IMPORTANCE OF AXIAL LENGTH IN THE DETECTION OF CARTOID ARTERY STIFFNESS INDUCED BY A HIGH FAT DIET

Abshire CA*, Reverte Ribo V**, Rosales CB**, Zimmerman MA*, Miller KS***, Prieto MC**, Lindsey SH*

* Pharmacology Department, Tulane University School of Medicine, New Orleans, LA
** Physiology Department, Tulane University School of Medicine, New Orleans, LA
*** Department of Biomedical Engineering, Tulane University, New Orleans, LA

Cardiovascular disease (CVD) is the leading cause of death worldwide and in the United States. Arterial stiffness, characterized by reduced compliance in large conducting arteries, is a major risk factor for CVD. Individuals with cardiometabolic risk factors such as obesity and insulin resistance have stiffer arteries and an increased risk of developing CVD. Recent evidence suggests that *ex vivo* arterial stiffening can be more fully characterized by performing pressure myography at multiple fixed lengths. Therefore, the aims of this study were to characterize the effect of a high fat diet on murine carotid stiffness using biaxial mechanical phenotyping.

At 4 weeks of age, some C57BL/6 male mice were placed the DIO Rodent Purified Diet with 45% Energy from fat (HFD, TestDiet 58V8) while control animals remained on a normal diet. At 39 weeks of age, common carotid arteries were harvested and cannulated for assessment of biaxial mechanical properties using pressure myography. After equilibration and pre-conditioning, *in vivo* carotid artery length was estimated by finding the length at which the artery caused minimal change to longitudinal force when subjected to pressures ranging from 70-150 mmHg. Pressure-diameter and force-length curves were obtained at the estimated *in vivo* length as well as 5% above and below the estimated *in vivo* length. Statistical analysis was performed using 2-way ANOVA with Graphpad Prism.

Baseline diameter of carotid arteries pressurized at 10 mmHg tended to be larger in HFD (388 ± 7 μm, n=5) versus control arteries (360 ± 13 μm, n=4, P=0.08). Pressure-diameter data obtained at the estimated *in vivo* length showed a significant interaction between diet and pressure ($P<0.001$) with the largest differences evident at pressures at and above 70 mmHg ($P<0.05$). HFD significantly decreased arterial compliance, a measure of the change in diameter at each 10 mmHg pressure step ($P<0.05$), especially at lower pressures. Finally, arterial distensibility was calculated as the percent change in outer diameter from the original diameter obtained at 10 mmHg. HFD significantly decreased distensibility ($P<0.05$), with the greatest differences found at pressures above 40 mmHg ($P<0.05$). Interestingly, the impact of diet on arterial compliance was significantly attenuated when experiments were performed at an axial stretch above or below the estimated *in vivo* length.

These data show a significant impact of HFD on carotid stiffness in male C57BL/6 mice. Of note, this difference was only detected when experimental conditions closely approximated the *in vivo* state. Additional analysis of this data will determine the impact of HFD and axial length on the force-length and stress-strain relationships. In conclusion, our study shows the importance of axial length in the analysis of diet-induced carotid artery stiffness.

A Generalized Kernel Method for Higher Order Interaction: An Imaging Genetics Analysis

Md Ashad Alam and Yu-Ping Wang

Department of Biomedical Engineering, Tulane University, New Orleans, LA 70118, USA

Technological advances are enabling the collection of multiview data in imaging genetics at increasing depth and with a decreasing costs. To date, a central goal of imaging genetics is to understand the interaction with pair of genetic variables or genetic and non-genetic variables such as genes with disease risk factors. However, understanding the interactions among more than two genetics variables is an emerging topic of imaging genetics. In this study, we propose a novel method named generalized kernel method for higher order interaction to achieve accurate implementation of interaction of multiple view data sets - a collection of single nucleotide polymorphisms (SNPs), deoxyribonucleic acid (DNA) methylations and functional magnetic resonance imaging (fMRIs). The proposed method is a semiparametric learning method on the reproducing kernel Hilbert space. Extensive simulation studies are conducted to evaluate the performance of the method. As a demonstration of application we applied to real data from the Mind Clinical Imaging Consortium to identify the effects of the interaction among candidate Schizophrenia genes corresponding to SNPs, methylation and region of interest (ROI) of fMRI data. Our method identified that ten genes from methylations have significant interactions with genes corresponding to SNPs and ROI.

This work was partially supported by NIH (R01GM109068, R01MH104680, R01MH107354), and NSF (#1539067)

THE ROLE OF EXTRAMEDULLARY HEMATOPOIESIS FOLLOWING SEVERE TRAUMA AND CHRONIC STRESS

Alamo IG*, Kannan KB**, Loftus TJ**, Ramos H**, Efron P**, Mohr AM**

*Department of Medicine/Office of Clinical Research and Training, Tulane University, New Orleans, LA.

** Division of Trauma/Department of Surgery, University of Florida, Gainesville, FL.

Severe traumatic injury is associated with bone marrow dysfunction that manifests as impaired erythropoiesis and loss of hematopoietic progenitor cells from the bone marrow. Extramedullary hematopoiesis (EMH), the development of blood cells outside the bone marrow, can occur in response to anemia, injury, and infection but has not been studied following severe injury and critical illness. In a clinically relevant rodent model of lung contusion (LC) and hemorrhagic shock (HS), we hypothesize that the addition of chronic stress (CS) increases EMH in the spleen. Male Sprague-Dawley rats (n=4-7/group) were subjected to LCHS and LCHS/CS. On day 7 spleen weight, growth of spleen erythroid progenitors including CFU-GEMM, BFU-E, and CFUE-E colonies, and spleen erythropoietin (EPO) and erythropoietic receptor (EPOr) expression were all assessed. Data was presented as mean±SD; *p<0.05 vs. naïve and **p<0.05 vs. LCHS by t-test. Seven days after LCHS, there was no significant difference in spleen size as compared to naïve. After the addition of CS to LCHS, spleen weight significantly increased by 22% (Figure 1). Spleen CFU-GEMM, BFU-E, and CFU-E growth following LCHS were comparable to that of naïve rodents (Table 1). However, LCHS/CS increased growth of spleen colonies by 28-39% (Table 1). Similarly, spleen EPO and EPOr expression following LCHS was comparable to naïve. LCHS/CS significantly increased splenic EPO expression by 23% but splenic EPOr expression decreased by 43% and LCHS/CS rodents had persistent anemia (Table 1). Following LCHS, chronic stress triggers splenic EMH that manifests as increased spleen weight, increased splenic erythroid colony growth, and increased splenic EPO expression; however, spleen EPOr expression is suppressed and despite EMH there is a persistent anemia. Further investigation of role of the EPO receptor in persistent anemia following severe trauma is warranted. This research was supported by the National Institutes of Health. AMM was supported by NIH NIGMS grant R01 GM105893-01A1.

Figure 1: Spleen weight.

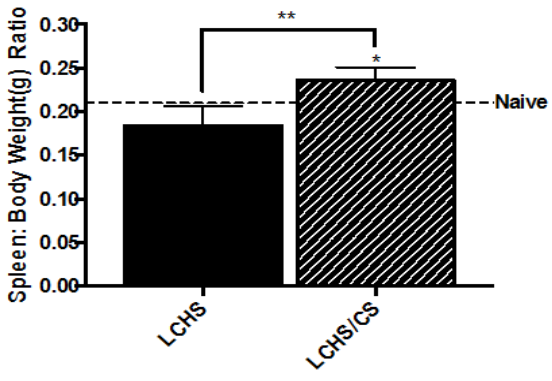

Table 1: Spleen erythroid colony growth, EPO and EPOr expression.

		Seven Days Following LCHS/CS	
	Naïve	LCHS	LCHS/CS
CFU-GEMM (colonies/plate)	11±2	9±3	**14±3****
BFU-E (colonies/plate)	12±3	15±1	**24±4****
CFU-E (colonies/plate)	14±1	16±2	**22±4****
Spleen EPO (cDNA/B-actin)	29±3	30±4	39±6
Spleen EPOr (cDNA/B-actin)	47±16	42±6	**27±5****
Hemoglobin (g/dL)	14.3±0.3	**12.3±0.7***	**10.8±0.9****

SEX DIFFERENCES IN THE EFFECT OF MEMBRANE AND NUCLEAR ERα SIGNALING ON GLUCOSE HOMEOSTASIS IN MICE.

Allard C*, Xu B*, Salwen B*, Levin ER**, Mauvais-Jarvis F*

*Department of Medicine, Tulane University Health Sciences Center, New Orleans, Louisiana 70112, USA

**Department of Medicine and Biochemistry, University of California, Irvine and the Long Beach VA Medical Center, California 90822, USA

Estrogens maintain energy homeostasis in females, but also in males, mostly via the estrogen receptor-α (ERα). Estrogens are involved in insulin sensitivity as well as pancreatic β-cell function and survival. Apart from its well-known nuclear receptor activity, a pool of ERα has been characterized at the membrane and allows rapid-membrane initiated signaling. The roles of extra-nuclear versus nuclear ERα signaling on glucose homeostasis *in vivo* in male and female mice is unknown.

We studied the phenotype of male and female mice expressing a Membrane-Only ERα (MOER) and a Nuclear-Only ERα (NOER). NOER mice showed almost no metabolic alterations, whereas MOER mice of both sexes were hyperglycemic and glucose-intolerant and exhibited a sex dimorphism related to glucose homeostasis. Female MOER were hyperinsulinemic, insulin resistant and glucose intolerant without alteration in glucose-stimulated insulin secretion (GSIS). In contrast, male MOER mice were not hyperinsulinemic and did not exhibit insulin resistance but showed impaired GSIS leading to glucose intolerance.

Our results highlight the importance of genomic events initiated by nuclear ERα in glucose homeostasis in male and female mice via different mechanisms. This study emphasize the necessity of pursuing pre-clinical studies in animals of both sexes as the identification of sex-specific biological processes will open avenue for gender-based treatments of metabolic disease.

Funding acknowledgement: NIH R01DK107444, ADA 7-13-BS-101 and 1-16-PDF-004.

SURGICAL OUTCOMES OF ROBOT-ASSISTED THYROIDECTOMY FOR THYROID CANCER; A 108 CASES ANALYSIS FROM USA AND FRANCE

Alzahrani H*, Aidan P**, Bu Ali D*, Murad F*, Alshehri M*, Noureldine S*, Al-Qurayshi Z*, Kang SW*, Kandil E*

*Surgery, Tulane University, School of Medicine, New Orleans, LA, United States.

**American Hospital of Paris, Paris, France.

Introduction:

Recently, many studies reported the safety and feasibility of robot-assisted thyroidectomy, but most of these studies were performed in South Korea. Although there were several small series and case reports from the United States, most of these cases were for benign disease. The aim of our study is to report the safety and feasibility of robot-assisted thyroidectomy for thyroid cancer in the western population.

Methods:

Retrospective review of all patients who underwent robot-assisted thyroidectomy over the last 5 years for thyroid cancer, in two centers, one in France and one in USA. Those were compared to a control group who underwent open thyroidectomy at the same period. We analyzed demographic data, operative outcome and early oncologic outcome measures including; pathological margins, biochemical (thyroglobulin level) and radiological evidence for recurrence

Results:

Total of 108 robotic cases and 233 conventional cervical operations were included. 28.70% of patients underwent central lymph node dissection and 9.26% had lateral neck dissection. The transaxillary approach was performed in 93.5% and the remaining underwent retroauricular approach. In the robotic cases, the mean age was 45.58±10.58 years and BMI was 26.09±6.47. The average nodule size was 2.05±1.5cm. The mean operative time was 161.1±55.99 minutes with 3 patients required conversion to conventional cervical approach. Complications were reported in 8(7.4%) patients including 1 hematoma, 3 seroma and 5 patients developed transient vocal cord paralysis. Two (1.92%) patients had focal positive margins and two (1.85%) developed recurrence 24 and 16 months following initial surgery. In comparison to patients who underwent open approach, the robotic approach had significantly longer operative time (p<001). On the other hand, there was no significant difference in the overall complication rate (p=0.15). The mean TG level was 0.16±0.4 in the robotic group compared to 0.6±0.1 in the conventional open group.

Conclusions:

Robot-assisted thyroid surgery is a safe and feasible approach for managing selected group of patients with thyroid cancer in the western population, and is associated with sound oncologic outcome comparable to the open approach.

Impact of Number of Cycles of Collagenase Clostridium Histolyticum on Outcomes in Patients with Peyronie's Disease

James Anaissie, B.S.*; Faysal A. Yafi, M.D.; Elizabeth J Traore, B.A.; Suresh C. Sikka; Waynge GJ Hellstrom, M.D.

Department of Urology, Tulane University School of Medicine, New Orleans, LA, USA
** Presenting author*

Introduction and Objective: Peyronie's disease (PD) is the abnormal accumulation of fibrous plaques in the tunica albuginea, leading to penile deformity. Collagenase Clostridium histolyticum (CCH) is a minimially invasive, Food and Drug Aministration (FDA)-approved, and effective treatment for PD. The objective of this study was to analyze the changes seen between the four cycles of CCH therapy in order to uncover any trends that may help guide therapy.
Methods: Consecutive patients treated with Xiaflex® for PD between 04/2014 - 09/2015 were identified from a prospective registry. Data was collected from patient electronic medical records. The primary outcome of interest was the change in curvature between each cycle of treatment (4 cycles total). Secondary outcomes included predictors of significant reduction in penile curvature. Significance was determined via two-tailed t-test for continuous variables, and Pearson's chi-square test for categorical variables. Repeated measures model was used to determine change in curvature per cycle.
Results: Among 78 patients who met inclusion criteria for analysis, 36 (46%) recieved four rounds of treatment. Median duration of PD was 15 months, ranging between 0 and 492 months. Mean pre-treatment curvature was 58.5 (18.0) degrees vs. a post-treatment curvature of 42.0 (18.4) degrees ($p<0.001$), with a mean change of -14.5 (14.2) degrees for patients regardless of number of cycles recieved. Curvature changed significantly from one cycle to the next except with the 4th cycle, as seen in figure 1. A reduction in curvature of -16.8 (11.1) degrees after the 1st cycle significantly predicted ≥20% reduction in pre-treatment curvature ($p<0.001$).
Conclusions: CCH therapy is an effective treatment for PD, although the therapeutic benefit may decline after the third cycle of treatment. Significant mprovement after the first cycle may be a predictor of ≥20% reduction in curvature at the conclusion of treatment.

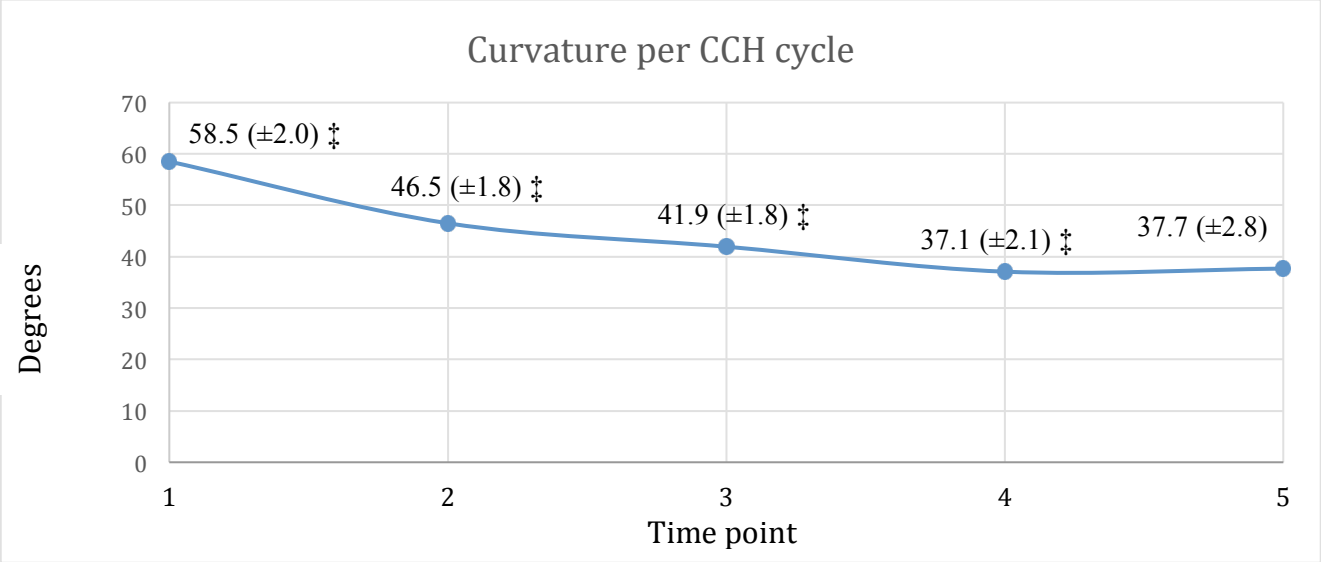

Figure 1: Repeated measures model for curvature improvement per cycle of collagenase Clostridium histolyticum (CCH). Time points: 1) curvature before 1st round, 2) curvature before second round, 3) curvature before 3rd round, 4) curvature before 4th round, and 5) final duplex curvature. ‡ indicates statistically significant improvement over previous cycle.

DIACETYL AND ACETYL PROPIONYL, BUT NOT THEIR METABOLITE ACETOIN, INDUCE HUMAN VASCULAR CELL DEATH AS COMPONENTS OF E-CIGARETTE AEROSOL

Anderson C*, Wang S*

*Department of Cell and Molecular Biology, School of Science and Engineering, Tulane University, New Orleans, LA

Electronic cigarettes have become the most popular alternative to conventional tobacco cigarettes among adults, and the most popular tobacco product among middle and high schoolers. While several recent studies confirm that e-cigarette aerosol can induce vascular cytotoxicity, very little is known about the specific compounds in e-cigarette liquid which cause that toxicity. Diacetyl and acetyl propionyl are volatile diketones and FDA approved food additives that have become popular flavoring agents for e-cigarette liquids. Here we investigate the effect these compounds have on human aortic cells. Initially, we employed neutral red uptake cell viability tests to determine the LC50 of each compound independently in cultured human aortic endothelial and smooth muscle cells. Then, we analyzed the literature to estimate a mean level of these compounds in the average e-cigarette. Using these two values, we were able to make custom e-cigarette liquid formulations and aerosolize them using a novel laboratory apparatus. The aerosol from these e-cigarette liquid formulations was applied to vascular cells in culture and cell viability was measured at 24 hours post-exposure. Additionally, these experiments were repeated with acetoin, the primary metabolite of diacetyl and acetyl propionyl, which is also used as a flavoring agent in e-cigarette liquids. Our results indicated that diacetyl and acetyl propionyl, but not acetoin, display a dose dependent cytotoxic effect in both aortic endothelial and smooth muscle cells both in isolation and as part of e-cigarette aerosol. Aortic smooth muscle cells are more tolerant of these compounds than endothelial cells (LC50 diacetyl = 58.23 ± 1.35 ppm and LC50 acetyl propionyl = 46.85 ± 1.49 ppm vs. LC50 diacetyl = 19.92 ± 1.54 ppm and LC50 acetyl propionyl =33.41 ± 1.55 ppm), but both cell types begin to show a noticeable cell death at concentrations >10 ppm of either compound. Acetoin displayed no cytotoxic effect at concentrations up to 1000 ppm. These results indicate that diacetyl and acetyl propionyl, but not acetoin, are dose dependent vascular risk factors when used as flavoring agents in electronic cigarette liquid, and support the need to regulate their use.

This work was supported by a Tobacco Product Regulatory Science Research Fellowship to C Anderson from the Tulane University School of Science and Engineering and a Startup Fund to S Wang from the Tulane University Department of Cell and Molecular Biology.

CHOP-INTERNATIONAL: AN OPEN ACCESS NUTRITION EDUCATION TOOL FOR PHYSICIANS, RESIDENT DOCTORS, AND MEDICAL AND PUBLIC HEALTH STUDENTS

Arman D*, Monlezun D*, Peters B**, Urday P*, Cutler H*, Pellicore D***, Lim H***, Sarris L*, Harlan TS*

*The Goldring Center for Culinary Medicine, Tulane University, New Orleans, LA.
**Abdominal Transplant Institute, Tulane Medical Center, New Orleans, LA.
***College of Culinary Arts, Johnson and Wales University, Providence, RI.

Dietary diseases drive some of this century's most pressing and costly global public health challenges, ranging from malnutrition-related infectious diseases such as HIV infection to overfeeding and linked chronic diseases such as type 2 diabetes mellitus and coronary heart disease. We seek to create clinically meaningful and costeffective education tools to help treat such conditions in a manner that is both population specific and evidence based. Tulane University School of Medicine's Goldring Center for Culinary Medicine (GCCM), a medical school-based teaching kitchen and research laboratory, utilized its novel collaboration of clinicians, registered dieticians, chefs, and culinary and medical students to create an open source international nutrition education resource comprised of region-specific recipes based upon the World Health Organization's Nutrient Intake Goals. Using staple ingredients from three sample Millennium Development Goals regions, GCCM has developed sample recipes from three continents for proof-of-principle testing. The recipes include nutrition facts, interchangeable and optional ingredients, and salient nutrition education discussion points for students and medical professionals to use with a variety of patient conditions. Community-based participatory testing of the efficacy of this tool will allow for the refinement of the complete tool in the United States, followed by global expansion in coordination with physicians and students from Tulane University School of Public Health and Tropical Medicine in Kenya, Indonesia, and Colombia.

Reinfection and Persist Infection After a Random Screening for Chlamydia in New Orleans

Asma Azizi, James Mac Hyman

Chlamydia trachomatis (Ct) is the most commonly reported STI in the United States with an estimated 1.7 million infections per year. According to the United States Add health there is a 4.9% prevalence of Ct among 18-26 years old sexually active individuals. There is a high prevalence of Ct rate among African American (AA) sexually active people aged 15-25 reside in New Orleans , 8% among men and 12% among women. We create and analyze an individual network-based model for the spread of Chlamydia trachomatis, Ct, in New Orleans. Based on partnership distribution, we made a bipartite sexual network for men and women. We Implemented a stochastic susceptible-infected-susceptible (SIS) Ct transmission model on this network and identified model parameters that agree with the known Ct incidence in New Orleans. We use the model to quantify the effectiveness of different intervention measures, such as screening and rescreening. For the rescreening, we come up with the proper time to rescreen infected people based on their sexual activity.

THE RELATIVE EFFECT OF INDIVIDUAL FACTTORS VERSUS COMMUNITY-LEVEL ACCESS MEASURES ON MODERN CONTRACETIVE USE IN KINSHASA, DRC: A MULTILEVEL ANALYSIS

Babazadeh S*, Bertrand J*, Anglewicz P*, Eitmann L*, Kayembe P**

***Department of Global Health Management and Policy, Tulane School of Public Health and Tropical Medicine
****Kinshasa School of Public Health, Kinshasa, Democratic Republic of Congo

Democratic Republic of Congo is the second largest country in Sub-Saharan Africa in land mass and third largest in population size (approximately 70 million inhabitants). With a natural increase of 2.7% a year, the population of the country will double by 2037. Furthermore, the country is ranked 186 of 187 in terms of Human Development Index (HDI). Similar to other francophone countries in West and Central Africa, the DRC has a high fertility rate, low modern contraceptive use and high unmet need. The country underwent a devastating period of political and social unrest from 1991 to the early 2000s, but has regained a sense of normalcy in the past decade.

This analysis was based on a household-level and a facility-level survey, conducted in Kinshasa, DRC as part of the fourth round of PMA2020 survey initiative by the Kinshasa School of Public Health in collaboration with Tulane University. Two-stage cluster sampling was used. At the first stage 58 enumeration areas (EA) were randomly selected. At the second stage, 30 households and 3-6 service delivery points were selected in each EA. Data collection took place between October 2015 and January 2016.Multilevel analysis was used to test the effect of explanatory variables (including both individual and community level) on modern contraceptive use. Individual level variables included age, education, number of live birth, wealth index, if husband had other wives, and exposure to FP messages via the media. Community level variables that measured the FP supply environment in each EA were number of hospitals or health centers offering FP methods, mean number of methods in those facilities, mean number of staff in the facilities, and mean number of days per week that the facilities offered FP services.

Among women married or in union 15 to 49 years old in Kinshasa, 23.8% used modern contraception as of 2016. Results of the multivariate analysis indicated that only two of the six individual variables were significantly associated with modern contraceptive use: age and number of live births. By contrast, three of the four community-level variables were significantly related : mean number of staff in health facilities offering FP in EA, mean number of days per week that facilities offering FP services were operational, and mean number of contraceptive methods available in FP facilities in the EA.Because PMA2020 collects both household- and facility-level data, it is possible to simultaneously analyze the effects of individual level factors and community-level factors (measuring the FP supply environment). This analysis is particularly illuminating, since the conventional associations between education or wealth and modern contraceptive use are not evident in Kinshasa. Rather, only age and number of living children (highly predictive of contraceptive use in countries worldwide) were associated with modern method use. Further analysis of these data will be conducted to determine if certain community-level factors (e.g., number of staff working in FP facilities in the EA) are a proxy for something larger. The final analysis – to be presented in Indonesia – will refine the measures of access, for example, to determine the mean distance that each respondent from the household survey lives to a facility delivering FP services.

These results reflect the importance of assessing the FP supply environment as well as the individual characteristics of women in the target population to better understand patterns of contraceptive use. These findings are particularly valuable given that access is a variable susceptible to programmatic action. The researchers are working closely with the National Program of Reproductive Health as well as local and international NGOs in a collective effort to increase modern contraceptive prevalence in Kinshasa.

THE MRE11-REGULATED CONSERVATIVE SEGREGATION OF TELOMERE CHROMATIN AND PHENOTYPIC HERITABILITY IN *SACCHAROMYCES CEREVISIAE.*

Baek IJ. and Lustig A.J.

Department of Biochemistry and Molecular Biology, School of Medicine, Tulane University, New Orleans, LA

Telomeres, nucleoprotein complexes at termini of linear chromosomes, are playing an essential role in telomere replication and end protection. The loss of these functions would lead to chromosome instability. The basic components of the telomere are beginning to be understood and consist of the reverse transcriptase, telomerase, enzymes that regulate telomerase and telomere size homeostasis. One process that remains unstudied is the nature of the segregation of telomeric protein to sister chromatids, one of the more poorly understood processes in epigenetic behavior. This process maintains the same telomere structure on both sister strands. In this study, we have defined the nature of telomere segregation through the continual segregation of a mutant allele of *MRE11* to sister chromatids. This allele, *mre11A470T* displays a bi-directional complementation telomere size phenotype. Integration of wild type at an ectopic position still gives rise to the mutant short telomere phenotype. In contrast, integration of *mre11A470T* in a wild type strain maintains the wild type phenotype. This indicates that the same telomeric chromatin segregates to both strands of DNA during replication to daughter cells even in the presence of the other allele. What is more, this phenotype is stable for at least 100 generations of growth indicating that this phenotypic maintenance is a very efficient and stable process. This segregation pattern appears to be mediated through the telosome structure. Telosomes are defined operationally by particles that are released with increasing concentration of micrococcal nuclease. While the wild type protein is released readily and forms a particle 200 bp larger than the telomere size, *mre11A470T* cells, are released only after more extensive digestion and are more diffuse than wild type telosomes. These data suggest that Mre11 is involved in the formation or maintenance of the telosome. The major component of the telosome is Rap1. A temperature sensitive mutation of *RAP1*, *rap1-5* has similar phenotypes growth and chromatin structures as wild type at semi-permissive conditions. The double mutant *mre11A470Trap1-5* has a similar chromatin phenotype as in the mre11A470T single mutant. However,

at the restrictive condition, *rap1-5* cells slowly cease growth. Unlike the single mutant, *mre11A470T* and *rap1-5* synergistically interact to decrease rates of viability.

This work was funded by the NIH grant GM, institutional funding, and the Tulane Cancer Center for support of this project.

ROLES OF THE INTERSTITIAL GENES BETWEEN THE TMPRSS2 AND ERG IN PROSTATE CANCER PROGRESSION

Bai S*, Cao S*, and Dong Y*

*Department of Structural and Cellular Biology, Tulane University School of Medicine, New Orleans, LA

Approximately 50% prostate cancers harbor the TMPRSS2-ERG gene fusion. The fusion leads to overexpression of the ERG gene under the control of the TMPRSS2 promoter. The TMPRSS2-ERG translocation can be generated by either deletion of the region between these two genes (referred to as Edel) or interchromosomal insertion. The Edel subtype appears to be more aggressive than the insertion subtype, indicating that the deletion of at least some of the interstitial genes between TMPRSS2 and ERG may contribute to the aggressiveness. The objective of this study was to identify these interstitial genes. We focused on 9 of the 16 coding genes in the interstitial region because of the commercial availability of their shRNA constructs. We knocked down their expression individually in the VCaP human prostate cancer cell line, which contains the TMPRSS2-ERG gene fusion through interchromosomal insertion. The knockdown of 3 genes, namely IGSF5, FAM3B and BACE2, promoted the growth of the cells. Conversely, ectopic expression of FAM3B suppressed the growth of ~~the~~ LNCaP human prostate cancer cells, which express very low level of endogenous FAM3B. Interestingly, overexpression of the 3'-UTR of FAM3B also caused suppression of cell growth, and this effect was eliminated when Dicer, a protein involved in miRNA biogenesis, was knocked out. These findings indicate that at least some of the interstitial genes may play a tumor suppressor role and that the tumor suppressor role may be mediated through both coding and miRNA-involved, non-coding functions of the gene.

INTRADERMAL VACCINATION WITH A *PSEUDOMONAS AERUGINOSA* VACCINE ADJUVANTED WITH A MUTANT BACTERIAL ADP-RIBOSYLATING ENTEROTOXIN PROTECTS AGAINST ACUTE PNEUMONIA

Baker SM*, Clements JD*, Morici LA*

*Department of Microbiology and Immunology, Tulane University School of Medicine

Pseudomonas aeruginosa is an opportunistic pathogen capable of causing acute pulmonary infections and is a leading cause of hospital-acquired and ventilator-associated pneumonia. With an estimated 6700 multidrug-resistant *P. aeruginosa* infections in the US annually, the need for a vaccine against this pathogen is critical. Growing evidence suggests that a successful *P. aeruginosa* vaccine may require antibody and Th1 $CD4^+$ T cells systemically and in the lungs to prevent pulmonary infection. The majority of *P. aeruginosa* vaccine studies in mice utilize intramuscular (IM) vaccination. However, IM immunization may not be the optimal route for eliciting mucosal immune responses. Recent work suggests that intradermal (ID) immunization can induce a mucosal immune response, as dermal dendritic cells process antigen and migrate to the draining lymph nodes, inducing the expression of mucosal homing markers on B and T cells. Additionally, ID immunization with mucosal adjuvants, such as the bacterial ADP-Ribosylating Enterotoxin Adjuvant (BARE) double mutant of *E. coli* heat-labile toxin (dmLT), can direct protective immune responses to mucosal tissues. Previously, we demonstrated that ID immunization with *P. aeruginosa* outer membrane proteins (OMP) adjuvanted with dmLT induced anti-pseudomonal IgG in the serum and bronchoalveolar lavage fluid (BALF) and antigen-specific $CD4^+$ T cells in the lungs, mediastinal lymph nodes, and spleen. To evaluate the protective efficacy of the ID *P. aeruginosa* vaccine in a lethal acute pneumonia model, we immunized C57Bl/6 mice with 1 μg of a *P. aeruginosa* OMP preparation combined with 1 μg of dmLT. Control mice were administered saline. Mice were then challenged with $7x10^6$ CFU of *P. aeruginosa* via oropharyngeal aspiration of the bacteria directly into the lungs. ID immunization with *P. aeruginosa* OMPs and dmLT provided significant protection against *P. aeruginosa* pneumonia, with 78% of immunized mice surviving and clearing the pulmonary infection compared to 100% mortality in saline immunized controls. Protection was associated with strongly binding, bactericidal antigen-specific serum and BALF IgG and IFN-γ-producing $CD4^+$ T cells in the lungs. These results demonstrate the ability of ID vaccination to stimulate protective antibody and cellular immune responses in the lung. The use of ID immunization with a BARE to target vaccine-induced immune responses to the lung has the potential to prevent respiratory infections and reduce the global morbidity and mortality caused by multidrug resistant pathogens.

DISRUPTING TUMOR-HOST COMMUNICATION, AN EFFECTIVE APPROACH TO CONTROL GLIOBLASTOMA DEVELOPMENT

Barabadi Z*, Pfnur A*, Ochoa JE**, Lin D*, Braun SE***, Alt E*, Izadpanah R*,**

*Heart and Vascular Institute, Applied Stem Cell Laboratory, Tulane University, New Orleans, LA
**Department of Surgery, Tulane University, New Orleans, LA
***Division of Gene Therapy, Tulane National Primate Research Center, New Orleans, LA

The role of chronic inflammation in formation of tumor microenvironment (TM) and subsequently in tumor development has been well established. Our novel data indicate a crucial role for TRAF3IP2 as a key player in inflammatory signaling pathways in TM. We studied the role of TRAF3IP2 in development and progression of glioblastoma (GBM). TRAF3IP2 was knocked down using lentiviral vector containing specific shRNA in U87 cells, a human GBM cell line. Silencing TRAF3IP2 has a remarkable effect on cell cycle and cause cell cycle arrest in S and G2/M phases and increase the apoptosis markers. A significant decrease in inflammatory cytokine levels in TRAF3IP2 knock down U87 cells ($U87_{TRAF3IP2KD}$) was observed in Elisa. In addition, NFκB induced TGFβ and IL17 secretion was significantly reduced in $U87_{TRAF3IP2KD}$ cells. Gene expression analysis showed decrease in the expression of matrix metalloproteinases (MMPs) and vascular endothelial growth factor (VEGF) and increase in the expression of adhesion genes such as melanoma cell adhesion molecule (MCAM). Also, scanning electron microscopy imaging showed a remarkable change in morphology of $U87_{TRAF3IP2KD}$ cells. For tumorigenesis studies, we subcutaneously injected the $U87_{TRAF3IP2KD}$ cells in the right flank of immune deficient mice. A group of animals were injected with U87 cells transduced with non-target shRNA as control. Resultant tumors from $U87_{TRAF3IP2KD}$ cells were significantly smaller in size compared to the control group tumors. In a different set of experiments, wild type GBM tumors were treated with lentiviral vector containing shRNA targeting TRAF3IP2 gene. The results of these experiment showed that treatment of wild type tumors can significantly prevent tumor growth compared to control groups. These studies suggest the crucial role of TRAF3IP2 in development of TM and consequently development of GBM, therefore controlling the expression of this gene disturbs TM structure and prevents tumor growth.

This work was supported by funds from Alliance of Cardiovascular researchers (545856A1).

OSTEOINDUCTIVE EFFECTS OF GLYCEOLLINS ON ADULT MESENCHYMAL STEM CELLS DERIVED FROM ADIPOSE TISSUE AND BONE MARROW

Bateman ME*, Strong AL*, Hunter RS*, Bratton MR**, Komati R***, Sridhar J***, Riley KE***, Hayes DJ****, Boue SM*****, Burow ME******, Bunnell BA*,*******

*Center for Stem Cell Research and Regenerative Medicine, Tulane University School of Medicine, New Orleans, LA

**Cell and Molecular Biology Core Facility, Xavier University of Louisiana, New Orleans, LA

***Department of Chemistry, Xavier University of Louisiana, New Orleans, LA

****Department of Biological and Agricultural Engineering, Louisiana State University and Agricultural Center, Baton Rouge, LA

*****Southern Regional Research Center, US Department of Agriculture, New Orleans, LA

******Department of Medicine, Tulane University School of Medicine, New Orleans, LA

*******Department of Pharmacology, Tulane University School of Medicine, New Orleans, LA

Osteoporosis is characterized by destruction of bone architecture, resulting in decreased bone mass density (BMD) and increased fracture susceptibility. While current therapies focus on reducing bone resorption, the development of anabolic therapies to regenerate bone may also be beneficial. Promising anabolic therapeutic candidates include phytoestrogen compounds, such as daidzein, which effectively induce osteogenesis of adipose-derived stem cells (ASCs) and bone marrow-derived mesenchymal stem cells (BMSCs). Glyceollins are structural derivatives of daidzein, and herein, the osteoinductive effects of glyceollins I and II were assessed in ASCs and BMSCs and compared to estradiol. The ability of glyceollins to promote osteogenesis of ASCs and BMSCs was evaluated in adherent and scaffold cultures. Relative deposition of calcium was analyzed using Alizarin Red staining, Bichinchoninic acid Protein Assay, and Alamar Blue Assay. To further explore the mechanism by which glyceollin II exerts its osteoinductive effects, docking studies of glyceollin II, RNA isolation, cDNA synthesis, and quantitative RT-PCR (qPCR) were performed. In adherent cultures, ASCs and BMSCs treated with estradiol, glyceollin I, or glyceollin II increased calcium deposition relative to vehicle-treated cells. During evaluation on PLGA scaffolds seeded with ASCs and BMSCs, glyceollin II was the most efficacious in inducing ASC and BMSC osteogenesis compared to estradiol and glyceollin I. Dose-response analysis in ASCs and BMSCs revealed that glyceollin II has the highest potency at 10 nM in adherent cultures and 1 μM in tissue scaffold cultures. At all doses, osteoinductive effects were attenuated by fulvestrant, suggesting that glyceollin II acts at least in part through estrogen receptor-mediated pathways to induce osteogenesis. Analysis of gene expression demonstrated that, similar to estradiol, glyceollin II induces upregulation of genes involved in osteogenic differentiation. The ability of glyceollin II to induce osteogenic differentiation in ASCs and BMSCs indicates that glyceollins hold the potential for the development of pharmacological interventions to improve clinical outcomes of patients with osteoporosis.

PREVIOUS MIDLIFE ESTRADIOL TREATMENT RESULTS IN LONG-TERM MAINTENANCE OF HIPPOCAMPAL ESTROGEN RECEPTOR ALPHA LEVELS IN OVARIECTOMIZED RATS: MECHANISMS AND IMPLICATIONS FOR MEMORY.

Black KL*, Witty CF**, Daniel JM* ***

*Tulane Brain Insitute, Tulane University, New Orleans, LA. **Neuroscience Program, Tulane University, New Orleans, LA. ***Psychology Department, Tulane University, New Orleans, LA.

Ovariectomized rats that have received previous administration of estradiol in midlife display enhanced cognition and increased hippocampal levels of estrogen receptor (ER) α months after estradiol treatment ended compared to ovariectomized controls. The present study aimed to investigate the mechanisms by which ERα levels are maintained following midlife estradiol exposure and the role of ERα in memory in aging females in the absence of circulating estrogens. Unliganded ERα has increased interaction with the ubiquitin ligase, C-terminus of Hsc-70 interacting protein (CHIP), leading to increased degradation of the receptor. In our first experiment, we tested the hypothesis that midlife estradiol exposure in ovariectomized rats results in decreased interaction between CHIP and hippocampal ERα, leading to increased levels of ERα. Middle-aged rats were ovariectomized and received estradiol or vehicle implants. After 40 days, implants were removed. One month later, rats were killed and hippocampi were processed for whole protein western blotting and co-immunoprecipitation, in which ERα was immunoprecipitated from lysate. As expected, ERα protein expression was increased in rats previously treated with estradiol compared to vehicle-treated rats. In rats treated with estradiol, there was a decrease in CHIP-ERα interaction, suggesting that previous estradiol treatment reduces interaction, slowing the degradation of ERα. In a second experiment, we determined the impact on memory of antagonism of ER in the absence of circulating estrogens. Rats were ovariectomized and implanted with estradiol capsules. Capsules were removed after 40 days. Rats received chronic i.c.v. infusion of ER antagonist, ICI 182 780, or artificial cerebrospinal fluid vehicle and were tested on a spatial memory radial-maze task. Rats treated with ICI 182 780 had significantly worse performance (more errors). These experiments provide evidence that previous midlife estradiol treatment maintains hippocampal ERα by decreasing its interaction with CHIP and that activation of these receptors provides cognitive benefits in the absence of circulating estrogens.

This work was supported by *National Institute of Aging* Grant RO1AG041374

ROBOT-ASSISTED THYROIDECTOMY; ANALYSIS OF TWO DIFFERENT APPROACHES

Bu Ali D*, Murad F*, AlQurayshi Z*, Kang SW*, Kandil E*

*Department of Surgery, Tulane University, School of Medicine, New Orleans, LA, United States

Introduction:
Several approaches have been described for Robotic thyroid surgery. However, their comparative studies have never been performed. The aim of this study is to compare the surgical outcome of transaxillary and retroauricular approaches in a single North American institution.

Methods:
Retrospective review of 73 patients scheduled for Robotic thyroid and parathyroid surgery over 3 years by one surgeon. Patients were divided into 2 groups the transaxillary (TA) and retroauricular (RA) approaches, and those were compared to 177 control matched group who underwent open approach. The patients were compared based on clinical pathological characteristics and surgical outcome.

Results:
33 patients underwent transaxillary approach and 40 had retroauricular approach. 69.7% of TA and 45.71% of RA procedures were done on outpatient basis, and there was no significant difference in operative time or intra-operative blood loss. No reported cases of conversion to open. There was no difference in the overall complication rate(p=0.75). In RA, there were 2(5.71%) cases of hematoma and 3(8.57%) cases of seroma, compared to none in the TA. Only one patient in the RA group required exploration for neck hematoma. One patient in the TA had transient vocal cord paralysis and 2 in the RA; however, no permanent paralysis was reported. In comparison to the open approach, there was no difference in complication rate (OR: 0.63, p=0.47), however; the operative time was significantly less in the control group (OR:0.01, p<0.001).

Conclusions:
Retroauricular and transaxillary approaches for robot-assisted thyroid surgery are both safe and feasible, with no additional complications risk compared to the open approach.

MAIT CELL CHARACTERIZATION AND RESPONSES DURING *MTB*/SIV INFECTION IN RHESUS MACAQUES

Bucşan AN*,**, Foreman TW*,**, Rout N*,***, Kaushal D*,**

*Department of Microbiology and Immunology, Tulane University School of Medicine, New Orleans, LA
**Department of Bacteriology and Parasitology, Tulane National Primate Research Center, Covington, LA
***Department of Immunology, Tulane National Primate Research Center, Covington, LA

Tuberculosis (TB) is a catastrophic infectious disease, affecting roughly one third of the world's population. Mucosal-associated invariant T (MAIT) cells are innate-like T cells that recognize vitamin B metabolites produced by bacteria, possess effector memory phenotype, and express tissue-homing markers driving migration to sites of infection. Previous research in both *Mtb* and HIV infections has shown that MAIT cells are depleted in the human periphery, with the hypothesis being that they are migrating to the tissue sites of infection. We investigated this hypothesis using rhesus macaques with active TB, latent TB (LTBI), and SIV-coinfection to explore the effects of different disease states on the MAIT cell populations in vivo. Early in infection, we observed that MAIT cells increased predominantly in the blood of actively infected rhesus macaques compared to those with LTBI. However, the frequency of MAIT cells increased at the site of infection, the lungs, in animals with LTBI. Furthermore, following infection, the chemokines expressed on MAIT cells reflected a shift towards a Th1 phenotype from a shared Th1/Th17 phenotype. In conclusion, we observed that MAIT cells with enhanced Th1 functions were migrating effectively to the site of infection during LTBI. The anti-mycobacterial effector functions of MAIT cells, particularly during the early stages of *Mtb* infection, may play an important role in protective long-term TB immunity. Better understanding the role of MAIT cells may enable us to develop better vaccines that target early TB pathogenesis by involving the innate immune response.

This work was supported by R01AI111914, R01AI111943, U19AI111211, P51OD011104, P51OD011104.

RISK FACTORS FOR PROGRESSION OF CORONARY ARTERY CALCIFICATION IN PATIENTS WITH CHRONIC KIDNEY DISEASE

Bundy JD*, Chen J*,**, and He J*,**

*Department of Epidemiology, Tulane University School of Public Health and Tropical Medicine, New Orleans, LA; **Department of Medicine, Tulane University School of Public Health and Tropical Medicine, New Orleans, LA

Coronary artery calcification (CAC) is highly prevalent among patients with chronic kidney disease (CKD) and predicts the risk for cardiovascular disease (CVD). Our objective was to examine the associations of novel risk factors with the progression of CAC among patients with CKD. In a random subsample of 1,123 participants from the Chronic Renal Insufficiency Cohort (CRIC) Study, CAC was measured at baseline and a follow-up visit using electron beam computed tomography (CT) or multidetector CT. Multiple logistic regression was used to evaluate risk factors for CAC progression, defined as an increase of Agatston score ≥100 units during follow-up. We also evaluated the change in square root transformed CAC score over time using mixed-effects regression models. Over an average of 3.3-year follow-up, 332 (29.6%) participants had CAC progression. After adjusting for age, sex, race/ethnicity, clinical site, follow-up time between CT scans, baseline CAC score, and established CVD risk factors including total cholesterol, HDL cholesterol, use of antihypertensive medications, systolic blood pressure, diabetes, and current smoking, lower estimated-glomerular filtration rate (eGFR) (OR 1.25, 95% CI 1.04-1.52, p=0.02), cystatin C (OR 1.19, 95% CI 1.01-1.40, p=0.04), serum phosphate (OR 1.35, 95% CI 1.13-1.60, p<0.001), and glycated hemoglobin (OR 1.27, 95% CI 1.05-1.53, p=0.01) were associated with CAC progression. In addition, lower eGFR, 24-hour urine albumin, cystatin C, serum calcium, serum phosphate, fibroblast growth factor-23, total parathyroid hormone, fibrinogen, interleukin-6, and tumor necrosis factor-α were associated with increase in CAC score from baseline in the multivariable-adjusted models. In conclusion, these data suggest that reduced kidney function, calcium and phosphate metabolism disorders, and inflammation, independent of established CVD risk factors, might play a role in CAC progression among patients with CKD.

HDAC2 MEDIATES TNBC PROGRESSION AND METASTASIS

Burks HE*, Matossian M*, Elliot SE*, Rhodes LV**, Collins-Burow B*, Burow ME*

*Department of Medicine, Section of Hematology and Oncology, Tulane University School of Medicine, New Orleans, Louisiana

** Department of Biological Sciences, Florida Gulf Coast University, Fort Myers, Florida

Triple negative breast cancer (TNBC), is the most aggressive subtype of breast cancer, with higher rates of metastasis and recurrence than other classified subtypes. The decreased survival rates seen in TNBC can be attributed in part to the lack of targeted therapeutics. HDAC inhibitors (HDACi) have emerged as a potential adjuvant therapy for patients with triple negative disease. Previously, our lab has identified Panobinostat, a pan-DAC inhibitor, as a successful therapy for the reversal of the metastatic phenotype in TNBC. However, this therapy lacks specificity and may have increased side effects as a result. In this study we aim to dissect the necessary HDACs responsible for driving and maintaining the metastatic phenotype of TNBC, with the goal of informing specific, well targeted HDACi therapies. Here we show that Romidepsin, an HDAC 1 and 2 specific inhibitor, is capable of recapitulating aspects of Panobinostat treatment in TNBC both *in vitro* and in a patient derived xenograft model *in vivo*. To parse the necessity and role of HDAC1 and HDAC2 individually, we created knockdown cell lines and analyzed them for changes in gene expression changes and their respective associated biological processes, including proliferation, migration, tumor growth and metastasis. We found that HDAC2 knockdown was able to significantly repress migration and proliferation in TNBC cells and their associated gene expression signatures *in vitro*. Furthermore, HDAC2 knockdown resulted in decreased tumor growth and metastasis an *in vivo* mouse model. These results illustrate the efficacy of FK228 in inhibition of oncogenic processes and implicate HDAC2 as a potential target for therapeutic intervention in TNBC.

PANCREAS-RELATED NEURONS CAN BE IDENTIFIED AND TARGETED FOR PATCH-CLAMP ELECTROPHYSIOLOGICAL RECORDING IN THE MOUSE BRAIN USING PSEUDORABIES VIRUS-152

Butcher SM*, Miyada K**, Zsombok A*,**

*Neuroscience Program, Brain Institute,Tulane University, and **Department of Physiology, Tulane University School of Medicine, New Orleans LA

Diabetes Mellitus, the most common metabolic disorder, is characterized by hyperglycemia as a result of insulin resistance or lack of insulin, and damage or failure of the insulin producing beta cells of the pancreas. Secretory function of the pancreas is partly controlled by the autonomic nervous system; however, diabetes mellitus is typically treated peripherally, for example, through insulin injections, or with drugs designed to stimulate insulin release from the pancreas or reduce glucose production in the liver. Investigation of the neural circuitry involved in the control of the pancreas could provide novel central nervous system targets for the treatment of diabetes mellitus. Pseudorabies Virus (PRV), a retrograde trans-synaptic viral tracer, when injected into the pancreas can be used to determine the neural circuits involved in the control of pancreatic activity. Mice with a C57bl/6 background injected with PRV-152 in the pancreas showed labelling in brainstem and hypothalamic nuclei important for metabolic regulation. Pancreas-related neurons were identified in the dorsal motor nucleus of the vagus (DMV), nucleus tractus solitarius (NTS), rostral ventrolateral medulla (RVLM), periaqueductal gray (PAG), parabrachial nucleus (PBN), paraventricular nucleus (PVN), lateral hypothalamus (LH), dorsomedial hypothalamus (DMH), arcuate nucleus (ARC), ventromedial hypothalamus (VMH), and the central amygdaloid nucleus (CeA). These results are consistent with PRV injections into the pancreas of Sprague-Dawley rats (Loewy and Haxhiu 1993) and C57bl/6 mice (Rosario et al 2016); however, both studies used PRV strains that require immunohistochemistry (IHC) to identify neurons; and do not allow for identification of pancreas-related neurons for *in vitro* patch-clamp electrophysiological recordings. By using PRV-152, a strain that expresses an EGFP reporter that is under control of the CMV promoter, IHC is not required to identify pancreas-related neurons, which can be targeted during patch-clamp recordings using a FITC microscope filter. During recordings from pancreas-related neurons in the PVN, insulin was applied to brain slices in the bath, and changes in frequency and amplitude of excitatory and inhibitory postsynaptic currents can be determined. This method can be used to investigate the effect of various hormones and neurotransmitters on signal transmission in pancreas-related neurons in the hypothalamus, and provide insight into how their activity is regulated in both normal and diabetic animals.

National Institutes of Health R01 DK099598 for AZ

Loewy AD, Haxhiu MA: CNS cell groups projecting to pancreatic parasympathetic preganglionic neurons. Brain Research 1993; 620:323-330

Rosario W, Singh I, Wautlet A, Patterson C, Flak J, Becker TC, Ali A, Tamarina N, Philipson LH, Enquist LW, Myers MG, Rhodes CJ: The Brain to Pancreatic Islet Neuronal Map Reveals Differential Glucose Regulation from Distinct Hypothalamic Regions. Diabetes 2016; 65(9): 2711-2723

Low Dose Rate Prostate Brachytherapy: Predictors of Failure, Sequelae, and Quality of Life

Cameron Callaghan, BA; Lin Wang, PhD; Abhishek V Alluri, MD; Katie M Vance, PhD; Andrew Lauve, MD; Cynthia Boyer, MD; William Russell, MD

Abstract

Purpose: To determine impact of patient characteristics (Age, Smoking, Alcohol, Family History of Prostate Cancer), comorbidities (DM, HTN, CVA, Gout, GERD, HLD, PVD, CAD, COPD), disease characteristics (T-stage, Grade, PSA, Prostate Volume) and six week post-implant PSA (6wPSA) on erectile and urinary symptoms, Health-Related Quality of Life (HRQOL), Biochemical Failure (BCF) and Biochemical Failure Free Survival (bFFS) in patients receiving Low Dose Rate Prostate Brachytherapy (LDR-BT).

Methods and Materials: Data from 694 consecutive patients receiving LDR-BT for localized prostate cancer at a single institution between 2002 and 2015 was collected for patient and disease characteristics, comorbidities, and 6wPSA. Changes in urinary and erectile function and HRQOL were measured using AUASS, IIEF-5 and CDC's HRQOL-14 questionnaires respectively. Pretreatment data was compared to BCF and bFFS using Multivariate Analysis (MVA), Receiver-Operator Characteristic (ROC) curves and Kaplan-Meier method.

Results: MVA demonstrated that for BCF; Alcohol, GERD and 6wPSA were associated with BCF (p= 0.011, 0.045, and 0.001 respectively). ROC curves between 6wPSA and Alcohol compared to BCF yielded areas under the curve of 64.7% (p<0.001) and 41.2% (p=0.030) respectively. MVA of bFFS demonstrated associations with Alcohol, Gleason score, HTN and TIA/CVA (p= 0.047, 0.009, 0.038 and 0.037). Kaplan-Meier curves of Gleason score were very significant compared by log-rank test (p=0.0059).MVA demonstrated association between AUASS Change and T-stage (p= 0.003) while higher pre-treatment IIEF-5 scores were more likely to result in non-failure (p=0.038). Smoking, Alcohol, FHx Prostate Cancer, Gleason score, and PVD were associated with ≥5 separate measures of HRQOL.

Conclusion: This study demonstrated 6wPSA and Alcohol were predictive of BCF while bFFS was most strongly associated with Gleason score. T-stage was associated with AUASS Change and higher pre-treatment IIEF-5 scores were less likely to experience BCF. HRQOL was broadly impacted by Smoking, Alcohol, FHx Prostate Cancer, Gleason score, and PVD.

TUMOR SUPPRESSIVE ROLE OF RIBOSOMAL PROTEIN L22 THROUGH P53 ACTIVATION

Cao B*, Zhou Z*, Liao P*, Liao JM*, Chao T*, Zeng S* and Lu H*

Department of Biochemistry & Molecular Biology and Tulane Cancer Center, Tulane University School of Medicine, New Orleans, LA, USA.

Ribosomal stress (RS) mediated by ribosomal proteins (RPs) in response to various cellular and environmental carcinogens or chemicals has been well appreciated to activate the tumor suppressor p53 by inhibiting MDM2 E3 ubiquitin ligase activity toward p53, and therefore plays a critical role in p53 associated regulation of cell cycle arrest, apoptosis and tumor suppression. Recently, we identified ribosomal protein L22 (RPL22) as another p53 activator. Different from other RPs involved in p53 activation, RPL22 is highly mutated (mostly deletion mutation) in various types of human cancer. In the present study, we demonstrated that ectopic expression of RPL22 suppresses the colony formation of cancer cells in a p53-dependent manner. Markedly, knockdown of RPL22 compromised p53 activation by ribosomal stress, resulting in rescue of Actinomycin D induced G1/G0 cell cycle arrest. Interestingly, in the human samples with RPL22 deletion, TP53 tends to remain wild-type. Mechanistically, RPL22 binds to MDM2 acidic domain and inhibits MDM2-mediated p53 ubiquitination and degradation, accompanied by extended half-life of p53. Ribosome-profiling analysis revealed that induction of ribosomal stress by Actinomycin D treatment leads to increased portion of RPL22 in ribosome-free form. In addition, RPL22 formed a complex with MDM2/RPL5/RPL11 and synergized with RPL11 to activate p53. Furthermore, the N terminus of RPL22 plays a critical role in inhibiting MDM2-mediated p53 downregulation. Our study may present the first to characterize the clinical relevance of RPL22 to tumorigenesis, highly likely through regulation of the MDM2/p53 pathway, and therefore provide a novel insight into understanding the significance of high mutation rate of RPL22 in human cancers.

This work was supported in part by NIH-NCI grants R01 CA095441, R01CA172468, R01CA127724, R21 CA201889-01A1, and R21 CA190775 to Hua Lu.

A BLUEPRINT OF ANDROGEN RECEPTOR SPLICE VARIANT TRANSACTIVATION

Cao S*, Xu D**, Qi Y*, Zhan Y*, Sartor O***, and Dong Y*.

*Department of Structural and Cellular Biology, Tulane University School of Medicine, Tulane Cancer Center, New Orleans, LA. **College of Life Sciences, Jilin University, Changchun, China. ***Department of Urology, Tulane University School of Medicine, Tulane Cancer Center, New Orleans, LA

Constitutively active androgen receptor splice variants (AR-Vs) have been implicated as one driver of castration-resistant progression of prostate cancer. AR-Vs can directly regulate the expression of both canonical AR targets and a unique set of cancer-related targets in the absence of androgen. Our previous studies showed that dimerization is required for AR-Vs to perform their *trans*-activating function. They can form homodimers to regulate their specific targets. They can also form heterodimers with the full-length AR (AR-FL) to induce AR-FL nuclear localization and transactivation in the absence of androgen. However, the critical steps leading to AR-V transactivation remain largely unknown. AR-V7 and AR^{v567es} are two major AR-Vs expressed in human prostate cancer specimens. We found that disruption of AR-V7 and AR^{v567es} homodimerization did not affect their nuclear localization, indicating that they can enter the nucleus as monomers. On the other hand, disrupting the heterodimerization between AR-V7 or AR^{v567es} and AR-FL abolished AR-V7 and AR^{v567es}-induced AR-FL nuclear localization. Ligand-binding assay showed that AR-V7 did not change the androgen-binding capability of AR-FL, indicating that AR-V7-mediated castration resistance is not through attenuating AR-FL ligand binding. AR-V7 chromatin immunoprecipitation assay further showed that mutating the dimerization interface of AR-V7 did not decrease the ability of AR-V7 to bind to the promoter of its target genes, UBE2C and CCNA2, indicating that dimerization is not required for AR-Vs to bind to DNA. Moreover, mutating the DNA-binding interface of AR-V7 had no effect on AR-V7 homodimerization and AR-FL/AR-V7 dimerization, suggesting that DNA binding may not be necessary for AR-V/AR-V or AR-FL/AR-V dimerization. Nonetheless, both the dimerization and the DNA-binding mutants of AR-V7 lost *trans*-activating activity. Taken together, our data suggest that AR-V DNA binding and dimerization are two independent but indispensable steps for AR-V transactivation. AR-V can enter the nucleus as a monomer, and then either forms a dimer before binding to DNA or binds to DNA as a monomer and then forms a dimer to trans-activate gene transcription. Our study may provide insights into developing more precisely targeted strategies to overcome AR-V-driven castration resistance.

Mesenchymal stromal cells (MSCs) are recruited by HIV-1 infected cells and facilitate provirus reactivation: Role of exosomes and PI3K/AKT signaling pathway

Chandra PK[1*], Gerlach SL[1], Khurana N[2], Wu C[3], Abdel-Mageed AB[2], Gimble JM[3,4,6], Braun SE[1,3,5], and Mondal D[1,3].

Departments of [1]Pharmacology, [2]Urology, [3]Center for Stem Cell Research and Regenerative Medicine, [4]Medicine, Tulane University School of Medicine, 1430 Tulane Avenue, New Orleans, LA. [5]Tulane National Primate Research Center, Covington, LA. [6]LaCell, LLC., New Orleans Bio-innovation Center, New Orleans, LA, USA. * Presenter

Background: Despite the availability of potent antiretrovirals (ARVs) against HIV-1, persistence of viral reservoirs remains a formidable challenge. Therefore, reservoir eradication would be critical towards a long-term cure. Factors that facilitate HIV-1 reactivation from latent reservoirs are not well understood. Mesenchymal stromal cells (MSCs) are multipotent and self-renewable cells that resides in almost all postnatal tissues. MSCs regulate the proliferation, activation, and effector function of T-lymphocytes, dendritic cells and macrophages via cell-to-cell contact or production of soluble factors. However, although MSCs are known to migrate towards sites of inflammation and release factors that activate second messenger signaling in neighboring cells, their effect on HIV-1 infected reservoir cells have not been addressed. MSCs may be attracted to sequestered HIV-1 reservoirs that release chemokines and inflammatory cytokines and may enable viral recrudescence.

Aim: To delineate the mechanism/s via which MSCs are recruited by latently infected cells and the signaling pathways activated by reservoir-recruited MSCs that enable viral reactivation in T-lymphocytes and monocytes, *in vitro*.

Methods: Well-established latently-infected monocyte lines (U1) and T-cell lines (ACH2 and J Lat-9.2) and primary human MSCs from both adipose-tissue and bone-marrow (AT-MSC and BM-MSC) were used for these studies. Conditioned medium (CM) from HIV-infected cells were tested in MSC migration studies and CM from MSCs from different donors were tested in HIV-1 reactivation experiments. In addition, CM was subjected to ultracentrifugation to isolate exosomes, which were then used in both migration and viral reactivation studies. Cell motility and migration were analyzed by both scratch-wound assays and trans-well migration assays. HIV-1 replication was assessed by p24 levels in culture supernatants by ELISA. U937 cells (promonocytes) stably transduced with a lentivirus expressing GFP, transcriptionally regulated by the HIV-LTR (U937-VRX494) was utilized in flow cytometry analysis of HIV-LTR function. To delineate the mechanism(s) of HIV-1 reactivation, experiments were carried out in the presence or absence of different signal transduction inhibitors. Western blotting was performed to study the different signaling pathways.

Result: Factors secreted by latently infected cells increased both motility and migration of MSCs. Increased migratory ability of MSCs was shown to be primarily due to exosomes isolated from HIV-infected cells. Virus reactivation from latently-infected cells was clearly evident following both direct co-culture with MSCs and exposure to MSC-CM, as evident by increased HIV p24 production. Studies using U937-VRX494 cells showed increased GFP expression following incubation with MSC-CM, which indicated provirus reactivation via the HIV-LTR. Heat-inactivation of MSC-CM decreased its capacity to activate HIV-1 and implicated a direct role for soluble factors secreted by MSCs. Studies using inhibitors of PI3K/AKT (LY294002), ROS (N-acetyl-L-cysteine), NFκB (Bardoxolone Methyl and Bortezomib), proteasome (MG132) and autophagy (chloroquine) clearly depicted that both ROS and PI3K/AKT pathways are responsible for HIV-1 reactivation. Western blot analysis confirmed the activation of PI3K(p110β) and pAKT(S473) in U1 cells by MSC-CM.

Conclusion: Results showed that HIV-infected cells secrete exosomes to increase the migratory phenotype of MSCs. These reservoir-recruited MSCs then secrete factors which activate latently infected cells by inducing oxidative stress and PI3K/AKT signaling. This type of host-virus interaction particularly in tissue reservoir has implications for anti-HIV therapeutics that target cellular signaling machinery.

Acknowledgement: Studies were supported by NIH grants to DM (AI116348) and SEB (AL110158).

Chaperone-mediated autophagy compensates for impaired macroautophagy in the cirrhotic liver to promote hepatocellular carcinoma

Srinivas Chava[1], Christine Lee[1], Yucel Aydin [2], Partha K Chandra[1], Asha Dash[1], Milad Chedid[1], Swan N Thung [3], Krzysztof Moroz[1], Nabeen C Nayak [4], Tong Wu[1], and Srikanta Dash[1]

1-Department of Pathology and Laboratory Medicine, 2-Department of Medicine, Division of Gastroenterology and Hepatology,Tulane University Health Sciences Center, New Orleans, Louisiana, USA. 3-The Lillian and Henry M. Stratton-Hans Popper Department of Pathology, Icahn School of Medicine at Mount Sinai, New York, NY 10029, 4-Senior Consultant and advisor, Sir Ganga Ram Hospital, Department of Pathology, New Delhi, India, 110060

Hepatocellular carcinoma (HCC) is the most common primary liver cancer that develops in the background of liver cirrhosis and the mechanism is unclear. Autophagy is a cellular lysosomal degradation process that has been implicated in the pathogenesis of chronic liver disease, liver fibrosis and HCC. We have reported previously that most of the HCC express p62, compared to the surrounding non-tumorous cirrhotic liver suggesting impaired macroautophagy in HCC. Macroautophagy and chaperone-mediated autophagy (CMA) are two major lysosomal degradation processes and they often compensate for each other to improve cell survival. We performed this investigation to verify whether a compensatory mechanism between two forms of autophagy is involved in the survival of HCC in the cirrhotic liver. The expressions of macroautophagy flux (p62, glypican-3) and CMA flux (Hsc70, LAMP2A) were examined by immunohistochemical staining of paraffin embedded tissues sections of 46 cirrhotic livers with HCCs related to viral and non-viral etiologies. Glypican-3 and p62 protein expression was not detected in any of the normal livers. Of the 46 cirrhotic livers with HCC, 39 (84%) showed increased expression of p62 and 38 (82%) showed increased glypican-3 expression as compared to negative expression in 100% of adjacent non-tumorous hepatocytes suggesting impaired macroautophagy flux in HCC. The impaired macroautophagy was present among HCC of viral and non-viral etiologies. More than 95% of HCC showed increased expression of LAMP2A as compared to the surrounding non-tumorous cirrhotic liver, suggesting that CMA flux is induced in HCC. High level expression of glucose-regulated protein 78 (GRP78, BiP) and heat shock cognate protein (Hsc70) were detected in 100% of the HCC and adjacent non-tumorous cirrhotic livers, which suggests that unresolved ER-stress is associated with HCC risk in liver cirrhosis. Interestingly, inhibition of CMA by hydroxychloroquine (HCQ) induced expression of p53 tumor suppressor, and cellular apoptosis plus inhibited HCC growth, whereas autophagy induction by mTOR inhibitor (Torin1) promoted HCC growth. Conclusions: Results of this study indicate that the

activation of CMA compensate with the impaired macroautophagy to promote HCC survival in the cirrhotic liver.

Biochemical Mechanism of TU-1, a New Antibiotic Drug

Chen Judy*

*Cellular and Molecular Biology Department, Tulane University, New Orleans, Louisiana

The advent of modern medicine in the 19th and 20th centuries drastically improved the knowledge, detection, and treatment of infectious diseases caused by bacteria. Unfortunately, the wide spread overuse and misuse of antibiotics has selected for a growing number of bacterial strains that have developed resistance to a wide range of therapeutic drugs. My research project seeks to investigate TU-1, a member of a new class of antibacterial drugs under development in the Mulllin lab. So far I have determined the minimum inhibitory concentration (MIC) of TU-1 for a variety of gram positive and gram negative bacterial pathogens, and have investigated the kinetics of growth inhibition of cultures of *Staphylococcus aureus* strain MLS1 at 1X, 2X, 4X, and 10X. From the killing kinetic experiment, I have found that strain TU-1 is bactericidal because at each of the 4 concentrations tested, viability of the *Staphylococcus aureus* cells dropped by more than 1000-fold. Using the same approach, I found that the viability of stationary phase cultures of strain MLS1 was unaffected by TU-1. The results from these initial tests suggest that TU-1 is a potent antibacterial agent that might hold promise for development into a therapeutic antibacterial agent. I am presently identifying the target of action of TU-1 in S. aureus.

The work was supported by the Georges Lurcy Grant program as well as the CELT Fund for Faculty/Student Scholarly and Artistic Engagement..

HEPATOCYTE SMOOTHENED SIGNALING PREVENTS FAS-INDUCED LIVER INJURY

Chen WN, Wang Y, Han C, Zhang JQ, Song K, Kwon H, Yao L and Wu T

Department of Pathology and Laboratory Medicine, Tulane University School of Medicine, 1430 Tulane Avenue SL-79, New Orleans, Louisiana 70112

While hedgehog (Hh) signaling pathway is inactive in adult healthy liver, it becomes activated during acute and chronic liver injury and thus modulates the reparative process and disease progression. The current study provides novel evidence for an active role of hepatocyte Hh signaling in protection against Fas-induced apoptosis and liver injury. We developed a novel mouse model with liver-specific knockout of Smo (Smo LKO) and the animals were subjected to Fas-induced liver injury *in vivo*. After treatment with the anti-Fas antibody Jo2, the Smo LKO mice showed higher mortality, higher serum transaminases levels, more apoptotic hepatocytes and more caspases/PARP cleavage compared to the matched wild type (WT) mice. Activation of Hh signaling in hepatocytes in the setting of Fas-induced injury was supported by the observation that Jo2 treatment enhanced hepatic expression of Ptch1, Smo and its downstream target Gli1 in WT mice, but not in Smo LKO mice. While the primary hepatocytes from WT mice showed increased Hh signaling activation in response to Jo2 treatment *in vitro*, the Smo KO hepatocytes were devoid of Hh activation and more sensitive to Jo2-induced apoptosis. The protein levels of NK-κB, p-NK-κB(Ser536), EGFR and p-Akt(Ser473) in Smo KO livers/hepatocytes were lower than in WT livers/hepatocytes; accordingly, hydrodynamic gene delivery of active NK-κB prevented Jo2-induced liver injury in Smo LKO mice. Our findings demonstrate that the Hh pathway in hepatocytes plays an important role for protection against Fas-induced apoptosis and that this mechanism involves activation of NK-κB-related signaling pathway.

Multivariate analysis of genomics data to identify pleiotropic genes and pathways for type 2 diabetes, obesity and dyslipidemia

Chen Yuan-Cheng[1,2], Xu Chao[2], Zhang Ji-Gang[2], Shen Jie[1], Zeng Chun-Ping[1], Peng Cheng[1], Wang Xia-Fang[1], Zhou Rou[1], Lin Xu[1], Guo Yang-Fang[1,3], Shen Hui [4], Deng Hong-Wen *[1,2,4]

[1]Department of Endocrinology and Metabolism, The Third Affiliated Hospital of Southern Medical University, Guangzhou 510630, PR China

[2] Department of Biostatistics and Data science, Tulane University School of Public Health and Tropical Medicine, New Orleans, LA 70112, USA

[3]Institute of Bioinformatics, School of Basic Medical Science, Southern Medical University, Guangzhou 510515, PR China

[4]Center for Bioinformatics and Genomics, Tulane University School of Public Health and Tropical Medicine, New Orleans, LA 70112, USA

* Corresponding author:

Hong-Wen Deng, Ph. D.

Department of Biostatistics and Data science, Tulane University School of Public Health and Tropical Medicine, New Orleans, LA 70112, USA

Tel: 504-988-1310

E-mail: hdeng2@tulane.edu

Abstract

Type 2 diabetes, obesity and dyslipidemia are three serious disorders to date. Previous studies showed there were genetic correlations among these three disorders, and indicated that many genes appeared to have pleiotropic effects on them. However, the pleiotropic genes of them are largely unknown. It is essential to systemically explore the pleiotropic genes and their effects on these three disorders. In this study, we performed a multivariate analysis of GWAS (Genome-wide associated study) data of six correlated traits related to type 2 diabetes, obesity and dyslipidemia by using Meta-CCA (meta-analysis using canonical correlation analysis), which is a novel method to identify pleiotropic genes using GWAS summary statistics from multiple correlated traits. 2720 gene were identified as significant genes after multiple testing (adjusted p-value <0.05). Further, to refine the identified genes, we tested their relations with the six traits respectively using VEGAS-2 (Versatile Gene-based Association Study –2), which is a gene-based algorithm to calculate the P-value of each gene using GWAS summary statistics. Only the genes significantly associated (adjusted p-value<0.05) with more than one trait were kept. Finally, 16 genes were identified as the pleiotropic genes. They were enriched in 5 pathways including statin pathway and PPAR Alpha pathway, which have been successfully used as drug target in the therapy for dyslipidemia. In summary, our study identified pleiotropic genes and pathways of type 2 diabetes, obesity and dyslipidemia, which may yield the common biological etiology and pathogenesis of these three disorders and provide promising insights for the therapy of the three disorders.

ACKNOWLEDGEMENTS

This authors were partially supported by grants from the National Institutes of Health [R01AR050496, R01AR057049, R01059781, R01MH104680]. CYC was also partially supported by the Foundation from China Scholarship Council (20150322).

A MECHANISTIC SUTDY OF RETINAL PIGMENT EPITHELIAL CELL DEATH IN RESPONSE TO CIGARETTE SMOKE EXTRACT TREATMENT

Chimienti J*, Majeste A*, Anderson C*, Hanus J*, Wang S*
*Department of Cell and Molecular Biology, Tulane University, New Orleans, LA 70118

The aim of this project is to investigate the cell death pathway triggered in Retinal Pigment Epithelial (RPE) cells by cigarette smoke extract (CSE) and test the role of antioxidants in preventing CSE induced RPE cell death. TUNEL staining demonstrates an increase in DNA damage with increasing concentrations of CSE and as the time period of CSE treatment is extended from 4 to 24 hours. By LC3 staining we observed lack of autophagosomes formation in ARPE-19 cells when treated with CSE for 4 and 24 hours, indicating a lack of autophagy. RIPK3-GFP shows aggregation of RIP3 kinase in cells treated with CSE as time and concentration progresses. p-MLKL, marker for programmed necrosis, staining demonstrates an increase of p-MLKL in cells with increasing concentration of CSE. Caspase-1 and caspases-3 staining do not show positive staining in CSE treated RPE cells, indicating no activation of pyroptosis or apoptosis. Pre-treatment of ARPE-19 cells with apoptosis inhibitor, z-VAD, does not show the same protective effects against CSE induced RPE cell death as pre-treatment with necrosis inhibitor, necrostatin-1. ARPE-19 cells pre-treated with antioxidants, Vitamin C, Vitamin E and 4-Acetoxyphenol (4-AC) show varied levels of protection against CSE induced RPE cell death. Results from p-MLKL staining, RIPK3-GFP, HMGB1-YFP and cell death inhibitor Necrostatin-1 indicate activation of the necrotic cell death pathway in CSE induced RPE cell death. RPE cells show protection against CSE induced cell death by antioxidant 4-AC.

Funding provided by Tulane University Summer Research program in Neuroscience.

COMPARATIVE MECHANICAL ASSESSMENT OF ARTERIAL STIFFNESS IN HIGH FAT MICE

Clark GC*, Abshire CA**, Reverte Ribo V***, Rosales CB, Zimmerman MA**, Prieto MC***, Lindsey SH**, Miller KS*

*Biomedical Engineering, Tulane University, New Orleans, LA, **Pharmacology, Tulane University School of Medicine, New Orleans, LA , ***Physiology, Tulane University School of Medicine, New Orleans, LA

Obesity is a metabolic disorder affecting 30-60% Americans. It results in cardiovascular complications that are the leading cause of morbidity and mortality. Studies show that vascular remodeling and arterial stiffening, actively contribute to the development of cardiovascular diseases in obese patients. Changes in the arterial mechanical properties can lead to cardiovascular dysfunction. The aim of this preliminary study is to validate a high fat fed murine model by characterizing alterations in arterial mechanics. It is hypothesized that high fat fed mice will have an increase in circumferential stress and stiffness. Male mice (C57Bl/6) at 4 weeks were separated in two groups: a normal diet (ND, n=5) (4.07 kcal/g, 24.7% protein, 13.3% fat, 62.1% carbohydrates) and high fat diet (HFD, n=6) (4.07 kcal/g, 18.1% protein, 46.1% fat, 35.8% carbohydrates). They were fed for 36 weeks. Pressure myography was used to perform a biaxial mechanical test on the common carotid artery (CCA). The four-fiber family model constitutive relations were used to calculate the CCA material properties. An unpaired student t-test compared the two groups with $p<0.05$ considered significant. The HFD mice weighed significantly more than the ND group (49.85± 3.049 and 30.0± 2.91 g). The systolic outer diameter (659 ± 23 and 655 ± 28 μm) and thickness (47 ± 2 and 50 ± 3 μm) , respectively, had no significant difference. The circumferential stress and strain for the ND were 81 ± 9 kPa and 1.76 ± 0.09 mm/mm. As for the HFD, the results were 107 ± 10 kPa and 1.77 ± 0.07 mm/mm, respectively. The significant difference in circumferential stress is possibly due to the increase in the HFD mice blood pressure. Between the ND and HFD, there was no significant difference in the collagen circumferential stress, 0.52 ± 0.71 and 0.40 ± 0.87 kPa, respectively. The CCA from the HFD mice is circumferentially stiffer that the ND (0.23 ± 0.08 and 0.16 ± 0.09 MPa), but it is statically proven to be insignificant. Although the HFD mice were theoretically experiencing an advanced stage metabolic disease, this study suggests that the CCA material properties are similar. A study performed by Billaud et al on a 6-week HFD murine model presented no change in compliance. However, there was a presence of collagen deposition in the high fat mice. As for a smaller artery, a decrease in compliance was evident at 6 weeks. Santelices et al showed that the aorta, a larger artery, experienced stiffening at 34 weeks of age. In conclusion, the HFD at 40 weeks is negligible because it did not promote a significant change in the CCA stiffness. To validate this, age can be added as another factor, and pulse wave velocity could be implemented throughout the diet. Also, histology can be utilized to confirm microstructural changes. Understanding the mechanisms underlying cardiovascular complications, not from just a chemical, but also a mechanical perspective is imperative to develop new detection, prevention, and treatment strategies.

Do Vented Suture Anchors Make a Difference in Rotator Cuff Healing?

Tyler R Clark*, Evan M Guerrero, Amos Song, Michael J O'Brien and Felix H Savoie

Department of Orthopaedics, Tulane University School of Medicine, USA

Abstract

Purpose: Ultrasound is well documented as an accurate tool to assess rotator cuff (RC) thickness, a proven marker of healing. There are no studies to date that compare healing in primary RC repairs between vented and non-vented suture anchors. The hypothesis is that vents allow stem cells and growth factors to assist healing in the rotator cuff.

Methods: Patients who had undergone primary RC repair were reviewed and divided into groups by those who received vented versus non-vented suture anchors. Healing was assessed by RC thickness as viewed on ultrasound at each patient's routine six week post-operative appointment.

Results: Forty patients were in the vented group and thirty patients were in the non-vented suture anchor group. One-third of patients in the vented anchor group were female (37.5%), and half of the patients in the non-vented group were female. The average days between surgery and follow up in the vented group and non-vented group were 42.1 and 40.8 respectively. The average age of the vented group was 55.0 years vs. 62.5 in the non-vented cohort. The average thickness for the vented group was 0.59 centimeters and for the non-vented group was 0.48 centimeters (p-value 0.0074). Rotator cuff thickness was signi cantly associated with implant type, patient's age ($r = -0.42$, $p = 0.0003$), and days post-op ($r = 0.34$, $p = 0.0043$).

Conclusions: The results of this study show that vented suture anchors provide greater healing potential for patients at six weeks post-operatively. We recommend continued investigation into this topic, with follow up at six months to evaluate rotator cuff healing at its full potential.

MODERATE PATHOLOGY IN RHESUS MACAQUES IN ASSOCIATION WITH PERSISTENCE OF BORRELIA BURGDORFERI WITHSTANDING ANTIBIOTIC TREATMENT

Crossland NA* and Embers ME*

*Division of Bacteriology and Parasitology, Tulane National Primate Research Center, Tulane University Health Sciences, Covington, Louisiana

Abstract

Borrelia burgdorferi (*Bb*) is the causative agent of Lyme disease (LD). Non-human primates serve as the most appropriate experimental animal model for LD due to their close genetic homology, multisystem involvement, and demonstration of all three stages of disease progression including early localized, early disseminated, and late-stage disease. This study investigated the histopathology and antigenic localization of *Bb* within inflamed tissues of the rhesus macaque (*Macaca mulatta*). Ten 4-year-old male rhesus macaques were infected with *Bb* strain B31 by the natural tick vector (*Ixodes scapularis*). Five animals remained untreated for the duration of the study, while five were treated with 28 days of oral doxycycline, beginning 4 months post-inoculation. Mild to moderate mononuclear inflammation was observed surrounding peripheral nerves, and in joint and cardiac tissues. Inflammation of the peripheral nervous system was more severe and frequent in untreated animals (3/4 untreated vs. 2/5 doxycycline-treated), while cardiac inflammation was more frequent and severe in doxycycline-treated animals (4/5 doxycycline-treated vs. 3/5 untreated). Inflammation of the central nervous system was only observed in doxycycline-treated animals (2/5 doxycycline-treated). Tissues from three age- and sex- matched control rhesus macaques were utilized for comparison; these control animals lacked significant inflammation of the heart, nervous system, and joints. Indirect immunohistochemistry is being utilized for the identification of *Bb* in affected tissues. This is the first study to investigate pathology associated with persistence of *B. burgdorferi* in the late stage of LD following antibiotic therapy and supports the notion that chronic Lyme disease symptoms may be attributable to inflammation in and around tissues that harbor persistent, host- adapted spirochetes.

This research was supported by the National Institutes of Health under the Louisiana Center of Biomedical Research Excellence (CoBRE) in Experimental Infectious Disease Research (2P20-RR020159-08) and the Ruth L. Kirschstein National Research Service Award (5T32OD011124-12) from Tulane University of Louisiana, and the Bay Area Lyme Foundation.

HIGH GLUCOSE-INDUCED UPREGULATION OF ANGIOTENSINOGEN IN CULTURED PROXIMAL TUBULAR CELLS

Cypress MW, Sato R, and Navar, LG

Department of Physiology, Hypertension and Renal Center of Excellence, Tulane University School of Medicine, New Orleans, LA

Angiotensinogen (AGT) expression is increased in the proximal tubule during high glucose exposure, and contributes to the development of diabetic nephropathy in a process mediated by reactive oxygen species (ROS) generation. Sodium-glucose cotransporter 2 (SGLT2) is located primarily in the S1 segment of the proximal tubule and is the primary transporter responsible for glucose reabsorption in the kidney. However, the role of SGLT2-dependent glucose transport in AGT upregulation has not been delineated. To establish the enhancing effects of SGLT2 on AGT expression, an experimental model that elicits AGT augmentation under high glucose conditions in S1 proximal tubular cells (PTCs) was utilized. Immortalized mouse PTCs isolated from the S1 segment (mPTCs) were used to characterize the effects of high glucose on AGT expression, ROS generation, and glycolytic activity. mPTCs were exposed to normal glucose levels (5 mM) or high glucose levels (15 mM or 25 mM) for 6, 12, or 24 hours. AGT protein was quantified using western blot analysis, and mRNA levels were measured by qRT-PCR. Sodium pyruvate was used to determine the role of glycolysis in AGT upregulation. A ROS-fluorescent probe was used to detect ROS accumulation during treatment. mPTC were pretreated with 2.5 mM tempol, an antioxidant, to evaluate if high glucose-induced AGT expression is mediated by ROS. Glycolytic activity was determined using the Seahorse metabolic analysis system. After 24 hours exposure in 15 mM or 25 mM glucose, AGT protein levels were increased compared to control by 4.39 ±0.71 fold and 6.15 ±0.58 fold, respectively. Increased AGT mRNA levels reached 31.1 ±3.52 fold at 24 hours treatment. AGT expression was increased by high glucose in a time-dependent manner. AGT protein levels after 25 mM treatment were highest after 24 hours compared to control. In contrast, AGT expression was not increased by mannitol, indicating that increased osmolality is not responsible for AGT upregulation by high glucose. Pyruvate also enhanced AGT expression 10.74 ±1.03-fold compared to control. 30 minutes after glucose exposure, glycolytic activity increased in 15 mM or 25 mM glucose compared to control by 1.88 ±0.58 fold and 1.97 ±1.37 fold, respectively. ROS generation increased by 3.03 ±0.29-fold during high glucose treatment. However, tempol attenuated AGT augmentation by 4.38 ±0.01-fold during high glucose, demonstrating that ROS generation is required for high glucose-induced AGT upregulation. The results obtained from these experiments demonstrate that AGT expression is upregulated in PTC under hyperglycemic conditions in a process mediated by increased glycolysis and consequent ROS generation. The data demonstrate that increased glucose transport leads the upregulation of AGT in mPTCs via increased glucose metabolism and ROS dependent mechanisms. This model will help elucidate the molecular pathways underlying the enhanced AGT expression in the proximal tubule under diabetic conditions.

This work was supported by the National Institutes of Health Center of Biomedical Research Excellence (COBRE: P30GM103337), National Institute of Diabetes and Digestive and Kidney Diseases (Satou: R01DK107694; Cypress: F31DK107185), and American Heart Association Predoctoral Fellowship (Cypress: 15PRE25090156)

Sex differences in levels of myelin basic protein in the orbitofrontal cortex of adult rats results from action of ovarian hormones during puberty.

*J. S. Darling[1], A. H. Nguyen[1], S. A. Rios[1], J. M. DANIEL[1,2];
[1]Neurosci., [2]Psychology, Tulane Univ., New Orleans, LA

Previous work from our lab has revealed that adult female rats have increased levels of myelin basic protein (MBP), a marker for myelination, in the orbitofrontal cortex (OFC) as compared to adult males. However, this sex difference in MBP in the OFC was not seen in prepubertal rats. In a follow-up experiment, we examined adult circulating levels of gonadal hormones for activational influence on this sex difference in myelination and found no impact. Therefore, we hypothesized that exposure to a rise in gonadal hormone levels during puberty mediates a sex difference in MBP in the OFC of rats. To test this hypothesis we compared the impact of gonadectomy prior to and after puberty on levels of MBP in the OFC of adult male and female rats. 36 rats (18 males, 18 females) were used in this experiment. One third of rats (28d of age) underwent gonadectomy prior to puberty, one third of rats (90d of age) underwent gonadectomy in adulthood, and one third of rats received sham surgeries (at either 28d or 90d of age). At 4 months of age, animals were killed and OFC were dissected and processed for western blotting. Consistent with our previous results, intact female rats had increased levels of MBP in the OFC than did males and there was no impact of adult gonadectomy on levels of MBP. A significant decrease in MBP in the OFC was found in female rats gonadectomized prior to the onset of puberty while no such effect was seen in males. These results indicate that exposure to gonadal hormones during puberty organizes and significantly increases adult levels of MBP in the OFC in female rats as compared to males. Future work will examine the ability of gonadal hormones acting during the pubertal period to influence previously described sex differences in OFC-dependent behaviors in adult rats.
Louisiana Board of Regents: LEQSF(2013-18)-GF-17

Manumycin A suppresses exosome biogenesis and secretion in prostate cancer cells via targeted inhibition of Ras/Raf/MEK/ERK1/2 signaling and hnRNP H1 in prostate cancer cells

Amrita Datta[1], Hogyoung Kim[1*], Madu Lal[5], Adedoyin Johnson[1], Ahmed Moustafa[1], Sudha Talwar, Jennifer Clare Jones[4], Debasis Mondal[2,3], Marc Ferrer[5], Asim B. Abdel-Mageed[1, 2,3]

Departments of Urology[1] and Pharmacology[2]and Tulane Cancer Center[3], Tulane University School of Medicine, New Orleans, LA 70012, [4]Center for Cancer Research, and [5]Division of Preclinical Innovation, National Center for Advancing Translational Sciences (NCATS), National Institutes of Health, Bethesda, Maryland 20850, United States.

Emerging evidence support a pivotal role for exosomes (Exo) in cancer progression through trafficking of oncogenic factors involved in metastasis and neoplastic reprogramming of tumor-tropic stem cells. This necessitates identification and incorporation of functionally validated Exo-targeting therapeutics in the clinical management of cancer. We employed quantitative high throughput screen on two libraries to identify Exo-targeting drugs; a commercially available collection of 1280 pharmacologically active compounds and a collection of 3300 clinically approved compounds. Fluorometric and tunable resistive pulse sensing analyses identified Manumycin-A (MA), a natural microbial metabolite, as an inhibitor of Exo biogenesis and secretion by castration-resistant prostate cancer (PC) cells, but not RWPE1 cells. MA attenuates ESCRT-0 protein Hrs, ALIX and Rab27a; key regulatory factors involved in late endosome biogenesis and secretion of Exo. MA mediates its effect through inhibition of Ras signaling pathway and the oncogenic splicing factor, hnRNP H1. The shRNA silencing of hnRNPPH1 lead to attenuation of Exo release by downregulating the endogenous levels of Rab27a, Alix and Ras in C4-2B cells. Selective MEK inhibitor, but not p38 MAPK or JNK inhibitors, suppressed the expression of ALIX, Rab27a, and hnRNP H1, thus corroborating a direct role of Ras/Raf/MEK/ERK1/2 pathway in mediating MA inhibitory effects on Exo biogenesis and secretion via hnRNP H1 in PC cells. Taken together the findings suggest that MA is a potential drug candidate to suppress exosome biogenesis and secretion by CRPC cells. Further preclinical studies are required to examine MA *in vivo* therapeutic efficacy against PC in combination with conventional therapy

Daytime Blue-enriched LED Light Enhances Nighttime Circadian Melatonin Inhibition of Rodent Hepatoma Metabolism and Growth.

Dauchy RT*, Wren-Dail MA*, Hoffman AE**, Xiang S*, Pointer DE***, Yuan L*, Hill SM*, Belancio VP*, and Blask*.

Melatonin, the nighttime circadian oncostatic hormone produced by the pineal gland in mammals, regulates linoleic acid (LA)-dependent metabolism and proliferation in rodent and human tumors *in vivo.* Melatonin inhibits LA-uptake and conversion to the mitogenic agent 13-hydroxyoctadecadienoic acid (13-HODE), a lipoxygenase product that enhances epidermal growth factor and insulin-like growth factor-I-induced mitogenesis. Previously our laboratory demonstrated how transmission of light in the blue-appearing portion of the visible spectrum (465-485 nm) through standard laboratory rodent caging during light phase results in amplification of the nighttime melatonin signal in rats and leads to suppression of human prostate tumor metabolism and growth. In this study we tested whether light phase exposure of hepatoma-bearing rats to white light-emitting diode (LED) lighting, enriched in blue emissions, results in amplified nighttime melatonin levels and influences tumor metabolism and growth. Male Buffalo rats (BUF/CrCrl; 250 g; n = 12/group) bearing "tissue-isolated" Morris hepatoma 7288ctc xenografts were maintained on a common lighting regimen 12L(172.0 ± 12.3 lx; 70.5 ± 5.0 $\mu W/cm^2$ [inside cage]; lights on 0600):12D under control broad spectrum cool white fluorescent (CWF) or experimental LED lighting in an AAALAC-accredited facility. After implantation tissue-isolated hepatoma latency-to-onset of growth and growth rates were significantly delayed ($P < 0.001$) in the LED group (21 days; 0.36 ± 03 g/d) versus CWF group (11 days;0.71 ± 0.03 g/d), respectively. When tumors reached an estimated weight of 6-8g animals they were prepared for arteriovenous measurements. Results showed that arterial plasma melatonin levels (mean ± 1 SD) were low in the light phase (1200 h) in both groups (1.0 ± 0.2 pg/mL), but significantly higher ($P < 0.001$) in LED (1065.0 ± 38.0 pg/mL) compared to CWF (154.0 ± 16.5 pg/mL) at peak, mid-dark phase (2400 h). Hepatoma xenograft cAMP levels, uptake-metabolism of LA to 13-HODE, aerobic glycolysis (Warburg effect) and growth signaling activities were significantly reduced in rats maintained in LED versus CWF lighting environments ($P < 0.001$). These findings are the first to show *in vivo* that amplification of nighttime melatonin levels by exposing rats to daytime blue-enriched LED light significantly reduces rodent hepatoma metabolic and proliferative activities.

*Departments of Structural & Cellular Biology and **Epidemiology, *** Surgery, Tulane University School of Medicine, 1430 Tulane Avenue, SL-49, Tulane, LA 70112-2699, USA; Telephone: #1-504-988-0398; FAX: #1-504-988-1687.

This work was supported in part by a Tulane University School of Medicine and Louisiana Cancer Research Consortium Startup Grant (#631455 to DEB), National Institutes of Health (NIH) grant (National Cancer Institute #1R56CA193518-01 to SMH and DEB) the American Association for Laboratory Animal Science Grants for Laboratory Animal Science (GLAS) Award (to RTD & DEB).

OPTIMIZING STATISTICAL POWER WHEN CORRECTING FOR MULTIPLE TESTING IN GENETIC ASSOCIATION STUDIES INVOLVING HUMAN LEUKOCYTE ANTIGEN (HLA) POLYMORPHISMS

Davis, R; Gragert, L

Department of Pathology and Laboratory Medicine, Tulane University School of Medicine, New Orleans, LA

Power analysis aims to minimize the type II error rate of a study design, and thus, sufficiently powered studies are well able to detect the effect of interest if an effect is present (i.e. power is a measure of sensitivity). Genome-wide association studies (GWAS) test for disease associations across many genetic loci. In GWAS there is typically only one minor allele, or single nucleotide polymorphism (SNP), per locus tested. Association statistics for significance and statistical power must account for these multiple tests. However, in association studies of the human leukocyte antigen (HLA) immune system genes, which reside in the major histocompatibility complex (MHC) on chromosome 6, each locus contains thousands of alleles in the general population. When assessing highly polymorphic genes such as HLA, the statistical problem of multiple testing must be addressed also in the dimension of the number of alleles tested per locus. The goal of this project was to develop an R package to apply power analysis in the context of multiple testing to optimize selection of HLA alleles where there would be adequate statistical power to detect effects. Testing too many rare alleles would increase the amount of correction for multiple tests with little hope of detecting additional associations. Meanwhile, testing too few alleles could miss relevant associations that the study is powered to detect. We are conducting secondary case-control association analyses for several different hematologic diseases utilizing a large dataset of bone marrow registry HLA typing. As a proof of principle, we applied our statistical power optimization to the case of Severe Aplastic Anemia (SAA), a rare and serious immune-mediated disease of the hematopoietic stem cells of the bone marrow that results in pancytopenia. Previous HLA association studies have consistently identified HLA-DRB1*15:01 as a positive risk allele. Our preliminary data indicates many other HLA allele associations are present. Power is dependent upon both the number of SAA cases and the HLA allele frequencies at six loci (A, B, C, DQB1, DRB1, and DRB3/4/5) in four populations (African Americans, Caucasians, Hispanics, and Asian-Pacific Islanders). HLA allele frequencies differ dramatically across different human populations; this affects power and thus the number of alleles to test in each population. In our SAA dataset, the Caucasian, African American, Hispanic, and Asian-Pacific Islander samples had 3429, 891, 708, and 376 cases, respectively, with 50,000 controls per population. The power analysis calculated unadjusted and Bonferroni-adjusted power per allele, per locus, and per population. With a set power threshold of 0.5 and an effect size of relative risk of 1.5, 46 alleles across all six loci and all four populations were calculated to have sufficient power for inclusion in the SAA association study considering a Bonferroni adjustment. As an example single-locus result, at the DQB1 locus in African Americans, 5 alleles met our threshold, and the remaining XXX rare DQB1 alleles with low power remaining untested. Overall compared to a previous approach which tested every HLA allele found in more than 5 disease cases, far fewer HLA alleles were tested, and adjusted P-values remained higher with no loss of significant allelic associations. We also developed a novel visualization that depicts power versus allele frequency curves per locus and population, showing where the threshold of selection of alleles occurs. By selecting only the more frequent alleles with sufficient power to detect an association for testing, discovery of statistically significant HLA associations is optimized. While this optimization method was developed for the HLA system, it is generalizable to other polymorphic genetic systems.

NATURALLY-DERIVED BACTERIAL NANO-PARTICLES DRIVE POTENT ADAPTIVE IMMUNE RESPONSES THROUGH SUPERIOR ENHANCEMENT OF INNATE IMMUNITY COMPARED TO OTHER VACCINE PLATFORMS.

Davitt CJH, Kurtz J, Kikendall N, Lee F, McLachlan J, Morici LA

Department of Microbiology and Immunology, Tulane University School of Medicine, New Orleans, Louisiana, USA

Vaccines are the most effective public heath measure discovered to date and have been correlated with an unprecedented increase in human lifespans globally. The 1950s to 80s witnessed an explosion of new vaccines, including non-living vaccines largely regarded as a safer platform for use in humans. These vaccines primarily induced antibody-mediated protection against conserved antigens and have been very effective against extracellular pathogens. Unfortunately, these strategies have not been able to deliver protection against pathogens with complicated intracellular lifecycles which often require cell-mediated immunity (CMI). Outer-membrane vesicles (OMVs) derived from Gram-negative bacteria are also an effective vaccine platform with precedence for safe use in humans. Unlike most subunit antigens and synthetic nano-particles, OMVs contain endogenous immunostimulatory ligands and deliver antigens in their native orientation. We hypothesized that OMVs derived from *Salmonella typhimurium* and *Burkholderia pseudomallei*, two complex intracellular pathogens, could drive potent CMI through superior engagement of innate immune cells compared to the widely utilized live attenuated (LA) and heat killed (HK) bacteria vaccine platforms. We intraperitoneally administered mice either LA or HK bacteria or OMVs for 6 hours and used flow cytometry and multiplex assays to measure innate immune activation dendritic cells (DCs), which are the most efficient drivers of CMI. DCs exhibited increased maturation, increased antigen-presentation through both major histocompatibility molecule class (MHCc) I and MHCcII pathways, and enhanced expression of co-stimulatory molecules following administration of OMVs versus LA or HK bacteria. In addition, OMVs stimulated production of significantly higher levels of key T cell polarizing cytokines compared to either HK or LA bacteria following administration *in vivo*. Following sub cutaneous vaccination of mice, OMVs induced a significant increase in the percentage of interferon gamma producing $CD4^+$ and $CD8^+$ antigen-specific T cells compared to immunization with HK bacteria. Lastly, vaccination of mice with OMVs induced comparable protection against oral *Salmonella* and aerosol *Burkholderia* challenge in mice compared to LA and superior protection compared to HK bacteria. Collectively these results establish OMVs as potent stimuli of innate immunity that promote enhanced CMI against bacterial pathogens and support the utility of the OMVs as a non-living vaccine platform against intracellular bacterial infections.

LOWER RATE OF SIV-ENCEPHALITIS (SIVE) IN PEDIATRIC COMPARED TO ADULT RHESUS MACAQUES WITH SIV INFECTION

Delery EC*, Filipowicz F**, Allers C*, Blair R***, Walker E*, Didier ES****, Kuroda MJ*, Kim W-K**

*Department of Immunology, Tulane National Primate Research Center, Covington, LA
**Department of Microbiology & Molecular Cell Biology, Eastern Virginia Medical School, Norfolk, VA ***Depart of Pathology, Tulane National Primate Research Center, Covington, LA
****Department of Microbiology, Tulane National Primate Research Center, Covington, LA

Relatively little is understood about HIV-associated neurocognitive disorders (HAND) but understanding mechanisms and development of encephalitis is critical to maintaining quality of life in HIV-positive patients. We previously reported that increased turnover of monocytes was indicative of tissue macrophage infection in SIV-infected adult macaques, which was also observed in the brain along with a higher SIV load that correlated with an increased rate of SIV-Encephalitis (SIVE). We also observed that the rapid AIDS disease progression in pediatric macaques correlated with earlier and sustained higher monocyte turnover following SIV infection. Therefore, we hypothesized that in pediatric macaques, brain macrophages may also be infected early following infection resulting in more severe or accelerated development of SIVE compared to adults. H&E staining was used to identify areas of encephalitis in paraffin-embedded, formalin-fixed cortical brain tissues from three different groups of rhesus macaques; SIV-infected infants (OI; n=2), infected adults without encephalitis (IAnoE; n=5), and infected adults with encephalitis (IAE; n=5). SIV-infected infants with encephalitis were not included in this study because no cases have been found to date. Tissue viral load and plasma viral load were measured by PCR. Monocyte turnover was calculated after BrdU injection and at necropsy using flow cytometric analysis. No statistical difference in plasma viral load was observed between SIV-infected infants and SIV-infected adults. SIV-infected infants showed equal turnover of monocytes compared to SIVE adults. However, none of the SIV-infected infants exhibited signs of SIVE and expressed a much lower brain DNA & RNA load compared to SIV-infected adults with SIVE, especially in the frontal cortex. These studies demonstrated that in SIV-infected adults, monocyte turnover correlated with increased tissue macrophage infection, including brain macrophages that reflected the severity of SIVE. However, a more rapid and sustained increased turnover of monocytes and increased tissue macrophage infection following SIV infection did not correlate with increased brain tissue infection. This study suggests that in pediatric cases, despite a more rapid rate of AIDS disease progression and higher level of tissue macrophage infection, the level of brain tissue infection remains limited. Future studies are warranted to elucidate why adults appear more likely to progress to SIVE than do pediatric macaques, and whether there exist protective mechanisms in the pediatric brain.

This study was supported by grants AI097059, HL125054, AI110163, AI116198, DA041017, MH108458 and MH107333 from the National Institutes of Health and P51OD011104 to the Tulane National Primate Research Center.

THE ASSOCIATION BETWEEN CHILDHOOD OBESITY AND ADULTHOOD CAROTID INTIMA-MEDIA THICKNESS IS MODIFIED BY SERUM ADIPONECTIN LEVELS

Du Y*, Zhang T**, Sun D*, Bazzano L*, Qi L*, He J*, Krousel-Wood M*, Whelton P*, Chen W*, Li S*

* Department of Epidemiology, Tulane University School of Public Health and Tropical Medicine, New Orleans, LA, USA

**Department of Biostatistics, School of Public Health, Shandong University, Jinan, China

Childhood obesity, measured by body mass index (BMI), is predictive of adult subclinical atherosclerosis as measured by carotid intima-media thickness (CIMT). However, accumulating evidence indicates that the consequences of childhood obesity are heterogeneous. We hypothesized that the association between childhood BMI and adult CIMT is modified by levels of adiponectin, an adipocytokine potentially connecting body fat and cardiovascular risk, measured in adults. The sample included 1,056 adults (71% white and 29% black, 57% female) aged 23.8-43.5 years who were previously examined as children in the Bogalusa Heart Study cohort, with an average follow-up period of 26.5 years. Childhood BMI, low-density lipoprotein cholesterol (LDL-C), high-density lipoprotein cholesterol (HDL-C), triglycerides (TG), and systolic blood pressure(SBP) at the first examination were standardized to age-, race-, and sex-specific z-scores. General linear models were used for data analyses. Results showed that significant childhood risk factors for adult CIMT included BMI ($P=0.047$), LDL-C ($P<0.001$), and SBP ($P=0.003$) after adjustment for age, race, sex, cigarette smoking, adiponectin levels (which was inversely associated with CIMT, $P=0.002$). Further, adult adiponectin levels significantly modified the association between childhood BMI and adult CIMT (P for interaction=0.045) such that significant association ($P=0.003$) between childhood BMI and adult CIMT was only observed in those with adiponectin levels above the median. These results suggest that serum adiponectin levels modify the association between childhood obesity and adult atherosclerosis, which has implications for risk stratification and targeted intervention for obese children with low levels of adiponectin.

ANALYSIS OF ERECTILE RESPONSES TO BRADYKININ IN THE ANESTHETIZED RAT

Justin A. Edward[1], Edward A. Pankey[1], Ryan C. Jupiter[1], George F. Lasker[1], Daniel Yoo[1], Vishwaradh G. Reddy[1], Taylor C. Peak[1], Insun Chong[1], Mark R. Jones[1], Samuel V. Feintech[1], Sarah H. Lindsey[1], Philip J. Kadowitz[1]

[1]Department of Pharmacology Tulane University School of Medicine, 1430 Tulane Avenue, New Orleans, Louisiana 70112-2699 USA

The kallikrein-kinin system is expressed in the corpus cavernosa, and bradykinin (BK) relaxes isolated corpora cavernosal strips. However, erectile responses to BK in the rat have not been investigated *in vivo*. In the present study, responses to intracorporal (ic) injections of BK were investigated in the anesthetized rat. BK, in doses of 1–100μg/kg ic, produced dose-related increases in intracavernosal pressure (ICP) and dose related decreases in mean arterial pressure (MAP). When decreases in MAP were prevented by intravenous injections of angiotensin II (Ang II), increases in ICP, in response to BK, were enhanced. Increases in ICP, ICP/MAP ratio, and area under the curve and decreases in MAP in response to BK were inhibited by the kinin B2 receptor antagonist HOE-140 and enhanced by the angiotensin-converting enzyme (ACE) inhibitor captopril and by Ang-(1–7). Increases in ICP, in response to BK, were not attenuated by the nitric oxide (NO) synthase inhibitor (N^{ω}-nitro-L-arginine methyl ester) or the soluble guanylate cyclase inhibitor (1H-[1,2,4]oxadiazolo[4,3-a]quinoxalin-1-one) but were attenuated by the cyclooxygenase inhibitor, sodium meclofenamate. Decreases in MAP were not attenuated by either inhibitor. These data suggest that erectile responses are mediated by kinin B2 receptors and modulated by decreases in MAP. These data indicate that ACE is important in the inactivation of BK and that erectile and hypotensive responses are independent of NO in the penis or the systemic vascular bed. Erectile responses to cavernosal nerve stimulation are not altered by BK or HOE-140, suggesting that BK and B2 receptors do not modulate nerve-mediated erectile responses under physiologic conditions. These data suggest that erectile responses to BK are mediated, in part, by the release of cyclooxygenase products.

COMPARISON OF PROSTATE BIOPSY FEATURES USING MONOCHROME VERSUS DUAL-COLOR FLUORESCENCE HISTOLOGY

Elfer K*, Sholl AB, Wang M*, Tulaman D*, Brown JQ*

*Department of Biomedical Engineering, Tulane University, 500 Lindy Boggs Center, New Orleans, LA 70118, USA
**Department of Pathology and Laboratory Medicine, Tulane University School of Medicine, New Orleans, LA 70112 USA

In biospecimen banking, there is currently a disconnect between creating an accurate estimate of specimen content and conserving biopsy tissue for later use. The traditional method for this evaluation is frozen section analysis (FSA), which allows for intraoperative analysis of biopsies and tumor margins. However, FSA is highly destructive in terms of preserving the tissue for multiple analyses. One alternative to FSA is the application of fluorescent stains paired with optical sectioning fluorescence microscopy. Fluorescence histology has been shown to be diagnostically accurate as well as capable of preserving the full specimen for later use. Currently, fluorescence microscopy takes two forms: a monochrome greyscale image and those images that have been pseudocolored. We demonstrate the use of the monochrome stain Acridine Orange (AO) and the pseudocolored stains, DRAQ5 and Eosin Y (D&E), using structured illumination microscopy (SIM) to achieve fluorescence histology on prostate biopsies. Fifty-two freshly excised prostate biopsies were exposed to either AO (22) or D&E (30) then processed with gold-standard hematoxylin and eosin (H&E) histology. Pathologist review found that D&E increased accuracy of diagnosis compared to AO. The pathologist also identified variations in features across all three methods allowing for direct comparisons in feature definition. One immediate difference between the two methods is the fact that in the monochrome grayscale image resulting from the AO stain, the primary source of contrast is image brightness against a dark background. Conversely, the dual-stain pseudocolored image inverts the intensity mapping so that images are colored against a bright background and the primary source of contrast is image color. For fluorescence histology to become an alternative to or paired method with FSA for rapid screening of biopsy quality and diagnosis at the point of care, both the instrumentation and the fluorescent agents must be well characterized and standardized in the clinic. With increase interest in tissue preservation and alternatives to FSA for rapid diagnostics, fluorescence histology must be carefully examined before adoption in the clinic. As with the myriad of analyses available to pathologists after initial diagnosis, the tools used in the early screening process must fit the needs of the clinician.

This work was supported by the National Science Foundation's Graduate Research Fellowship, NIH NCI R21CA159936and NIH NCI R33CA196457.

TRPV1 EXPRESSING NEURONS IN THE HYPOTHALAMUS

[1]Enix CL, [2]Butcher SM, [1]Molinas A, [1]Miyada K, [1]Anwar IJ, [1,2]Zsombok A

[1]Department of Physiology, School of Medicine, and [2]Neuroscience Program, Brain Institute, Tulane University, New Orleans LA, USA

Transient receptor potential vanilloid type 1 (TRPV1)-dependent mechanisms participate in the regulation of whole body glucose homeostasis through both peripheral and central mechanisms. Our previous studies have demonstrated that TRPV1 increases excitatory neurotransmitter release, thus controlling pre-autonomic neurons in the paraventricular nucleus (PVN) of the hypothalamus. A mouse model for identification of TRPV1-expressing neurons was established, as prior to this study the location, projection and target sites for these neurons remained largely unknown. Through crossing $TRPV1^{cre}$ mice with tdTomato reporter mice, a unique mouse model was generated in order to visualize TRPV1-expressing neurons within the entire hypothalamus. After perfusion the brains were sectioned and mounted to identify TRPV1-expressing cells based on their red fluorescence. An abundance of TRPV1-expressing neurons were observed in the PVN, dorsomedial hypothalamic nucleus, and lateral hypothalamus. Further studies to characterize the cellular and phenotypic properties of TRPV1-expressing neurons were conducted using whole-cell patch-clamp electrophysiology and immunostaining for neuronal cell type markers, respectively. The electrophysiological studies determined the pre- and postsynaptic properties of $TRPV1^{tdTomato}$ neurons in the PVN and dorsomedial hypothalamus; while the immunostaining studies revealed no co-localization with vasopressin and oxytocin. The $TRPV1^{tdTomato}$ mouse model proves to be a useful tool to study the role and properties of TRPV1 receptors in autonomic control. Further studies are necessary to determine the exact role of these neurons with respect to whole body glucose homeostasis.

Funding NIH R01DK099598 (AZs), and Hypertension COBRE (P30GM103337) and DeBakey Scholar Program (CLE).

Macrophage Persistence in Adipose Tissue of Rhesus Macaques

Author Block Marissa Fahlberg[1], Xavier Alvarez[2], Cecily Midkiff[2], Elizabeth Didier[2], Marcelo Kuroda[2]. [1]Tulane University, New Orleans, LA; [2]Tulane University National Primate Research Center, Covington, LA

Abstract:
BACKGROUND: HIV/SIV establishes lifelong infection by integrating proviral DNA into the genome of susceptible long-lived immune cells. In order to eliminate the virus, cellular reservoirs must be discovered and removed. Previous work showed the existence of short and long-lived macrophages in the lung of rhesus macaques (RM), and these long-lived macrophages are permissible to SIV infection and replication. Given recent publications describing adipose as a tissue reservoir for HIV in HAART-treated patients, we chose to investigate the abundance of macrophages in adipose tissue and the proportion that are long-lived to determine their potential as viral reservoirs.
MATERIALS and METHODS: Mesenteric adipose tissue from three RM infected with SIVmac239 intravenously and three uninfected RM were analyzed by confocal microscopy to determine frequency of CD163+ macrophages among nucleated cells. An additional two macaques (one SIVmac239-infected, one uninfected) were injected with dextran intravenously, an inert molecule which can be phagocytosed by macrophages and detected at later time points. At necropsy, tissues were fixed and paraffin-embedded prior to antigen detection with fluorescent antibodies and dextran was detected by confocal microscopy.
RESULTS: CD163+ macrophages constituted 10.5% ± 2.0 of all nucleated cells in the adipose of three uninfected macaques, which differed significantly from infected macaques where macrophages made up 22.0% ± 3.1 of all nucleated cells. We detected dextran in cells within adipose tissue from both injected rhesus macaques at the time of death. The time points at which they died were 43 days (uninfected animal) and 50 days (infected animal) post-injection.
CONCLUSION: Macrophages constitute a significant proportion of nucleated cells in adipose tissue of both uninfected and infected macaques, highlighting their importance in homeostatic and diseased states. The incorporation of dextran within these macrophages for up to 50 days is indicative of a long-lived tissue-resident macrophage subtype with potential to be a reservoir for HIV/SIV.

JOINT DETECTION OF ASSOCIATIONS BETWEEN DNA METHYLATION AND GENE EXPRESSION FROM MULTIPLE CANCERS

Jian Fang*, Ji-Gang Zhang**, Hong-Wen Deng**, Yu-Ping Wang*

*Department of Biomedical Engineering, Tulane University, New Orleans, LA, USA

**Department of Biostatistics and Bioinformatics, Tulane University, New Orleans, LA, USA

DNA methylation plays an important role in the development of various cancers mainly through the regulation effect on gene expression, hence the study on the relation between DNA methylation and gene expression is of particular interest to better understand cancers. Recently, an increasing number of datasets are available from multiple cancers, which encourages the studies on both similarity and difference among genomic alterations across tumor types. However, most of the existing pan-cancer analysis methods perform simple aggregation, which may miss the heterogeneity of the interactions. Here, we wish to put forward an approach for discovering associations between DNA methylation and gene expression profiles from multiple cancers. The approach is able to detect both shared and group-specific interactions. Different from the single variate methylation-gene correlation analysis, we focus on the interactions from any loci and multivariate effects. The method consists of two stages. In the first stage, we extract a densely correlated module that includes a set of methylated sites and a set of shared or group-specific genes using joint sparse CCA. This stage can provide a global view of a principal correlated pattern and help identify important biological processes among them. In the second stage, we detect significant partial correlations inside the detected module based on the joint sparse precision matrix estimation method. This is motivated by the fact that although the detected methylation and genes are densely and highly correlated with each other, most of their interactions are indirect due to complex gene regulations, co-expressions, co-methylations, and etc. To overcome this limitation, we propose to use a partial correlation analysis, which has the potentials in the distinction between direct and indirect interactions. Hence, the second stage can identify gene and methylation pairs that are closely correlated, providing some key interactions underlying the module detected in the first stage. We apply the method to TCGA data with 1166 samples from 4 cancers including breast invasive carcinoma(BRCA), lung squamous cell carcinoma(LUSC), colon adenocarcinoma(COAD), and ovarian serous cystadenocarcinoma(OV). The two-stage method has shown to be effective in extracting interactions from different aspects. From the joint sparse CCA analysis, many interesting pathways have been enriched by both methylated sites and genes, e.g. ERBB2, Oncostatin M, PI3K, and the interactions between pathways enriched by methylated sites and genes were found. From the joint partial correlation analysis, we have also detected some significant pairwise interactions, which were identified to be closely related to epigenetic dysregulation in one or more cancers.

This work was partially supported by NIH (R01GM109068, R01MH104680, R01MH107354, R01AR059781), and NSF (#1539067)

Development of a novel ophthalmic therapeutic biocide with unusual potency against *Acanthamoeba* spp.

Fears AC*, Metzinger RK**, Killeen SZ***, Reimers RS****, and Roy CJ*,***

*Department of Microbiology and Immunology, Tulane School of Medicine, New Orleans, LA
**Department of Ophthalmology, Tulane University School of Medicine, New Orleans, LA
***Division of Microbiology, Tulane National Primate Research Center, Covington, LA
****Department of Environmental Health Sciences, Tulane School of Public Health and Tropical Medicine, New Orleans, LA

There are numerous etiologies associated with infectious keratitis, many of which are extraordinarily difficult to effectively treat to resolution. *Acanthamoeba castellanii* is a saprophytic infectious multiform protozoa associated with sight-threating eye infection. Suspected *Acanthamoeba*-associated keratitis requires remarkable diagnostic effort, and once confirmed few therapeutic clinical options currently available due to the recalcitrant nature of this organism to their environment and antimicrobial agents. In order to meet this therapeutic need, a pH-balanced isotonic biocide comprised of novel active ingredients was developed in our laboratories for ocular instillation to treat this protozoal infection. The candidate biocide was evaluated for activity against *A. castellanii* trophozoites using an alamar blue-based cellular respiration quantitative *in vitro* assay and concurrently compared to biocidals chlorhexidine (5% v/v) and povidone iodine (10% v/w) for antiprotozoal activity. Cultures of ≈10^4 trophozoites/well were commixed with 50 µl of the respective biocide. Contact times for biocidals under evaluation ranged from one minute to four hours before mechanical removal from the culture, addition of reagent, and analysis. Results showed remarkable effectiveness of the novel biocidal formulation, achieving 100% kill at one-min contact time. In contrast, partial kill with comparator biocides were achieved only after four hours of contact time. In a separate assay, *A. castellanii* cultures were subjected to encystation media to test biocidal effectiveness against the cyst form of the protozoa. *A. castellanii* cysts at ≈10^4/well were subjected to commixing with biocides and then were examined microscopically (10x) using trypan blue on a hemocytometer; live-dead counts were performed in no less than five grid fields. Results showed the novel biocide killed 100% of protozoal cysts at 30 min contact time; comparator products achieved a maximal cyst kill of only 20-30% after four hours contact time. Preliminary results show great promise of the novel biocide for development as a therapeutic for *A. castellanii*-associated keratitis and also suggests the possibility of use as a broad spectrum antimicrobial therapeutic for infectious keratitis of varied and/or unknown etiology.

Funded by Tulane School of Medicine Department of Ophthalmology Endowment, Tulane School of Medicine Office of the Dean, and Tulane National Primate Research Center NIH/OD Base Grant.

Norepinephrine activates synchronized inhibitory synaptic inputs to BLA principal neurons

Xin Fu, Jeffrey Tasker

Emotional arousal facilitates memory formation and norepinephrine released in the basolateral amygdala (BLA) during arousal is thought to play an important role in this facilitatory effect. Diverse GABAergic interneurons in the BLA have been shown to be essential for gating the activities of the principle neurons through feed forward inhibition or disinhibition during fear conditioning (Wolff, 2014). Norepinephrine (NE) thus may regulate the activity of the local interneurons to control the concerted neural outputs from BLA. Using whole-cell patch clamp recordings in amygdala slices, we found that norepinephrine application induces a significant increase in the frequency and amplitude of inhibitory postsynaptic currents (IPSCs) in BLA principal neurons. Also, we consistently observed 3 different types of IPSC bursting activity induced by NE. The effects of NE on IPSCs were blocked by pre-application of the a1 adrenergic receptor antagonist prazosin and of the sodium channel blocker TTX, indicating that NE stimulates different subtypes of presynaptic interneurons in the BLA by acting on a1 adrenoceptors. Dual recordings revealed synchronization of the IPSC bursts between pairs of BLA principal neurons. These data suggest that NE can synchronize BLA network activity via a1 receptor-mediated activation of upstream inhibitory interneurons and feedforward synaptic inhibition. This work was supported by NIH R01MH104373.

STANDARDIZATION OF GOOD MANUFACTURING PRACTICE-COMPLIANT DRUG RELEASE FILMS FOR POST-SURGICAL DELIVERY OF ANTI-FIBROTIC AGENTS TO SUBCONJECTIVAL SPACE

Fullerton ML*, John VT**, Ayyala RS***, Blake DA****

*Bioinnovation Program, **Department of Chemical and Biomolecular Engineering, Tulane University, New Orleans, LA, ***Department of Ophthalmology, **** Department of Biochemistry and Molecular Biology, Tulane University School of Medicine, New Orleans, LA

Glaucoma is the second leading cause of blindness in the world and currently has no cure. For many glaucoma patients, pharmaceutical treatments can reduce and control the intraocular pressure (IOP), which causes the optical nerve damage associated with this disease. For patients that are either non-compliant with or unresponsive to pharmaceutical interventions, surgery is the next option. This surgery creates a new pathway to drain the excess fluid from the aqueous chamber of the eye to a space (the bleb) between the sclera and the conjunctiva. Such surgical treatments are hindered by the formation of fibrotic scar tissue inside the bleb wall. This fibrous tissue gradually reduces the flow of fluid from the bleb, which results in a 50% failure rate in valve implants after 5 years. Previously, we developed a slow-release drug delivery device that can be implanted at the surgery site and can release anti-fibrotic agents to inhibit the growth of fibrous tissue and the failure rate. This device uses a biodegradable polylactic-co-glycolic acid (PLGA) film with a breath-figure morphology to enable a dual loading of both 5-flurouracil (5-FU) and mitomycin-C (MMC) after implantation. Following device design and animal testing, the manufacturing required rigorous standardization in order to improve reproducibility and to prepare the product for development in a good manufacturing practice (GMP) facility. This included selection of standard PGLA molecular weights, control of drug content in each film, and quality assurance procedures for drug loading and delivery. We found that PLGA of molecular weight 38-54 kDa best delivered encapsulated 5-FU in the required period. Additionally, a lower molecular weight PLGA of 7-17 kDa performed best as the top breath figure layer for loading MMC. To enhance our quality assurance procedures, we developed an extraction method to dissolve films and confirm the reproducibility of drug loading. In vitro release studies confirmed that the MMC loaded on the top layer released within the first 24 h and that the 5-FU released in a linear fashion over the first 30 days. Future studies will include demonstration that the γ-sterilization procedures required by the FDA do not affect drug release kinetics or drug potency. The tests facilitate the development of slow release devices, improve quality assurance/ quality control and prepare our device for transition to a GMP facility prior to use in human trials.

Spontaneous Membrane Translocating Peptides: Mechanism and Motifs

Taylor Fuselier and William C. Wimley

Department of Biochemistry and Molecular Biology, Tulane University School of Medicine, New Orleans, LA 70112

We previously used an orthogonal high-throughput screen to select peptides that spontaneously cross synthetic lipid bilayers without permeabilization. Interestingly, many of the 12-residue *spontaneous membrane translocating peptides* (SMTPs) selected from the library contained a consensus *LRLLR* motif. We hypothesized that the conserved *LRLLR* motif could be a minimal motif for spontaneous membrane translocation. To test this and to explore the mechanism of spontaneous membrane translocation, we synthesized six arginine spacing variants of *LRLLR* and compared their membrane partitioning, translocation, and perturbation to one of the parent SMTPs, called TP2. Several motif variant peptides translocate into synthetic vesicles with rates that are similar to TP2. However, the actual motif peptide, LRLLR, was not the fastest, showing that sequence context is important for translocation efficiency. While none of these peptides permeabilize bilayers, the motif peptides translocate faster at higher peptide to lipid ratios, suggesting that bilayer perturbation and/or cooperative interactions are important for their translocation. On the other hand, TP2, which was actually selected in the screen, translocates dramatically faster as its concentration is *decreased*, suggesting that TP2 translocates as a monomer and is inhibited by lateral interactions in the membrane. We tested variants with shorter and longer arginine sidechain analogs and found that neither translocate as fast as those with arginine. Finally, we tested concatenated motifs and measured slow translocation compared to the motifs alone. In summary, multiple variants of the conserved motif translocate as well as TP2, showing that amino acid composition is an important factor, but one that is influenced by sequence context. These results also show that rational engineering of SMTPs is not yet possible, providing even more reason to pursue SMTP discovery with synthetic molecular evolution.

THE IMPACT OF ADJUVANT RADIATION THERAPY BEFORE OR AFTER ARTIFICIAL URINARY SPHINCTER PLACEMENT: A MULTI-INSTITUTIONAL ANALYSIS

Gabrielson AT*, Haney NM*, DeLay KJ*, Chiang J*, Stewart C*, Yafi FA**, Angermeier K***, Lacy J***, Wood H***, Boone T****, Kavanagh AG*****, Gretzer M******, Boyd S*******, Doyle JL*******, Hellstrom WJ*

*Tulane University Department of Urology, New Orleans, LA, **University of California Irvine Department of Urology, Irvine, CA, ***Cleveland Clinic Department of Urology, Cleveland, OH, ****Houston Methodist Urology Associates, Houston, TX, *****University of British Columbia Department of Urologic Sciences, Vancouver, BC, ******University of Arizona Department of Urology, Tuscon, AZ, *******University of Southern California Department of Urology, Los Angeles, CA

Introduction and Objective: Artificial Urinary Sphincter (AUS) remains the gold standard in the management of male stress urinary incontinence following radical prostatectomy. However, the impact of AUS placement before or after adjuvant radiation therapy has limited coverage in the literature. The objective of this study was to determine if the timing of radiation therapy has an impact on AUS outcomes, as well as identify predictors of AUS-related complications.

Methods: A retrospective review was conducted across five academic institutions of men who received AUS placement and adjuvant radiation therapy between 1993 and 2016. A total of 306 men were included in the study. Out of the 306 men, 292 (95.4%) received radiation before AUS placement (Group 1) and 14 (4.6%) men received radiation after AUS placement (Group 2). Collected variables included demographics, type of prostate cancer therapy, and AUS device specifications. Primary endpoints included complication rates, revision rates, and number of pads per day before and after AUS treatment. Bivariate analysis was used to examine the association between pretreatment comorbidities and the incidence of AUS-related complications postoperatively.

Results: Median duration of follow-up for the entire cohort was 30 months (range 4-148 months). Group 1 was followed for a median of 29 months (range 4-148 months), while Group 2 was followed for a median of 49 months (range 12-141 months). There was no difference between groups in the percentage of men who experienced postoperative complications ($P = 0.832$). In Group 1, 26.0% of patients experienced postoperative complications while 28.6% of patients in Group 2 experienced postoperative complications. While the number of pads per day decreased significantly from before AUS placement to after AUS placement, there was no significant difference in the average number of pads used per day between Group 1 and Group 2 ($P = 0.907$). The number of pads used per day in Group 1 before AUS placement was 5.24 +/- 3.12 which decreased to 1.13 +/- 1.31 ($P < 0.001$). In Group 2, the number of pads used per day before surgery was 6.09 +/- 1.97 which decreased to 1.53+/-0.99 pads per day after AUS placement ($P < 0.001$). The percentage of men requiring revision in Group 1 was 31.2%, while the percentage of revisions in Group 2 was 14.3%($P = 0.028$). The median time to revision was 14 months and 18.5 months for Group 1 and Group 2, respectively. The presence of peripheral vascular disease (PVD) and coronary artery disease (CAD) was associated with increased incidence of AUS-related complications (primarily refractory incontinence and cuff erosion) in both Groups ($P = 0.032$). The following factors were not significant: age, race, smoking, hypertension, diabetes mellitus, dyslipidemia, BMI, AUS device specifications, type of radiation therapy. Demographic data is included in Table 1, prior treatment history and perioperative data is included in Table 2, and postoperative follow-up parameters are included in Table 3.

Conclusions: The timing of radiation therapy does not have a significant impact on complication rates or urinary continence as represented by number of pads used post-AUS placement. There is a non-statistical association between lower revision rates in patients who underwent radiation after AUS placement, as compared to before AUS placement. Patients with pre-existing PVD or CAD may experience more frequent postoperative complications, but this study is underpowered. Further research is needed to confirm these findings.

TABLE 1: Demographic and Comorbidities data

	Total 306	**Radiation before AUS 292 (95.4%)**	**Radiation after AUS 14 (4.6%)**
Median Age	71 (51-88)	71 (51-88)	68 (59-79)
Race	197 Caucasian 25 African-American 13 Hispanic 4 Other 67 Unspecified	187 Caucasian 24 African-American 13 Hispanic 4 Other 64 Unspecified	10 Caucasian 1 African-American 0 Hispanic 0 Other 3 Unspecified
Smoking	153 Nonsmoker 88 Smoker 65 Unspecified	145 Nonsmoker 85 Smoker 62 Unspecified	8 Nonsmoker 3 Smoker 3 Unspecified
HTN	96 No disease 144 Hypertensive 66 Unspecified	89 No disease 140 Hypertensive 63 Unspecified	7 No disease 4 Hypertensive 3 Unspecified
DM	181 No disease 59 Diabetic 66 Unspecified	173 No disease 56 Diabetic 63 Unspecified	8 No disease 3 Diabetic 3 Unspecified
Dyslipidemia	114 No disease 126 Dyslipidemia 66 Unspecified	108 No disease 121 Dyslipidemia 63 Unspecified	6 No disease 5 Dyslipidemia 3 Unspecified
PVD/CAD	166 No disease 74 PVD/CAD 66 Unspecified	157 No disease 72 PVD/CAD 63 Unspecified	9 No disease 2 PVD/CAD 3 Unspecified
Median BMI	28.7 (20.1-42.4)	28.7 (20.9-42.4)	26.9 (20.1-37.3)

TABLE 2: Description of prostate cancer treatments prior to AUS placement and intraoperative/device parameters

	Total 306	**Radiation before AUS 292 (95.4%)**	**Radiation after AUS 14 (4.6%)**
Previous Surgery	54 None 129 Open RP 9 Laparoscopic RP 45 Robotic RP 10 Local 59 Unspecified	54 None 122 Open RP 8 Laparoscopic RP 39 Robotic RP 10 Local 59 Unspecified	0 None 7 Open RP 1 Laparoscopic RP 6 Robotic RP 0 Local 0 Unspecified
Hormonal Tx	160 None 108 Hormonal Tx 38 Unspecified	153 None 101 Hormonal Tx 38 Unspecified	7 None 7 Hormonal Tx 0 Unspecified
Type of Radiation	28 Brachytherapy 251 EBRT 18 Both 9 Unspecified	28 Brachytherapy 237 EBRT 18 Both 9 Unspecified	0 Brachytherapy 14 EBRT 0 Both 0 Unspecified
Surgical Approach	287 Perineal 19 Trans-scrotal	275 Perineal 17 Trans-scrotal	12 Perineal 2 Trans-scrotal
Separate Abdominal Incision for PRB	22 None 284 Separate incision	19 None 173 Separate incision	3 None 11 Separate incision
Cuff Type	299 Single 5 Tandem 2 Unspecified	287 Single 3 Tandem 2 Unspecified	12 Single 2 Tandem 0 Unspecified
Size Cuff	14 Size 3.5 99 Size 4 159 Size 4.5 19 Size 5 6 Size 5.5 2 Size 6 7 Unspecified	13 Size 3.5 89 Size 4 156 Size 4.5 19 Size 5 6 Size 5.5 2 Size 6 7 Unspecified	1 Size 3.5 10 Size 4 3 Size 4.5 0 Size 5 0 Size 5.5 0 Size 6 0 Unspecified
PRB Size	14 Size 51-60 291 Size 61-70 1 Size 71-80	14 Size 51-60 277 Size 61-70 1 Size 71-80	0 Size 51-60 14 Size 61-70 0 Size 71-80
PRB Location	182 Space of Retzius 122 Ectopic 2 Unspecified	172 Space of Retzius 118 Ectopic 2 Unspecified	10 Space of Retzius 4 Ectopic 0 Unspecified

Table 3: Description of post-operative complications and follow-up parameters

	Total 306		**Radiation before AUS 292 (95.4%)**		**Radiation after AUS 14 (4.6%)**	
Postoperative Complications	226 None 80 Complications		216 None (74%) 76 Complications (26%)		10 None (72%) 4 Complications (28%)	
Type of Postoperative Complications	6 Infection 32 Erosion 14 Sub-cuff atrophy 44 Persistent Incontinence 4 Mechanical Failure 12 – Other (3 mixed complication events)		6 Infection 32 Erosion 13 Sub-cuff atrophy 42 Persistent Incontinence 4 Mechanical Failure 10 Other (2 mixed complication events)		0 Infection 0 Erosion 1 Sub-cuff atrophy 2 Persistent Incontinence 0 Mechanical Failure 2 Other (1 mixed complication event)	
Number of Revisions	93 Total Revisions 35 Explants 42 Cuff Revisions 4 PRB Revision 3 Pump Revision 3 Placement of 2nd Cuff 2 Other (4 mixed revision events)		91 Total Revisions (31%) 35 Explants 40 Cuff Revisions 4 PRB Revision 3 Pump Revision 3 Placement of 2nd Cuff 2 Other (4 mixed revision events)		2 Total Revisions (14%) 0 Explants 2 Cuff Revisions 0 PRB Revisions 0 Pump Revisions 0 Placement of 2nd Cuff 0 Other (0 mixed revision events)	
Median Time to First Revision (months)	15 (1-134)		14 (1-134)		18.5 (10-27)	
Median Duration of Follow-up (months)	30 (4-148)		29 (4-148)		49 (12-141)	
Average # Pads pre-op vs. post-op	*Pre-op* 5.29+/-3.08	*Post-op* 1.13+/- 1.30	*Pre-op* 5.24+/-3.12	*Post-op* 1.13+/-1.31	*Pre-op* 6.09+/-1.97	*Post-op* 1.53+/-0.99

GABA AND GLYCINE: FINE TUNING FOR INHIBITORY CONTROL OF BRAINSTEM RVLM NEURONS

Gao H* and Derbenev AV**

*Department of Physiology, School of Medicine, **Brain Institute, Tulane University, New Orleans, Louisiana

Presympathetic neurons in the rostral ventrolateral medulla (RVLM) are best known for their contribution to the control of sympathetic nervous system and homeostatic functions of the body. Both glycine and GABA were identified as fast inhibitory neurotransmitters in the RVLM. Traditionally, GABA is essential for the control of the excitability of neurons in the RVLM. In addition to GABA, glycine also inhibits RVLM neurons. Despite the critical role of GABA and glycine as inhibitory neurotransmitters, surprisingly little is known about the mechanisms of GABA and glycine release and co-inhibition of the RVLM neurons. Using whole-cell patch-clamp recordings from presympathetic neurons identified with PRV-152, we examined release of GABAergic and glycinergic in the rat brainstem slices containing RVLM neurons. We tested the hypothesis that release of glycine requires network activation. With pharmacological tools, we found that inhibitory postsynaptic currents (IPSCs) recorded from RVLM neurons composed from both GABAergic and glycinergic events and in steady state conditions GABA is the predominant inhibitory neurotransmitter. Interestingly, after activation of the neuronal network in the RVLM we found that GABAergic and glycinergic neurotransmission is reversed. Our work supports the hypothesis that both GABA and glycine act as inhibitory co-transmitters. We have found that presynaptic release of GABA and glycine generates IPSCs and provides the basis for inhibition in non-activated neuronal network in the RVLM. Before activation of neuronal network 64% of IPSCs were generated by GABA and 36% of IPSCs were generated by glycine. Surprisingly, we found that activation of neuronal network produced switch between GABAergic and glycinergic IPSCs. After activation of neuronal network 37% of IPSCs were generated by GABA and 63% of IPSCs were generated by glycine. Our work support the hypothesis that both GABA and glycine are inhibitory neurotransmitters in the RVLM, but release of GABA and glycine strictly depends on activity of neuronal network.

This work was supported by NIH HL122829 for AVD.

REPAIR ARTICULAR CARTILAGE DEFECTS USING HUMAN ADIPOSE TISSUE-DERIVED ADULT STEM CELLS

Ge D[1], Liu S[1], Ma L[1], Zhang, Q[1,11], Wu V[1,2], O'Brien M[2], Mead RN[2], Savoie F[2], Gimble J[3,4] Wu X[3], Bunnell B[4,5,6], Gilbert M[5], Miller K[7], Wang A[8], Myers L[9], You Z[1,2,4,10,11]

[1]Department of Structural and Cellular Biology, [2]Department of Orthopaedic Surgery, [4]Tulane Center for Stem Cell Research and Regenerative Medicine, [5]Tulane National Primate Research Center, [6]Department of Pharmacology, [7]Department of Biomedical Engineering, [8]Department of Pathology and Laboratory Medicine, [9]Department of Global Biostatistics and Data Science, [10]Tulane Cancer Center and Louisiana Cancer Research Consortium, [11]Tulane Center for Aging, Tulane University, New Orleans, LA; [3]LaCell LLC, New Orleans, LA.

Articular cartilage damage caused by trauma and diseases is recalcitrant to repair or regeneration. Tissue engineering and regenerative medicine are potential strategies to treat articular cartilage defects. The current therapy strategies such as autologous chondrocyte implantation (ACI) have their own limitations such as availability of normal donor cartilage. This limitation may be overcome by tissue engineering using human adipose tissue-derived adult stem cells (ASCs) isolated from liposuction tissues that are unlimited in the sources, because approximately 280,000 liposuction procedures are done annually. Our previous studies discovered that doublecortin (DCX) is expressed by limb mesenchymal stem/progenitor cells and uniquely expressed in articular chondrocytes, suggesting that DCX may guide ASCs to differentiate into articular chondrocytes. This idea is preliminarily supported by our finding that low-level DCX expression in human adipose-derived ASCs leads to increased expression of matrilin 2 and growth and differentiation factor 5 (GDF5), two markers of articular chondrocytes, in the cartilage tissues derived from ASCs. We hypothesized that consistent expression of DCX in ASCs may promote differentiation of the ASCs into articular chondrocytes that can be used to treat cartilage injuries. We developed an *in vitro* differentiation system to produce articular cartilage. ASCs were transfected with either HRST-DCX-GP-eGFP or HRST-eGFP lentiviruses to express DCX (experimental group) or eGFP only (control group). Additional untreated control group was repaired with fibrin sealant. We set up the pellet culture system to generate cartilage pellets. The chondrocyte quantity and quality controls were performed to confirm that the products were free of bacteria, yeast, virus, or endotoxin contamination. The cartilage pellets were used to repair the knee defects surgically created in 10 rabbits. At different time-points after surgery, the outcomes of repair were evaluated. Our preliminary results showed that the experimental group had better repair than the fibrin sealant control group. Our ongoing study will expand the number of rabbits, perform repair in rhesus macaques, and extend the follow-up to 24 months.

This work was supported by the Office of the Assistant Secretary of Defense for Health Affairs through the Peer Reviewed Orthopaedic Research Program under Award No. W81XWH-15-1-0444. Opinions, interpretations, conclusions and recommendations are those of the author and are not necessarily endorsed by the Department of Defense; the U.S. Army Medical Research Acquisition Activity, 820 Chandler Street, Fort Detrick MD 21702-5014 is the awarding and administering acquisition office; the conducts of research using animals, recombinant DNA, and toxic materials followed the guidelines of Department of Agriculture and NIH.

MICROFLUIDIC CAPTURE AND QUANTIFICATION OF HIV

Genemaras, KJ*, Kundrod, KA**, Fraser, JC***, Cheng, X***, Garry, RF****

*Bioinnovation Program, Tulane University, New Orleans, LA
**Department of Bioengineering, Rice University, Houston, TX
***Bioengineering Program, Lehigh University, Bethlehem, PA
****Department of Biomedical Sciences, Tulane University, New Orleans, LA

Approximately 35 million people worldwide are living with HIV and need to regularly monitor the efficacy of their treatments. The standard laboratory-based tests are not accessible in resource-limited settings, where the prevalence of HIV is concentrated. Thus, there is a need for the development of an inexpensive, portable, and easy-to-operate technology for HIV treatment monitoring that can be used at the point of care. Our solution is a microfluidic device with an incorporated novel porous membrane that has been proven effective in the capture of HIV and uses cyclic voltammetry for quantification of viral load.

The membrane was fabricated through the deposition of a binary suspension of silica (diameter = 1um) and polystyrene (diameter = 0.1um) beads in a PDMS well. The polystyrene was melted and allowed to set, forming a solid structure, and the silica was etched out with 50% hydrofluoric acid. The final membrane was a structure with pore sizes comparable to HIV virions. The membrane was encased in PMMA with stainless steel electrodes making contact with the membrane. Finally, inlet and outlet tubing were incorporated, and the device was sealed with epoxy. The membrane was functionalized with avidin, and HIV was captured to the membrane. Avidin-functionalized gold nanoparticles were bound to the captured virus, and liquid silver was catalyzed to solidify by the gold, forming larger structures around the captured virus that acted as resistors. An ion solution was injected into the device, and peak current during cyclic voltammetry was recorded.

The results of the study confirmed the concept that using a potentiostat, cyclic voltammetric signal reduction can be observed as bead-capture increases within the membrane (Figure 1). A measurable reduction in peak current was observed between the devices containing captured virus compared with the devices containing no virus, confirming that physical blocking of ion movement was present. In addition to technical feasibility, the test required a test sample of 100uL and the testing time was less than 1 hour. Current methods for analysis of viral load involve PCR amplification of viral RNA. These methods are accurate but time intensive and require a sterile lab infrastructure. However, for this device, projected operation procedures are simpler and projected instrumentation cost is lower than existing technology, making scale-up of manufacturing and distribution more feasible.

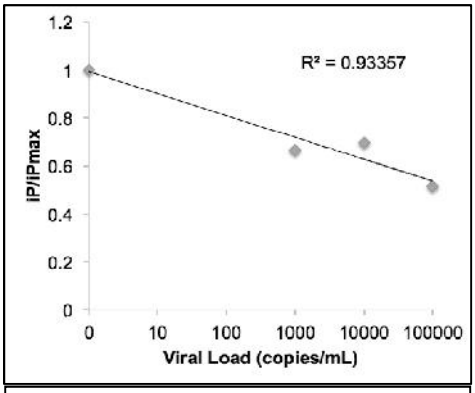

Figure 1. Standard peak current versus viral load. This will be used as a calibration curve to calculate viral load in an unknown sample.

With technical and financial improvements over current approaches, our design has the potential to be the revolutionary technology for HIV viral load diagnostics that society currently lacks. With a design that drastically increases accessibility to viral load testing, this technology has the potential to help patients and clinicians better manage HIV infections, preventing mortality from failing treatment regimens.

This work was supported by the National Institutes of Health No. 1R21AI081638.

THE MEMBRANE-ACTIVE PHYTOPEPTIDE CYO2 INCREASES ANTI-HIV EFFICACY BY SIMULTANEOUSLY INCREASING DRUG UPTAKE AND BY DISRUPTING VIRAL PARTICLES

Gerlach SL[*,], Chandra PK[*], Upal R[***], Göransson U[****], Wimley WC[*****], Braun SE[*], and Mondal D[*]**

Departments of [*]Pharmacology and [*****]Biochemistry, Tulane University School of Medicine. [**]Department of Biology, Dillard University. [***]Department of Immunology, Florida International University, Miami, FL. [****]Division of Pharmacognosy, Department of Medicinal Chemistry, Uppsala University, Sweden. [*]Presenter

Despite the availability of potent antiretrovirals (ARV) subtherapeutic drug entry into HIV-1 infected cells enable viral propagation and facilitate the selection of drug resistance. Resurgence in plasma viremia, occurring during the time needed for drug susceptibility assessment in the clinic, causes the development of newly infected reservoir pool. Therefore, novel adjuvant strategies that increase ARV efficacy and suppress the resurging viral load will be of significant value in patients. The membrane targeting effect of cyclotides and their ability to specifically recognize phosphatidyl-ethanolamine (PE) enriched lipid membranes provides a promising approach, to simultaneously increase drug entry and cause viral particle disruption. Indeed, the lipid envelope of HIV particles is rich in PE, Cholesterol (Chol) and sphingomyelin (SM). In addition, the plasma membranes of productively infected cells are enriched with raft-like regions containing these phospholipids. In this respect, the prototypic bracelet cyclotide, Cycloviolacin O2 (CyO2) has the strongest affinity to PE-rich membranes, and shows the highest efficiency in membrane destabilization. Therefore, we investigated whether low doses of CyO2 can be used to form multimeric pores in HIV-1 infected cells in order to increase ARV uptake, and whether low dose CyO2 can also directly target the HIV-1 envelope to disrupt the infectivity of viral particles. Fluorescent dye (Sytox-green) uptake assays showed that subtoxic concentrations CyO2 (<0.5 mM) rapidly increased pore-formation in productively infected T-cells (HuT78 and PM1) and monocytes (U1). CyO2 coexposure rapidly enhanced the intracellular levels of a radiolabeled HIV-1 protease inhibitor (HPI), tritiated saquinavir [^{3}H-SAQ]. Indeed, in both short-term (2-6 h) and long-term (72 h) exposure studies, CyO2 was able to increase ($p<0.05$) the antiviral efficacy of two HPIs, SAQ and nelfinavir (NEL) as evident by decreased HIV-1 p24Gag levels in culture supernatants (by ELISA). Pore-formation by CyO2 was significantly lower in the uninfected cells and primary endothelial cells, implicating specificity for infected cell membranes. Interestingly, a subtoxic dose of CyO2 was also effective in suppressing HIV-1 infection and p24 production by itself ($p<0.05$). Mechanistic studies were first carried out to determine the effect of CyO2 on proviral gene expression via the HIV-1 LTR. In two cell lines, J-Lat (T-cells) and U937-VRX (monocyte), containing an integrated provirus that directs GFP reporter expression, CyO2 did not suppress HIV-1 LTR function. However, studies using a replication defective viral like particle (VLP) that expresses GFP following infection and chromosomal integration, clearly indicated that CyO2 suppresses the infectivity of VLPs. Indeed, CyO2 exposure of cell-free virus (CFV) followed by ultracentrifugation to pellet intact viral particles clearly showed a direct effect of CyO2 in disrupting infectious virions. Significant decreases in internal viral contents (p24 protein and viral RNA) and decreased infectivity of the viral titer were evident following exposure to CyO2 alone. Indeed, pre-exposure to CyO2 (<0.5 mM) suppressed viral infectivity in PM1 cells ($p<0.05$) and enhanced ($p<0.05$) antiviral efficacy of the HIV-1 entry inhibitor, Enfuvirtide. Thus, adjuvant treatment with subtoxic doses of CyO2 may be a promising strategy in HIV-positive patients.

Acknowledgement: Studies were supported by NIH grants to DM (AI116348) and SEB (AL110158).

Young Children's Physiological Reactivity During Memory Recall: Associations with Posttraumatic Stress and Parent Physiology

Sarah A. O. Gray, Rebecca Lipschutz, & Michael Scheeringa

Objective: Autonomic reactivity is implicated in stress response and social engagement – both key components of posttraumatic stress disorder (PTSD) – but few studies have examined autonomic reactivity in pediatric samples, and no known studies have examined physiological synchrony among children with PTSD and caregivers. **Method:** In a sample of 247 young children, most (85%) of whom had exposure to trauma and 40% who met criteria for PTSD, we examined children's patterns of respiratory sinus arrhythmia (RSA) at baseline and in response to a memory recall task, as well as correspondence between parents' and children's RSA. **Results:** Children with PTSD demonstrated significantly higher reactivity than other groups during their recollection of a traumatic memory, but not during other memory tasks. Regarding synchrony, caregivers' and children's RSA were more significantly and positively correlated during the trauma recall task among children who had had exposure to a potentially traumatic event but did not meet PTSD criteria, suggesting physiological synchrony may be protective in contexts of trauma. **Conclusions:** Young children with PTSD demonstrated heightened reactivity during a traumatic memory recall task. While more work is needed to understand the meaning of parent-child physiological synchrony, these data suggest that children's psychopathology is associated with physiological synchrony processes among young children with exposure to trauma.

Keywords: Trauma, Posttraumatic Stress Disorder, Parenting, Synchrony, Respiratory Sinus Arrhythmia, Emotion Regulation

Knockdown of ABCB5 transporter sensitizes CD133^{+} melanoma subpopulation to RAS-RAF pathway inhibitor-based therapy

Erik A. Green[1], Saboori Sobti[1], Paul Friedlander[2], Mary T. Killackey[1], Emad Kandil[1], Mohamed Hassan[1]

[1]Department of Surgery, Tulane University, Medical School, New Orleans, LA 70112, USA; [2]Department of Otoaryngology, Tulane University, Medical School, New Orleans, LA 70112, USA.

Background: Despite the improved treatment options for melanoma patients, prognosis of patients with advanced malignant melanoma remains poor. Neoplastic clones are maintained by a small fraction of cells with stem cell properties. The focus of this study was to determine whether the resistance of CD133^{+} melanoma subpopulation to available chemotherapeutics is attributed to the elevated expression of the stem cell marker, ATP-binding cassette sub-family B member 5 (ABCB5), which may be responsible for drug efflux and subsequent chemo-resistance of CD133^{+} melanoma subpopulations. **Material and Methods:** Immunogenetic separation of CD133^{+} cells from established melanoma cell lines BLM/NRAS-mutated and A375/BRAF-mutated, colony formation assay, Scratching assay, Cell viability assay, Flow cytometry analysis, Western Blot analysis. **Results:** The CD133^{+} melanoma subpopulations isolated from established NRAS-mutated and BRAF-mutated melanoma cell lines have been confirmed for their ability to self-renew and to migrate. Data from the cell viability assay revealed that the CD133^{+} subpopulations derived from either NRAS-mutated or BRAF-mutated cells were resistant to trametinib and dabrafenib, respectively, when compared to CD133^{-} subpopulations. The knockdown of the stem cell marker ABCB5 sensitized CD133^{+}cells to trametinib as well as to dabrafenib-induced cell death, as evidenced by MTT assay and Western blot analysis of PARP. Trametinib and dabrafenib-induced cell death was associated with the inhibition of the basal phosphorylation of extracellular regulating kinase 1 and 2 (ERK1 and2) and the expression of mitogen activated protein kinase phosphatase-1 (MKP-1) expression together with the activation c-jun-N-terminal kinase (JNK) and p38 pathways. **Conclusion:** Knockdown of ABCB5 by its specific siRNA is essential to overcome the resistance of CD133^{+} melanoma subpopulation to NRAS/BRAF pathway-based therapy.

Membrane active peptides as a potential therapeutic option for enveloped viruses

Guha S[1], Hoffmann AR[2], He J[1], Garry RF[2], Wimley WC[1*]

[1]Department of Biochemistry and Molecular Biology, Tulane University School of Medicine, New Orleans, LA,
[2]Department of Microbiology and Immunology, Tulane University School of Medicine, New Orleans, LA
*Corresponding author

Every year, influenza affects populations all across the world, and every year, new vaccines must be developed due to the intrinsically high rate of mutation and reassortment in influenza virus. Currently, there are two classes of antiviral drugs available to treat influenza virus infection, neuraminidase inhibitors and M2 inhibitors, but both classes have limited efficacy and resistant strains of virus are common. Due to the difficulty in treating influenza and other enveloped viruses, there is an urgent need for new classes of antiviral agents. One potentially useful, but underdeveloped type of inhibitor is the peptide entry inhibitor (PEI). PEIs interfere with the key early steps by which enveloped viruses bind, fuse, enter, and eventually infect their target cells. By testing a large number of membrane active peptides in an influenza infection model system, we identified a panel of peptides which have potent inhibitory activity against the virus. We have hypothesized that some of these peptides directly interact with viral and/or host cellular membrane lipids and disrupt viral binding and fusion. This hypothesis leads to the prediction that membrane-active peptides, in general, will inherently have inhibitory activity against enveloped virus due to the nature of virus-host entry mechanisms. We have used cell biology and biophysics to compare the peptide activity against synthetic membrane vesicles with the antiviral activities of each peptide. Taken together, our results show that interfacially active PEIs have the potential to be useful therapeutics which can possibly be applied to different enveloped viruses.

MODULATION OF MEDIAL ENTORHINAL CORTEX LAYER II CELL CIRCUITRY BY STRESS HORMONES

Hartner JH*, Schrader LA* **

*Neuroscience Program, School of Science and Engineering, Tulane University, New Orleans, LA
**Department of Cell & Molecular Biology, School of Science and Engineering, Tulane University, New Orleans, LA

Acute and chronic stress can cause spatial memory deficits, but the underlying mechanisms affecting the known memory pathways remain unclear. Until the discovery of spatially- tuned grid cells within layer II of the medial entorhinal cortex (MEC – LII), spatial memory research has focused primarily on the hippocampus, where the effects of stress are well-characterized. However, spatial memory processing has recently been shown to require functional interaction between the hippocampus and the entorhinal cortex, and the inhibitory network within the MEC is particularly important for the firing properties of the grid cells. Despite the crucial role of the MEC in spatial memory processing, the effects of stress on this region have not been studied. Stress simultaneously activates both the autonomic nervous system (ANS) and the hypothalamic-pituitary-adrenal (HPA) axis to release norepinephrine (NE) and glucocorticoids respectively. The effect of NE, glucocorticoids, and a potential interaction between the two systems within the MEC has not been investigated. Given that glucocorticoid receptor (GR) expression is abundant in nearly all types of neural tissue, and that NE receptors are highly-expressed in the MEC, both glucocorticoids and norepinephrine may have rapid effects on the cell networks within MEC – LII.

In this study, we used whole-cell patch clamp electrophysiology of MEC slice preparations from male mice to test the effects of bath application of dexamethasone (1μM), a synthetic glucocorticoid, as well as NE (100μM) on excitability and synaptic inputs of both MEC – LII principal cells and parvalbumin-positive (PV^+) interneurons. Dexamethasone treatment had no significant effect on frequency or amplitude of either miniature or spontaneous excitatory postsynaptic currents in MEC – LII principal cells. Interestingly, the frequency of spontaneous inhibitory postsynaptic currents (sIPSCs), but not miniature IPSCs, was significantly decreased by dexamethasone application in both principal cell types of MEC – LII. Treatment with the naturally circulating glucocorticoid, corticosterone (100nM), significantly decreased the frequency, but not amplitude, of sIPSCs in both principal cell types. Together, these results suggest that the glucocorticoid-induced decrease of IPSC frequency requires hyperpolarization of presynaptic inhibitory interneurons. Application of norepinephrine (NE) increased frequency and amplitude of sIPSCs in 50% of MEC – LII principal cells. Interestingly, in cells pre-treated with dexamethasone, NE increased the frequency and amplitude of sIPSCs in more than 90% of cells. These findings suggest that dexamethasone caused an increase in the proportion of NE-responsive cells in MEC – LII. We are currently using a Pvalb-tdTomato mouse line that expresses RFP exclusively in PV^+ inhibitory interneurons to investigate the effects of both NE and dexamethasone on inhibitory cell excitability and synaptic activity in MEC – LII. Preliminary

recordings from PV^+ interneurons show an increase in cell excitability following NE application due to a depolarization of the membrane potential. Further characterization of the effects of stress hormones on the functional circuitry within MEC – LII requires an investigation of the effects of dexamethasone and NE on the pre-synaptic inhibitory connections within MEC – LII. Given the importance of the inhibitory network in spatial mapping properties of the MEC, these results contribute to our understanding of the effects of stress on spatial mapping and memory formation, and suggest the intriguing possibility of modulation of network processing upstream of the hippocampus.

Supported by NSF grant IOS 1146853

IDENTIFICATION OF NTRK3 AND SIK 1 AS POTENTIAL THERAPEUTIC TARGETS FOR DESMOPLASTIC SMALL ROUND CELL TUMOR

Hartono AB*, Hmeljak J**, Spraggon L**, Ladanyi M**, Lee SB*

* Department of Pathology and Laboratory Medicine, Tulane University School of Medicine, New Orleans, LA

** Memorial Sloan Kettering Cancer Center, New York, NY

Desmoplastic small round cell tumor (DSRCT) is a rare and aggressive malignant cancer associated with the chromosomal translocation t(11;22)(p13;q12) that produces a novel chimeric protein, EWS-WT1. The translocation causes a fusion of the N-terminal domain of EWS to the C-terminal domain of WT1, generating an aberrant oncogenic transcription factor. EWS-WT1 is essential in the formation of DSRCT; however, current research has not clearly elucidated how EWS-WT1 leads to the pathogenesis of DSRCT. Consequently, conventional chemotherapy is ineffective and the prognosis remains extremely poor for DSRCT patients. Our lab generated a gene expression profiling data by using a patient-derived cell line (JN-DSRCT-1) and knocking down the expression of EWS-WT1 via shRNA. By comparing the altered gene expression profile in JN-DSRCT-1 when EWS-WT1 is depleted against primary DSRCT tumor specimens, we found that more than 200 genes have reduced expressions when EWS-WT1 expression is depleted. Among them, 17 genes encode a kinase, an important class of signaling proteins that are also amenable for targeted inhibition with small compounds. We systematically depleted the expression of each of the 17 kinases via siRNA in JN-DSRCT-1 cell line and showed that several of the kinases, such as NTRK3 and SIK1, when depleted result in cytotoxicity. To determine the oncogenic roles of these kinases, we established a doxycycline-inducible (Tet-ON) shRNA system that uses an optimized MiR-30 backbone to induce RNAi knockdown in JN-DSRCT-1 cells. Using this Tet-ON shRNA vector system, we currently have generated several stable cell lines carrying shRNA against EWS-WT1, NTRK3, and SIK1 as well as a luciferase control. When treated with doxycycline, our stable cell lines showed decreased cell growth, which suggests that these kinases are essential in JN-DSRCT-1 cell viability or survival. We are currently generating more stable cell lines that carry shRNA against the other identified oncogenic kinases. Once established, we will examine their effects on cell growth and dissect the downstream signaling pathways. Furthermore, we will inject JN-DSRCT-1 cells carrying the TET-ON shRNA vector subcutaneously into NOD.SCID mice and once tumors have grown, we will administer doxycycline to silence the kinases and monitor tumor growth. By performing an in vivo model, we will be able to identify the kinases that can be targeted for drug development against DSRCT.

THE DELTA PEPTIDE OF EBOLA VIRUS HAS POTENT VIROPORIN ACTIVITY

He J[1], Melnik L[2], Komin A[3], Starr CG[1], Fuselier T[1], Wiedman G[3], Morris CF[2], Hristova K[3], Gallaher W[4], Garry R[2] and Wimley WC[1]

[1]Biochemistry and Molecular Biology and [2]Microbiology and Immunology, Tulane University Medical Center, New Orleans, LA; [3]Materials Science and Engineering, Johns Hopkins University, Baltimore, Maryland; and [4]Mockingbird Nature Research Group, Pearl River, Louisiana

The Delta peptide, cleaved from the soluble glycoprotein (sGP) of Ebola virus (EBOV), is a partially conserved, 40-residue nonstructural polypeptide that has no known function. This peptide shows high similarity in amino acid composition to membrane permeabilizing peptides, including a peptide in the diarrhea-inducing viroporin, NSP4, of Rotavirus. In addition, EBOV disease (EVD) survivors from West Africa have antibodies against the Delta peptide. Therefore, we hypothesize that the Delta peptide has an important role as a viroporin in EVD pathology. Here we show that a peptide corresponding to the serum-stable, conserved C-terminal sequence of Delta peptide permeabilizes and kills nucleated mammalian cells, and potently increasing ion permeability across synthetic lipid bilayers. Importantly, this permeabilizing activity is eliminated by the reduction of the disulfide bond between conserved cysteines. We conclude that EBOV Delta peptide does not form large unregulated pores through membranes, but rather increases ionic permeation, which is similar to other viroporins. By this mechanism, it could contribute to EVD pathology in human through vascular leakage, enterotoxic effects, or other cytotoxic pathways.

KINETICS OF NEUTROPHILS IN HEALTHY AND SIV-INFECTED RHESUS MACAQUES

He Z*, Allers CH**, Fujioka H****, Didier ES***, Kuroda MJ**

*BMS Program, School of Medicine, Tulane University, New Orleans, LA **Division of Immunology, Tulane National Primate Research Center, Covington, LA ***Division of Microbiology, Tulane National Primate Research Center, Covington, LA ****Center for Computational Science, Tulane University, New Orleans, LA

We previously showed that macrophages, in addition to CD4+ T cells, play critical roles in the development of AIDS in macaques. Neutrophils are the most abundant leukocytes in peripheral blood and play important roles in host immunity. Therefore, we aimed to study the kinetics and turnover of this large leukocyte subset as a basis to begin to determine the role of neutrophils in AIDS disease pathogenesis using the SIV/macaque model. The kinetics of neutrophils were evaluated using in vivo Bromodeoxyuridine (BrdU) pulse-chase analyses in both healthy and SIV-infected rhesus macaques. We first defined neutrophils in blood as HLA-DR^{-}, CD14^{dim}, CD3^{-}, CD20^{-} from the forward and size scatter, and this was further confirmed by myeloperoxidase staining. Mathematical model was applied to estimate target cells kinetics and daily production. Interestingly, both neutrophils and monocytes showed a similar half-life of 1.63±0.16 and 1.01±0.15 days, respectively. The production of neutrophils and monocytes was calculated as 1.42x10^{9} cells/L/day and 3.09x10^{8} cells/L/day. The kinetics of the neutrophils precursors in bone marrow were also analyzed. During SIV infection, no significant change in the neutrophils kinetics was observed at the acute stage and we are currently analyzing neutrophils kinetics during the chronic phase as well as during progression to AIDS. Our study demonstrated the following: 1) Massive production of neutrophils in the uninfected control macaques suggested a continuous need for replenishing these cells during steady state. 2) Maturation in the bone marrow required approximately 5-6 days before neutrophils were released into the circulation which may explain why the major cell subset in bone marrow is comprised of neutrophils. 3) Neutrophils may have limited effect during SIV acute infection. Preliminary results also suggested that turnover of neutrophils was independent of monocyte turnover during AIDS progression suggesting their individual roles during AIDS development.

This work was supported by grants from National Institutes of Health (NIH) AI097059, HL125054, AI091501 and AI110163 and P51OD011104 to the Tulane National Primate Research Center.

Pioglitazone Improves Neuronal Health After Cavernous Nerve Injury Via Insulin Growth Factor-1

Daniel J Heidenberg, Nora Haney, Bashir Rezk, Sudah Talwar, Samuel Okpechi, Matt Honda, Bryant Song, Kevin Swann, Salah Awadallah, Kenneth J DeLay, Suresh Sikka, Asim Abdel-Mageed, Phillip J Kadowitz, Wayne JG Hellstrom

Department of Urology, Tulane University School of Medicine, New Orleans, LA 70112, USA

Purpose: To investigate the mechanism of action of pioglitazone on the pelvic ganglion neurons and cavernous nerve in a rat model of bilateral cavernosal nerve crush injury (BCNI), in order to determine a clinically exploitable pathway to treat post-prostatectomy erectile dysfunction.

Methods: 26 Sprague-Dawley rats weighing 350-400 grams were divided into four groups: (a) sham procedure, (b) BCNI, (c) BCNI + postsurgical pioglitazone (Pio), (d) BCNI + Pio + JB-1, an Insulin-Growth Factor-1 (IGF-1) antagonist (JB). Sham and BCNI-only rats were treated with phosphate-buffered saline (PBS), and both Pio and JB rats received 14 days treatment of 6.5 mg pioglitazone. The PBS and pioglitazone were administered by oral gavage. Sham, BCNI only and Pio rats had osmotic mini pumps placed subcutaneously, which delivered saline. JB rats received 100 mg/kg JB-1 trifluoroacetate salt dissolved in saline, delivered by subcutaneous osmotic mini pump. After treatment, animals underwent surgery for endpoint cavernosal response to define hemodynamic parameters of erectile function, reported as the ratio of intracavernosal pressure to mean arterial pressure. The Major Pelvic Ganglions (MPG) and cavernosal nerves were resected at 2 weeks in all rats and processed for Western blot and immunohistochemistry to examine neuronal nitric oxide synthase (nNOS), IGF-1, ERK ½, IGF-1R.

Results: Animals treated with pioglitazone after BCNI experienced improvements in the ratio of intracavernosal pressure to mean arterial pressure, with the Pio group achieving results similar to the sham group. Animals treated with JB-1 in addition to Pioglitazone after BCNI achieved results similar to BCNI only. At 7.5 V, the ICP/MAP data reveals sham, 0.627; BCNI, 0.294; Pio, 0.582; JB, 0.286 ($P < .05$). Both 5V and 2.5 V showed similar results. Western blot and immunohistochemistry results support the surgical data and indicate that PGZ's positive effects are mediated by intercellular IGF-1 mediated activity.

Conclusion: JB-1 reverses the positive effects of pioglitazone on erectile function in rats undergoing BCNI, indicating that pioglitazone acts through IGF-1.

MUTATOR PHENOTYPE OF DNA POLYMERASE EPSILON MUTANTS IN CANCER: CRISPR/CAS9 CELL LINE GENERATION

Hodel KP*, Pursell ZF*
*Department of Biochemistry and Molecular Biology, Tulane University School of Medicine, New Orleans, LA,USA

The bulk of nuclear DNA synthesis during replication of the eukaryotic genome is carried out by three DNA polymerases: Pols α, δ, and ε. Through its role in leading strand synthesis, Pol ε is responsible for replicating up to half of the genome. As such, DNA synthesis errors made by Pol ε during replication pose a considerable source of potential genomic mutagenesis. Exonuclease domain mutations in Pol ε in human endometrial, colorectal and brain cancers are associated with significantly elevated genomic mutation burdens, in some cases exceeding 500 mutations per Mb. Proofreading and post-replication mismatch repair activities normally help to prevent subsequent fixation of these errors into novel mutations. By the time tumors defective for these activities are detectable, however, they have acquired more than 10,000 exomic mutations, complicating efforts to understand the relative contributions of each pathway toward genome stability.

To address this, we used CRISPR/Cas9 to inactivate Pol ε proofreading in mismatch repair-proficient and -deficient human cell lines. In the absence of mismatch repair, proofreading deficiency in a single polymerase allele caused a large and rapid increase in a unique mutation signature, consistent with what has been suggested by tumors from patients with biallelic mismatch repair deficiency (bMMRD). Somewhat surprisingly, restoration of mismatch repair was sufficient to suppress the explosive overall mutation accumulation. However, the appearance of the unique proofreading-deficient mutation signature itself was not suppressed. These results provide support for the idea that variability in mismatch repair efficiencies can help drive somatic evolution in tumors and yield novel insight into the mechanisms of how replication infidelity contributes to tumor development.

THE EFFECT OF MEDIA TYPE ON NERVE PRESENCE IN CULTURED MICROVASCULAR NETWORKS WITH BLOOD VESSELS AND LYMPHATICS

Nicholas A. Hodges, Ryan W. Barr, Walter L. Murfee
Department of Biomedical Engineering, Tulane University, New Orleans, LA

Introduction: Neurovascular patterning represents an emerging area of microvascular research and is critical for tissue remodeling. While overlapping molecular signals highlight links between angiogenesis and neurogenesis, advancing our understanding of their spatial and temporal coordination is limited by a lack of *in vitro* models that contain both systems. One such potential model is the rat mesentery culture model, which our laboratory has recently introduced as an *ex vivo* tool to investigate cellular dynamics during angiogenesis and lymphangiogenesis in an intact microvascular network scenario. The objective of this study was to evaluate the effect of media type on the maintenance or growth of nerve presence in the rat mesentery culture model.

Materials and Methods: Adult male Wistar rat mesenteric tissue windows were harvested, rinsed in sterile DPBS and media and then cultured per media group: 1) neural basal media (NBM), 2) NBM with 20ng/mL nerve growth factor (NGF), and 3) NBM with NGF and 20% fetal bovine serum (FBS). On day 3 tissues were labeled for PECAM and class III β-tubulin or PECAM and NG2. Unstimulated (not cultured) tissues were also labeled as a control group. Nerve presence was quantified by the ratio of network feeding arterioles with nerve alignment to the total number of arterioles.

Results and Discussion: PECAM labeling in uncultured and cultured tissues identified arterioles, venules, capillaries and lymphatic vessels. In class III β-tubulin labeled tissues, nerve presence along feeding arterioles was decreased for the culture groups (NBM: 0.03 ± 0.03; NBM + NGF: 0.35 ± 0.11; NBM + NGF + 20% FBS: 0.38 ± 0.08) compared to the uncultured day 0 control group (0.91 ± 0.04). The addition of NGF and NGF + FBS caused an increase in nerve presence versus the NBM only group. Interestingly for the NG2 labeled tissues, nerve presence along feeding arterioles in media groups was not significantly different than the uncultured group.

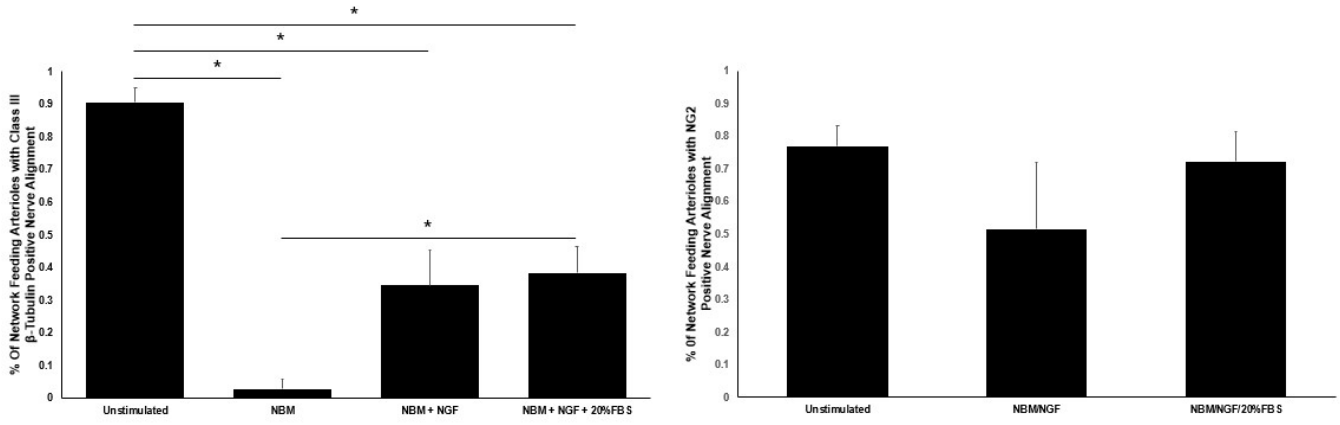

Figure 1. Quantification of the ratio of network feeding arterioles with nerve alignment. Left: Nerves were labeled with class III β-tubulin. Right: Nerves were labeled with NG2. * represents a significant difference ($p < 0.05$).

Conclusions: The results from this study support that media type can influence nerve presence in cultured microvascular networks and suggests that nerves undergo differentiation.

Acknowledgements: This work was supported by NIH 5-P20GM103629-04 to W.L.M.

OUTER MEMBRANE VESICLES DERIVED FROM *BURKHOLDERIA* POSSESS BROAD-SPECTRUM ANTIMICROBIAL PROPERTIES

Hoffmann JP*, Baker SM*, Morici LA*

*Department of Microbiology and Immunology, Tulane University School of Medicine, New Orleans, LA

As bacteria continue to rapidly evolve new mechanisms of drug resistance, there is an urgent need for novel strategies to treat them. Outer membrane vesicles (OMVs) are naturally produced by all Gram-negative bacteria and are formed when a small section of the outer membrane buds off as a nano-sized particle. Previous studies have shown that OMVs display bacteriolytic activity against both Gram-negative and Gram-positive bacteria. Here, we pursued the use of OMVs as a novel antimicrobial by investigating the potential bacteriolytic properties of OMVs derived from the soil bacterium, *Burkholderia thailandensis*. First, we used a Kirby Bauer-like assay and broth serial dilution assay to examine the bacteriolytic activity of OMVs *in vitro* against both Gram-positive and Gram-negative bacteria. OMVs were also tested for their ability to degrade purified peptidoglycan *in vitro*. Next, we used liquid chromatography-mass spectrometry (LC-MS) to identify putative OMV components that could confer bacteriolytic activity. Lastly, zymography was performed using both whole autoclaved cells and purified peptidoglycan as a substrate to further elucidate the proteins responsible for antimicrobial activity. We found that *B. thailandensis* OMVs significantly inhibited the growth of Gram-negative and Gram-positive bacteria, including drug resistant *Acinetobacter baumannii* and *Staphylococcus aureus,* in both broth culture and Kirby Bauer assays. We also demonstrated that OMVs degraded purified peptidoglycan in a dose dependent manner. LC-MS analysis identified nine putative enzymes with potential lytic activity. Zymography assays and gene knock-out studies are underway to further examine the bacteriolytic properties of each identified enzyme. In conclusion, OMVs derived from *B. thailandensis* possess antimicrobial properties against drug resistant bacteria. Numerous OMV enzymes potentially confer these properties and represent an untapped resource of novel antibiotics.

Acute predator threat induces sex-specific hippocampal plasticity and contextual fear generalization.

Homiack DR* and Schrader LA*,**

* Brain Institute, ** Cell and Molecular Biology, Tulane University New Orleans, LA

Post-traumatic stress disorder (PTSD) is characterized by the development of paradoxical memory disturbances characterized by powerful, intrusive memories with concurrent amnesia for details of the traumatic experience. However, in spite of evidence that women are at higher risk to develop PTSD, most animal research has focused on the processes by which male rodents develop adaptive fear memory. As such, the mechanisms which underlie the development of PTSD-like memory disturbances are poorly understood, particularly with respect to the female brain. In this investigation, we exposed adult male and female Wistar rats to the synthetic alarm pheromone 2,4,5-trimethylthiazole (TMT) to assess the activation of signaling cascades associated with hippocampus-dependent long-term memory and the development of generalized fear behavior.

Expression of phosphorylated CREB (S133), but not total CREB was dramatically reduced immediately following 30 minute TMT exposure throughout the male, but not the female hippocampus. Consistent with activation of the previously described CREB shut-off cascade, we also observed inactivation of ERK/MAPK and nuclear translocation of Jacob in the male hippocampus. Follow-up experiments showed that TMT exposure dampens glutamate reuptake, which may contribute to activation of the CREB shut-off cascade. To probe the long-term behavioral effects of predator odor exposure, we designed a novel predator odor context discrimination paradigm to assess the ability of TMT-exposed Wistar rats to distinguish between threat-associated and neutral contexts. We report that TMT-exposed female rats exhibited context discrimination impairments relative to TMT-exposed male rats, suggesting the intriguing possibility that females are more susceptible to developing generalized fear behavior following predator threat.

Funding: NSF grant - IOS 1146853

Louisiana Board of Regents LEQSF (2012-17) – GF-15

Tulane University Neuroscience Bridge Funding

A Novel Computational Model of the Carotid Artery to Determine Fluid Dynamic Effects on Atherosclerotic Plaque Instability

Hymel SJ*, Cosgrove KM**, Woods TC***, Bazan HA** and Khismatullin DB*
* Department of Biomedical Engineering, School of Science and Engineering, Tulane University
** Section of Vascular/ Endovascular Surgery, Department of Surgery; Ochsner Clinic
*** Department of Physiology and the Tulane Heart & Vascular Institute, School of Medicine, Tulane University

Atherosclerotic plaque progression within the carotid artery is thought to be due to a combination of a pro-inflammatory state and various hemodynamic conditions, including wall shear stresses (WSS) and volumetric strain. We aimed to create a computational model of the carotid from non-invasive imaging scans to evaluate the effects exerted by fluid dynamics on plaque composition and geometry. A computational model was created from an institutional database of patients who underwent carotid endarterectomy (CEA). Patients underwent duplex ultrasonography (DUS) and computed tomography angiography (CTA) of the carotid prior to intervention. CTA images were evaluated in a 3D-imaging software for vessel and plaque geometry; plaque composition was based on Hounsfield units (HU) from CTA scans. The geometrical data was then transported into a 3D-processing software (ScanIP+FE), wherein a patient-specific computational mesh was created. This mesh was then transferred to a Multiphysics software where a model was created from the mesh. The velocity curves, obtained from DUS of the common (CCA), internal (ICA) and external (ECA) carotid artery were used to set as the physiological boundary conditions of the vessel. In order to evaluate velocity streamlines by time, we ascertained the WSS and volumetric strain along the carotid artery where the model was subjected to dynamic fully-coupled, fluid-structure time-simulation through one cardiac cycle. 3D-geometry analysis revealed the different mass densities in the ICA plaque. Here, we present a comparison of 10 patients with > 80% carotid stenosis who were acutely symptomatic (n=5) or asymptomatic (n=5). Time-dependent analysis of patient-specific computational models demonstrated increased velocities in the stenotic portion and incremental increases in WSS along the ICA lesion. The highest WSS was located at the site of the greatest plaque burden during the peak velocity of the cardiac cycle which is seen in the shoulder region of the ICA depending on the structure and location of the patient's plaque. Volumetric strain was found to be lowest at the site of the greatest stenosis, related to the highest degree of calcification, due to less deformation and higher material density of the plaque. Within the central region of the plaque, the maximum strain occurred at maximum systolic velocity; however, only certain sections of the plaque had greater deformation depending on the material composition of that region, then returned to minimum strain with respect to the rest of the model. Each patient has different plaque geometry and material properties, which affect the regions of the highest WSS and lowest volumetric strain. Based on our model, we hypothesize that these variances will affect the stability of the plaque with the change in the dynamics of the plaque region. Time-dependent fluid simulations from this novel model adds to previously validated results from prior computational models in biomedical engineering. The benefit of a patient-specific model creation has the potential to compare changes in WSS and volumetric strain at various points across individual carotid plaques, along with predicting plaque rupture and stroke in the future.

Research reported in this publication was supported by National Institutes of Health (R01HL127092 and U54GM104940) and the SVS Clinical Seed Grant 2014 'Biomarkers in Carotid Disease' (HAB).

THE INTERGENERATIONAL IMPACT OF MATERNAL ADVERSE CHILDHOOD EXPERIENCES ON INFANT CELLULAR STRESS AND AUTONOMIC STRESS REACTIVITY: FROM THE PLACENTA TO THE INFANT

Jones CW*, Esteves KC**, Theall KP***, Drury SS*,**

*Tulane Brain Institute, Tulane University, New Orleans, LA

**Department of Psychiatry, Tulane University School of Medicine, New Orleans, LA

***Department of Global Community Health and Behavioral Sciences, Tulane University School of Public Health and Tropical Medicine, New Orleans, LA

Adverse Childhood Experiences (ACEs) have a negative impact on biological, physiological, and psychological functioning that can persist across the lifespan and across generations. Exposure to a high number of ACEs predicts stress and age-related chronic disease within the individual, in part through epigenetic and/or stress-related physiological mechanisms. Further, ACE exposure is associated with negative early parenting and birth outcomes, yet the intergenerational impacts of ACEs on biological and physiological pathways in the offspring of ACE exposed individuals remains understudied. To address this gap, this study explored the impact of maternal ACEs on markers of cellular stress indexed by telomere length (TL), across four fetally-derived tissues of the human placenta and longitudinal buccal TL across the first 18 months of life. Additionally, the impact of maternal ACEs on infant autonomic stress reactivity, indexed by respiratory sinus arrhythmia (RSA), at four months of age was explored. RSA is a measure of heart rate variability where increased RSA in response to a stressor connotes increased parasympathetic influence on the heart to mitigate the stress response. Given the established race differences in TL, where Black individuals exhibit longer initial TL than White individuals and the opposite relationship in placental TL, we explored racial differences in all analyses. Crude differences between high and low maternal ACEs (high >4 exposures) from N=51 placentas (N=204 placental tissue samples) revealed decreased TL depending on tissue tested (p=0.12 to p=0.001). When controlling for relevant covariates, high maternal ACEs significantly predicted decreased TL across all tissues (β=-0.09; p=0.05) and placentas from White pregnancies exhibited longer TL than Black pregnancies at trend level (β=-0.10; p=0.07). Longitudinal assessments of TL in DNA extracted from buccal swabs at 4, 12, and 18 months of age revealed shorter TL in the high ACE group in Black infants (β=-0.24; p=0.07) and longer TL in White infants in the high ACE group (β=0.29; p=0.06). Assessment of infant autonomic stress response revealed that high ACEs predicted lower RSA (β=-0.100; p=0.010), suggesting greater parasympathetic nervous system withdrawal during a dyadic stressor. There was some evidence that this effect was driven by Black infants (β=-.15; p=.01), instead of White infants (β=-.06, p=.38).These findings indicate that maternal exposure to a greater number of early life adversities, prior to conception, is associated with differences in both cellular stress and autonomic stress reactivity in the next generation across a range of different tissue types. Altered autonomic stress reactivity, evidenced by parasympathetic withdrawal (e.g. decreased RSA during a stressor), suggests that the same stress-related physiological mechanisms impacted by high ACE exposure within the mother is also found within her infant during the first years of life. This study suggests that maternal ACE exposures are transmitted across generations not only through the impact on birth outcomes and parental mental health and behavior, but also through biological stress systems. These findings highlight the need to develop interventions targeting these high risk mothers during pregnancy and the first years of life to mitigate the biological impact on infants during critical periods of development.

This work was supported by the Altria Foundation and NIH R01MH101533 (SSD).

BIOCHEMICAL AND MOLECULAR STUDIES ON ARGININE METABOLISM IN *AEDES AEGYPTI* FEMALE MOSQUITOES, VECTORS OF SEVERAL HUMAN DISEASES

Joseph V*, Petchampai N*, Isoe J**, Scaraffia PY*

*Department of Tropical Medicine and VBIDRC, Tulane University, New Orleans, LA, USA **Department of Chemistry and Biochemistry, The University of Arizona, Tucson, AZ, USA.

Mosquitoes are vectors of tremendous medical importance. In recent years, the population of *Aedes aegypti* has spread significantly increasing the risk of pathogen transmission in human populations. The implementation of effective strategies for controlling mosquito populations requires a better understanding of mosquito metabolism. Mosquitoes lack a gene encoding ornithine transcarbamylase, also called carbamoyltransferase. Therefore, they do not have a functional urea cycle for ammonia disposal, such as the one present in most terrestrial vertebrates, which converts arginine into an essential amino acid in mosquitoes. In addition to the degradation of uric acid for urea synthesis by an amphibian-uricolytic pathway, mosquitoes can synthesize urea by a reaction catalyzed by arginase, which is active but independent of a urea cycle. Arginase uses arginine, either provided in the diet or from turnover of endogenous proteins, to produce ornithine and urea. It was previously reported that both metabolic pathways, uricolysis and argininolysis, are tightly regulated by a unique cross-talk signaling mechanism. Since this sophisticated metabolic regulation of urea affects the fixation, assimilation, and excretion phases of ammonia metabolism, as well as the synthesis and /or excretion of other nitrogen waste products, we are interested in expanding our current understanding of arginine metabolism in mosquitoes. By using qRT-PCR, we analyzed arginase and ornithine decarboxylase (ODC) transcript expression in mosquito tissues dissected from sugar- and blood-fed females. Our results indicate that each gene is differentially regulated in response to blood feeding, showing specific patterns in each tissue during a gonotrophic cycle. Additionally, we monitored the effect of silencing ODC by using a specific inhibitor. Chemical inhibition of ODC significantly impairs mosquito behavior and decreases mosquito survival. Furthermore, ovary development is severely affected, oviposition is delayed and the number of eggs laid by those females treated with an ODC inhibitor is significantly reduced. Taken together, our data suggest that arginine plays several key roles in blood-fed mosquitoes.

This work is supported by NIH/NIAID Grant R01AI088092 (to PYS).

RNA-BINDING MOTIF PROTEIN 10 REGULATES p53 DEPENDENT APOPTOSIS AND CELL GROWTH ARREST

Jung JH[*], Zeng SX[*], and Lu H[*]

[*]Department of Biochemistry & Molecular biology, and Tulane Cancer Center, Tulane University School of Medicine, New Orleans, LA, USA

RNA-BINDING MOTIF PROTEIN 10 **(**RBM10), also called S1-1, is an RNA-binding protein frequently deleted or mutated in lung cancer cells. Recent reports indicate that knockdown of RBM10 in human cancer cells enhances growth of mouse tumour xenografts suggesting that RBM10 acts as a tumour suppressor. RBM10 also regulates alternative splicing and control cancer cell proliferation. However, the underlying molecular mechanisms remain unclear. Here, our group for the first time reports that RBM10-induced apoptosis and inhibited cell proliferation are partially dependent on p53. Overexpression of RBM10 decreased cancer cell proliferation and also induced apoptosis through the caspase family proteins. Furthermore, overexpression of RBM10 increased p53 stability and decreased p53 ubiquitination. Consistently, knockdown of RBM10 decreased p53 stability. RBM10 also bound to p53 and MDM2 via the N-terminal domain of MDM2 and inhibited p53-MDM2 interaction. Intriguingly, RBM10 is not required for p53 activation by chemotherapy drugs, such as doxorubicin, actinomycin D, and 5-FU. Analysis of cancer genomic databases reveals that patients with wild type RBM10 and p53 survive longer than do those with mutated p53 or less RBM10. Together, our results demonstrate that RBM10 plays a critical role in cancer cell proliferation and apoptosis through the regulation of MDM2 and p53.

This work was supported in part by NIH-NCI grants R01 CA095441, R01CA172468, R01CA127724, and R21 CA190775 to Hua Lu.

Identification of novel peptide sequences with improved nuclear delivery of peptide nucleic acids (PNAs)

W. Berkeley Kauffman, William Wimley

Peptide Nucleic Acids are DNA mimics featuring a peptide-like backbone and nucleobases that bind nucleic acids, are capable of impacting gene expression, are resistant to degradation, and show promise as therapeutic agents. Although PNAs are cell-impermeant and intracellular delivery has been a challenge, cell-penetrating peptides show some promise as delivery vehicles. To improve nuclear PNA delivery we have constructed a library of 8192 unique peptide sequences based on the well-known cell penetrating peptides Tat and Penetratin. These sequences are covalently linked to the N-terminus of an 18-residue PNA sequence (PNA705) that blocks an aberrant splice site in a recombinant luciferase gene (pLuc705) stably expressed in Hela cells thereby correcting its function. A live cell screen of the library peptides has generated several PNA Delivery Peptides (PDEPs) capable of delivering PNA705 to the nucleus of Hela705 cells with greater efficiency than the well-known cell penetrating peptides used as a basis for the screen. As varying the PNA sequence will change the nucleic acid target without changing its physicochemical properties significantly, we envision these PDEP sequences serving as delivery vectors for therapeutically beneficial PNA sequences in cell based systems. This will provide researchers with a valuable tool moving forward and has the potential for significant translational value.

Targeted Degradation of AR and its Spliced Variant AR-V7 by the Phytochemical Sulforaphane: New Therapeutic Opportunity for Prostate Cancer

[1,3]Namrata Khurana, [1]Hogyoung Kim, [2]Partha K. Chandra, [1]Sudha Talwar, [3]Pankaj Sharma, [1]Asim B. Abdel-Mageed, [#,1]Suresh C. Sikka, [#,2] Debasis Mondal

Departments of [1]Urology and [2]Pharmacology, Tulane University School of Medicine, 1430 Tulane Avenue, New Orleans, LA 70112, USA.

[3]Amity Institute of Biotechnology, Amity University, Noida, U.P. 201313, India.

Abstract

Androgen deprivation therapy (ADT) suppresses the growth of prostate cancer (PC) cells expressing the ligand-dependent full length androgen receptor (AR-fl). However, the recurrence of castration resistant prostate cancer (CRPC) can occur due to the induction of constitutively active (ligand-independent) AR splice variants, particularly AR-V7. Therefore, strategies to suppress both AR-fl and AR-V7 levels will be of significant therapeutic benefit in CRPC patients. Our previous published studies showed that sulforaphane (SFN), an isothiocyanate phytochemical, can enhance the rate of degradation of AR-fl in several PC cell lines, e.g. LNCaP and C4-2B. In the current study, we monitored the efficacy of SFN in targeting both AR-fl and AR-V7 levels in the CRPC cell line, CWR22RV1 (22RV1). As compared to LNCaP and C4-2B cells, the AR-V7- expressing 22RV1 cells were significantly ($p<0.05$) more resistant to the potent anti-androgen, enzalutamide (ENZ). However, co-exposure to SFN (5-25 μM) significantly ($p<0.01$) enhanced the efficacy of ENZ, as evident from MTT cell-viability assays and scratch-wound migration assays. Western immunoblot studies showed that SFN decreases the half-life of both AR-fl and AR-V7 proteins ($p<0.01$). Immunofluorescence microscopy (IFM)

showed that SFN treatment down-regulated both cytosolic and nuclear AR levels, and Enzyme linked immunosorbent assays (ELISA) demonstrated decreased expression of the AR-regulated protein, prostate specific antigen (PSA). The SFN-induced degradation of both AR-fl and AR-V7 proteins was linked to increased protein ubiquitination and proteasomal activity in the 22RV1 cells. Previous studies have shown that SFN can inhibit the chaperone activity of heat-shock protein 90 (HSP90) and induce the potent antioxidant transcription factor, Nuclear factor erythroid-2-like 2 (Nrf-2). Therefore, we investigated whether combined exposure of clinically approved drugs that inhibit HSP90 (e.g. Ganetespib) and activate Nrf-2 (e.g. Bardoxolone-methyl) can similarly suppress AR levels in 22RV1 cells. Indeed, co-exposure to low physiologic doses (<1 μM) of Ganetespib and Bardoxolone-methyl caused rapid degradation of both AR-fl and AR-V7. Most importantly, co-exposure to this safe pharmaceutical combination augmented the efficacy of ENZ, and decreased both cell viability and migration of 22RV1 cells in vitro. Therefore, the multimodal actions of SFN can cause rapid decrease in both AR-fl and AR-V7 protein levels in 22RV1 cells. Our findings also implicated that a combination of HSP90 inhibitor (Ganetspib) and Nrf-2 activator (Bardoxolone-methyl) may be an effective adjunct to current ADT in CRPC patients, especially those expressing AR-V7.

Using Tulane Student-Run Clinics to Fight the Growing Hepatitis C Epidemic

Kim MM*, Counts CR**, McClung E**, Preston SC*, Lee F*, McGonigle KM*, Nix LM*, Carley TF*, Mallya S*, Kanter J***

*Tulane University School of Medicine, New Orleans, LA
**Department of Global Health Management and Policy, Tulane University School of Public Health and Tropical Medicine, New Orleans, LA
***New Orleans Department of Health, New Orleans, LA

Hepatitis C virus (HCV) is a major cause of liver disease worldwide and a considerable cause of morbidity and mortality. HCV disproportionately affects the disenfranchised, especially people of low socioeconomic status and those who inject drugs. Through our medical student-run HCV screening and treatment program, we sought to examine the prevalence of HCV in Orleans Parish, LA (New Orleans) and determine the impact of our program's current treatment cascade. Voluntary HCV screening using a HCV rapid antibody test began at the largest homeless shelter in New Orleans in March of 2015. Screening efforts expanded to six other homeless shelters, substance abuse rehabilitation centers, and free clinics throughout New Orleans. A number of important changes were made to progressive iterations of the testing protocols, including the addition of electronic information tracking, standardized client education sessions, and an improved treatment cascade. Since inception, over the course of 471 shifts totaling over 800 volunteer hours, 47 testers have performed 724 tests. Currently, patients that test positive for HCV antibodies are encouraged to participate in the program's treatment cascade consisting of a HCV RNA test, liver ultrasound, follow-up appointment with a primary care physician, and ultimately an appointment at the Viral Hepatitis Clinic to be considered for free/reduced-price treatment. The program focuses on the disenfranchised population in New Orleans, specifically the homeless, those with a history of substance abuse, and the formerly incarcerated. For a variety of reasons, these groups are at higher risk of HCV infection than the general population, and are therefore deserving of special consideration. A total of 665 individuals throughout New Orleans were screened. Approximately 25% of all screened clients initially tested positive, of those just under 50% have had their RNA confirmed, and slightly over 25% have obtained the necessary liver ultrasound. Thus far, five patients have started to receive curative treatment, and one patient has completed the treatment. HCV is a growing major health concern across the country. This student-run program demonstrates that New Orleans is currently suffering from epidemic proportions of this disease within specific disenfranchised populations. However, when concerted efforts are made, progress can be seen. This is a small program, with relatively little funding, however it's ability to have an impact has been substantiated. Given the current opioid epidemic facing the US and the growth of HCV as a result, more research is needed on how best to ensure that those with the disease receive efficient and effective care, while those at high risk of contracting HCV are adequately informed of preventative measures.

SINGLE NUCLEOTIDE POLYMORPHISM IN DLGAP2 AFFECTS CORTICAL WHITE MATTER VOLUME IN CHILDREN EXPOSED TO SEVERE PSYCHOSOCIAL DEPRIVATION

King JL*, Esteves K*, DeBoever P**, Drury SS*
*Tulane University School of Medicine, Psychiatry and Behavioral Sciences. New Orleans, LA
**Flemish Institute of Technology, VITO. Antwerp, Belgium

Background: Discs large homolog associated protein 2 (DLGAP2) is a gene that encodes SAP90/PSD-95-associated protein 2 (SAPAP2), a post-synaptic density protein commonly found at glutamatergic synapses. In previous studies genetic polymorphisms in DLGAP2 have been linked to severe mental illness such as autism and schizophrenia. White matter (WM) volume deficits are a common problem with these diseases, and DLGAP2 has been linked to WM deficits in autism. In other studies DLGAP2 has been found to interact with traumatic experiences to predict development of PTSD. Leveraging previous analyses that revealed DLGAP2 was both differentially methylated and exhibited differential salivary gene expression levels based on extreme differences in early caregiving this study explored whether single nucleotide polymorphisms (SNPs) in DLGAP2 were associated with WM in subjects enrolled in the Bucharest Early Intervention Project (BEIP). The BEIP, conducted entirely in Romania, is a randomized control trial examining the impact of foster care compared to institutional care on child development that included a control group of children without exposure to institutional care. Children from several institutions in Bucharest were randomized to be placed in the foster care group (FCG) or remain in institutions as the care as usual group (CAUG). Community controls not in an institution constituted the never institutionalized group (NIG).

Methods: A subset of 74 BEIP individuals (29 CAUG, 25 FCG, and 20 NIG) between the ages of 8-11 years (avg. 9.8 years) received T1-weighted MRI scans on a Siemens Magnetom Avanto 1.5T syngo system with a 16-channel head coil and total cortical WM volume was determined with the FreeSurfer image analysis suite. Individuals were genotyped for three SNPs in DLGAP2 (rs2301963, rs2235112, and rs2293909), selected based on allele distribution and previous findings in the literature. SNP genotyping was performed using TaqMan SNP Gentoyping Assays from ThermoFisher Scientific. Initial allele frequencies were examined for Hardy-Weinberg Equilibrium (HWE) and compared to expected frequencies from the NCBI data base. The association between genotype and total cortical white matter volume was examined. Data was analyzed using SAS 9.3.

Results: Genotypes did not deviate from HWE with allele frequencies that were similar to previous studies and reported allele frequencies in the NCBI data base. Genotype was not significantly different between caregiving groups, and was not associated with DNA methylation or gene expression. Previous analyses revealed significant group and sex differences in WM. Genotype did not significantly predict WM, however within females there was a significant interaction between genotype and caregiving group. Specifically within females there was no group difference in WM for those that were not AA at rs2235112. However in females with the AA genotype at rs2235112, group remained significant suggesting that the impact of institutional care on total WM within the BEIP subjects was driven by the effect within AA females. No group or genotype differences were found in males.

Conclusions: Negative early life experiences have significant, lasting effects on the brain. Individuals with certain genetic polymorphisms may be more at risk than peers with without these genetic markers.

Funding: Bill and Melinda Gates Foundation Grand Challenges Exploration and R21 MH094688-01

IMPACT OF MICROBIOME MANIPULATION ON AGE-RELATED MICROBIAL COMMUNITY ALTERATIONS AND IMMUNE SYSTEM DYSFUNCTION

Kodroff LH*, Norton EB*

*Department of Microbiology and Immunology and Tulane Center for Aging, Tulane University School of Medicine, New Orleans, Louisiana

Aging is associated with high levels of chronic inflammation and declining immune function. Gut microbiota may impact this process as the composition is altered with both disease and old age. Toll-like receptors (TLRs) recognize pattern associated molecular patterns, such as those found on intestinal bacteria, and play an important role in activating immune responses. We examined whether administration of exogenous gut microbiota from young animals could improve dysbiosis and impaired immune functioning, including TLR expression, in older mice. To test this in two experiments, after antibiotic administration (Exp. A) with ampicillin in drinking water, young (14 weeks), middle-aged (50 weeks), and old (100 weeks) were fed either young fecal material or PBS by oral gavage; (Exp. B) or with a cocktail of antibiotics in drinking water, old mice were fed either old or young fecal material. Three weeks after this fecal microbiota transplant (FMT) mice were euthanized and spleens were harvested for flow cytometric analysis of immunologic markers. Fecal material was collected from individual mice throughout the duration of the experiments and analyzed for microbial communities by 16S rRNA gene sequencing.

In Exp. A, antibiotics effectively lowered the concentration of bacterial DNA in the fecal material. FMT also altered microbial community structure and diversity in older mice. After being treated with antibiotics, the differences between groups treated with PBS or FMT were most pronounced in the oldest age group. In Exp. B, difficulties were encountered getting mice to drink the antibiotic cocktail, which the mice found unpalatable (likely impacting ability of FMT to successfully colonize intestines). Regardless, in both Exp. A and Exp. B, TLR2 and TLR4 expression on immune cells was differentially altered based on age, FMT, or type of antibiotic treatment. These studies help determine if manipulation of the gut microbiome can reverse age-related immune dysfunction and become a therapeutic treatment to improve immunity in older populations.

This work was supported in part by NIH COBRE grant (P20 GM 103629**)**

FORMULATIONS FOR DRUG DELIVERY THROUGH THE MAMMARY PAPILLA

Kurtz SL*, Lawson LB**

* Bioinnovation PhD Program, Tulane University, New Orleans, LA
** Department of Microbiology and Immunology, Tulane University School of Medicine, New Orleans, LA

Breast cancer is the most frequently diagnosed cancer and the second leading cause of cancer-related deaths in women. Of patients diagnosed with breast cancer, the fastest growing subtype is ductal carcinoma in situ (DCIS) or Stage 0 disease. In DCIS patients, cancer cells remain localized within the ducts or lobules of the breast. The ducts form an expansive tree-like structure that extends throughout the entire breast and may serve as a conduit for local delivery of therapeutics. Targeting drug action at the site of disease would eliminate side effects associated with systemic treatments. This study examines how liposomal formulations influence delivery through the nipple using a model hydrophilic dye, Sulforhodamine B (SRB), and a model lipophilic dye, Nile Red (NR). A porcine nipple was positioned in a Franz diffusion cell and the formulations were applied topically. With equivalent dye concentrations applied to the donor surface, we noted higher permeation into and through the nipple with SRB (hydrophilic) as compared to NR (lipophilic) after 48 hours. However, when we further looked at the distribution of each dye within the tissue using fluorescence microscopy, we saw a distinction in the amount of dye in the duct versus the surrounding tissue. Fluorescence micrographs show that lipophilic NR is retained within the ducts while the hydrophilic SRB diffuses throughout the entire tissue section, suggesting that hydrophobicity impacts the ability of molecules to diffuse from the duct into the surrounding tissue. This suggests that lipid-based carriers may be effective for delivery of cancer therapeutics or preventative agents targeting the mammary ducts, where DCIS is localized, rather than distribution throughout the breast tissue. We then assessed three different liposome formulations encapsulating SRB. The liposome compositions included neutral liposome, an ionic liposome, and a surface-modified liposome. After 3 hours, the neutral, non-surface modified liposomes were best able to penetrate into the tissue with ~45% retained in the tissue followed by surface-modified liposomes (~30%), ionic liposomes (~25%) and lastly, free SRB (13%). When the proportion of SRB within the tissue was analyzed as a function of tissue depth, our results suggest that not only are the neutral, non-modified liposomes penetrating the tissue more rapidly, but the SRB encapsulated within these liposomes is also deeper compared to other liposome formulations and free SRB. For these vesicles, vesicle diameter did play a role in dye transport as smaller (100 nm) liposomes showed increased permeation as compared to larger vesicles, while no size difference was found for other liposome compositions. Together, our results support the impact of liposome encapsulation for increasing transpapillary delivery efficiency.

PHOTOACOUSTIC IMAGING TO MEASURE PLACENTAL TISSUE HYPOXIA IN A PREECLAMPTIC STATE

Lawrence DJ*, Wu C*, Bayer CL*
*Department of Biomedical Engineering, Tulane University, New Orleans, LA

Preeclampsia is a disorder occurring in 5-8% of pregnancies characterized by hypertension and proteinuria. One of the initiating conditions of preeclampsia is placental hypoxia. Photoacoustic (PA) imaging is an imaging modality that can provide noninvasive, real-time images of physiological changes *in vivo*. PA imaging uses nanosecond pulsed light energy to generate images. Its contrast is derived from the absorption properties of native contrast agents, in this case oxy- and deoxy-hemoglobin. We performed PA imaging on a timed pregnant rat model to estimate placental oxygen saturation. The results were the oxygen saturation map overlaid on an ultrasound image of the anatomy. Using these techniques, we will induce preeclampsia with a reduced uterine perfusion pressure (RUPP) surgical model to observe the changes in placental oxygen saturation.

Chaperone-mediated autophagy compensates for impaired macroautophagy in the cirrhotic liver to promote hepatocellular carcinoma

Srinivas Chava[1], Christine Lee[1], Yucel Aydin [2], Partha K Chandra[1], Asha Dash[1], Milad Chedid[1], Swan N Thung [3], Krzysztof Moroz[1], Nabeen C Nayak [4], Tong Wu[1], and Srikanta Dash[1]

1-Department of Pathology and Laboratory Medicine, 2-Department of Medicine, Division of Gastroenterology and Hepatology,Tulane University Health Sciences Center, New Orleans, Louisiana, USA. 3-The Lillian and Henry M. Stratton-Hans Popper Department of Pathology, Icahn School of Medicine at Mount Sinai, New York, NY 10029, 4-Senior Consultant and advisor, Sir Ganga Ram Hospital, Department of Pathology, New Delhi, India, 110060

Hepatocellular carcinoma (HCC) is the most common primary liver cancer that develops in the background of liver cirrhosis and the mechanism is unclear. Autophagy is a cellular lysosomal degradation process that has been implicated in the pathogenesis of chronic liver disease, liver fibrosis and HCC. We have reported previously that most of the HCC express p62, compared to the surrounding non-tumorous cirrhotic liver suggesting impaired macroautophagy in HCC. Macroautophagy and chaperone-mediated autophagy (CMA) are two major lysosomal degradation processes and they often compensate for each other to improve cell survival. We performed this investigation to verify whether a compensatory mechanism between two forms of autophagy is involved in the survival of HCC in the cirrhotic liver. The expressions of macroautophagy flux (p62, glypican-3) and CMA flux (Hsc70, LAMP2A) were examined by immunohistochemical staining of paraffin embedded tissues sections of 46 cirrhotic livers with HCCs related to viral and non-viral etiologies. Glypican-3 and p62 protein expression was not detected in any of the normal livers. Of the 46 cirrhotic livers with HCC, 39 (84%) showed increased expression of p62 and 38 (82%) showed increased glypican-3 expression as compared to negative expression in 100% of adjacent non-tumorous hepatocytes suggesting impaired macroautophagy flux in HCC. The impaired macroautophagy was present among HCC of viral and non-viral etiologies. More than 95% of HCC showed increased expression of LAMP2A as compared to the surrounding non-tumorous cirrhotic liver, suggesting that CMA flux is induced in HCC. High level expression of glucose-regulated protein 78 (GRP78, BiP) and heat shock cognate protein (Hsc70) were detected in 100% of the HCC and adjacent non-tumorous cirrhotic livers, which suggests that unresolved ER-stress is associated with HCC risk in liver cirrhosis. Interestingly, inhibition of CMA by hydroxychloroquine (HCQ) induced expression of p53 tumor suppressor, and cellular apoptosis plus inhibited HCC growth, whereas autophagy induction by mTOR inhibitor (Torin1) promoted HCC growth. Conclusions: Results of this study indicate that the

activation of CMA compensate with the impaired macroautophagy to promote HCC survival in the cirrhotic liver.

Posttraumatic Stress Disorder associated with Hurricane Katrina Predicts Incident Cardiovascular Disease Events among Elderly Community-dwelling Adults

Zach Lenane, BA&Sc, Tulane University School of Medicine, Tulane University School of Public Health and Tropical Medicine
Erin Peacock, PhD MPH, Tulane University School of Medicine
Marie Krousel-Wood, MD MSPH, Tulane University School of Medicine, Tulane University School of Public Health and Tropical Medicine, Ochsner Health System

Introduction
Cardiovascular disease (CVD) is the leading cause of death among US adults and its prevalence is increasing, despite efforts to identify and address risk factors. Posttraumatic stress disorder (PTSD) has been identified as a potential risk factor for CVD, though the results to date have focused on male veterans with combat-related PTSD. To our knowledge, there are no prospective analyses/reports among older community-dwelling adults following Hurricane Katrina. The purpose of this study was to explore the link between PTSD associated with Hurricane Katrina and incident CVD among elderly adults using data from the Cohort Study of Medication Adherence among Older Adults (CoSMO).

Methods/Study Population
PTSD associated with Hurricane Katrina and incident CVD events were assessed among 2075 hypertensive participants age ≥65 who were enrolled in a managed care organization in southeastern Louisiana. Baseline surveys were conducted between August 2006 and September 2007. PTSD was assessed using the civilian PTSD CheckList (PCL-17) and two cut points, ≥37 and ≥44, for primary and secondary analyses, respectively. Participants were followed through February 2011 for a composite CVD outcome of MI, stroke, CHF, or CVD death. Multivariable logistic regression was performed with thirteen covariates identified in bivariate analysis: age, sex, race, marital status, education, hypertension knowledge, comorbidities, number of antihypertensive medication classes, dissatisfaction with healthcare, reduced medications due to cost, number of visits to healthcare provider in last year, depression, and coping.

Results
Participants were 59.8% female and 30.4% black, with a mean age of 75 years. The prevalence of PTSD using the primary and secondary cut points was 6.1% and 4.2%, respectively. In total, 240 (11.5%) participants had a CVD event during a median 3.8 year follow-up. After multivariable adjustment, the odds ratios and 95% confidence intervals (CI) for CVD event for the primary and secondary analyses were 1.90 (95% CI: 1.17, 3.09) and 3.74 (95% CI: 2.05, 6.81), respectively.

Conclusion/Discussion
PTSD following Hurricane Katrina was associated with an increased risk of incident CVD events among elderly adults. This finding from a prospective cohort study supports earlier reports suggesting PTSD is an independent risk factor for CVD. To our knowledge, this association has not been previously reported among a cohort of elderly community-dwelling adults. This study included hypertensive, elderly, insured participants living in southeastern Louisiana following Hurricane Katrina and may not be

generalizable to all people with PTSD. Strengths of this study include its longitudinal design, the identification of incident CVD, the diversity of the study population with respect to gender, race and CV risk, and reduced confounding due to access to care and insurance status. Future research is needed to confirm this finding in other populations and to assess if efforts to minimize the impact of PTSD following disasters reduce CVD risk and premature CVD events among older adults.

Conflict of Interest

The authors have nothing to disclose.

Research reported in this publication was supported by the National Center For Advancing Translational Sciences of the National Institutes of Health under Award Number TL1TR001418. The content is solely the responsibility of the authors and does not necessarily represent the official views of the National Institutes of Health.

INFLUENCE OF PHYSICIAN EMPATHY ON PERCEPTIONS OF INTERACTIONS

Lentz CJ*

*Molix Social Relations Lab, Tulane University School of Medicine, New Orleans, LA

Given the shift from paternalistic medicine, the relationship between the patient and physician has begun to play a much greater role in healthcare. Effective patient-physician relationships have led to improved health outcomes and decreased litigation. The present study aimed to examine the influence of empathy on patients' impressions of a physician and the estimated length of the visit. Empathy was manipulated via scripted patient-physician interactions. Participants randomly viewed one of five ostensible videos depicting an office visit between a patient and physician. Data for 69 participants, aged 18 to 64 who self-identified as Caucasian, Asian, Asian Indian, and African American, were collected. Following the video, participants completed a 41-item questionnaire to evaluate their perception of the physician and estimated length of visit. All empathy manipulations led to increased positive perception and longer estimated length of visit when compared to the neutral condition. The full MANOVA model was not significant but suggested that participants had higher positive perceptions and increased estimated length of visit in the condition with the physicians that used reflection/naming of the emotion. Limitations of the study, implications, and suggestions for further research were discussed.

Epigenomic Profiles Identify Age Associated Chromatin State Transitions in Nephron Progenitors

*Li Y, *Baddoo MC, *Liu J, *Saifudeen ZR, **Adli M, *El-Dahr SS
*Pediatrics, Tulane University, New Orleans, LA; **Biochemistry, University of Virginia, Charlottesville, VA.

Background: Cited1+/Six2+ cells are lineage-restricted multipotent nephron progenitor cells (NPC). Unlike young NPC, which are actively engaged in self-renewal and are resistant to inductive signals, old NPC differentiate at a faster rate limiting their life span. We hypothesized that “aging” alters the epigenomic landscape of NPC, which favors differentiation over renewal.
Methods: NPC were isolated using a magnetic activated cell sorting protocol from E13 and E19 CD1 mouse kidneys and expanded in NPEM growth factor medium for 48 hrs to generate pure Cited1+/Six2high NPC. To identify genome-wide open chromatin regions (OCR – nucleosome-free active promoters and enhancers), NPC were subjected in triplicates to ATAC-seq (Assay for Transposase-Accessible Chromatin with high throughput sequencing). Peak calling, annotation, transcription factor binding motifs and overlapping peaks between E13/E19 samples were performed using HOMER and iCis-Target. OCR were integrated with publicly available RNA-seq and ChIP-seq databases.
Results: We identified 956 and 1438 annotated genes carrying at least one OCR in E13 vs. E19 NPC, respectively, of which 5-7% are differentially expressed. OCR clustered around the transcription start site and at distant 5’ or 3’ or intragenic sites. Progenitor genes (e.g., c-Myc, Osr1, Six2, Meox1, Eya1, cell cycle and epigenetic regulators) featured age-related attenuation of OCR peak scores and density. Transcriptionally silent β-catenin target genes (e.g., Wnt4, Lef1, Axin2, Jag1, Pax8) consistently harbored OCR in curated enhancers as well as in novel candidate enhancers in old but not young NPC. AP-1, Six2, Sall1/2, WT1, Pax2, Smads, c-Myc, p53, and E2F were amongst the most commonly identified transcription factors in OCR footprints.
Conclusions: Young and old Cited1+ NPC exhibit distinct epigenomic landscapes. OCR footprints identified candidate networks of transcriptional regulators in NPC. Chromatin of old NPC displays biochemical signs of epigenetic poising which may explain, at least partly, the enhanced propensity of old NPC to differentiation vs. self-renewal.
Funding: NIDDK Support

Mutant p53 Gains Its Function via c-Myc Activation upon CDK4 Phosphorylation at Serine 249 and Consequent PIN1 Binding

Liao P[1,2], Zeng S[1,2], Zhou X[2], Chen T[3], Cao B[1,2], Jung J[1,2], Del Sal G[4], & Lu H[1,2]*

[1]Department of Biochemistry & Molecular Biology, [2]Tulane Cancer Center, and [3]Haywood Genetics Center, Tulane University School of Medicine; New Orleans, LA 70112, USA;
[4]Laboratorio Nazionale CIP, Area Science Park Padriciano and Dipartimento di Scienze della Vita, Universita degli Studi di Trieste, Trieste, Italy.

TP53 missense mutations significantly influence the development and progression of various human cancers via their gain of new functions (GOF) through different mechanisms. Here we report a unique mechanism underlying the GOF of p53-R249S (p53-RS), a p53 mutant frequently detected in human hepatocellular carcinoma (HCC) that is highly related to hepatitis B infection and aflatoxin B1. A CDK inhibitor blocks p53-RS's nuclear translocation in HCC, whereas CDK4 interacts with p53-RS in the G1/S phase of the cells, phosphorylates it, and enhances its nuclear localization. This is coupled with binding of a peptidyl-prolyl cis-trans isomerase NIMA-interacting 1 (PIN1) to p53-RS, but not the p53 form with mutations of 4 serines previously shown to be crucial for PIN1-binding. As a result, p53-RS interacts with c-Myc and enhances c-Myc-dependent rDNA transcription important for ribosomal biogenesis in the nucleus. Altogether, these results unveil a CDK4-PIN1-p53-RS-c-Myc pathway as a novel mechanism for the GOF of p53-RS in HCC.

This work was supported in part by NIH-NCI grants R01 CA095441, R01CA172468, R01CA127724, R21 CA201889-01A1, and R21 CA190775 to Hua Lu.

CCDC3: A NEW p63 TARGET INVOLVED IN REGULATION OF LIVER LIPID METABOLISM

Liao W[*], Liu H[*,**], Zhang Y[*], Jung JH[*], Chen J[*], Su X[***], Kim YC[****], Flores ER[***], Wang SM[****], Czarny-Ratajczak M[*****], Li W[******], Zeng SX[*] and Lu H[*]

[*]Department of Biochemistry & Molecular Biology and Tulane Cancer Center, [**]Department of Pediatrics (current address), and [*****]Department of Medicine, Center for Aging, Tulane University School of Medicine, New Orleans, LA, 70112, USA; [***]Department of Molecular Oncology, Cancer Biology and Evolution Program, H. Lee Moffitt Cancer Center, Tampa, Florida, USA; [****]Department of Genetics, Cell Biology and Anatomy, University of Nebraska Medical Center, 986805 Nebraska Medical Center, Omaha, NE 68198, USA; [******]Laboratory of General Surgery, The First Affiliated Hospital, Sun Yat-sen University, Guangzhou, Guangdong 510080, P.R. China.

TAp63, a member of the p53 family, has been shown to regulate energy metabolism. Here, we report coiled coil domain-containing 3 (CCDC3) as a new TAp63 target. TAp63, but not ΔNp63, p53 or p73, upregulates CCDC3 expression by directly binding to its enhancer region. The CCDC3 expression is markedly reduced in TAp63-null mouse embryonic fibroblasts and brown adipose tissues and by tumor necrosis factor alpha that reduces p63 transcriptional activity, but induced by metformin, an anti-diabetic drug that activates p63. Also, the expression of CCDC3 is positively correlated with TAp63 levels, but conversely with ΔNp63 levels, during adipocyte differentiation. Interestingly, CCDC3, as a secreted protein, targets liver cancer cells and increases long chain polyunsaturated fatty acids, but decreases ceramide in the cells. CCDC3 alleviates glucose intolerance, insulin resistance and steatosis formation in transgenic CCDC3 mice on high-fat diet (HFD) by reducing the expression of hepatic PPARγ and its target gene CIDEA as well as other genes involved in de novo lipogenesis. Similar results are reproduced by hepatic expression of ectopic CCDC3 in mice on HFD. Altogether, these results demonstrate that CCDC3 modulates liver lipid metabolism by inhibiting liver de novo lipogenesis as a downstream player of the p63 network.

This work was supported in part by NIH-NCI grants R01 CA095441, R01CA172468, R01CA127724, R21 CA201889-01A1, and R21 CA190775 to Hua Lu.

QUANTIFYING CHANGES IN CYTOCHROME P450 2E1 ACTIVITY DUE TO DIET-INDUCED OBESITY

Lichtler RC*, Wilson MJ*, Wickliffe JK*

*Department of Global Environmental Health Sciences, Tulane University School of Public Health and Tropical Medicine, New Orleans, LA.

Obesity, a global public health concern, has been implicated in an increasingly wide range of medical conditions. Recently, several obesity-related health outcomes have been linked to oxidative stress, a term that describes the cumulative effect of an excess of reactive oxygen species in the body. The cytochrome P450 enzymes, a group of proteins responsible for metabolizing toxicants in the liver, often produce reactive oxygen species in the process. Specifically, it is known that when induced beyond normal levels of expression by certain environmental toxicants, cytochrome P450 2E1 (CYP2E1) can create oxidative stress conditions. In an attempt to quantify the relationship between obesity and oxidative stress, we hypothesized that diet-induced obese (DIO) mice would have elevated CYP2E1 activity. To further our understanding of the mechanisms of CYP2E1, we developed experimental methods for testing if obesity alone, without any additional treatment, can also induce CYP2E1 expression and activity. Preliminary data have indicated a small but significant elevation in CYP2E1 activity in DIO mice, when measured via an *in vitro* enzyme activity assay performed on endoplasmic reticulum membranes isolated from mouse liver tissue. These results are consistent with previous data that indicate increased CYP2E1 expression, as well as an overall increase in oxidative stress markers in the livers of DIO mice. While further testing is needing to demonstrate consistency of findings, our results contribute to a growing body of knowledge regarding the specific mechanisms of obesity-related oxidative stress.

This work was supported by the Tulane University 170th Early Career Professorship Award and the Gulf of Mexico Research Initiative Award.

A novel function of nebivolol: stimulation of stem cell proliferation and inhibition of differentiation

Lin D*, Ochoa JE*, Barabadi Z**, Pfneur A**, Braun SE***,Phil kadowitz****, Izadpanah R*, Alt E*

* School of Medicine, Heart and Vascular Institute, Tulane University , New Orleans, LA 70112
**Department of Surgery, Tulane University, New Orleans, LA 70112
*** Division of Regenerative Medicine, Tulane National Primate Research Center, Tulane University,18703 Three River Road, Covington, LA 70433
****Department of pharmacology, Tulane University, New Orleans, LA 70112

Abstract

Tissue engineering is often limited by the time required for culture expansion of cells necessary for scaffold seeding. Thus, a simple means by which the rate of stem cell proliferation could be accelerated could represent a significant advance. Here, nebivolol, a highly selective β1-blocker, was investigated on its effect on proliferation of adipose-derived stem cells (ASCs). Cell counting assay indicated that the number of ASCs with nebivolol treatment showed a significant increase of 51.5% compared to control ($p<0.01$). Further analysis of the mechanism revealed that by cell cycle analysis the percentage of cells in G1 phase with nebivolol treatment significantly decreased compared ($p<0.01$), suggesting that nebivolol shortens the G1 phase of ASCs resulting faster proliferative rate. Clonogenic assay showed that nebivolol significantly increased colony-forming units of ASCs ($p<0.01$), which is consistent with the effects of nebivolol on promotion of ASC proliferation. In addition, ASC differentiation assay indicated that nebivolol affected not only the adipogenic differentiation potential as indicated by significantly reduced expression of CCAAT Enhanced Binding Protein alpha ($P<0.001$) and lipoprotein lipase ($P<0.001$), but also osteogenic differentiation as shown by inhibition of alkaline phosphatase ($P<0.01$). Taken together, these results showed nebivolol accelerated ASC proliferation through shortening G1 phase although it inhibited both adipogenic and osteogenic differentiation of ASCs, which provides a novel and simple approach to accelerate stem cell expansion in vitro before cell differentiation. Withdrawal of nebivolol reconstituted the normal differentiation capacity of the cells.

POTENTIAL ROLE OF TH17 CYTOKINES IN THE AGING PROCESS CONTRIBUTES TO PROSTATE CARCINOGENESIS

Liu S*, You Z*,**,***,****, Rowan BG*,***, Zhang Q*,**

*Department of Structural & Cellular Biology, **Tulane Center for Aging, ***Tulane Cancer Center and Louisiana Cancer Research Consortium, and Tulane Center for Stem Cell Research and Regenerative Medicine, ****Department of Orthopaedic Surgery, Tulane University School of Medicine, New Orleans, LA.

Aging is a major risk factor for prostate cancer (PCa). The immune system deteriorates with age and plays critical roles in age-related cancer formation. IL-17 producing $CD4^+$ T (Th17) cells, which produce IL-17A, IL-17F and IL-22, promote autoimmunity in mice and have been implicated in the pathogenesis of autoimmue/inflammatory diseases in humans. However, the Th17 immune response in the aging process is still not clear. Recent studies have shown that (Th17) immune responses are elevated in aging humans and mice and present a reciprocal relationship between Th17 and Treg cells. Changes to the Th17/Treg ratios in combination with altered cytokine expression during aging may contribute to an imbalance between the pro- and anti-inflammatory immune responses. This has been demonstrated as a higher susceptibility to developing inflammatory diseases with increasing age. Data supporting the role of inflammation in PCa come from a variety of fields. However, the causal relationship among inflammation, aging and PCa is unknown. In the present study, we compared the inflammatory responses of young and aged mice which were either wild-type (C57BL/6) or prostate-specific *Pten*-null. We found that both aged wild-type and *Pten*-null mice had significantly increased inflammatory cytokines including IL-6, TNFα, and IL-1β in prostate tissues compared with young mice. Induction of Th17 cells from $CD4^+$ naïve T cells was significantly increased in the aged wild-type and *Pten*-null mice compared with the young mice. The mRNA expression of IL-17A, IL-17F, IL-22, and RORγt in $CD4^+$ T cells was also significantly increased in the aged wild-type and *Pten*-null mice. Furthermore, Th17 cells and mRNA levels of IL-17A, IL-17F, IL-22 and RORγt were dramatically elevated in naïve T cells from the aged wild-type and *Pten*-null mice compared to the young ones. More interestingly, the mRNA levels of Th17 cytokines in naïve T cells from the aged *Pten*-null mice were dramatically higher than that from the wild-type mice. In addition, the proportion of Th17 ($CD4^+RORγt^+$) cells and Tregs ($CD4^+Foxp3^+$) were significantly increased in the aged wild-type and *Pten*-null mice. $CD4^+$ T cells and/or naïve T cells were harvested from the aged and young mice and differentiated in Th17 cell conditions for 4 days. Then, their conditioned media were collected. When the human prostate cancer cell line LNCaP and mouse prostate cancer cell line PTEN-CaP8 were exposed to the conditioned media from $CD4^+$ T cells and/or naïve T cells of the aged mice, their cell viability and migration increased significantly compared with the cancer cells treated with the conditioned media from $CD4^+$ T cells and/or naïve T cells of the young mice. These results indicate that age-related elevated Th17 cytokines may play a role in prostate carcinogenesis. Mechanistic studies of how the age-related elevated Th17 cytokines promote prostate carcinogenesis are ongoing.

This work was supported by NIH-National Institute of General Medical Sciences COBRE P20GM103629 (PI: S. Michal Jazwinski; Pilot Project PI: Q.Z.).

A mechanism underlying the production of androgen receptor splice variants in prostate cancer after endocrine therapies

Ma T[*,**], Zhan Y[*,**], Qi Y[**], Bai S[*,**], and Dong Y[*,**]

*Department of Structural and Cellular Biology, Tulane Cancer Center, New Orleans, Louisiana.
**College of Life Sciences, National Engineering Laboratory for AIDS Vaccine, Jilin University, Changchun, China.

Resistance to androgen-directed therapies is the major challenge in prostate cancer treatment. Many preclinical and clinical studies have shown that the expression of androgen receptor splice variants (AR-Vs), which lack the ligand-binding domain and are constitutively active, is increased after androgen-directed therapies and may contribute to the failure of the therapies. However, how the expression of AR-Vs is increased is still unclear. Androgen-bound full length AR (AR-FL) is known to interact with a 400-bp region in intron 2 of the AR gene, named androgen receptor binding site 2 (ARBS2), to repress the transcription of the AR gene. We hypothesized that, as a result of disrupting this negative autoregulatory loop, androgen-directed therapies induce the production of AR pre-mRNA, leading to increased expression of AR-FL and AR-V mRNAs. To test this hypothesis, we first used the CRISPR gene-editing technology to delete the ARBS2 region from the LNCaP95 human prostate cancer cell line, which expresses both AR-FL and AR-Vs. We found that ARBS2 deletion attenuated the effect of androgen deprivation on AR-V expression. Moreover, androgen deprivation can no longer increase AR-V levels after AR-FL was eliminated from LNCaP95 cells by using an AR-FL-specific degrader. We further assessed the stability of AR-FL and AR-V proteins in response to androgen deprivation and found that, while the AR-FL protein requires androgens for stabilization, the AR-V proteins have high, androgen-independent stability. Taken together, our findings indicate that, in response to androgen-directed therapies, the loss of AR negative autoregulation leads to coordinated increase of AR-FL and AR-V mRNAs. This, together with androgen-independent, high stability of AR-V proteins, results in a selective accumulation of AR-V proteins in castration-resistant prostate cancer. Our study therefore provided a mechanism of AR-V production after androgen-directed therapies, and this mechanism may help explain the ability of high testosterone treatment to restore sensitivity of castration-resistant prostate cancer to androgen deprivation therapy.

.

TITLE: MECHANISTIC ROLE OF EOSINOPHILS IN THE INITIATION AND PROGRESSION OF PANCREATITIS PATHOGENESIS

MANOHAR M*, VERMA AK*, VENKATESHAIAH SU*, AND MISHRA A*

*Department of Medicine, Tulane Eosinophilic Disorders Centre (TEDC), Section of Pulmonary Diseases, Tulane University School of Medicine, New Orleans, LA, 70112, USA

Several clinical reports indicated that IL-18 and eosinophils are induced in patient with chronic pancreatitis and pancreatic malignancy. However, the etiology and pathogenesis of eosinophilic pancreatitis (EP) is poorly understood and termed as rare disease. Accordingly, we tested the hypothesis that IL-18 and IL-5 synergy may be critical in promoting EP pathogenesis. We performed qPCR, ELISA, western blot, immunofluorescence and immunohistochemical analyses to detect eosinophils, mast cells, collagen, associated cytokines and chemokines in experimental and human pancreatitis. Herein, we show the evidence of tissue eosinophilic microabscesses, mast cells and collagen accumulation in non-malignant and malignant human pancreatitis. Additionally, we observed more prominent collagen accumulation, fibrotic lesions and degranulated eosinophils in malignant pancreatic tissue samples compare to non-malignant pancreatic samples. A similar characteristics such as acinar cells atrophy, increased accumulation of tissue eosinophils, mast cells and induced levels of IL-5, IL-18, Eotaxin-2, TGF-β1, Collagen-1, Collagen-3, fibronectin and α-SMA was observed in cerulein-induced chronic mouse model of pancreatitis. Mechanistically, we show that IL-5 deficiency in mice protect pancreatic pathogenesis including fibrosis in cerulein-induced mouse model of pancreatitis, indicating a critical role of eosinophils in disease pathogenesis. Taken together, our combined clinical and experimental data indicates that eosinophils accumulation and degranulation may be critical in promoting pancreatic fibrosis that may leads to pancreatic malignancy.

Funding: NIH RO1 AI080581 (AM)

PATIENT-DERIVED TRIPLE NEGATIVE BREAST CANCER XENOGRAFTS AS A TRANSLATIONAL MODEL TO SCREEN FOR NOVEL KINASE PATHWAYS

Matossian MD*, Burks HE*, Bowles A**, Sabol RA**, Hoang VT*, Bunnell B**, Zuercher WJ***, Drewry DH***, Wells C***, Alfortish A****, Moroz K****, Burow ME*, Collins-Burow B*

*Tulane University School of Medicine, Department of Medicine
**Tulane University School of Medicine, Department of Stem Cell Research and Regenerative Medicine
***Louisiana Cancer Research Center, Biospecimen Core
****Eshelman School of Pharmacy, University of North Carolina, Chapel Hill, NC

Overall, triple negative breast cancers (TNBCs) constitute 12% of all breast cancers, and is approximately twice more prevalent in African-American populations. Louisiana has a high proportion of African-American residents (32.5% in 2015), and thus hosts a higher population of TNBC patients. TNBCs have an aggressive phenotype that is elusive to the targeted therapeutics used to treat other breast cancer subtypes. Certain kinase families have been extensively studied as regulators of epithelial-mesenchymal transition (EMT), a process involved in the initiation of cancer metastasis. Discovery of novel kinase targets within the subset of uncharacterized kinases could provide important insight into future targeted therapies. However, current models utilized in target discovery research are limited by the inability to accurately recapitulate the complex stromal architecture and heterogenous genetic and molecular composition of breast cancer. Furthermore, immortalized cell lines are limited to a 2D environment and over time acquire mutations that may not reflect the primary tumor. Recently, our laboratory has successfully established two TNBC patient-derived xenograft (PDX) models derived from African-American patients, and generated cell lines (TU-BCx-2K1, TU-BCx-2O0) and mammospheres. One of these models, 2O0, presents tumor architecture, cellular composition, genomic (qRT-PCR) and protein (western blot) expressions that are concordant with a claudin-low subtype, which has higher rates of metastasis and recurrence. Furthermore, we show that both TNBC models metastasize to the lungs, and exhibit molecular characteristics consistent with mesenchymal phenotypes. We utilized these translational PDX models to screen a library of small molecule inhibitors that represent a variety of kinase pathways to identify novel therapeutic targets and/or pathways that are specific to TNBC subtypes. We found in a preliminary cell morphology screen using three TNBC cell lines (MDA-MB-231, BT549, MDA-MB-157), two small molecule inhibitors that increased epithelial marker (CDH1) gene expression, suppressed mesenchymal (VIM, c-FOS, SNAI1, ZEB1) expression and/or suppressed cellular motility in transwell migration assays. We observed after *ex vivo* treatments with our PDX tumors the two compounds increase the epithelial marker CDH1 expression, and suppress mesenchymal markers (VIM, MMP2, c-FOS, SNAI1, ZEB1) expressions. We confirm these findings in the TU-BCx-2K1 cell line. Kinase array data revealed candidate kinases responsible for the observed EMT changes in the two compounds of interest (NEK5, NEK9, NEK1 potentially affect cell motility; SRC-family kinases, TAOK2, STK10 potentially affect EMT gene changes); we plan to utilize the PDX cell lines to characterize these kinases in EMT. We aim to ultimately discover novel therapeutic targets specific to different TNBC molecular subtypes.

A Comparison of Human Platelet Lysate and Silk 3D Adipose Tissue Constructs using Adipose Tissue -Derived Stromal Vascular Fraction.

McCarthy ME*, Frazier TP*, Gimble JM*

* Tulane Center for Stem Cell Research and Regenerative Medicine, Tulane School of Medicine, New Orleans, LA

Background:
Owing to its ease of collection and abundant supply of heterogeneous stem/progenitor cell populations, adipose tissue has emerged as an attractive cell source in tissue engineering and regenerative medicine. Often considered a waste product of liposuction surgeries, the stromal vascular fraction (SVF) of lipoaspirate has been shown to demonstrate enormous regenerative potential in damaged tissues or organs through paracrine and differentiation mechanisms. Currently, SVF calls are being investigated for multiple clinical indications such as nerve regeneration, burn wounds, and diabetes-related complications. Together, these properties have resulted in the recent adoption of SVF in cosmetic surgery clinics across the country.

Traditionally, silk-based biomaterials have offered exceptional benefits over conventional synthetic polymer scaffolds, offering a low immunogenicity, slow degradation rates, plasticity during processing, and suitable mechanical properties for implantation. Additionally, media supplemented with 7.5% human platelet lysate (hPL) has been shown to result in a 3D scaffold after addition of SVF. This scaffold is entirely cell-derived, is of human origin, and offers the benefit of having no immunogenic properties. Previous studies have shown that hPL increases adhesion of mesenchymal stem cells (MSCs) and encourages both neovascularization and bone regeneration.

Objective:
In this study, we investigated and compared the ability of Silk Fibroin (SF) and hPL scaffolds to promote the generation of a functional 3-dimensional humanized fat pad in-vitro.

Design/Methods:
SVF cells will be isolated, sub-cultured, and either seeded in SF or hPL scaffolds. In-vitro cell/matrix constructs will be cultured over extended periods, and assayed for biological properties including: cell surface antigen profiles via flow cytometry, adipogenic differentiation potential via quantification of intracytoplasmic lipid deposition, cell growth as measured by proliferation and colony forming unit (CFU) assays, and adipose tissue functionality assays via glucose uptake and chemokine (adiponectin and leptin) secretion.

Main Outcomes and Measures:
Statistical analyses will be performed using the Student's t-test for analyzing CFU-Fs and cell growth, while one-way and two-way ANOVAs and Bonferroni's Post-test will be used to compare immunophenotypical changes and functional assays.

Results:
Initial in-vitro hPL-SVF 3D cultures demonstrate enhanced proliferation and show potential for the formation of humanized adipose 3D matrices capable of adipogenic potential. More work will be conducted to investigate the aforementioned outlined parameters.

This work is supported by NSF grant: 1621439 entitled "Tissue engineered human fat on a chip - a novel tool for metabolic drug discovery."

CHARACTERIZATION OF MACROPHAGES SERVING AS A VIRAL RESERVOIR IN PEDIATRIC SAIDS

Merino KM*, Sugimoto C**, Cai Y***, Allers C*, Alvarez X*, Maness NJ*, Walker E*, Penney T*, Slisarenko N*, Haupt E*, Didier ES* and Kuroda MJ*

*Divison of Immunology, Tulane National Primate Research Center, Covington, La
**Department of Environmental Biology, School of Medicine, Hokkaido University, Sapporo, JAPAN
*** HIV-1 Immunopathogenesis Laboratory, The Wistar Institute, Philadelphia, PA

Background: In SIV-infected adult *Macaca mulatta,* increases in peripheral monocyte turnover indicates destruction of short-lived tissue macrophages and predicts progression to SAIDS. This increased turnover also correlates with infection (but not death) of long-lived tissue macrophages. Higher baseline monocyte turnover rates are consistently measured in neonates, and disease progression is faster than in adults. Our data has shown that increase in monocyte turnover with increased tissue macrophage infection is associated with rapid SAIDS progression in infants. We hypothesize that early and high infection of macrophages soon after pediatric SIV inoculation results in establishment of a viral reservoir in long-lived tissue macrophages prior to initiation of antiretroviral therapy (ART). **Materials and Methods:** In rhesus infants infected with SIV_{mac251}, cell turnover is measured using BrdU uptake. Flow cytometry and confocal imaging allow phenotypic characterization of cells in blood, tissues, and cultures. PCR and *in situ* hybridization s used to quantify SIV RNA and DNA in plasma, tissues, sorted cells and CSF. Plasma cytokine analysis will be performed using Milliplex bead panel. ART consists of dolutegravir, PMPA or tenofovir, and emtricitabine. **Results:** Infant macaques euthanized post-infection (without ART) confirm previous data and will be used to quantify macrophage infection in cases of high monocyte turnover. Animals euthanized after various lengths of ART provide data on reservoir seeding, viral persistence and immune activation status. ART-treated infants with discordant viral loads are evaluated to identify the source of viral replication despite ART treatment. In treated animals, regardless of viral load, no differences are observed in activation status, absolute number, or kinetics of CD4 and CD8 T-cells, indicating ART is preventing T-cell infection similarly in treated animals. Confocal imaging of tissues is used to compare infection in long-lived macrophages and CD4 T-cell infections in animals with contrasting viral load. Viral RNA and DNA PCR analysis of tissues and sorted cells should confirm that uncontrolled viral load during ART treatment can be attributed to infected macrophages. **Conclusions:** Ongoing works suggest that the magnitude of long-lived macrophage infection may dictate the effectiveness of ART in pediatric SIV infection.

This study was supported by grants R01AI097059, R01HL125054 and R21AI116198 from the National Institutes of Health to MJK and P51OD011104 to the Tulane National Primate Research Center.

A IMMUNODEFICIENT MOUSE MODEL MIMICS HUMANS IN LACKING A-GAL EPITOPES

Mohammedsaleh FM[***], Lin D[****], Chandra P[*], Robinson JE[**], Izadpanah R[****], Alt E[****], Mondal D[*], Abdel-Motal U[*****], Braun SE[*, ***, ****]

Departments of [*]Pharmacology, [**]Pediatrics, [***]Tulane National Primate Research Center, [****]Applied Stem Cell Laboratories, Tulane University School of Medicine, New Orleans, LA. [*****]Sidra Medical and Research Center, Doha, Qatar.

The α-gal epitope (Galα1-3Galβ1-(3)4GlcNAc-R) is synthesized on glycoproteins and glycolipids of new world monkeys and non-primate mammals by the glycosylation enzyme α1,3 galactosyltransferase (α1,3GT). However, old world monkeys and primates (human and non-human) have a natural mutation in this gene. Therefore, these species do not make α-gal epitopes, but instead produce abundant antibodies against natural α-gal epitopes. Actually, these antibodies generate the strong rejection of tissues in xenograph transplantation in NHP models. Since mice have been a crucial tool for investigating complex human diseases including immunological responses, new strains of mice were developed with reduced innate and adoptive immune responses. These NSG mice are based on the NOD (non-obese diabetic) background, but are also deficient in the prkdc^{scid} and IL-2 receptor gamma genes. Therefore, NSG mice are permissive for engraftment of human hematopoietic stem cells and other human tissues; however, they would be an inappropriate model to study α-gal epitopes. To circumvent this issue, we breed α1,3GT knockout mice into the NSG strain and initiated characterization of endogenous immune responses and engraftment of human hematopoietic stem cells in NSG/α-gal^{null} mice. Immunofluorescence staining and flow cytometric analysis showed NSG/α-gal^{null} mice lack T cells, mature B cells, and NK cells. Tissue sections of liver, kidney, skin, and heart obtained from NSG/α-gal^{null} mice were examined with a confocal laser-scanning imaging system and showed no staining for the α-gal epitopes. To facilitate production of α-gal antibodies, we synthesized V_H and V_L domains from α-gal antibodies and demonstrated α-gal specific antibody production by immunofluorescence staining and ELISA. Ongoing studies are measuring engraftment of human cord-blood CD34$^+$ hematopoietic stem/progenitor cells and production of human natural antibodies to α-gal epitopes. The new Hu-NSG/α-gal^{null} mouse model can be used for preclinical evaluation of viral and tumor vaccines carrying α-gal epitopes with natural anti-α-gal antibodies providing an endogenous adjuvant for more efficient processing of antigens.

This work is supported by the Qatar Foundation (SEB), and the Alliance for Cardiovascular Research (SEB), and NIH NIAID R21 AI116348 (DM).

LACK OF ASSOCIATION BETWEEN LYMPH NODE METASTASIS AND NODULE SIZE IN DIFFERENTIATED THYROID CANCER

Mohsin K*, Bu Ali D*, Monlezun D*, Kandil E*

*Tulane University School Of Medicine, Surgery, New Orleans, LA, USA

Introduction: Several studies have reported the association between large thyroid nodules and the increased incidence of lymph node metastasis in differentiated thyroid cancer. We aim to investigate the use of thyroid nodule size in predicting lymph node (LN) metastasis in differentiated thyroid cancer (DTC).

Methods: This is a retrospective review of all patients who underwent thyroidectomy for DTC by a single surgeon in an academic institution over 5 years. Clinicodemographic data, histopathological data and preoperative ultrasound features including nodule size and presence of internal vascularity or calcification were analyzed. Patients were divided into two groups based on the presence of positive LN metastasis.

Results: A total of 139 patients were included, 28 (20.9%) had positive LN metastasis and 106 (79.1%) were non-metastatic. There was no significant difference in nodule size on ultrasound between the two groups. The mean nodule size for the group with metastatic LN was 2.7 ± 1.5 cm, and 2.5 ± 1.4 cm for the non-metastatic group ($p=0.48$). In addition, there was no association between larger nodule size and presence of positive LN metastasis, even in the combination with other ultrasound features such as calcification and internal vascularity ($p>0.05$). However, there was a significant association of positive LN metastasis with the presence of positive BRAF mutation (OR: 14.32, $p<0.001$, Sens.= 87.5%, Spec. = 67.2%, PPV= 48.8%, NPV= 93.8%, Acc.= 72.5%)

Conclusion: Larger thyroid nodule size on ultrasound is not associated with increased risk of LN metastasis in DTC. However, the presence of positive BRAF mutation was predictive of increased risk of presence of metastatic LN.

CELLULAR PROPERTIES OF LIVER-RELATED PVN NEURONS IN DB/DB MOUSE

Molinas AJR[*], Gao H[*], Qiao X[*], Miyata K[*], Zsombok AZ[**]

[*]Department of Physiology, School of Medicine, and [**]Neuroscience Program, Brain Institute, Tulane University, New Orleans LA, USA

Transient receptor potential vanilloid type 1 (TRPV1) has been shown to play a role in the modulation of glucose homeostasis. Preautonomic, liver-related neurons in the paraventricular nucleus (PVN) of the hypothalamus contribute to the regulation of sympathetic and parasympathetic outflow to the liver. Our previous findings demonstrated that liver-related PVN neurons are controlled by TRPV1-dependent excitatory neurotransmission. In this study, liver-related PVN neurons were identified with a retrograde, trans-neuronal viral tracer and whole-cell patch-clamp recordings were conducted. We tested the hypothesis that the TRPV1-dependent synaptic control of liver-related PVN neurons is reduced in db/db mice. Application of the exogenous TRPV1 agonist, capsaicin (1μM) increased the average frequency of miniature excitatory post-synaptic currents (mEPSCs) in liver-related PVN neurons from lean mice. In contrast, in db/db mice capsaicin application did not change the overall frequency of mEPSCs. Capsaicin did not alter the frequency of miniature inhibitory post-synaptic currents (mIPSCs) neither in lean or db/db mice. We did not observe significant difference in the basal frequency of mEPSCs and mIPSCs in liver-related PVN neurons of lean and db/db mice. On the other hand, the amplitude of mIPSCs was smaller in liver-related PVN neurons of db/db mice compared with lean mice. GABA-mediated inhibitory tonic currents as a bicuculline-dependent inward shift of the holding current were also revealed in liver-related PVN neurons. Our data did not show difference in the magnitude of tonic inhibition between the groups. Together, this study suggests that the TRPV1-dependent control of liver-related PVN neurons is diminished in the db/db mouse. These findings are consistent with our previous data demonstrating synaptic plasticity of hypothalamic autonomic circuits in hyperglycemic conditions, and further suggest dysregulation of neuronal activity at the level of the PVN in obese-diabetic state.

Molinas AJR and Gao H contribute equally to this work. This work was supported by NIDDK R01DK099598

ARTIFICIAL INTELLIGENCE-BASED HEALTH SYSTEM OPTIMIZATION WITH CULINARY MEDICINE: MULTI-SITE 5-YEAR COHORT STUDY WITH NESTED RANDOMIZED TRIALS OF 3,082 PATIENTS AND MEDICAL TRAINEES AND PROFESSIONALS

Monlezun DJ*,**, DeValle N*, Tran D*, Budnick I*, Shepard R*, Arman D*, Carr C*, Desai AN*, Lakhmani P*, Saccoccia B*, McGowan G*, Grant A*, McGowan C*, Feigenbaum SB*, Cardello F*, Coleman J*, Pedroza K*, Dotson K*, Niu T***, Leong B*, Sarris L*, Harlan TS*

*The Goldring Center for Culinary Medicine, Tulane University School of Medicine, New Orleans, USA; **Department of Global Health Management & Policy, Tulane University School of Public Health & Tropical Medicine, New Orleans, USA; ***Department of Biostatistics & Data Science, Tulane University School of Public Health & Tropical Medicine, New Orleans, USA

Health systems globally are faced with extinction and failure in their patient duty if they falter in providing clinically efficacious, cost-effective healthcare. Despite the known causal link between the nutrition-related chronic disease epidemics and the world's top morbidity cause, cardiovascular disease, there is no evidence-based and scalable model of nutrition education and intervention for and with medical professionals. Therefore, the medical school-based teaching kitchen, The Goldring Center for Culinary Medicine (GCCM) at Tulane University School of Medicine, launched the largest known multi-site cohort study with nested randomized controlled trials (RCTs) across 30 medical centers and 3,082 medical professionals, trainees, and patients to establish the standard in scalable, evidence-based nutrition education within a population health management framework. This study, Cooking for Health Optimization with Patients (CHOP) with its four sub-studies, additionally featured not only the first known systematic review and meta-analysis on this subject to determine best practices. CHOP also serves as the first known nutrition education study utilizing the latest artificial intelligence-based machine learning techniques to complement the traditional statistical approaches to provide real-time, precise treatment estimates for causal inference and assessment of hands-on cooking and nutrition education for medical professionals and trainees, and improved patient psychometric and biometric outcomes. (1) The first sub-study, CHOP-Medical Students, demonstrated in propensity score-adjusted fixed effects multivariable regression across 2,291 students that GCCM versus traditional clinical education significantly improved student's adherence to the Mediterranean Diet (MD) (Odds ratio [OR] 1.32; 95% confidence interval [CI] 1.00-1.73; p=0.048), and total mastery of 25 nutrition counseling topics for patients (OR 1.69; 1.34-2.11; p<0.001). (2) The second sub-study, CHOP-Meta-analysis, demonstrated that though the average effect size (ES) across the 10 nutrition education studies among medical trainees was 10.36 (95%CI 6.87-13.85; p<0.001), the only study meeting the STROBE criteria for high quality, the published version of CHOP-Medical Students above, had significantly triple the ES (31.67; 95%CI 29.91-33.43). (3) The third sub-study, CHOP-CME, demonstrated that among 230 physicians, GCCM education significantly increased their odds of providing patients nutrition education (OR 3.97; 95%CI 1.35-11.64; p=0.012). (4) The final sub-study, CHOP-Community, demonstrated that GCCM education versus the standard of care significantly increased patient adherence to the MD (OR 1.94; 1.04-3.60; p=0.038). The four sub-studies within CHOP taken together provide the first known multi-site cohort and randomized trial evidence of superiority of hands-on cooking and nutrition education compared to standard of education and medical care to improve patient outcomes through improved medical student and physician training. CHOP utilized the latest in causal inference-based statistics, randomized trials for causal assessment, and machine learning to provide robust, precise estimates of comparative treatment effectiveness. Beginning with Tulane University School of Medicine,

GCCM has since grown these past 5 years to 30+ medical centers providing over 20,000+ hours of hands-on cooking and nutrition education. Its umbrella study has utilized the latest rigorous study design and analysis methodologies to provide a blueprint to optimize health systems through sustainable improvements in population health management that is clinically and cost effective, and so can reduce health inequities while improving individual outcomes.

STRUCTURAL BASIS FOR CD4+ T-CELL EPITOPE DOMINANCE IN PESUDOMONAS EXOTOXIN A DOMAIN III

Moss DL*, Mettu R**, Landry SJ*

*Department of Biochemistry and Molecular Biology, Tulane University School of Medicine, New Orleans, LA

**Department of Computer Science, Tulane University, New Orleans, LA

The CD4+ T-cell adaptive immune response is initiated by antigen-specific peptides bound to class II major histocompatibility complex (MHC) molecules. There are three main factors that influence the processing of protein antigens: protein folding, proteolysis, and MHC binding. Current T-cell epitope prediction methods rely on MHC binding affinity which are inadequate, most likely because they ignore protein folding and proteolysis. Recently a recombinant immunotoxin (RIT), comprised of pseudomonas exotoxin A domain III (PE-III) and a cancer specific antibody fragment, has been described as a potentially highly effective treatment for cancer. Initially, treatment with this RIT was limited by the development of neutralizing antibodies in patients. Pastan and coworkers attempted to eliminate the human CD4+ T-cell epitopes by mutating six residues within domain III of PE. The resulting protein is referred to as T18. The intention of these mutations was to eliminate the T-cell epitopes by disrupting the MHC binding of PE-III peptides. However, we predict that the mutations altered PE-III folding stability and proteolytic susceptibility, resulting in reduced activation of PE-III specific CD4+ T-cells. For this study we have purified WT PE-III, four variants of PE-III with single-residue mutations found in the T18 mutant, and the six-residue-mutated T18. All five mutant proteins exhibit significantly altered resistance to chemical- and acid-induced unfolding compared to WT PE-III. All of the mutant proteins also exhibit increased resistance or susceptibility to proteolysis compared to WT PE-III. One mutant in particular, R494A, exhibited decreased folding stability and increased proteolytic susceptibility. The immune response elicited by this mutant was drastically reduced compared to WT PE-III as measured by both T-cell response and PE-III specific antibody titer, which was similar to the reduced responses observed for the six-residue-mutated T18. Our data support a model for antigen processing in which protein antigen folding and proteolysis strongly influence the presentation of peptides to T-cells. These data can be used for the development of more accurate epitope prediction methods.

This work is supported by NIH grant R21 #AI122199

EVALUATION OF SMOOTH MUSCLE CELL FUNCTION IN THE RAT MESENTERY CULTURE MODEL

Motherwell JM[*], Azimi AS[*], Spicer K[*], Alves N[**], Breslin JW[**], Katakam PV[***], Murfee WL[*]

[*]Department of Biomedical Engineering, Tulane University, New Orleans, LA
[**]Department of Molecular Pharmacology and Physiology, University of South Florida, Tampa, FL
[***]Department of Pharmacology, Tulane University School of Medicine, New Orleans, LA

An emerging challenge in tissue engineering biomimetic models is recapitulating the physiological complexity associated with real tissues. Recently, our laboratory introduced the rat mesentery culture model as an *ex vivo* experimental platform for investigating the multi-cellular dynamics involved in angiogenesis within an intact microvascular network using time-lapse imaging. A critical question remains whether the vascular smooth muscle cells maintain their functionality. The objective of this study was to determine if vascular smooth muscle cells along arterioles in cultured microvascular networks maintain the ability to constrict. Adult Wistar rat mesenteric tissues were harvested, rinsed in sterile DPBS and media, then placed underneath a commercially available polycarbonate membrane insert. Tissues were cultured up to 3 days with either minimum essential media (MEM) or MEM supplemented with 10% serum. Tissues were maintained at 37°C and 7.4 pH while exposed to topically administered vasoconstrictors (50mM KCl or 20nM Endothelin-1 (ET-1)) for 5 minutes; arterioles were observed. After 3 days in culture, tissues were viable and arterioles maintained their ability to constrict in response to both KCl and ET-1. The percent arteriolar constriction in *ex vivo* tissues cultured in 10% supplemented media was decreased at 3 days for both constrictors compared to the responses in pre-culture *ex vivo* control tissues. Day 3 serum stimulated microvascular networks were angiogenic characterized by increased capillary sprouting and vessel density. The mechanism of action for the receptor-mediated vasoconstriction induced by ET-1 was confirmed using antagonists BQ-123 and BQ-788. Day 0 *ex vivo* tissues were incubated with BQ-123 (3μM) and BQ-788 (3μM) for 30 minutes prior to exposure to 20nM ET-1; control tissues were incubated without the antagonists. The combined presence of BQ-123 and BQ-788 resulted in significantly reduced ($p<0.05$) arteriole constriction (23 ± 5.4%; n=12) compared to control tissues (41 ± 4.1%; n=9). Interestingly, the arteriole constriction response to KCl in day 3 tissues cultured in media without serum was not significantly different than the uncultured group suggesting that angiogenesis versus culture conditions might influence smooth muscle cell function. The functionality in cultured tissues and association of impaired vasoconstriction during angiogenesis were confirmed with intravital microcopy experiments. No significant difference was observed for arteriole constriction response to 50mM KCl between the freshly harvested *ex vivo* Day 0 tissues (33 ± 3.1%; n=10) and the unstimulated Day 0 tissues evaluated intravitally (35 ± 4.3%; n=13). Intravital comparison of unstimulated and tissues stimulated by an *in vivo* wound healing stimulus also confirmed impaired vasoconstriction in angiogenic networks. This study demonstrates functional constriction of vessels within intact microvascular networks *ex vivo* and supports the novelty of the rat mesentery culture model as a biomimetic tool for microvascular research.

The research reported in this abstract was supported by the National Institutes of Health under Award Numbers 5-P20GM103629-04, R01AG049821, and NS094834.

THYROID AND PARATHYROID SURGERIES IN OCTOGENARIANS. DOES AGE INFLUENCE OUTCOMES?

Murad F, Emejulu O, Bu Ali D, Kholmatov R, Mohsin K, Alzahrani H, Monlezun D, Killackey M, Kandil E.

Tulane University, Department of Surgery, New Orleans, LA, United States.

Introduction:
Surgical procedures for various thyroid and parathyroid diseases are common, and the incidence of thyroid malignancies increases with age, necessitating surgical intervention for older patients. We aim to evaluate the safety of thyroid and parathyroid surgeries in patients over 80 years of age.
Methods:
This is a retrospective review of all octogenarians who underwent thyroid or parathyroid surgery at a North American institute, over a five-year period by a single surgeon. Those patients were compared to a randomly selected control group of younger patients who underwent the same procedures. We collected demographics clinicodemographical data, procedure type, length of hospital stay, and perioperative complications.
Results:
22 octogenarian patients (mean age: 83.6±2.98 years, females 63.6%) were compared to 233 younger patients (mean age: 53.1± 12.43 years, females 65.7%). The overall postoperative complication rates in the octogenarian group were significantly higher (OR 5.38, 95%CI 1.68-17.23, P =0.005). Postoperative complications included transient hoarseness (OR 4.54, 95%CI 1.10-18.80, P=0.037), and transient post-operative confusion (OR 31.13, 95%CI 1.23-786.86, P=0.04). Hypocalcemia, wound infection, hematoma and seroma were not higher in octogenerians (P>0.05 for all). There was a tendency to keep octogenarian patients over 24 hours postoperatively (OR 11.35, 95%CI 2.78-46.25, p=0.04). Risk of complications was associated with increasing age by one year (OR 1.03, 95%CI 1.00-1.06, p=0.036), and the odds of length of stay over 24 hours by 5% (OR 1.05, 95%CI 1.00-1.09, p=0.038).
Conclusions:
Patients over 80 years of age undergoing thyroid and parathyroid surgery tend to have a higher risk of overall complications rates and a longer post-operative hospital stay compared to younger patients. Thorough counselling in octogenarian patients should be performed. However, further multi-institutional studies with are warranted.

Disclosure: No financial relationships or commercial interests.

FOCUSED ULTRASOUND REPROGRAMS ETHANOL-TREATED PROSTATE CANCER CELLS BACK TO NORMAL

Murad HY*, Yu H*, Luo D*, Halliburton G*, Sholl A**, Khismatullin D*
*Department of Biomedical Engineering of Tulane University, New Orleans, LA 70118 USA
**Department of Pathology and Laboratory Medicine of Tulane University, New Orleans, LA

Introduction: Prostate cancer is the most incident cancer in men. Since the majority of prostate cancer patients are elderly men, often not suitable for invasive procedures, there is a need for minimally invasive therapies (e.g., focused ultrasound). Previous ex vivo and in vitro studies conducted in our laboratory showed that high-intensity focused ultrasound (HIFU) synergistically enhanced tumor destruction by ethanol injection. The objective of this study was to investigate the molecular mechanisms behind the anti-cancer effects of HIFU. We tested the hypothesis that focused ultrasound (FUS) drastically reduces the metastatic potential of chemically-treated cancer cells via overproduction of heat-shock protein 70 (HSP70), death receptor Fas, its ligand FasL, and inhibition of NFκB. Suspensions of cultured DU145 and PC3 prostate cancer cells were placed in 0.2ml tubes for *in vitro* experiments or injected into athymic nude mice to create xenografts *in vivo*. The cells were left untreated or exposed to FUS alone, 4% ethanol, or FUS+4% ethanol. The FUS signal was generated by a 1.1 MHz transducer, with acoustic power ranging from 4.1 to 20 W. Fas and FasL expression were measured by flow cytometry, HSP 70 and NFκB protein levels were determined by Western blot analysis at 2, 24, and 72 hours post-treatment. To confirm that cancer cells lose aggressiveness, we measured the number of cancer cells adhered to TNF-α-activated endothelium as well as tested the ability of cells to form multi-cellular spheroids. Prostate cancer cells significantly increased their expression of Fas, FasL, and HSP 70 immediately after being exposed to FUS+4% ethanol and continued to produce these molecules at a significantly higher amount than untreated, ethanol, or FUS alone alone-treated cells. Static adhesion assay showed that cells in the combined treatment were less likely to attach to endothelium. Cells exposed to both ethanol and FUS were unable to form three-dimensional tumor spheroids. Athymic nude mice bearing DU145 xenografts were left untreated or exposed to FUS alone, 4% ethanol, or FUS+4% ethanol. Tumors exposed to combination were the only treatment that led to tumor regression in vivo, based on caliper measurements and histological analysis. Although Hsp70 plays a key role in cancer initiation and progression, its overproduction interferes with NF-κB signaling, thereby causing apoptosis and reduced expression of adhesion molecules required for metastasis. Here, we showed that FUS induces Hsp70 overproduction, inhibits NFκB, and promotes cell apoptosis via an increase in expression of Fas and its ligand FasL. These factors lead to phenotypic changes in cancer cells that reduce their aggressiveness.

This study has been supported by National Science Foundation grant 1438537, American Heart Association grant 13GRNT17200013, Louisiana Board of Regents grant LEQSF-EPS(2012)-PFUND-292, George Lurcy and Oscar Lee Putnam grants of Newcomb-Tulane College, and Tulane CELT research grant.

HSP90 FAMILY PROTEINS IN THE MALARIA PARASITES: ESSENTIAL AND NON-REDUNDANT ROLES DURING INTRAERYTHROCYTIC AND MOSQUITO DEVELOPMENT

Murillo S. C*, Aly A* and Pizarro J*.

*Department of Tropical Medicine, School of Public Health and Tropical Medicine, Tulane University, New Orleans, Louisiana, USA

Malaria is a lethal vector-borne disease caused by a *Plasmodium* parasites. The emergence of resistance to Artemisinin in South-east Asia and the scarcity of alternative antimalarial drugs, drives the urgency to develop new antimalarial options that mitigates the appearance of drug resistant strains, and sustain disease control and elimination programs. Drug repurposing is a viable alternative to identify antiplasmodial compounds. We hypothesize that Heat Shock Protein 90 (HSP90) inhibitors, originally developed as anticancer agents, could serve as starting point to identify new antimalarial drugs. Because, these inhibitors limit parasite growth in vitro and in vivo with very limited toxicity against host cells. In order to validate HSP90 as an antimalarial drug target against *Plasmodium*, we used a genetic approach to evaluate the chaperone essentiality in the parasite blood stages. Our strategy included the targeted deletion of *Plasmodium yoelii* HSP90 gene by homologous recombination. The 5' and 3' UTR regions of the genes of *P. yoelii* 17XNL strain were amplified and inserted into the transfection plasmid (pAA20). Linearized plasmids were transfected into *P. yoelii* parasites by electroporation, and transfected parasites were injected into mice, and selected by treating the mice with pyrimethamine for 7 days. The disruption of the targeted gene was confirmed by diagnostic PCR. In addition, we also targeted three additional HSP90 family members to evaluate the potential compensatory role of these additional protein chaperones. We were unable to generate knockout parasites for any of the four HSP90 family members. All the parasites recovered from the deletion experiment were wild type parasites, suggesting that the chaperones have an essential and non-redundant role in *Plasmodium* blood stage development. To discard the possibility of genomic inaccessibility in any of the four targets locus, we generated transgenic parasites expressing C-terminal GFP-tagged chaperones by genetic recombination. The transgenic parasites for each HSP90 family member allowed us to determine its cellular localization in both asexual and sexual stages. To investigate the chaperones in the mosquito stages, female *Anopheles stephensi* mosquitoes were fed on mice infected with the different transgenic parasites. Ookinetes and oocysts were isolated from mosquito midguts. Fluorescent microscopy images of live GFP-expressing parasites were taken for each developmental stage. Tagged proteins were obtained for three out of the four HSP90 family members. We found each of them in a distinct subcellular compartment within the cytoplasm of the parasite. Our results highlight the essential non-redundant cellular roles of HSP90 family members and validate the protein chaperone as potential drug targets candidate

RESILIENCE NOT MET: PRELIMINARY CHARACTERIZATION OF UNIVERSITY CAMPUS PREPAREDNESS HIGHLIGHTS LACK OF COMPREHENSIVE STANDARDS

Murphy, S.*, Lichtveld, M.*

* Department of Global Environmental Health Sciences, Tulane University School of Public Health & Tropical Medicine, New Orleans, LA

Health departments charged with public health emergency preparedness, hospitals under the Joint Commission's (TJC) purview, and public sector emergency management agencies all have strict preparedness and operational response mandates and requirements to meet, to validate through exercises, and incorporate corrective actions for overall preparedness and response efficiencies related to the protection of life and property. Standards such as positioning an experienced and educated professional in a full-time capacity to direct emergency management activities, establishing a radio communication system which is interoperable with local responders, and basing an emergency operations plan on a valid, updated hazard vulnerability assessment or threat and hazard identification and risk assessment are critical benchmarks of bolstering community preparedness and ultimately its resilience. Preparedness planning represents a core component of the five key mission areas of emergency management: prevention, protection, mitigation, response, and recovery. Institutions of higher education (IHEs) are a core stakeholder in assuring disaster resilience. Yet, no formal preparedness assessment strategy exists to quantify disaster readiness of IHEs.

Hypothesis: Proximity to the Atlantic Hurricane Basin's threat zone and recent experience with emergency situations influences an IHE's preparedness level.

Study aims:

1) Conduct a gap analysis of disaster preparedness at IHEs located in the Atlantic Hurricane Basin's threat zone
2) Identify preparedness benchmarks to assess disaster readiness of IHEs
3) Develop a baseline assessment tool to quantify IHE disaster preparedness

Preliminary data highlight improvement areas, including the primary requirement of having an experienced, full-time employee charged solely with emergency preparedness responsibilities. Of universities with enrollment of 20,001 students or more, 91% have an obvious web presence showcasing full-time professionals responsible for emergency management and operational continuity. However, these figures drop significantly with decreased enrollment. Of those universities with enrollment of 10,001-20,000, only 42% are compliant with this single best practice. Those with enrollment of 6,001-10,000, only 30% offered compliance and those with enrollment of 3,001-6,000 and those with 2,000-3,000 enrollment only had 23% and 13% compliance respectively.

These findings characterize the current baseline landscape and are the basis of impending, more rigorous analytical research. While preliminary data suggest there is a correlation with enrollment, it remains inconclusive whether geographic location is a factor, even in areas recently struggling with disaster response and recovery.

Future research will further characterize external influences driving the lack of adoption of existing best practices, and characterize external factors influencing IHE preparedness as a contributor to overall community resilience.

THE IMPACT OF HSP90 OVEREXPRESSION ON LEISHMANIA AMAZONENSIS METACYCLOGENESIS AND INFECTION

Nation CS*, McNolty AK**, Bryant N**, Stryker GA**, Dondji B**, Kelly B***, Pizarro JC*

*Department of Tropical Medicine, Tulane SPHTM, New Orleans, LA
**Biological Sciences, Central Washington University, Ellensburg, WA
***Department of Molecular Biology, Immunology and Parasitology, LSUHSC, New Orleans, LA

The incidence of Leishmaniasis is increasing worldwide due to many factors including the inadequacy of available drugs, the appearance of drug resistant parasites and disruption of vector control programs. Thus, the identification of new drug targets is crucial to combat this disease. A major transition in this protozoa parasite's life cycle is the differentiation from the promastigote (vector form) into the intracellular amastigote (human form) to successfully establish an infection. However, the molecular mechanisms driving this important process remain unknown. Upon entering the host, the parasite undergoes differentiation triggered by an increase in temperature followed by a decrease in pH within the macrophage. In addition to these signals, previous studies have also shown that pharmacological inhibition of HSP90 induces this transformation *in vitro* in the absence of changes in temperature or pH. We hypothesize that the protein chaperone HSP90 is a key regulator in parasite development, and will have an impact on infection. The specific role of this protein was further characterized through overexpression of HSP90, because viable null mutants cannot be obtained. Parasites overexpressing HSP90(pXG_HSP90) grew at similar levels when compared to both wild type and parasites carrying empty vector. Interestingly pXG_HSP90 parasites showed significant morphological differences evidenced by microscopy and flow cytometry analysis. These differences included shortened flagella, thus not differentiating into the canonical metacyclic (infective promastigote) morphology characterized by elongated flagella and decreased cell size. However, pXG_HSP90 parasites were still able to undergo a normal axenic differentiation into amastigote like forms. The HSP90 overexpressing parasites also demonstrated a difference in GP63 activity, a surface metallopeptidase and virulence factor. These differences were correlated with increased macrophage invasion capabilities *in vitro* shown by pXG_HSP90 parasites. However, these transgenic parasites were less infective than WT parasites *in vivo* in the mouse model. We then explored differences in proteomic profiles between the WT and transgenic parasites to identify potential virulence factors and drug targets. Taken together these data confirm the importance of HSP90 in the parasite's complex life cycle. Specifically, during metacyclogenesis, the process of differentiating into infective forms. This will inform the identification of novel drug targets to combat this disease.

THE ROLE OF ANGIOTENSIN II AND VITAMIN D ON NATRIURETIC PEPTIDE RECEPTOR-A GENE EXPRESSION

Nguyen CN, Kumar P, Pandya K, and Pandey KN

Department of Physiology, Tulane University Health Sciences Center and School of Medicine, New Orleans, LA.

Physiologically, atrial and brain natriuretic peptides (ANP and BNP) bind guanylyl-cyclase-A/natriuretic peptide receptor-A (GC-A/NPRA) and produce intracellular cGMP, a vital second messenger implicated in hypertension and cardiovascular homeostasis. In this manner, ANP and BNP stimulate natriuresis, endothelial permeability, diuresis, vasorelaxation, and antiproliferation to decrease blood pressure and maintain blood volume homeostasis. Thus, elucidating molecular mechanisms of *Npr1* (coding for GC-A/NPRA) gene expression and regulation has vital implications for the treatment of hypertensive patients. The purpose of this study is to reveal the epigenetic regulation of *Npr1* expression and NPRA levels by Angiotensin II (Ang II) and vitamin D, two stimuli that have been implicated in *Npr1* promoter activity. Mouse mesangial cells (MMCs) were cultured in Dulbecco's modified Eagles medium containing 10% fetal bovine serum and ITS (insulin, transferrin, and sodium selenite) and maintained at 37° C in an atmosphere of 5% CO2/95% O2. The cells were treated with varying concentrations of Ang II and vitamin D for 24 h in DMEM containing 0.1% BSA. Nuclear extract, whole cell lysate, and histones were prepared from these cultures. Through Western blot analysis, we showed NPRA protein expression decreased by 60% in Ang II-treated MMCs compared to control cells. Ang II treatment significantly attenuated ANP-stimulated intracellular concentrations of cGMP compared with ANP-stimulated cells. Treatment of MMCs with Ang II increased histone deacetylase (HDAC) activity in a dose-dependent manner. On the other hand, treatment of MMCs with vitamin D markedly induced NPRA protein expression. In summary, our results show that Ang II treatment decreases NPRA protein expression and signaling whereas vitamin D enhances NPRA protein levels, an important player in the control of hypertension and cardiovascular homeostasis.

This work was supported by the NIH grant (HL57531 and H62147).

.

INAUHZIN ANALOG: A SMALL MOLECULE ACTIVATOR OF p53

Nguyen D, Zeng SX, Zhang Q, Wu R, Zhang Y, Wang G, and Lu H

Department of Biochemistry and Molecular Biology, Tulane University School of Medicine, New Orleans, United States

Because the tumor suppressor p53 is indispensible for the protection and maintenance of genome-wide stability, cancers often find ways to disable its function, as over 50% of all human cancers harbor either p53 gene mutations or posttranslational modifications that abrogate its activity. A paramount challenge in translational research has been to develop molecules that can reactivate the p53 pathway in human cancers in order to repress or reverse tumor growth. Our lab has discovered Inauhzin (INZ), a small molecule non-genotoxic activator of p53. INZ accomplishes this by directly associating with and inhibiting two independent cellular targets: Sirt1 and IMP dehydrogenase. We have recently developed a third generation analog of INZ, which we have INZ-A, which has increased potency and improved metabolic stability. Studies with INZ-A reveal that, in addition to the two established mechanisms, INZ-A may also target an additional two cancer-related pathways. The first involves Glucose-regulated protein 78 (GRP78, also known as Hspa5 and BiP), a member of the heat shock 70 family of molecular chaperones. Not only is GRP78 highly upregulated in tumor cells, but its expression pattern is also expanded to subcellular locations outside of the endoplasmic reticulum, such as the cell surface and the nucleus. Our research indicates that INZ-A requires GRP78 for full activity, an exciting revelation that suggests cancer-specific targeting. The second pathway involves the activation of autophagy, which appears to be important for INZ-A's cytotoxicity. Taken together, INZ-A represents the first paradigm of anti-cancer drugs that can target multiple cancer-related protein molecules and pathways, which might overcome the drug resistance possibility developed against any singular molecule-target drug.

This work is supported by: NIHR01 CA172468-05 and R21 CA190775-02 to Hua Lu.

2017 Annual Meeting
ePoster submission details

ID: 5479

Title: Scarring Alopecia: The Knowledge, Attitudes and Referral Patterns of Hair Stylists and Barbers

Description:

Introduction: Hair loss is a source of psychological distress, and has a negative impact on quality of life. Although there are limited treatment options, early recognition and treatment of scarring alopecia may halt or slow disease progression. Work up for underlying systemic disease may be indicated. Therefore, emphasis should be placed on identifying patterns of hair loss and referral for appropriate medical work up and management.

Hairdressers can act as valuable liaisons between healthcare providers and members of the community. Interventions targeting melanoma screening, hypertension, and intimate partner violence have successfully utilized hairdressers as lay health workers to provide screening and health education to clients. Stylists are in a unique position to detect scalp and neck pathology.

Objective: This study aims to assess knowledge and attitudes of hair dressers and barbers concerning scarring and non-scarring alopecia.

Methods: Cross-sectional data were obtained from a questionnaire administered to hair professionals in person by members of the study team. The study population included English-speaking adult over age 18 working as a hairdresser or barber. Descriptive statistics were tabulated using Microsoft Excel.

Results: Data were obtained from 118 respondents from 51 different hair salons. 2 salons specifically catered towards an African American population and 4 served only men. The majority of salons served a primarily Caucasian population. A standard haircut ranged from $14.95-$100 with a median price of $40 for a women's cut and $27 for a men's cut. 68.6% of participants received some hair loss training while in training. Half of the respondents stated they were somewhat confident in their abilities to identify scarring versus non-scarring hair loss, whereas 34.7% were not at all confident. 56.7% of respondents believe that a scalp exam by a hairdresser is somewhat helpful for finding the cause of hair loss. 79.6% of stylists were willing to learn more about the different types of hair loss. The majority preferred attending a continuing education seminar or using the Internet to receive information. If stylists were trained to identify the different types of hair loss, the majority (90.6%) would discuss the topic with clients.

Conclusions: Survey results indicate that hairdressers frequently interact with patients suffering from hair loss. Hairdressers are interested in learning more and discussing hair loss with their clients. These results provide evidence that hairdressers are engaged in alopecia screening and education and are receptive to additional training and education to expand this role. Limitations of this study include limited demographic

diversity. Future studies may expand to include more diverse population, and focus on specific health training initiatives to most appropriately prepare stylists to accurately evaluate hair loss.

Categories:	Education & Community Service Hair & Nail Disorders
Type:	Research Study
Disclosure:	False
Content Agree:	True
Author Verify:	True

Author(s)

Primary Author: Rachel Evers-Meltzer BS
Co-Author 1: Virginia Tracey MD, MPH
Co-Author 2: Aderonke Obayomi BS
Co-Author 3: Julia Accetta BS
Co-Author 4: Andrea Murina MD

Contact

Virginia Tracey
1430 Tulane Avenue
#8036
New Orleans, LA United States 70112
p: 504-988-5114
e: valldred@tulane.edu

BIOMECHANICAL ROLES OF GLYCOSAMINOGLYCAN CLUSTERS IN TENDON HOMEOSTASIS

O'Cain CM*, Heard WMR***, Savoie FH***, Roccabianca S**, Anderson RC*, Miller KS*

* Department of Biomedical Engineering, Biological Growth & Remodeling Lab, Tulane University, New Orleans, LA, US
** Department of Mechanical Engineering, Soft Tissue Mechanics Lab, Michigan State University, East Lansing MI, US
*** Orthopedic Surgery, Tulane School of Medice, Tulane University, New Orleans, LA, US

Tendiopathy is a general term referring to a diseased tendon with compromised structural integrity caused from either overuse and/or pathological factors. Tendinopathy lead to swelling, pain, reduced functionality, and increased risk of tendon rupture if ignored. Towards this end, the objective of this study was to develop a finite element model, which considered the role of GAGs and their interactions with the surrounding collagen matrix to examine a potential etiology of compromised tendon structural integrity. Therefore, we hypothesize that larger GAG clusters will lead to changes in stress, which may be sufficient to damage neighboring collagens fibers delaying the remodeling process of the tendon, and preventing proper homeostatic conditions.

To initialize the finite element model, the best-fit material parameters were calculated from uniaxial tensile data obtained in the rat Achilles tendon via nonlinear regression. To consider the role of GAGs in tendon mechanical response, parametric studies were performed to evaluate the role of GAG geometry and fixed charge density while subjected to 1–4% axial strain. The bounds for cluster sizes were calculated from histological images from rat supraspinatus tendon with and without overuse pathology using ImageJ.

As the ratio of short to long axis increased, an increase in radial stress and decrease axial stress was observed. As fixed charge density was increased, larger radial stresses were observed in all cases, however the effect on axial stress was minimal. A greater influence was observed on the overuse models compared to the control for radial stress.

The study supports the hypothesis that increased GAG size significantly impacts the local mechanical environment and may augment the surrounding collagen microstructure and induce mechanobiological consequences. The study suggests the structural integrity of tendon may depend on GAG geometry and the interaction between GAG clusters and the other tendon constituents. Future work will further investigate the mechanobiological implications and the impact of GAG clusters on tendon growth and remodeling in healthy and pathological states.

This work was supported by a grant from the Oscar Lee Putnam Cultural and Intellectual Enrichment Program.

EFFECTS OF TERIFLUNOMIDE ON PERIPHERAL BLOOD MONONUCLEAR CELLS AND MITOCHONDRIAL FUNCTION IN MULTIPLE SCLEROSIS

*Ogunsakin O, *Perez Juanazo S, *Wong S *Morava E, *Kozicz T

*Hayward Genetics Center, Tulane University School of Medicine, New Orleans.

Teriflunomide (TF) is an oral, immunomodulatory drug for treatment of relapse in multiple sclerosis (MS). TF functions as a selective and reversible inhibitor of the mitochondrial enzyme, Dihydroorotate Dehydrogenase (DHODH). DHODH plays an important role in de novo pyrimidine (uridine) synthesis. Previous documented studies showed that in Multiple Sclerosis (MS), TF blocks proliferation of activated B and T lymphocytes through inhibition of pyrimidine synthesis. However, fewer studies have elicited mechanism of actions and other therapeutic effects of TF. Objectives of this study focused on exploring and understanding TF actions on mitochondrial of MS via uridine dependent and independent mechanism in vitro systems (Peripheral Blood Mononuclear Cells (PBMCs)).

Cell proliferation in PBMCs will be measured using CellTrace™ Violet proliferation dye (Invitrogen). To investigate the possibility that any inhibition of activation or proliferation of PBMCs in the presence of TF could be due to cytotoxic effects, the viability of stimulated lymphocytes in the presence or absence of TF will be assessed based on staining with LIVE/DEAD® viability dye. For cytokine/chemokine measurement, the human 26-plex Luminex kit will be used to analyze supernatant samples of PBMCs. Protein glycosylation assays will be measured using Western blot analysis, immunocytochemistry, and ICAM-1 isoelectric focusing. Because it is a major surface protein, ICAM-1 will be utilized as a marker for TF induced changes in ICAM-1 glycosylation.

Effects of TF on Mitochondrial structure and function to analyse cellular bioenergetics of PMBCs will be measured using Seahorse XF^e 24 XF^e Extracellular Flux Analyser. This experiment will involve; XF Cell Mito Stress Test (functional mitochondrial measurements to understand cellular activation, proliferation, differentiation, and dysfunction of PMBC); XFp Cell Energy Phenotype Test (metabolic Potential of PMBC); and XF Glycolysis Stress Test (parameters of glycolytic flux of PMBC after treatments).Statistical analysis on effects of TF on various indices of PBMCs function will be tested using multifactorial analysis of variance (ANOVA) and appropriate post-hoc analysis (Tukey-Kramer test). A value of $p<0.05$ will be considered significant.

Previous studies that showed effects of TF on activation of lymphocytes did not show documented evidences to explain mechanisms by which TF exerts its influence on immune cells, especially in MS. Our studies plan to further elucidate roles of TF in three (3) mechanistic approaches; to characterize and confirm TF prevents activations of cytokines in MS, to elucidate TF's glycolytic effects on protein potentially affecting cell to cell contact activation and homing of lymphocytes in preventing attack host cells, and finally, to characterize and describe TF's effects on mitochondrial enzymes with potential to disrupt oxidative phosphorylation and affect cellular activation with potential immunological outcomes.

THIS WORK IS SUPPORTED BY A GRANT FROM GENZYME.

VIRTUAL REALITY GOGGLES: A NOVEL METHOD FOR VISUAL FIELD PERIMETRY

Panse KM*, Lim L*, Frenkel J*, Hawkey N*, Wenk C**, Ayyala R, Ma X**, Ayyala R*

*Tulane University School of Medicine, Department of Ophthalmology, New Orleans LA.
**Tulane University, Department of Computer Science, New Orleans, LA.

Glaucoma is a blinding disease associated with characteristic progressive optic nerve damage and visual field loss. Visual field testing in the form of automated perimetry is critical in the clinical diagnosis and monitoring of glaucoma. Currently, most visual field mappings are obtained by computerized perimeters such as the Humphrey Field Analyzer machine. These machines are built for a physician's office and are bulky, expensive and not portable. We report development lmoland testing of a software program compatible with the Oculus Rift, a commercially available virtual reality goggle technology that provides a more comfortable test environment than the standard instrumentation. We conducted a total of 36 visual field exams on 18 subjects-- 9 volunteers and 9 visual field defect patients. Healthy patients rated the ease of staying focused statistically significantly higher than ease of staying focused during the Humphrey test (4.33 +/- .71 vs. 2.22 +/- .83 with a $p < 0.5\%$) on a scale of 1 to 5. Diseased patients similarly ranked the Oculus VF to be significantly easier to stay focused during compared to the Humphrey test (4.89 +/- .33 vs. 3.11 +/- 1.45 with $p < 1\%$). Healthy patients ranked their overall experience with the Oculus VF to be significantly higher than the Humphrey test (4.22 +/- .83 vs. 2.78 +/- .01 with $p < 0.5\%$). Diseased patients ranked their overall experience with the Oculus VF to be significantly better than their experience with the Humphrey test (4.89 +/- .83 vs. 3.88 +/- .92 with $p = 1.2\%$). The positive predictive value and negative predictive value of the algorithm were .80 and .91, respectively. The present research is a proof of concept study exploring the practicality, comfort, and efficacy of our Oculus Rift virtual reality perimetry test. Our usability study indicates patients' acceptance of the virtual-reality goggle, head-mounted device. Our future work will involve improving the current algorithm to achieve greater efficacy.

This work was supported by a grant from the Carol Lavin Bernick Family Foundation.

THE INFLUENCE OF SOCIALIZATION ON PSYCHIATRIC DISEASE OUTCOME

Parkinson WM*, Earls L*

*Cell and Molecular Biology, Tulane University, New Orleans, LA

Adolescents with autism, social anxiety and other psychiatric conditions are often exposed to over-stimulating surroundings that can cause further withdrawal or exacerbate preexisting symptoms. Enigmatically, individuals with psychiatric disorders often also experience extreme social isolation, which may also contribute to disease outcome. Approximately 1 in 4000 individuals are affected by 22q11 deletion syndrome (22q11DS), widely known as DiGeorge syndrome. The psychiatric phenotype of 22q11DS is complex, and includes a high risk for autism spectrum disorders (ASD), social anxiety, and schizophrenia. While 22q11DS patients are studied by multiple groups around the world, it is difficult to intervene with the social habits of patients to understand how social interaction and social stress impact disease outcome. Mouse models of 22q11DS show similar deficits in learning and memory, socialization and neurological function, providing an excellent model for studying the effects of socialization on disease outcome.

The goal of this study is to compare the effects of three post-weaning social paradigms on 22q11DS outcomes. We will compare constant social interaction with post-weaning social isolation and regular brief isolation periods, a paradigm that we refer to as social respite. We will compare the effects of these paradigms on anxiety, adult social interaction, and adult cognitive function. We will identify molecular mechanisms for the effects of social interaction paradigms using next generation RNA sequencing. This study will determine whether intervening in isolated or over-stimulating environments may positively affect quality of life for 22q11DS patients. Further, this study will uncover the molecular correlates of socialization, providing a framework for future therapeutics targeted at this aspect of 22q11DS and other diseases.

CHARACTERIZATION OF A BIOLOGICALLY DERIVED GRAFT FOR NIPPLE-AREOLAR COMPLEX RECONSTRUCTION

Pashos NC[*, ***]; Martin EC[*]; Chaffin A[****]; Bunnell BA, Ph.D.[*, **]

[*]Center for Stem Cell Research and Regenerative Medicine, Tulane University School of Medicine, New Orleans, LA 70112; [**]Department of Pharmacology Tulane University School of Medicine, New Orleans, LA 70112; [***]Bioinnovation PhD Program, Tulane University, School of Science and Engineering, New Orleans LA 70118; [****]Department of Surgery, Tulane University School of Medicine, New Orleans, LA 70112;

There exists a need for a reproducible off-the-shelf ready graft for Nipple – Areolar Complex (NAC) reconstruction. There are more than 2.8 million breast cancer survivors in the United States, many of who have undergone reconstructive surgery. Approximately 36% of patients with early stage diagnoses and 60% of patients with late stage diagnoses undergo mastectomies. Moreover, immediate breast reconstruction following mastectomies has become more common, significantly increasing at from 20.8% in 1998 to 37.8% in 2008. This increasing trend is not surprising as there is evidence to suggest that NAC reconstruction affects psychological wellbeing of female patients who have undergone mastectomies. Evidence also suggests that woman are more comfortable with getting a mastectomy if the nipple can be spared during the mastectomy procedure, or if nipple reconstruction is possible if a nipple-sparing mastectomy is not an option. Current strategies for NAC reconstruction are limited to surgical techniques that create a NAC-like structure from existing local tissue, secondary site grafting, or 3D tattooing, or a combination of surgical reconstruction with tattooing. Generating a tissue engineered, biocompatible NAC graft for use in place of surgically created NAC structures is a promising approach to NAC reconstruction following mastectomies.

To date, no tissue engineering strategies have been targeted towards the regeneration of the NAC structure. By isolating a biological-derived collagen-rich acellular NAC scaffold, the NAC native micro and macro structural components are maintained. Once derived, NAC scaffolds would be onlay engrafted onto the patient, allowing for host resident-skin cells to repopulate the NAC scaffolds.

Using a Rhesus Macaque Non- Human Primate tissue model, it has been demonstrated that biological scaffolds were reproducibly derived from native tissues with maintenance of extracellular matrix (ECM) proteins and cellular adhesion molecules, with effective removal of nuclear material—significant reduction of DNA. This study details the in vitro material and biological characterization of ECM and cell-ECM interactions through: gene expression of stem

cell differentiation profile and percentage of proliferation/ apoptosis of reseeded cells, histological analysis, and protein quantification/analysis. NSF DGE-144646

OBESITY-DERIVED ADIPOSE STEM CELLS ENHANCE CANCER CELL TUMORIGENESIS THROUGH THE EXPRESSION OF CARCINOMA-ASSOCIATED FIBROBLAST MARKERS

Pei DT*, Strong AL*, Hurst CG*, Burow ME**, Bunnell BA*, ***

* Center for Stem Cell Research and Regenerative Medicine, Tulane University School of Medicine, 1430 Tulane Avenue, SL-99, New Orleans, LA 70112

** Department of Medicine, Tulane University Health Sciences Center, New Orleans, LA 70112

*** Department of Pharmacology, Tulane University School of Medicine, New Orleans, LA 70112

Obesity is associated with an increased risk of developing breast cancer. Increased adiposity induces the expression of certain markers that cause hypoxia, angiogenesis, and inflammation, which are processes that provide the perfect microenvironment for cancer cell proliferation. Of particular interest to our lab is the emerging role of adipose-derived stromal/stem cells (ASCs), which are an integral component within the tumor stromal layer. ASCs have been hypothesized to undergo conversion into carcinoma-associated fibroblasts (CAFs) and crucial in stimulating subsequent cancer cell proliferation. Therefore, identifying the mechanism by which ASCs convert into CAFs and the effects of obesity on this conversion is of particular interest. In this study, ASCs derived from lean subjects (body mass index (BMI) <25; lnASCs) and obese subjects (BMI>30; obASCs) were co-cultured with the breast cancer cell line, MCF7, for seven days. ASCs were subsequently FACS sorted and serially co-cultured with a new population of MCF7 cells that had never been exposed to ASCs. In order to characterize and induce an aggressive phenotype of CAFs, cells were serially co-cultured for a total of three passages and the gene expression profile was assessed. Analysis by qRT-PCR showed a higher induction of CAF markers (alpha smooth muscle actin and NG2) in obASCs following serial co-culture with MCF7s compared with lnASCs. Furthermore, induction of CAF markers occurred at earlier time points in obASCs compared to lnASCs. These results suggest that obASCs may be converted to more aggressive CAFs faster than lnASCs. After one passage, leptin and aromatase expression were also upregulated in obASCs compared to lnASCs. This may support an additional pathway of tumorigenesis, in which overexpression of leptin and aromatase in obASCs may induce the proliferation of estrogen receptor positive MCF7 cells. Together, these results suggest that obesity-associated alterations to ASCs enhance the conversion of these cells into CAFs to support the growth and progression of breast cancer.

This work was supported by Tulane School of Medicine.

High-fat diet induced leptin and Wnt expression: RNA-sequencing and pathway analysis of mouse colonic tissue and tumors

Penrose HM*, Heller S*, Cable CE*, Nakhoul HN*, Baddoo M**, Flemington EK*, Savkovic SD*

*Department of Pathology, Tulane University School of Medicine, New Orleans, LA 70112
**Tulane Cancer Center, Tulane University School of Medicine, New Orleans, LA 70112

Obesity, an immense epidemic affecting approximately half a billion adults, has doubled in prevalence in the last several decades. Epidemiological data support that obesity, due to intake of a high-fat, western diet, increases the risk of colon cancer; however, the mechanisms underlying this risk remain unclear. Here, utilizing next generation RNA sequencing, we aimed to determine the high-fat diet (HFD) mediated expression profile in mouse colon and the AOM/DSS model of colon cancer. Mice on HFD had significantly higher colonic inflammation, tumor burden, and a number of differentially expressed transcripts compared to mice on regular diet (RD). We identified 721 transcripts differentially expressed in mouse HFD colon that were in a shared pattern with colonic tumors (RD and HFD). Importantly, in mouse colon, HFD stimulated an expression signature strikingly similar to human colon cancer, especially those with inflammatory microsatellite instability. Furthermore, pathway analysis of these transcripts demonstrated their association with active inflammation and colon cancer signaling, with leptin and Wnt as the top two transcripts elevated in mouse HFD colon shared with tumors. Moreover, in mouse colon, HFD-stimulated tumorigenic Wnt pathway activation was further validated by upregulation of β-catenin transcriptional targets. Finally, in human colon cancer, upregulation of leptin pathway members was shown with a large network of dysregulated transcripts being linked with worse overall survival.

This work was supported by NIH R01 award (CA160809)

SEX-DEPENDENT VARIABILITY IN PROTEIN EXPRESSION OF RENAL SPHINGOSINE-1-PHOSPHATE SIGNALING PATHWAY AND BLOOD PRESSURE OF INTRAUTERINE GROWTH RESTRICTED MICE

Perez de Lara Rodriguez CE*, Intapad S*

*Department of Pharmacology, Tulane University, New Orleans, Louisiana

Many studies from other groups and ours reported intrauterine growth restriction (IUGR) programs hypertension in adult male offspring but the mechanisms are unclear. We previously showed that sphingosine-1-phosphate (S1P) may play a role in hypertension of adult male IUGR mice and whole kidney S1PR3 expression is altered in male IUGR during- and post-nephrogenesis. Although the potential role of the S1P signaling pathway on blood pressure (BP) of male IUGR is reported, whether different sexes exhibit variations in these parameters is still unclear. This study aimed to determine whether IUGR in mice induced by placental insufficiency programs sex differences in BP and renal S1P signaling protein expressions. C57BL/6J mice underwent sham or reduced uterine perfusion (RUP) surgery at day 13 of gestation with delivery at full term. At 24 weeks of age, we assessed BP via carotid catheter in the conscious state. Male IUGRs developed hypertension (control: 112.1+2.1, IUGR: 125.0+3.7 mmHg; n=7, $p<0.05$) while female IUGRs were normotensive (control: 113.8+3.8, IUGR: 117.8+2.8 mmHg; n=5, ns). Moreover, male IUGR BP was significantly decreased ($p<0.05$) after systemic acute administration of a nonspecific S1PR agonist (1 mg/kg BW I.P., FTY720) similarly to what we had previously reported. We assessed the expression pattern of S1P signaling protein in kidney using immunohistochemistry (IHC) with n=3-4 animals for each group. Digital images were prepared for analyses using ImageJ. Antigen-positive area was automatically separated using a color deconvolution plugin. Mean gray value was then measured and optical density was calculated and reported as percent of control. Males and females exhibited similar patterns of S1PR1 expression and no differences were observed between controls and IUGRs. Male IUGRs had similar S1PR2 expression to control males while female IUGRs exhibited a 25% increase compared to female controls. For S1PR3, no differences were observed in female IUGRs compared to female controls. However, male IUGRs had a 48% decrease in S1PR3 compared to male controls ($p<0.05$). Lower SPHK1 values were observed in male (74%, $p<0.05$) and female (29%) IUGRs compared to their respective controls. SPHK2 levels decreased by 38% in male IUGRS compared to male controls while there was a 129% increase ($p<0.05$) in female IUGRs compared to female controls. Together our data suggest that IUGR programs sex differences in BP and opposing patterns of renal S1P signaling protein expression in males and females. Thus, S1P signaling is a potential mechanism underlying the sex differences in BP of IUGRs.

This work was supported by Career Developmental Grant from American Society of Nephrology to S.I. and Scientist Development Grant from American Heart Association to S.I

REGULATORY PROPERTY OF PYRUVATE KINASE 1 FROM *AEDES AEGYPTI,* A PRIMARY VECTOR OF ZIKA VIRUS

Petchampai N, Murillo-Solano C, Pizarro JC, Scaraffia PY

Department of Tropical Medicine and Vector-Borne Infectious Disease Research Center (VBIDRC), Tulane University, New Orleans, LA, USA

The mosquito species *Aedes aegypti* is an obligate vector of numerous arboviruses that cause disease in humans, including dengue, chikungunya, yellow fever and Zika. Due to the anautogenous reproductive strategy of *A. aegypti*, female mosquitoes are required to take at least one blood meal prior to egg production. Because *A. aegypti* preferentially feed on human blood, this mosquito species is considered highly efficient in disease transmission and is therefore a significant concern for public health. Pyruvate kinase (PK) is the enzyme that catalyzes the conversion of phosphoenolpyruvate to pyruvate during glycolysis, and is crucial for the metabolism of carbohydrates. In most organisms, one or more allosteric effectors control PK activity; however, the mechanism that regulates PK in mosquitoes is unknown. In this study, two genes (AaPK1 and AaPK2) that code for PKs were identified from a BLAST search of the *A. aegypti* genome. The gene AaPK1, which encodes a 529 amino acid protein with an estimated molecular weight of ~57 kDa, was cloned into the pET-51b(+) Ek/LIC vector. The protein was expressed in Rosetta-2 *Escherichia coli*, and was purified using Ni-NTA resin and size exclusion chromatography. The kinetic parameters of recombinant AaPK1 were determined, and the effects of several sugars and amino acids on the enzyme kinetic parameters were also tested. Interestingly, we found that AaPK1 exhibited allosteric behavior and was regulated by fructose-1-phosphate and fructose-2,6-bisphosphate. Additionally, amino acids (including alanine, glutamine, proline, and serine) showed a classic allosteric activation of AaPK1. Given that PK plays a critical role in carbohydrate metabolism and carbohydrates provide valuable energy reserves for female mosquitoes, the regulatory property of AaPK1 may be useful for the design of species-specific inhibitors that control mosquitoes and, subsequently, the diseases they transmit.

This work is supported by NIH/NIAID Grant R01AI088092 (to PYS).

PREVIOUS EXPOSURE TO ESTRADIOL IN OVARIECTOMIZED FEMALE MICE RESULTS IN LASTING MEMORY ENHANCEMENT AND MAINTENANCE OF ESTROGEN RECEPTOR-DEPENDENT GENE TRANSCRIPTION IN THE HIPPOCAMPUS.

Pollard KJ*, Wartman H*, and Daniel JM**
Tulane University, New Orleans, LA; Tulane Brain Institute*, Department of Psychology**

The long-term effects for the brain and memory of short-term use of estrogen therapy following surgical or natural menopause in women are unknown. We have found that a 40-day continuous estradiol exposure in ovariectomized (OVX) rats improves hippocampal-dependent memory and increases hippocampal expression of the estrogen receptor alpha (ERα) up to seven months after treatment has ceased. Furthermore, increased hippocampal expression of ERα alone is sufficient to elicit memory enhancement in OVX rats. However, the cellular functions through which ERα mediates memory enhancement in the absence of circulating estrogens remain unknown. The goal of the current work is to determine if these phenomena also apply to mice and to determine if previous estradiol treatment after ovariectomy results in lasting increases in estrogen receptor transcriptional activity in the hippocampus. Two experiments were conducted, in which mice were ovariectomized and treated with continuous estradiol or vehicle via silastic capsules for 40 days, at which point all capsules were removed. In Experiment 1, C57BL/6 mice were tested for hippocampal-dependent memory performance on a radial-arm maze task several weeks after treatment was complete. Experiment 2 was conducted with transgenic "ERE-LUC" mice, which express the firefly luciferase protein whenever estrogen receptors are transcriptionally active. Four weeks after estradiol treatment had terminated, hippocampi of ERE-LUC mice were harvested and luciferase protein content was analyzed. In Experiment 1, OVX mice that received previous estradiol treatment outperformed OVX controls on the radial-arm maze task. Preliminary data from Experiment 2 suggest that OVX mice that received previous estradiol treatment had significantly higher levels of ERα expression and ERE-dependent gene transcription in the hippocampus than OVX controls. These results suggest that ERα can improve hippocampal dependent memory through its classic role as a nuclear transcription factor in the hippocampus of female mice lacking circulating estrogens.

RELATIONSHIP BETWEEN DAYTIME SLEEPINESS AND POOR PHYSICAL PERFORMANCE IN MIDDLE-AGED ADULTS OF THE BOGALUSA HEART STUDY

Pollock BD*, Stuchlik P*, Guralnik J**, Bertisch SM***, Redline S***, Chen W*, Harville EW*, Bazzano LA*.

*Tulane University School of Public Health and Tropical Medicine, New Orleans, LA
**University of Maryland School of Medicine, Baltimore, MD
***Harvard Medical School, Boston, MA

Studies conducted in elderly and frail adult populations, especially those with heart failure, have shown a consistent relationship between poor sleep and poor physical performance. Likewise, a similar association between poor sleep and lower performance has been found in extremely fit, elite athletes. However, this relationship has not been examined in healthy, middle-aged adult populations. Here, we test the cross-sectional association of daytime sleepiness with poor physical performance in our large, bi-racial cardiovascular cohort. From 2013-2016, 1,223 adults from the Bogalusa Heart Study attended study visits to assess physical and cognitive performance and answer questionnaires pertaining to sleep habits. The Epworth Sleepiness Scale (ESS) was used to measure daytime sleepiness on an ordinal scale from 0-24. Short Physical Performance Battery (SPPB), which consists of chair stands, balance testing, and walk speed, was the outcome measure, with a score of <10 out of 12 being considered poor physical performance. Multivariable logistic regression, adjusted for age, race, sex, sleep duration, employment status, BMI, and symptoms of sleep apnea was used to test the association between ESS [both continuously and dichotomized to abnormal (ESS>10) vs. normal (ESS≤10)] and poor physical performance. Our study population had a mean(SD) age of 48.1(5.2) and was 58.6% female and 34.7% black. Mean(SD) ESS was 6.3(4.7). 252 (20.6%) adults exhibited poor physical performance. After covariate adjustment, ESS was significantly associated with an increased risk of poor physical performance (Odds Ratio per 1 SD increase=1.17; 95% Confidence Interval=1.01-1.35; *p*=0.03). As a dichotomous exposure, an abnormal ESS resulted in a 53% increased risk of poor physical performance (OR=1.53; 95% CI=1.05-2.23; *p*=0.03). Even among relatively healthy middle-aged adults, daytime sleepiness appears to be associated with poor physical performance.

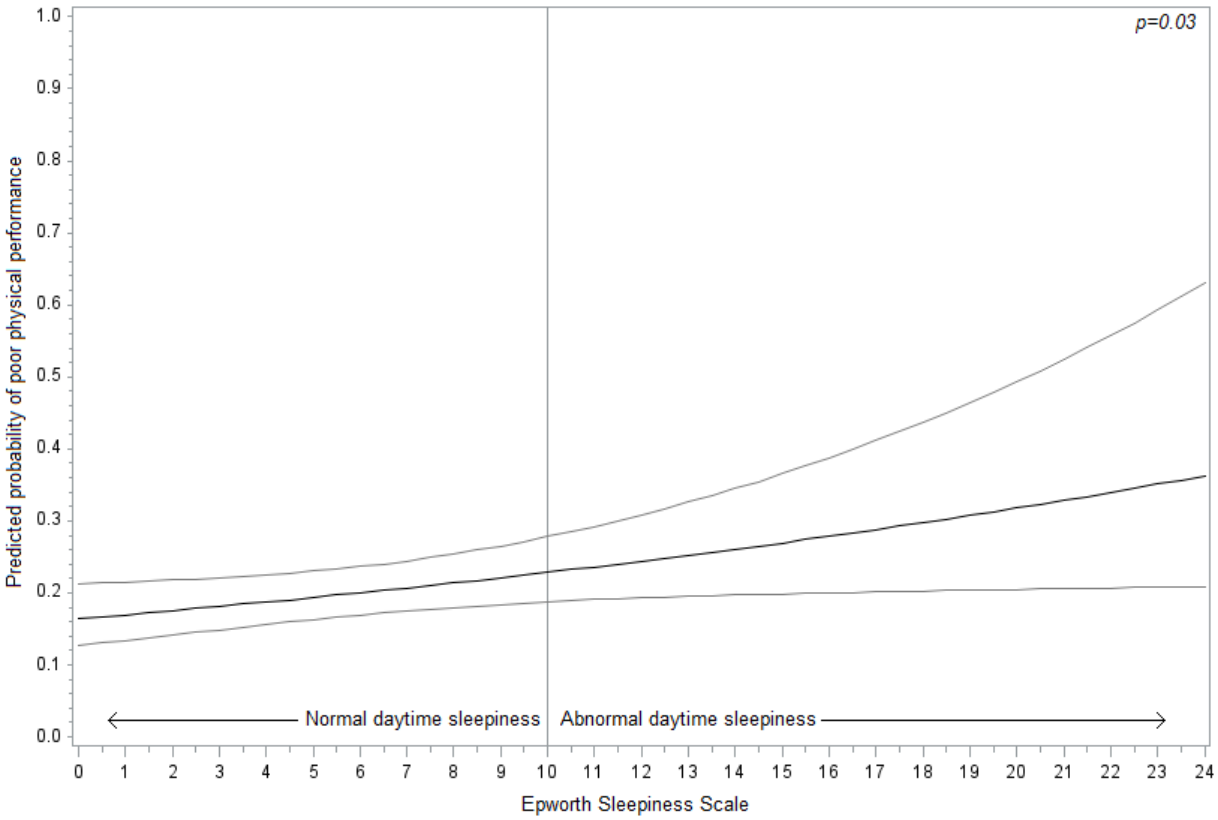
p=0.03
Predicted probability of poor physical performance
1.0
0.9
0.8
0.7
0.6
0.5
0.4
0.3
0.2
0.1
0.0
Normal daytime sleepiness
Abnormal daytime sleepiness
0 1 2 3 4 5 6 7 8 9 10 11 12 13 14 15 16 17 18 19 20 21 22 23 24
Epworth Sleepiness Scale

ACTION POTENTIAL FREQUENCY ADAPTATION CORRELATES WITH INHIBITORY DRIVE IN PYRAMIDAL NEURONS OF THE SOMATOSENSORY CORTEX

Popescu IR*, Lee K**, Mostany R*,**

*Department of Pharmacology, Tulane University School of Medicine, New Orleans, LA
**Neuroscience Program, Tulane Brain Institute, New Orleans, LA

Action potential firing frequency in response to a constant stimulus shows considerable decrease (adaptation) in some neocortical pyramidal neurons, and little or no adaptation in others. These two groups of pyramidal neurons have been shown to have either thin or thick tufted dendritic trees, to receive inputs mostly from local or remote areas, and to project either only within or also beyond the telencephalon, and therefore are very likely to perform different functions. Here we show that inhibitory postsynaptic potentials (IPSCs) in mouse layer 5 non-adapting pyramidal neurons occur with a mean frequency that is several fold higher than in the adapting pyramidal neurons. The difference in frequency is preserved when action potential firing is blocked in acute brain slices, suggesting that it is not caused by higher levels of activity in the GABAergic interneurons that synapse on non-adapting pyramidal neurons, but is most likely due to the presence of more synapses on the larger dendritic trees of these cells. Layer 5 pyramidal neurons expressing the Thy1 protein, which have been shown to be thick tufted, to send axonal projections beyond the telencephalon, and to be non-adapting, also had several fold higher IPSC frequencies when compared with adapting cells. Since a specific balance between excitatory and inhibitory synaptic inputs is thought to be important for neuronal function, the much larger inhibitory drive to non-adapting neurons implies that the excitation/inhibition balance of this subclass of pyramidal neurons is particularly susceptible to perturbation in conditions which diminish GABAergic function, such as, for example, aging.

Support: NIA/NIH R01AG047296, COBRE on Aging and Regenerative Medicine P20GM103629, Louisiana Board of Regents RCS LEQSF(2016-19)-RD-A-24, and startup funds from the Tulane University School of Medicine to RM.

Identification of Enhancer-SNPs Associated with Osteoporosis

Chuan Qiu[1], Hong-Wen Deng[1], Hui Shen[1]

1. Center for Bioinformatics and Genomics, Department of Global Biostatistics and Data Science, School of Public Health and Tropical Medicine, Tulane University, New Orleans, LA 70112, USA

Background

Most of the disease-associated SNPs discovered to date located in noncoding intragenic and intergenic regions, such as enhancer. Enhancer is a short (50-1500 bp) noncoding segments of DNA which can be bound with proteins to regulate transcriptional programs. A large number of weakly osteoporosis -associated loci are enriched in enhancer regions and disease-associated noncoding-SNPs frequently lie in cell-type-specific enhancer elements. To identify potential enhancer-SNPs among the weakly osteoporosis -associated loci, we conducted a meta-analysis of genome-wide association studies (GWAS) for osteoporosis, specifically focusing on enhancer-SNPs in osteoporosis -relevant cell type.

Methods

We retrieve weakly osteoporosis -associated SNPs (5xE-8< P-value < 5xE-5) from Genetic Factors for Osteoporosis Consortium (GEFOS-2) and download the enhancer regions in 20 primary cell types from Functional Annotation of Mammalian Genome (Fantom5). A total of 1206 osteoporosis -associated SNPs were mapped to 20 cell type enhancers. Then, meta-analysis was performed to identify significant enhancer-SNPs in 5 osteoporosis GWA Studies.

Results

There were 430 weakly osteoporosis-associated SNPs located in CD4+ T-cell enhancer regions, 282 SNPs located in osteoblast enhancer regions and 376 SNPs located in natural killer cell. Enrichment analysis shows these SNPs are enriched in enhancers regions which are preferentially active in immunological cell types. Meta-analysis identified 27 enhancer SNPs which were significantly associated with osteoporosis (4.14xE-5 [0.05/1,206]). Interestingly, several loci display clusters of osteoporosis -associated SNPs which are located within the same or neighboring enhancer. These haplotypes may have a greater likelihood to influence enhancer activity than SNP on its own.

Conclusion

In this study, we identified a number of osteoporosis-associated SNPs in T cells, osteoblast and Natural killer cells through altering the activity of immune cell enhancer. These results provided novel insights into the pathogenesis of osteoporosis.

MODELING THE MITIGATION OF ZIKA AND CHIKUNGUNYA BY INFECTING MOSQUITOES WITH WOLBACHIA BACTERIA

Qu Z*, Xue L**, Hyman JM*

*Department of Mathematics, Tulane University, New Orleans, LA
** Department of Mathematics, Harbin Engineering University, Harbin, HLJ, China

The ongoing mosquito-borne epidemics such as Chikungunya and Zika virus have significantly affected human health and are of increasing concern worldwide. We develop and analyze an ordinary differential equation (ODE) model to assess the potential effectiveness of infecting mosquitoes with the Wolbachia bacteria, which is a natural parasitic microbe that stops the proliferation of the harmful viruses inside the mosquito and blocks the disease transmission. A sustainable release for the maternally transmitted Wolbachia bacteria in a wide mosquito population can be difficult due to the Wolbachia-induced fitness change and cytoplasmic incompatibility. Our model captures the complex vertical transmission cycle by including aquatic and adult life stages of mosquitoes as well as single and pregnant stages for female mosquitoes. We derive important dimensionless parameters and observe a critical threshold condition for a successful introduction of Wolbachia endemic: the infection will only persist if the fraction of the infected mosquitoes passes the threshold. This threshold effect is reflected by a backward bifurcation with three coexisting equilibria of the ODE system: a stable disease-free equilibrium, an unstable intermediate-infection endemic equilibrium and a stable high-infection endemic equilibrium. We also perform sensitivity analysis on epidemiological and environmental parameters to determine their relative importance to Wolbachia transmission and prevalence.

Acknowledgement: This research was partially supported by the NSF-MPS/NIH-NIGMS award NSF-1563531 and the NIH-NIGMS Models of Infectious Disease Agent Study (MIDAS) award U01GM097661. The content is solely the responsibility of the authors and does not necessarily represent the official views of the National Science Foundation or the National Institutes of Health.

MSCS ACTIVATE THE LATENT PROVIRUS IN HIV-1 INFECTED MONOCYTES: PUTATIVE ROLE OF AKT SIGNALING AND C/EBPB IN AUGMENTING TAT TRANSACTIVATION OF THE HIV-1 LTR

Ramachandran M[*], Chandra PK[*], Gerlach SL[*], Wu C[***], Gimble JM[**,****], Mondal D[*,**], and Braun SE[*,**,***]

Department of Pharmacology[*], Center for Stem Cell Research and Regenerative Medicine[**], Tulane National Primate Research Center[***], Tulane University School of Medicine. LaCell, LLC[****], NOBIC.

Despite the efficacy of combined antiretroviral therapy (cART) in suppressing plasma viral load, persistently active tissue HIV-1 reservoirs remain a significant hurdle towards long-term cure. Additionally, constant provirus reactivation and propagation at subtherapeutic drug levels can facilitate a rapid selection of drug-resistant viral mutants. Host factors that regulate proviral latency and reactivation within sequestered tissue reservoirs of HIV-1 are not well understood. Although a number of past studies have suggested that mesenchymal stromal cells (MSC) play a crucial role in regulating the effector function of hematopoietic stem cells, both lymphocytes and monocytes, the role of tissue-resident MSCs in regulating infectivity in HIV-infected reservoirs has not been thoroughly addressed. Our previous *in vitro* studies showed that conditioned medium (CM) from MSCs can significantly ($p<0.05$) activate the latent provirus from HIV-infected monocytic cells (U1). This latency-reactivation by MSC-CM was as potent as the known provirus-inducer, phorbol myristate acetate (PMA). Unexpectedly, studies using signal transduction inhibitors clearly indicated that the MSC-CM mediated provirus induction occurs via the PI3K/AKT pathway, in contrast to PMA-stimulated provirus reactivation, which occurs via protein kinase-C (PKC)-induced NF-κB signaling pathway. Most interestingly, we documented that despite constitutive expression of the HIV-1 transactivator (Tat) protein, the U1 cells are latently infected. These findings suggested that both stimulation of U1 cells, either via PMA or MSC-CM, may induce host factors that are needed to increase Tat transactivation function. In these studies, using U937 cells carrying an integrated HIV-1 vector that regulates green fluorescent protein (GFP) expression via the HIV-1 long terminal repeat (LTR), i.e. U937-VRX494 model, we documented that both PMA and MSC-CM stimulation activates HIV-1 LTR mediated gene expression and its Tat transactivation function. Indeed, cotransfection of U937-VRX494 cells with a Tat expression plasmid clearly showed that exposure to both PMA and MSC-CM can activate Tat function. Previous studies have shown that the PI3K/AKT signaling pathway can activate the function of CCAAT-enhancer binding protein (C/EBP) transcription factors. Furthermore, several studies have shown that C/EBPβ can directly interact with the Tat-transactivation complex to facilitate HIV-1 LTR transactivation. Transient transfection of U937-VRX494 cells or of U1 cells with both Tat and C/EBPβ (LAP or LIP) expression plasmids showed significant increases in LTR-directed GFP expression and virus production, respectively. This induction was seen even in the absence of PMA stimulation. Stimulation with MSC-CM further augmented LTR function in cells cotransfected with Tat and C/EBPβ (LAP or LIP) expression plasmids. Our findings suggest a novel host-virus interactive pathway that enable latency reactivation and implicate novel anti-HIV therapeutics that target cellular signaling machinery that facilitates Tat transactivation of the latent provirus. Studies to delineate the role of PI3K/AKT pathway and C/EBPβ (LAP or LIP) in MSC-CM induced Tat transactivation are currently underway. In addition, studies using HIV-1 LTR deletion mutants are being carried out to further demonstrate the role of a novel NF-κB-independent pathway in MSC-induced latency reactivation.

Acknowledgement: Studies were supported by NIH grants to DM (AI116348) and SEB (AL110158).

ROLE OF ELASTIN IN VAGINAL WALL BIAXIAL MECHANICAL RESPONSE WITH EXPERIMENTAL AND MATHEMATICAL APPROACHES

Robison KR*, Akintunde AR*, Desrosiers L**, Knoepp LR**, Miller KS*

*Department of Biomedical Engineering, Tulane University, New Orleans, LA
**Female Pelvic Medicine & Reconstructive Surgery, Ochsner Clinical School, New Orleans, LA

Pelvic organ prolapse (POP) is a global health concern characterized by the atrophy of the vaginal wall and the prolapse of the pelvic organs. Although little is known about the underlying pathology of POP, a dysfunction of the elastin metabolism within the vaginal extracellular matrix has been implicated [1-3]. The mechanical mechanisms by which elastic fiber damage may contribute to prolapse, as well as the role of elastin in normal vaginal mechanical function, however, are poorly understood [1-3]. Therefore, the objective of this study is to determine the role of elastin in the biaxial mechanical properties of the murine vaginal wall using both experimental and mathematical tools. We hypothesize that a loss of elastin will decrease vaginal wall distensibility.

Experimental evaluation of vaginal mechanics demonstrated that intraluminal exposure to elastase for 45 minutes induced marked changes in the vaginal distensibility. To mathematically evaluate the role of elastin in vaginal mechanics, several microstructural models were selected as candidates to describe vaginal wall behavior before and after elastase digestion. Within the candidate models, all but the diagonal two-fiber family were found to be over-parameterized. Thus, a two-fiber family model with two symmetrical diagonal families of collagen (average R^2 value of 0.90 and 0.84 for control and elastase groups respectively) was selected as the best candidate to describe the biaxial testing data.

In this study, the loss of elastin induced significant changes in the load-bearing capability and geometry of the vagina, suggesting that the mechanical role of elastin in particular may be an important therapeutic target for prolapse. Intraluminal exposure to elastase resulted in a decrease in compliance and an increase in resistance to deformation at low strains. These results may be explained by the substantial dilation in vaginal caliber following digestion, which may be indicative of prolapse-like symptoms. While the constitutive model selected in this study describes the biaxial mechanical behavior of the control group reasonably well, the model is less accurate in predicting the mechanical response of the elastase group. Further, we hypothesized that a loss of elastin would be reflected in the constitutive relation by a decrease in the elastin-associated parameter. However, the average values of this term (313.8 and 357.51 kPa for control and elastase, respectively) did not show this, suggesting that the organization of elastin within the vaginal wall may not be isotropic within the ground matrix, as was previously thought. Ongoing work to rigorously quantify the microstructure of the vagina (including elastin-collagen interactions) is being pursued in order to refine this model and validate the microstructural implications of each parameter.

REFERENCES [1] Drewes P et al., *Am J Path*, 170(2):578-589, 2007. [2] Rahn D et al., *Am J Ob Gyn*, 198(5):590.e1-6, 2008. [3] Downing, K et al., *J Mech Beh Biomed Mat*, 29:190-8, 2014.

Barriers to HPV Vaccine Access

Rogg K*, Grimes C*, Goodman E*, Naresh A*, Robinson W*
Tulane University School of Medicine, New Orleans, La

We sought out to examine barriers to utilization of the human papilloma virus (HPV) vaccine for women in an urban center in the southern United States. We conducted focus groups with patients in a general obstetrics and gynecology clinic in an urban area in the southern United States. Participants were divided into three groups: (1) young women who had received the HPV vaccine (2) young women who had not received the HPV vaccine (3) mothers of adolescent daughters. The focus groups consisted of a series of open-ended questions developed by the research team regarding HPV and HPV vaccination. The focus groups demonstrated that knowledge of HPV and the HPV vaccine was generally low in all study groups. Most non-HPV vaccinated women and mothers indicated that a health care provider had never discussed nor offered the HPV vaccine. Other factors were not considered major barriers. As the major factor in lack of HPV vaccination in our study population was lack of awareness of the HPV vaccine possibly resulting from lack of a health care provider recommendation for this vaccine. Low rates of HPV vaccination in this community may continue to contribute to disproportionally high rates of cervical cancer in this southern city in the United States.

MULTI-SCALE MODELING OF PARENCHYMLA/AIRWAY INTERACTIONS

Ryans J[*], Fujioka H[**], Halpern D[***], Gaver DP[*]

[*]Biomedical Engineering Department, Tulane University, New Orleans, LA
[**]Center for Computational Science, Tulane University, New Orleans, LA
[***]Department of Mathematics, University of Alabama, Tuscaloosa, AL

Acute lung injury (ALI) is an onset form of non-cardiogenic pulmonary edema that can be triggered by local or systemic inflammation. ALI and its more severe form known as acute respiratory distress syndrome (ARDS) can lead to widespread alveolar collapse and small airway closure. Additionally, this affects the parenchymal tethering mechanics that contribute to maintain patency. The primary method of treating ALI/ARDS is the use of mechanical ventilation, yet this can lead to ventilator-associated lung injury (VALI). To investigate the pathophysiological effects of ALI/ARDS on lung parenchyma, a reduced-dimension multi-scale model was developed for an anatomically based airway tree with surrounding lung parenchymal tethering mechanics.

This new model builds upon the airway/acinar system that investigated plug propagation during ventilation (ref). That model includes time varying airway radii, airway liquid-lining thickness, and acini volume, with airway closure and the formation and movement of liquid plugs. To describe the effects of parenchymal tethering, work by Fujioka et al. (2013) was expounded upon to elucidate the mechanical interactions between airways and alveoli that are transmitted by parenchyma. To do so, finite element models of connected truncated octahedral alveoli were prescribed with a heterogeneous pressure distribution to represent the effects of ALI. Here we scale the effective shear modulus as a function of the change in alveolar pressure with collapsed alveoli. We will present reduced dimension parametric descriptions that will faithfully articulate the meso-scale interactions. Additionally, Langmuir kinetics were utilized to prescribe the dynamic surface tension based on the surfactant concentration within the interfacial film as described in Otis et al (1994).

This model was used to simulate adverse of ALI/ARDS conditions, and was compared to previous experimental and clinical studies. In particular, the pressure-volume (P-V) hysteresis loops were compared to determine how closely the model predicted impacted lung behavior. Additionally, the effects of parenchymal tethering on airway closure/reopening were investigated, along with effects on liquid plug propagation behavior. The modeling approach allows for a new method to simulate the mechanics of ALI/ARDS, which can be developed to examine other pulmonary pathophysiological conditions such as cystic fibrosis and emphysema. Further work will encompass the implementation of this model to assess the utility of mechanical ventilation, and to explicate ventilator regimes that will mitigate VALI.

This study was supported by National Science Foundation Grant CBET-1033619 and Research Traineeship Grant DMS-1043626. Computational resources were supported in part using high performance computing (HPC) resources and services provided by Technology Services at Tulane University, New Orleans, LA.

ADIPOSE STEM CELLS FROM OBESE INDIVIDUALS PROMOTE METASTASIS OF BREAST CANCER PATIENT DERIVED XENOGRAFT

Sabol RA*, Bowles AC*, Cote A*, Dutreil M*, Matossian M*, Collins-Burow B***, Burow ME***, Bunnell BA*,****
***Center for Stem Cell Research and Regenerative Medicine, Tulane University School of Medicine, New Orleans, LA 70125
****Department of Pharmacology, Tulane University School of Medicine, New Orleans, LA, 70125
*****Department of Medicine Section Hematology and Oncology, Tulane University School of Medicine, New Orleans, LA 70125

Obesity is an established risk factor for breast cancer. Obese women have an increased incidence and mortality of breast cancer, however the mechanisms(s) through which obesity enhances tumorigenesis are not well understood. Current models used to study breast cancer *in vivo*, specifically immortalized cell lines or orthotopic xenografts, are limited by the lack of tissue architecture and human stromal components. Passaging immortalized cell lines results in irreversible alterations of genetic information and behavioral characteristics. Patient-derived xenografts (PDX) have emerged as a novel translational tool for cancer research with the potential to more accurately recapitulate the molecular and behavioral aspects of cancer. Further, PDX represent primary patient tumors providing evidence in the context of humans *in vivo*. Our team has developed a system to investigate the obesity-breast cancer axis. The protocol involves implanting PDX tumor line 2K1 coated in matrigel alone or co-transplanted with adipose-derived stem cells from lean (lnASCs) and obese (obASCs) donors. PDX tumors were implanted bilaterally into the mammary fat pad of female SCID/Beige mice and passaged when the tumor volume grew to 750-1000 mm^3. Tumors with obASCs show increased circulating tumor cells as well as increased metastasis. These data suggest that obASCs promote metastasis of triple negative breast cancer PDX.

THE IMPACT OF ALCOHOL-DYSBIOSIS ON HOST DEFENSE AGAINST PNEUMONIA.

Samuelson, D.R.*, Maffei, V.J.***, Blanchard, E.E.***, Luo, M.***, Taylor, C.M.***, Shellito, J.E.*, Ronis, M.J.****, Molina, P.E.**, and Welsh, D.A.*

*Department of Medicine, Section of Pulmonary/Critical Care & Allergy/Immunology, Louisiana State University Health Sciences Center, New Orleans, LA, USA. **Department of Physiology, Louisiana State University Health Sciences Center, New Orleans, LA, USA. ***Department of Microbiology, Immunology and Parasitology, Louisiana State University Health Sciences Center, New Orleans, LA, USA. ****Department of Pharmacology and Experimental Therapeutics, Louisiana State University Health Sciences Center, New Orleans, LA, USA.

Alcohol consumption perturbs the normal intestinal microbial communities (alcohol-dysbiosis). To begin to investigate the relationship between alcohol-mediated dysbiosis and host defense we developed an alcohol-dysbiosis fecal adoptive transfer model, which allows us to isolate the host immune response to a pathogenic challenge at a distal organ (i.e., the lung). This model system allowed us to determine if the host immune responses to *Klebsiella pneumoniae* are altered by ethanol-associated dysbiosis, independent of alcohol use. We hypothesized that alcohol-induced changes in intestinal microbial communities would impair pulmonary host defenses against *Klebsiella* pneumonia. Mice were treated with a cocktail of antibiotics daily for two weeks. Microbiota-depleted mice were then recolonized by gavage for 3-days with intestinal microbiota from ethanol-fed or pair-fed animals. Following recolonization groups of mice were sacrificed prior to and 48 hrs. post respiratory infection with *Klebsiella pneumoniae*. We then assessed susceptibility to *Klebsiella* infection by determining colony counts for pathogen burden in the lungs. We also determined lung and intestinal immunology, intestinal permeability, as well as, liver damage and inflammation. We found that increased susceptibility to *Klebsiella pneumoniae* is, in part, mediated by the intestinal microbiota, as animals re-colonized with an alcohol-induced dysbiotic intestinal microbial community have significantly higher lung burdens of *Klebsiella pneumoniae* ($5x10^4$ CFU v. $1x10^3$ CFU) independent of EtOH. We also found that increased susceptibility in alcohol-dysbiosis recolonized animals was associated with a decrease in the recruitment and/or proliferation of CD4+ and CD8+ T-cells ($1.5x10^9$ cells v. $2.5x10^9$ cells) in the lung following *Klebsiella* infection. However, there were increased numbers of T cells in the intestinal tract following *Klebsiella* infection, which may suggest that T cells are being sequestered in the intestinal tract to the detriment of host defense in the lung. Interestingly, mice recolonized with an alcohol-dysbiotic microbiota had increased intestinal permeability as measured by increased levels of serum intestinal fatty acid binding protein (55 ng/mL v. 30 ng/mL). Alcohol-dysbiotic microbiota also increased liver steatosis (Oil Red-O staining) and liver inflammation (>2 fold expression of IL-17 and IL-23). Our findings suggest that the commensal intestinal microbiota support mucosal host defenses against infectious agents by facilitating normal immune responses to pulmonary pathogens. Our data also suggest that increased intestinal permeability coupled with increased liver inflammation may impair the recruitment/proliferation of immune cells in the respiratory tract following infection. The role of the microbiota during host defense will be important areas of future research directed at understanding the effects of microbial dysbiosis in patients with AUDs.

This work was supported by The National Institute on Alcohol Abuse and Alcoholism grants # R24-AA019661, P60-AA009803, and T32-AA07577; The National Heart Lung and Blood Institute grant #P01-HL076100; and by The National Institute of General Medical Sciences of the National Institutes of Health, which funds the Louisiana Clinical and Translational Science Center grant #1 U54 GM104940.

CHARACTERIZATION OF THE RENIN-ANGIOTENSIN SYSTEM IN INDUCED PLURIPOTENT STEM CELL-DERIVED HUMAN KIDNEY ORGANOIDS

Sato R[1], Dugas CM[1], Jiao L[2], El-Dahr S[2], Saifudeen Z[2]

[1]Department of Physiology, and Hypertension and Renal Center of Excellence, [2]Department of Pediatrics, Tulane University School of Medicine, New Orleans, LA

Intrarenal renin-angiotensin system (RAS) plays crucial roles in the progression of kidney injury in which augmentation of proximal tubular angiotensinogen (AGT) is a key mechanism. Furthermore, intrarenal RAS has been shown to contribute to kidney development. Our recent studies, using adult rodent models and cultured renal cells, demonstrated that histone deacetylase 9 (HDAC9) is an epigenetic repressor of proximal tubular AGT. Organoids forming multicellular structures can serve as *ex vivo* models to investigate organ development, molecular mechanisms and pathophysiological functions, and also have potential utilities in drug screening and clinical therapies. In addition to kidney organoids derived from embryonic and adult stem cells, technologies using induced pluripotent stem cells (iPSCs) have also rapidly evolved in the last few years. Accordingly, this study was performed to evaluate expression of RAS genes and regulation of AGT expression by HDAC9 in iPCS-derived kidney organoids (per published protocol, Takasato et al, 2015, Nature Protocols). Human iPSCs were pre-treated with CHIR99201, an inhibitor of glycogen synthase kinase, for five days to induce differentiation. Thereafter, the cells were transferred to transwell membranes. The cells were cultured on the membrane for 18 days followed by treatment with fibroblast growth factor 9. During the 18-day culture, cells were harvested on day 0, 5, 12 and 18 to determine absolute mRNA copy numbers of developmental markers and RAS components by droplet digital PCR and immunostaining. Induction of markers for renal structures including proximal tubules as well as morphological tubular maturation were observed during the culture. Moreover, immunostaining revealed that there were podocytes, proximal tubules and distal tubules in the organoids. Angiotensin II type 1 receptor mRNA levels were higher than other RAS components on day 0 and the receptor expression was downregulated on day 5. Expression of angiotensin II type 2 receptor was stimulated on day 5 and then decreased until day 18. Renin expression was strongly induced on day 5 and sustained until day 18. Expression of angiotensin-converting enzyme was moderately increased during the experimental period. AGT expression was elevated on day 12 and remained until day 18. On the other hand, HDAC9 levels were decreased as of day 18. In further experiments using pre-treatments with various concentrations of CHIR99201, AGT mRNA levels on day 18 were increased in a CHIR99201 concentration-dependent manner. In contrast, HDAC9 levels were downregulated in accordance with the CHIR99201 concentration, indicating a negative correlation between AGT and HDAC9 expression. Importantly, application of an inhibitor which exhibits higher affinity to HDAC9 than other HDACs resulted in augmentation of AGT expression (2.25±0.21-fold compared to control) in the organoids. The results of this study suggest that all of the RAS components required to generate angiotensin II and the receptor are expressed and independently regulated during the development of iPSC-derived human kidney organoids. Furthermore, HDAC9 has a suppressive effect on AGT expression in the human iPSC-kidney organoids, consistent with the effect observed in rodent models. Comparison of these findings with those previously published in embryonic kidneys may help to characterize the developmental potential and maturity of iPSC-derived human kidney organoids generated by current techniques. Although persisting scientific issues and technical difficulties currently avert the generation of functional nephrons in embryonic stem cell- or iPCS-derived kidney organoids, we recognize the need for additional experimental data and detailed evaluation of iPSC-derived kidney organoids in the current form, to improve and develop the technology further.

This work was supported by the NIDDK (DK107694-01) and the NIGMS (P30GM103337) for R.S.

LARGE-CONDUCTANCE POTASSIUM CHANNELS AS A POTENTIAL THERAPEUTIC TARGET IN FRAGILE X SYNDROME

Sawyer EJ*, Zingale AR*, Schrader LA**

*Neuroscience Program, Brain Institute, Tulane University

**Department of Cell and Molecular Biology, School of Science and Engineering, Tulane University

Fragile X Syndrome (FXS) is the most common inherited intellectual disability in humans, and the most common monogenic cause of autism spectrum (AS) symptoms. FXS is caused by the transcriptional silencing of the FMR1 gene on the X chromosome, which codes for the protein FMRP. Large-conductance potassium (BK) channels are part of the molecular machinery that regulates neuronal membrane potential following action potential propagation and synaptic transmission, and are themselves regulated by FMRP through an interaction between FMRP and the β-subunit of the BK channel. We have recently shown that BK channel activity is regulated in an activity-dependent manner, highlighting the importance of BK channels for synaptic remolding. Mice that have had the *fmr1* gene silenced or removed are a commonly-used animal model of FXS. In *fmr1* knockout mice, BK channel hypoactivity is associated with neuron firing irregularities and aberrant synapse formation, and systemic activation of BK channels in these partially rescues AS-related symptoms. We hypothesized that medial prefrontal cortical (mPFC) infusion of the BK channel activator BMS-204352 would be sufficient to rescue AS-related executive function abnormalities commonly observed in *fmr1* knockout mice. Single-housed knockout mice treated with BMS and subjected to a behavioral battery displayed improved social recognition, yet unchanged anxiety or motor activity relative to saline-treated control knockouts. We are currently investigating the effect of BK channel activation on group-housed wild type and knockout mice in social approach, social recognition, and compulsive burying tests. Future molecular and electrophysiological research will assess the role of BK channels in mPFC synaptic plasticity in *fmr1* knockout mice.

This work is supported by the Simons Foundation SFARI grant.

ENDEMIC LASSA FEVER AS A PHYSIOLOGIC MODEL FOR EPIDEMIC VIRAL HEMORRHAGIC FEVERS IN FEMALE AND MALE PATIENTS

Schieffelin JS*, Grant DS**, Hartnett JN***, Shaffer JG****, Garry RF***

* Department of Pediatrics, School of Medicine, Tulane University, New Orleans, LA
** Kenema Government Hospital, Kenema, Sierra Leone
***Department of Microbiology and Immunology, School of Medicine, Tulane University, New Orleans, LA
****Department of Global Biostatistics and Data Science, School of Public Health and Tropical Medicine, Tulane University, New Orleans, LA

Lassa fever (LF), a viral hemorrhagic fever (VHF) caused by Lassa virus (LASV) in the family *Arenaviridae*, is endemic to West Africa. Circulatory instability, increased vascular permeability and diffuse hemorrhagic manifestations are common characteristics of VHFs, including LF. Most VHFs, including Ebola Virus Disease (EVD) and Crimean-Congo Hemorrhagic Fever, occur sporadically in unpredictable outbreaks. However, LF occurs seasonally in endemic countries. If sufficient similarities exist, LF can serve as a model for testing novel supportive care strategies for all VHFs. Acutely ill subjects meeting the case definition of a suspected LF patient as well as healthy controls (asymptomatic household contacts) were recruited at the Kenema Government Hospital (KGH) VHF ward. All enrolled subjects were tested by ELISA for the presence of LASV antigen as well as anti-LASV IgM and IgG. All enrolled subjects were categorized as LASV Ag+/IgM-, Ag-/IgM+, Ag-/IgM- (non-Lassa febrile illness – NLFI) or healthy control. Patients admitted to KGH had samples drawn on hospital days 1,2,3,4,7 and 10. Nine different analytes were tested on available samples from 89 suspected LF patients, 41 household contacts and 15 confirmed EVD patients. Levels of sVCAM-1 and sICAM-1, markers of endothelial dysfunction, were significantly higher ($p<.001$) among Ag+/IgM- patients vs Ag-/IgM+, NLFI and contacts. While no sex differences in sVCAM-1 were seen, sICAM-1 levels were higher ($p=.02$) among male compared to female IgM+ patients. Higher levels of other endothelial dysfunction markers, angiopoietin-1 and -2 as well as markers of coagulation abnormalities, such as von Willebrand factor, PAF acetylhydrolase activity, tissue factor and plasminogen activator factor-1 were higher among Ag+ LF patients than EVD patients and normal controls. However, none reached significance. These results identify specific biomarkers associated with the vascular permeability and coagulopathy seen in severe LF. Further work is needed to determine if levels of these biomarkers differ among males and females and if LF would be a valid model for the treatment of other VHFs.

This work was supported by NIH grants 5K12HD043451-14 and 1U19AI115589-02

THE DEVELOPMENT OF A PARTICIPANT-INFORMED MHEALTH INTERVENTION TO PROMOTE HEALTHY EATING AMONG OVERWEIGHT AFRICAN AMERICAN MEN AND WOMEN

Sheats, JL*, Rose D*, Bazzano L**, Bordnick P***, Krousel-Wood MT**

**Global Community Health and Behavioral Sciences Department, Tulane University School of Public Health and Tropical Medicine, New Orleans, LA.*
***Epidemiology Department, Tulane University School of Public Health and Tropical Medicine, New Orleans, LA.*
****School of Social Work, Tulane University School of Public Health and Tropical Medicine, New Orleans, LA.*

Scores from the Healthy Eating Index reveal that African American adults have a poorer diet quality (e.g., low total vegetable intake (dark green, orange), increased added sugars) relative to White and Hispanic adults (Go, Casavale, et al., 2013)-- which has implications for their higher rates of cardiovascular disease (Go, A. S., Mozaffarian, D., et al., 2013). The integration of mobile health (mHealth) technologies (e.g., smartphones) into health behavior change interventions has enabled the development and testing of innovative efforts to promote behaviors such as healthy eating. Although cellphone and smartphone ownership has increased among African Americans (PewResearch, 2013) the development and testing of mHealth interventions with minority populations has been relatively limited. The purpose of this exploratory study is to: 1) qualitatively identify African American men and women's barriers and facilitators to using mobile phone-based technologies designed to improve eating behaviors; 2) determine the acceptability and preferences for different mobile phone-based intervention modes (i.e., text messaging vs. mobile applications); 3) understand what information in the mobile phone-based intervention messages will motivate and better support healthy eating behaviors among the target population; and 4) obtain feedback to inform the integration of culturally-centered, theory-based intervention messages.

Overweight/obese African American adults (N=24) aged 21 years and older residing in New Orleans, LA will be recruited from local health clinics to participate in sex-based focus groups (N=2). Participants will be recruited through study advertisements and snowball sampling methods. Interested and eligible participants will complete a study questionnaire to assess demographics, health behaviors, and attitudes about the use of health-promoting technology. Following each of the audio recorded focus groups, conventional content analysis will be conducted to code and categorize data into key themes in aggregate and by sex. Descriptive statistics will be conducted to assess data obtained from study questionnaires and qualitative findings in aggregate and by sex as well. Results will provide insights about the acceptability and feasibility of using mHealth strategies to improve eating behaviors among overweight/obese African American adults and will highlight any differences by sex. The proposed study is important in that it will fulfill a need to develop more participant-informed/tailored mHealth interventions for minority populations and inform the development of a mHealth intervention that has the potential to reach more members of the target population-- which may in turn reduce the numerous challenges that occur in traditional clinical and community-based health eating interventions (e.g., overall convenience, transportation, time limitations, social-cultural attitudes toward research, etc.) (Campbell et al., 2012; Chisolm & Sarkar, 2015; Farmer, Jackson, Camacho, & Hall, 2007; Song, Cramer, & McRoy, 2015).

This work was funded, in part, by NIH K12HD043451-14 (BIRCWH).

REPORT ON WEST NILE INFECTIONS IN LOUISIANA

Sheikh Mohammad*, Hoff Clarrisa**, Ratard Raoult***

*Preventive Medicine Resident Department of Family and Community Medicine, Tulane University, **Program Director Preventive Medicine Department of Family and Community Medicine, Tulane University, ***State Epidemiologist Louisiana Office of Public Health.

This report focuses on human surveillance. The main goal of human surveillance is to describe the disease burden in different populations, annual trends and the data to disseminate information to the medical community, and the vector control information for prevention. Passive reporting system is used in the state for surveillance and reports are commonly received in the National Electronic Disease Surveillance System Base System (NEDSS). Health care facility staff enters data on reportable diseases. The Infectious Disease (ID) epi section can receive lab result directly through ELR, mail and fax. ID Epi disease surveillance specialists have real-time access and alerted to the data entered. They review the data, process the report, and complete case investigations. Data is submitted to the NEDSS at CDC. Access 2010 was used to analyze the data. 80% of West Nile (WN) infections are asymptomatic; 19% have fever, 1% is Neuro-invasive Disease (NID). From 2002 to 2014; 937 cases are of NID; it represents 80% of all WN-NID, the total number has been 1,170. If this represents only 1% of all WN infections, then there were approx. 117,000 persons infected. Out of a population of 4.5 million residents, it represents 2%. In 2002 the M: F ratio was 1:1 but it is increased to 1.5 for the period 2003-2014. The main difference between M and F occurs at the higher age groups. The proportion of African-American is around 30% of WNV-NID cases. In 2002, the incidence of new cases of NID remained between 0.1 to 5 /100,000 from infancy to age 50, and then increased sharply to 15 and up to 25 /100,000 for the older age group. Overall the case fatality rate was 8 to 9% of NID. It is strongly associated with age ranging from 2% in younger ages to 10% in the 60s-70s and to 25% in over 85. It appears that ecological changes caused by temperature, rainfall and other meteorological conditions influence mosquito and bird populations and are the major factors in the trends of WN. There are no consistent patterns in incidence and area. The consistent patterns are seasonal transmission starting from June to August and ending in October to December. Prevention consists of an early warning system to detect the presence of virus, reduction of the numbers of mosquitoes by destroying mosquito larvae, killing adult mosquitoes, prevent mosquitoes from biting people, and diagnose encephalitis early.

Disruptions in Surgical Workflow: Perceptions and Implications

David Silver[1], Alan Kaye MD PhD[2], Elyse Cornett PhD[3], Charles Fox MD[3], Douglas Slakey MD MPH[4]

1. Tulane University, New Orleans, Louisiana
2. Department of Anesthesiology, Louisiana State University Health Sciences Center, New Orleans, LA
3. Department of Anesthesiology, Louisiana State University Health Sciences Center, Shreveport, LA
4. Department of Surgery, Tulane University, New Orleans, Louisiana

Background: Surgical flow disruptions (SFD) are defined as deviations from the natural progression of a procedure which are potentially compromising to the safety of the operation. Investigators have previously demonstrated that flow disruptions can increase the mental workload and likelihood of surgical errors. However, no prior study has evaluated how individual members of the operating room team perceive SFDs. This study, therefore, investigated the frequency, cause, and significance of flow disruptions from the perspective of operating room team members.

Methods: An online (Survey Monkey) questionnaire consisting of 16 questions was used. Operating Room (OR) personnel at three academic medical centers were emailed a link a maximum of 3 times. The questionnaire was designed to validate operating room team members' definition of disruptions and what the consequences of SFDs were.

Results: There were 111 unique responses (85% completion rate). 40% of respondents were between the ages of 25-34 and 56% were male. Nurse anesthetists made up the largest group of respondent (32%). 60% of the respondents spend 30 hours or more a week in the operating room. Of respondents 65% reported that surgical flow disruptions happen either "several times a day" or "every procedure." 40% ranked "poor communication" as the most frequent cause of SFDs. When stratified, respondents who identified as attending surgeons felt impacts in patient safety and staff burnout were the most likely consequence of SFDs. Scrub technician and nurses, on the other hand, felt that economic consequences were the most likely result of SFDs.

Conclusions: This study focused on the perspective of individual team members regarding SFD. The data demonstrates that OR team members recognize that surgical flow disruptions are a significant issue and believe poor communication is a significant factor. Responses confirm the belief that SFD compromise patient safety and lead to personnel burnout. By understanding surgical flow disruptions from this perspective, researchers and administrators will be better equipped to design interventions for optimizing OR outcomes, including patient safety.

THE DIVERGENCE OF PERSONAL FREEDOM AND THE PUBLIC HEALTH GOOD

Smith, HJ*

*Tulane University School of Medicine, New Orleans, Louisiana, USA

Public health is a field that wrestles with challenging and emotionally salient subject matter ranging from distributive justice of limited health resources to the production of culturally competent health initiatives. Such topics often spark significant differences of opinion on the best course of action for these challenges and how to most appropriately accomplish the goals once agreed upon. This process of formulating the optimal course of action and investigating how to best actualize it are central to the mechanisms of ethical deliberation. As such, the roots of public health decision-making and motivations are fundamentally questions of ethics. Two particular topics that illustrate the centrality of ethics in public health are quarantine and vaccination. The discussions surrounding quarantine and vaccination involve a wide variety of important themes, including value judgments, cultural variation, justice, consequentialism, deontology, etc. Yet the primary ethical argument resting at the core of quarantine and vaccination concerns the preservation of personal freedom and autonomy vs. the maximization of utilitarian health. Therefore, the central question that must be asked is: at what point do concerns for the overall health good of a population override the freedoms of individuals? The United States provides an interesting dissociation of these values, particularly in the recent events surrounding the measles outbreaks and Ebola healthcare workers. Though the U.S. is a country that proudly proclaims to hold individual freedom and autonomy above all else, its citizens readily toss these ideals aside when approached by the specter of media-significant infectious diseases. This research discusses the ethical nature of public health, outlines the history and background of quarantining and vaccination, and illustrates the ethical and public health arguments surrounding the two concepts. The work concludes by offering a novel method with which to construct and implement ethically optimal public health policy, and demonstrates its utility by applying it to two case examples involving quarantine and vaccination.

Functional analysis of thyroid cancer cells with stem/progenitor cell properties

Saboori Sobti[1], Erik A. Green[1], Paul Friedlander[2], Koji Tsumagari[1], Mary T. Killackey[1], Mohamed Hassan[1], Emad Kandil[1]

Department of Surgery and Department of otolaryngology, Tulane University School of Medicine, New Orleans, LA 70112, USA

Background: Cancer–initiating cells have been recently identified in thyroid carcinoma as $CD44^{+}/CD24^{-/low}$ cells, which exclusively retain tumorigenic activity and display stem cell–like properties. We hypothesized that thyroid cancer progression, and resistance to therapeutic modalities could be attributed to the presence of a small fraction of thyroid cancer stem cells (TCSCs). The aim of this study is to purify and functionally characterize TCSCs derived from thyroid cancer established cell lines based on their self-renewal capacity and drug resistance

Material and methods: Flow cytometry analysis of thyroid cancer subpopulations, colony formation assay, Immune fluorescence staining, cell viability assay and Western blot were applied in this study.

Results: Thyroid cancer subpopulation ($CD44^{+}/CD24^{-/low}$) was purified and TCSC were found to consist of undifferentiated cells. $CD44^{+}/CD24^{-/low}$ thyroid cancer cells possess a self-renewal potential, extensive proliferation as clonal non-adherent spherical clusters as evidenced by colony formation assay and cell viability assay, when compared with the parental cells. Interestingly, expression of additional stem cell marker such as CD133, CD166 and Oct-4 were identified in $CD44^{+}/CD24^{-/low}$ cultures. TCSCs were found to be resistance to anti-cancer agents including, vineblastine, bortezomib and dabrafenib.

Conclusion: Thyroid cancer cells with stem/progenitor cell properties consist of undifferentiated cells and are resistant to anti-cancer agents. These also represent a suitable in vitro model to study the mechanisms regulating thyroid cancer progression and to develop therapeutic strategies.

DEVELOPING NOVEL ANTIMICROBIAL PEPTIDES WITH ENHANCED HEMOCOMPATIBILITY THROUGH SYNTHETIC MOLECULAR EVOLUTION AND RATIONAL DESIGN

Starr CG*, He J*, Wimley WC*

*Department of Biochemistry and Molecular Biology, Tulane University, New Orleans, LA, USA

Antimicrobial peptides (AMPs) have long been considered excellent candidates for development as antibiotic agents to combat the imminent threat of drug-resistant bacterial pathogens. Yet, the promise that AMPs display in the laboratory has not yielded correlative clinical success. We hypothesized that a major reason for the disparity is AMP interaction with and toxicity towards host cells. Here, we validate this theory using human red blood cells as model eukaryotic cells. The potency of a well-studied antimicrobial peptide, ARVA, decreases from minimum sterilizing concentrations (MSC) of ~2 μM in the absence of RBCs to >30 μM in the presence of RBCs at $1x10^9$ cells/ml; equal to 20% of human physiological concentration. To circumvent this roadblock to clinical utility, we have adopted a high-throughput approach of screening a second-generation antimicrobial peptide library, based on the aforementioned ARVA AMP, for activity in the presence of RBCs. We present data from screening that indicates our new library contains peptides that retain activity in the presence of RBCs; greatly outperforming the template peptide. Additionally, we show data on nine peptides discovered in our screens that have been characterized and compared to the template sequence. The peptides discovered show reduced antimicrobial potency as compared to the parent sequence when RBCs are not present, but increased efficacy in the presence of concentrated erythrocytes. Finally, we show that the consensus sequence from peptides discovered in the library, when synthesized with all D-isomer amino acids to eliminate proteolysis, performs as well as the parent sequence in the absence of RBCs and retains this potent activity when RBCs are present. Additionally, all of the novel AMPs are significantly less toxic than the parent compound. Ultimately, our results suggest that combining the power of combinatorial library screening with refinement from rational sequence engineering is an effective approach to developing novel antimicrobial peptides that retain activity under physiological conditions.

This work was supported by the Louisiana Board of Regents (LABOR) and the National Institute of Health (NIH).

OBESITY MINIMIZES THE EFFICACY OF HUMAN ADIPOSE-DERIVED STEM CELLS FOR BONE TISSUE ENGINEERING APPROACHES

Strong AL*, Hunter RS*, Jones RB*, Bowles AC*, Dutreil MF*, Gaupp D*, Hayes DJ**, Gimble JM*,***, Levi B****, McNulty MA*****, Bunnell BA*

*Center for Stem Cell Research and Regenerative Medicine, Tulane University, New Orleans, LA; **Department of Biological and Agricultural Engineering, Louisiana State University, Baton Rouge, LA; ***LaCell LLC, New Orleans, LA; ****Department of Surgery, Section of Plastic and Reconstructive Surgery, University of Michigan Health Systems, Ann Arbor, MI; *****Department of Comparative Biomedical Sciences, School of Veterinary Medicine, Louisiana State University, Baton Rouge, LA

Craniomaxillofacial defects secondary to trauma, tumor resection, or congenital malformations are frequent unmet challenges, due to suboptimal alloplastic options and limited autologous tissues such as bone. Significant advances have been made in the application of adipose-derived stem/stromal cells (ASCs) in the pre-clinical and clinical settings as a cell source for tissue engineering approaches. To fully realize the translational potential of ASCs, the identification of optimal donors for ASCs will ensure the successful implementation of these cells for tissue engineering approaches. In the current study, the impact of obesity on the osteogenic differentiation of ASCs was investigated. ASCs isolated from lean donors (body mass index <25; lnASCs) and obese donors (body mass index >30; obASCs) were induced with osteogenic differentiation medium as monolayers in an estrogen-depleted culture system and on three-dimensional scaffolds. Critical size calvarial defects were generated in male nude mice and treated with scaffolds implanted with lnASCs or obASCs. lnASCs demonstrated enhanced osteogenic differentiation in monolayer culture system, on three-dimensional scaffolds, and for the treatment of calvarial defects, whereas obASCs were unable to induce similar levels of osteogenic differentiation in vitro and in vivo. Gene expression analysis of lnASCs and obASCs during osteogenic differentiation demonstrated higher levels of osteogenic genes in lnASCs compared to obASCs. Collectively, these results indicate that obesity reduces the osteogenic differentiation capacity of ASCs such that they may have a limited suitability as a cell source for tissue engineering.

A COMPREHENSIVE NEXT GENERATION SEQUENCING-BASED VIROME ASSESSMENT IN BRAIN TISSUE SUGGESTS NO MAJOR VIRUS - TUMOR ASSOCIATION

Strong MJ[*,**], Blanchard E[***], Lin Z[*,**], Morris CA[****], Baddoo M[*,**], Taylor CM[***], Ware ML[*****,******], Flemington EK[*,**,******]

[*]Department of Pathology, Tulane University, New Orleans, LA; [**]Tulane Cancer Center, New Orleans, LA; [***]Department of Microbiology, Immunology & Parasitology, Louisiana State University School of Medicine, New Orleans, LA; [****]Department of Microbiology and Immunology, Tulane University School of Medicine, New Orleans, LA; [*****]Department of Neurosurgery, Ochsner Medical Center, New Orleans, LA; [******]Co-corresponding authors: mware@ochsner.org, eflemin@tulane.edu

Glioblastoma multiforme (GBM) is a devastating disease with poor survival rates. Despite years of research, there has been little change in the median survival time. Human cytomegalovirus (HCMV) was reported in GBM over a decade ago and this finding has the potential to increase our understanding of the disease and it offers a potential tumor specific therapeutic target. Because of this promise, there is a fair amount of time, energy and money being directed towards understanding and utilizing this connection for eventual therapeutic purposes. Despite these ongoing efforts and the time lapsed since the discovery of HCMV in GBM, the association remains controversial. The objective of this study was to utilize the capabilities of next generation sequencing (NGS) to investigate the reported association between GBM and HCMV. A large-scale comprehensive virome assessment was performed on publicly available sequencing datasets from the Cancer Genome Atlas (TCGA), including RNA-seq datasets from primary GBM ($n = 157$), recurrent GBM ($n = 13$), low-grade gliomas (LGG) ($n = 514$), recurrent LGGs ($n = 17$), and normal brain ($n = 5$), and whole genome sequencing (WGS) datasets from primary GBM ($n = 51$), recurrent GBM ($n = 10$), and normal matched blood samples ($n = 20$). In addition, RNA-seq datasets from MRI-guided biopsies ($n = 92$) and glioma stem-like cell cultures ($n = 9$) were analyzed. Sixty-four DNA-seq datasets from 11 meningiomas and their corresponding blood control samples were also analyzed. Finally, three primary GBM tissue samples were obtained, sequenced using RNA-seq, and analyzed. After in-depth analysis, the most robust virus findings were the detection of human papillomavirus (HPV) and hepatitis B reads in the occasional LGG sample (4 samples and 1 sample, respectively). In addition, low numbers of virus reads were detected in several datasets but detailed investigation of these reads suggest that these findings likely represent artifacts or non-pathological infections. For example, all of the sporadic low level HCMV reads were found to map to the immediate early promoter intimating that they likely originated from laboratory expression vector contamination. Despite the detection of low numbers of Epstein-Barr virus reads in some samples, these likely originated from infiltrating B-cells. Finally, human herpesvirus 6 and 7 aligned viral reads were identified in all DNA-seq and a few RNA-seq datasets but detailed analysis demonstrated that these were likely derived from the homologous human telomeric-like repeats. Other low abundance viral reads were detected in some samples but for most viruses, the reads likely represent artifacts or incidental infections. This analysis argues against associations between most known viruses and GBM or meningiomas. Nevertheless, there may be a low percentage association between HPV and/or hepatitis B and LGGs.

This work was supported by National Institutes of Health (NIH) grants R01AI101046, and R01AI106676 to EKF; a Ruth L. Kirschstein National Research Service Award F30CA177267 from the National Cancer Institute to MJS; a Louisiana Clinical and Translational Science Center Pilot grant (U54GM104940 from NIH) to ZL, and NIH grant P20GM103518 to Prescott Deininger.

Sleepiness and subclinical measures of atherosclerosis in a bi-racial cohort: The Bogalusa Heart Study

Patrick Stuchlik, Benjamin Pollock, Wei Chen, Emily Harville, Suzanne Bertisch, Susan Redline, Lydia Bazzano

INTRODUCTION: That adverse health outcomes, including atherosclerosis, are associated with sleep disturbance is well-documented; however, evidence from diverse populations on the magnitude of this association, or investigating sleepiness as an outcome, is scarce.

METHODS: We examined data from the Bogalusa Heart Study, a long-term community-based observational study of a biracial cohort, with first measurements in childhood in 1973. Men and women (n=546) who underwent a measure of carotid intima-media thickness (IMT), calculated as the composite IMT (cIMT), mean of six segments (common and internal carotid, and carotid bifurcation, each left and right), and completed the Epworth Sleepiness Scale (ESS), were included. Multivariable logistic regression was employed to model the association between ordinal self-rated sleepiness and cIMT per standard deviation, adjusted for age, sex, smoking status (at time of IMT measurement), hours of sleep, symptoms of sleep disturbance, and previous heart attack. Based on previous race-specific findings, data were analyzed separately by race.

RESULTS: Of whites (n=356), 59.6% were female and 22.5% were current smokers. Mean (SD) age was 43.1 (4.4) years, and cIMT was 0.6 (0.1) mm. Of African-Americans (n=190), 66.8% were female, 34.7% were current smokers. Mean (SD) age was 42.8 (4.6) years, and cIMT was 0.7 (0.2) mm. Multivariate modeling found a significant race-cIMT interaction term (p=0.04). In stratified analyses, the adjusted odds of abnormal sleepiness (vs. normal sleepiness) were 1.40 times greater (95% CI: 1.04-1.90) per 1-SD increase in cIMT in whites, while among black participants, the odds ratio (95% CI) was 1.01 (0.68-1.50).

CONCLUSIONS: There was a significant association between unfavorable subclinical measures of atherosclerosis and excessive daytime sleepiness among white participants.

	ESS 0-7 (n=381)	*ESS 8-9 (n=62)*	*ESS 10-15 (n=79)*	*ESS 16-24 (n=24)*
Black, %	30.7	41.9	39.2	66.7
Female, %	62.7	61.3	55.7	75.0
Age, y	42.7 (4.6)	43.7 (4.0)	43.8 (3.7)	42.4 (4.4)
Smoker, %	25.2	35.5	27.9	25.0
cIMT, mm	0.65 (0.15)	0.67 (0.16)	0.70 (0.17)	0.67 (0.12)

All values are mean (SD) unless noted otherwise

GENE-BASED PATHWAY ANALYSIS FOR OSTEOPOROSIS: INSIGHTS FROM GENOMIC-WIDE ASSOCIATION STUDIES

Su KJ*, Zhu W*, Xu C*, Deng HW*

* Center for Bioinformatics and Genomics, Department of Global Biostatistics and Data Science, Tulane University, New Orleans, LA, USA 70112.

Background: Osteoporosis is a chronical human complex disease with decreased bone strength and increased risks of fracture, which has been characterized by low bone mineral density (BMD). To date, genome-wide association studies (GWASs) have been applied for osteoporosis and identified more than 100 susceptibility loci, which only account for a small proportion of the insights into osteoporosis. To further explore the pathologic mechanism of osteoporosis, we performed a series of gene-based pathway analyses with multiple pathway databases based on the largest meta-analysis of GWASs in the bone field.

Methods: Firstly, we examined BMD-associated genes by analyzing the summary statistics of the sequencing project of the GEnetic Factors for OSteoporosis Consortium (GEFOS.seq) with BMD of the femoral neck (FN), lumbar spine (LS), and forearm (FA), respectively. To improve the power of identifying the candidate genes, we collected the overlapping results of gene-based association analyses through two different strategies (the all-SNP test and the best-SNP test). Next, these overlapping genes were selected for pathway analysis through Enrichr and Gene Ontology (GO) enrichment analysis implemented by the Database for Annotation, Visualization and Integrated Discovery (DAVID). Additionally, to validate the discovery of pathway analysis, we conducted a weighted gene co-expression network analysis (WGCNA) to identify the BMD-related gene-set in a transcriptomics data from bone biopsy for subsequent pathway analysis.

Results: We identified overlapping associated genes between the results of two approaches, including 709 genes on the FN, 693 on the LS, and 463 on the FA. The pathway analysis revealed a total of 16 significant pathways (FDR < 0.05), including Wnt signaling pathway, RANKL/RANK signaling pathway, and Hedgehog signaling pathway. Three bone-related biological processes terms were identified on both the FN and LS (FDR < 0.05), e.g., skeletal system development, ossification, and bone development. Additionally, Cellular responses to stress pathway was significantly enriched in a BMD-associated gene set identified by WGCNA (FDR < 0.05), which highly response to the regulation of RANKL-dependent osteoclast differentiation.

Conclusion: This study not only identified several known bone-related pathways, but also investigated more potential risk pathways that may provide new insights into the pathological mechanism of osteoporosis.

This study was partially supported by grants from National Institutes of Health [P50AR055081, R21AG27110, R01AR057049, R01AR059781], and Edward G. Schlieder Endowment to Tulane University.

DEVELOPMENT OF THE *EX VIVO* MOUSE MESOMETRIUM MODEL TO INVESTIGATE MULTICELLULAR DYNAMICS DURING ANGIOGENESIS

Suarez-Martinez AD*, Kaplan D*, Huang K**, Meadows S**, Bierschenk S***, Sperandio M***, Murfee WL*

*Departmental of Biomedical Engineering, Tulane University
**Department of Cell and Molecular Biology, Tulane University
***Walter-Brendel-Centre of Experimental Medicine, Ludwig-Maximilians Universität, Munich, Germany

The development of biomimetic *in vitro* or *ex vivo* models that can incorporate the complexity of intact microvascular networks would enable the investigation of multicellular dynamics associated with angiogenesis and novel experimental platforms for pre-clinical therapy testing. Recently, our laboratory has introduced the rat mesentery culture model as such a tool. The applicability of this model would be enhanced with the use of murine tissue, yet unfortunately, the mouse mesentery is avascular. A potential analog to the mesentery is the mesometrium, the connective tissue of the uterine horns. The objective of this study was to demonstrate that the mouse mesometrium contains intact microvascular networks that can be cultured to investigate multicellular dynamics during angiogenesis. Mesometrium windows, defined as the translucent connective tissues attached to the uterine horns, were harvested from adult C57Bl/6 female mice and cultured in minimum essential media with 20% fetal bovine serum for 3 and 5 days. The tissues were immunohistochemically labeled with platelet endothelial cell adhesion molecule (PECAM), neuron-glial antigen 2 (NG2), and alpha-smooth muscle actin (α-SMA) to identify endothelial cells, pericytes, and smooth muscle cells, respectively. The mesometrium proved to have an intact microvascular network with arterioles, venules and capillaries. Arterioles and venules were differentiated by the PECAM-positive cell morphology, and the α-SMA-positive cell morphology that wraps the vessels. α-SMA and NG2 labeling confirmed the presence of smooth muscle cells along the larger vessels and pericytes along capillaries. After 5 days in culture, tissues remained viable as confirmed with a LIVE/DEAD assay. Compared to day 0, uncultured tissues, capillary sprouts per venule length was dramatically increased by day 3 and day 5 (Day 0: 0.09 ± 0.02; Day 3: 4.10 ± 0.75; Day 5: 4.37 ± 0.60 spouts/mm). For day 3 and day 5, capillary sprouting preferentially occurred of venules versus arterioles. Furthermore, while the number of capillary sprouts were comparable for day 3 and day 5, sprouts appeared to be longer on day 5. Capillary sprouts were also observed to contain NG2-positive, and SMA-negative pericytes. These results introduce the mouse mesometrium culture model as a novel *ex vivo* approach for elucidating pericyte-endothelial cell dynamics associated with capillary sprouting at specific vessel locations in a real microvascular network scenario.

This work was supported by the following grants: NIH R01AG049821, NIH P20GM103629.

MELATONIN-INDUCED SUPPRESSION OF RSK2 EXPRESSION IN HER2-POSITIVE HUMAN BREAST CANCER CELLS REPRESSES METASTASIS

Summers WM*, Mao L*,**,***, Xiang S*,**,***, Yuan L*,**,***, Dauchy RT*,**,***, Reynolds A*, Wren-Dail MA*,***, Pointer D****, Frasch T*,***, Blask DE*,**,***, Hill SM*,**,***

*Department of Structural and Cellular Biology, Tulane University School of Medicine, New Orleans, Louisiana.
**Tulane Cancer Center and Louisiana Cancer Research Consortium, New Orleans, Louisiana.
***Tulane Center for Circadian Biology, Tulane University School of Medicine, New Orleans, Louisiana.
****Department of Surgery, Tulane University School of Medicine, New Orleans, Louisiana.

The importance of circadian/melatonin signaling in the suppression of breast cancer metastasis has been reported by numerous laboratories, including our own. To date, the mechanisms underlying the anti-metastatic actions of melatonin have not been well defined. Recently, we evaluated the anti-metastatic actions of melatonin on the ERa-negative, Her2-positive SKBR-3 breast tumor cell line and ERa-positive MCF-7 cells overexpressing a constitutively active HER2.1 construct (MCF-7Her2.1 cells). Activation of Her2, via expression and/or phosphorylation-dependent activation of numerous kinases and transcription factors, drives drug resistance and metastasis in breast cancer. Rsk2, a key signaling node activated by the Her2/Mapk/Erk pathway, has been shown to induce numerous signaling pathways associated with epithelial-to-mesenchymal transition (EMT) and metastasis. Signaling pathways involved include Creb, Stat3, cSrc, Fak, Pax, Fascin, and actin polymerization. Our data showed that melatonin, both endogenous and exogenous, significantly represses this invasive/metastatic phenotype of through suppression of mechanisms involved in EMT, either by promoting mesenchymal-to-epithelial transition (MET), and/or by inhibiting key signaling pathways involved in later stages of metastasis. This data, in addition to our earlier studies, supports the importance of elevated and extended duration of nocturnal melatonin levels in repressing the metastatic progression of breast cancer. Melatonin inhibition of Rsk2 represses the metastatic phenotype in breast cancer cells via suppression of EMT or inhibition of other mechanisms that promote metastasis. Thus, disruption of the melatonin signal may promote metastatic progression in breast cancer.

MITOCHONDRIAL MECHANISMS OF DRUG-INDUCED DISRUPTION OF BLOOD-BRAIN BARRIER

Sure VN*, Unis GD*, Baker T*, Rajaprabhakaran G*, Abraham VM*, Cama Z*, Jain NP*, Chen A*, Mondal D*, and Katakam PVG*.

* Department of Pharmacology, Tulane University School of Medicine, New Orleans, Louisiana, USA.

Anti-HIV drugs have been found to significantly reduce HIV-associated neurocognitive disorders. Toxicity resulting from long-term use of protease inhibitors such as Nelfinavir has been implicated in the mild cognitive disorders but the exact underlying mechanisms are poorly understood. We hypothesized that nelfinavir causes the disruption of blood brain barrier (BBB) by promoting mitochondrial oxidative stress and impairing mitochondrial respiration. Our studies examined the effects of nelfinavir in human brain microvascular endothelial cells (BMECs). Cell viability following 48 h Nelfinavir treatment of hBMECs was determined using CCK-8 assay. Measurements of superoxide levels were made by electron spin resonance spectrometry using spin probes for total (1-Hydroxy-3-methoxycarbonyl-2,2,5,5-tetramethyl-pyrrolidine) and mitochondrial superoxide (mito-Tempo-H). Oxygen consumption rates (OCR) were measured by Seahorse Analyzer. The levels of mtDNA were measured by qPCR using the mitochondrial genes ND1 and ND5, which were normalized to the nuclear genes SLCO2B1 and SERPINA1. BBB permeability measurements were performed by using 40 kDa and 150 kDa-FITC-dextran transfer across monolayers of BMECs grown in transwells. In addition, transendothelial electrical resistance (TEER) measurements were also made across the monolayers of BMECs grown in transwells. Nelfinavir treatment caused an increase in cell proliferation of BMECs at low doses (0.5 µM-1.5 µM) but decreased viability at high doses (5 µM-10 µM). Nelfinavir at therapeutic doses promoted the generation of total and mitochondrial superoxide in BMECs. In addition, nelfinavir dose-dependently diminished the basal OCR and reserve mitochondrial respiratory capacity in BMECs. Nelfinavir also reduced the mitochondrial DNA copy number. Moreover, nelfinavir dose-dependently promoted increased transcellular permeability in BMECs. Thus, nelfinavir induced mitochondrial oxidative stress promotes diminished mitochondrial respiratory capacity and decreased cell proliferation leading to the disruption of BBB.

This work was supported by Louisiana Board of Regents Support Fund-Research Competitiveness Subprogram (LEQSF(2014-17)-RD-A-11) and American Heart Association National Center Scientist Development Grant (14SDG20490359).

OIL-WATER EMULSIONS STABILIZED BY ALUMINOSILICATE MICROSTRUCTURES: ALTERNATIVES TO CHEMICAL DISPERSANTS IN OIL SPILL RESPONSES

Swientoniewski LT*, Yu T**, Zhang D**, Blake DA*

*Department of Biochemistry and Molecular Biology, Tulane University School of Medicine, New Orleans, LA
**Department of Chemistry and Macromolecular Studies Group, Louisiana State University, Baton Rouge, LA

Oil spills are a significant source of pollution in the Gulf of Mexico. During the Deep Water Horizon (DWH) Spill, ~210 million gallons of oil were released into the Gulf. In response to this spill, an unprecedented 1.8 million gallons of chemical dispersant were applied to the ocean surface and subsurface. These dispersants contain one or more surfactants that decrease interfacial tension at the oil-water interface and break the oil into smaller droplets. This increased surface area enhances the colonization and subsequent biodegradation by marine bacteria. While studies are still ongoing, there is evidence that Corexit dispersants used during the DWH spill have negative impacts on coral growth, fish embryos, phytoplankton food webs, and the distribution of bacterial species in the marine ecosystem. Consequently, there is a need for 'green and natural' dispersants with reduced environmental impact. The objective of our study is to test the ability of aluminosilicate (AS) microstructures (including tubes, sheets, and diatomaceous earth) for their ability to aid bacterial biodegradation of crude oil. These AS microstructures form stable emulsions by adsorbing to the oil-water interface. Emulsification can proceed with energies equivalent to that provided by ocean turbulence, and increasing the hydrophobicity of the AS surface increases emulsion stability. We are studying the ability of these AS microstructures to enhance oil degradation using two model bacterial species: *Alcanivorax borkumensis* (degrades alkanes) and *Cycloclasticus pugetii* (degrades polycyclic aromatic hydrocarbons). Halloysites (sheets of naturally occurring AS rolled into tube-like formations) stimulated growth of *A. borkumensis* in a minimal media supplemented with 0.1% hexadecane. Loading of the interior of these nanotubes with a second, non-alkane nutrient (pyruvate) did not further enhance cell proliferation. Surface modifications of halloysites and other AS microstructures will include functionalization with amphipathic polypeptoid, synthesized by the Zhang lab at LSU. Preliminary tests of these polypeptoids (biocompatible peptidomimetic polymers) have shown that these novel polymers do not inhibit bacterial growth at concentrations at least 10x greater than what will be present in the final, functionalized AS microstructures.

This work is supported by the grant GOMRI2015-V-358 from the Gulf of Mexico Research Institute.

MICROSCOPIC ANALYSIS OF THE MACROPHAGE POPULATION OF THE INTESTINAL TRACT THAT REFLECTS DISEASE PROGRESSION IN SIV-INFECTED RHESUS MACAQUES

Takahashi N[*], Allers C[*], Midkiff C[**], Alvarez X[**], Didier ES[***] and Kuroda MJ[*]

[*]Division of Immunology, [**]Division of Comparative Pathology and [***]Division of Microbiology, Tulane National Primate Research Center, Covington LA

Background: We have reported that increased monocyte turnover was a better predictor of AIDS disease progression in SIV-infected macaques than CD4+ T cell levels. We further demonstrated that the increased death rate of lung interstitial macrophages (IM) caused by SIV infection directly correlated with the magnitude of overall lung tissue damage. In contrast to IM, SIV infection of long-lived alveolar macrophages (AM) did not induce cell death suggesting that these long-lived macrophages exhibit a different function during SIV. The intestinal tract is also a site of high viral replication and therefore, we extended these finding to examine the effects of SIV on different subsets of macrophages of the GI tract in rhesus macaques. Our recent data by flow cytometry suggested that destruction of CD163+CD206+ macrophages and accumulation of CD163+CD206- macrophages correlated with high monocyte turnover in the intestinal tracts of SIV-infected rhesus macaques. Here, we examined the phenotypes of macrophages and their localization in the intestinal tract by immunofluorescence to fully understand the role of macrophages in the GI tract during AIDS.

Method: We used confocal microscopy to analyze the phenotype and location of macrophage subpopulations in intestinal tissues collected from SIV-infected macaques with high monocyte turnover signifying disease progression.

Results: CD163+CD206- macrophages, equivalent to IMs, were frequently observed in the lamina propria of intestinal tissues in SIV-infected macaques whereas CD163+CD206+ subset, equivalent to AMs, was dominant in SIV-uninfected healthy macaques. Interestingly, CD163+CD206+ macrophages in the mucosa were equally observed in uninfected and infected macaques.

Conclusion: Combined with previous flow cytometry data, these results suggest that monocytes that newly arrived at intestinal tract differentiate to CD163+CD206+ macrophages and destruction of CD163+CD206+ subset in conjunction with accumulation of CD163+CD206- immature subset in the lamina propria contribute to the high monocyte turnover observed in SIV-infected macaques rapidly progressing to AIDS. The data also suggest that CD163+CD206+ macrophages in the mucosa may not be affected during SIV infection.

This work was supported by grants from National Institutes of Health (NIH) AI097059, AI087302, AI091501 and AI110163.

Targeting MALT1 with the Small Molecule Inhibitor MI2 Induces a Caspase-Dependent Apoptosis and Inhibits the NF-κB Pathway in Chronic Lymphocytic Leukemia Primary Cells.

Georges Tanios[1], Patricia Lobelle-Rich[1], Ashwin K. Vasudevamurthy[1], Tom Atkinson[1], Ali Baghian[1], Delong Liu[2], Hana Safah[1], Erik K. Flemington[3] , and Nakhle Saba[1].

[1]Section of Hematology and Medical Oncology, Department of Medicine, Tulane University, New Orleans, LA, USA
[2]Hematology Branch, National Heart, Lung, and Blood Institute, National Institutes of Health, Bethesda, MD, USA
[3]Department of Pathology, Tulane University, New Orleans, LA, USA

Targeting the B-cell receptor (BCR) pathway in chronic lymphocytic leukemia (CLL) with the Bruton Tyrosine Kinase (BTK) inhibitor Ibrutinib has transformed the treatment paradigm of this disease. Ibrutinib is currently indicated for treatment of CLL regardless of the line of therapy. However, ibrutinib is not curative, and relapses secondary to C481S mutation in *BTK* and gain of function mutations in *PLCγ2* (R665W and L845F) are being reported.
The protease *mucosa-associated lymphoid tissue lymphoma translocation 1* (MALT1) is the active component of the CARD11-BCL10-MALT1 (CBM) signaling complex. CBM mediates NF-κB activation downstream of BTK and PLCγ2 within the BCR pathway, which makes of MALT1 an ideal therapeutic target in ibrutinib-resistant clones. Notably, the chemical compound MI2 ($C_{19}H_{17}Cl_3N_4O_3$) binds to- and suppresses the protease activity of MALT1, and was found to be active against activated B-cell-like diffuse large B-cell lymphoma. However, the role of MALT1 inhibition in CLL has not been investigated.
We studied the efficacy of MI2 against a cohort of CLL samples (N=21), and explored its mechanism of action. PBMCs from patients with CLL were tested against serial dilutions of MI2 (0.125-8μM) for 48 h in 96-well plates, and MTS assay was performed to quantify cell viability. We observed a dose-dependent cytotoxicity in all samples, with an inhibitory concentration at 25% (IC25) < 2μM observed in the majority of the samples. MI2 cytotoxicity was independent of the *IGHV* mutational status, CD38 expression, cytogenetics, previous therapy status, and MALT1 protein level (immunoblot on purified CLL cells). To study the drug apoptosis and drug selectivity, we examined apoptotic induction in both CLL cells and T-cells of the same patients. PBMCs from five patients with CLL were treated with MI2 for 48 h and compared to untreated control. At the end of the incubation, cells were stained with CD5, CD19, and Annexin-V, then analyzed using flow cytometry. We found that MI2 induced a dose-dependent apoptosis in CLL cells (defined as CD5+/CD19+) in all samples, with only mild toxicity to their corresponding T-cells (T-cells represent a fraction of each patient's PBMCs defined as CD5+/CD19-). This minimal toxicity to T-cells was not statistically significant when compared to untreated control T-cells, and may reflect a T-cell receptor signaling-independence of circulating T-cells, which are mostly composed of terminally differentiated effectors. To determine whether the induced apoptosis is caspase-dependent, we treated PBMCs of CLL patients (N=5) with MI2 (0.5-4 μM) in the presence or absence of 100μM of the pan-caspase inhibitor z-VAD-fmk for 48 h. We found that z-VAD-fmk completely prevented the induction of apoptosis in CD19+/CD5+ CLL cells as determined by Annexin-V staining (flow cytometry), and decreased MI2-induced PARP cleavage (Immunoblot).
To determine the effect of the microenvironment on MI2 toxicity, we cultured primary CLL cells with and without MI2 (0.5-4μM) for 48 h, in the presence or absence of Nurse-Like Cells (NLC) (N=5) or anti-IgM (N=4). NLCs and anti-IgM cross-linking of BCR are *in-vitro* models for the protective effect of the microenvironment. Co-culture with NLCs or with anti-IgM improved the viability of the untreated primary CLL samples. Similar to ibrutinib, MI2 continues to be effective

against CLL cells in the presence of NLCs or anti-IgM, but higher concentrations are required to achieve the desired cytotoxicity against CLL cells. There was no cytotoxic effect on NLCs.
To investigate the effect of MI2 on tumor biology, 1 µg of total RNA from purified CLL cells (treated for 8 h with MI2, N=3; and untreated control, N=3) was subjected to RNA sequencing. Out of 56,650 tested genes, there were 438 genes whose expression changed ≥2-fold at $P<0.05$ (312 down- and 126 up-regulated), several genes are known NF-κB targets. The observer-independent method, Gene Set Enrichment Analysis (GSEA), clearly identified the canonical NF-κB among of the top affected pathways.
Further studies aim to verify the RNA sequencing data at the protein level, to determine MI2 efficacy against ibrutinib-resistant clones *in vitro*, and against CLL growth in mice *in vivo*.

Supported by *Hope Foundation SWOG Early Exploration and Development (SEED) Award*. We thank the *Louisiana Cancer Research Center (LCRC)* biospecimen core and our patients for the donation of samples to make this research possible.

DISTRIBUTION AND OVIPOSITION INTENSITY OF *AEDES AEGYPTI* AND *AEDES ALBOPICTUS* IN THE GREATER NEW ORLEANS REGION.

Thongsripong P*, Jameson SB*,**, Michaels SR*,***, Wesson DM*

*Department of Tropical Medicine, Tulane University, New Orleans, LA
**Department of Pediatrics, University of Mississippi Medical Center, Jackson, MS
***City of New Orleans Mosquito, Termite and Rodent Control Board, New Orleans, LA

Aedes aegypti and *Ae. albopictus* are vectors of multiple emerging pathogens including Zika, dengue and chikungunya. The presence of these mosquitoes in the southern United States could potentially result in local transmission of these viruses in the region. In this ongoing longitudinal study, we investigate the distribution of *Ae. aegypti* and *Ae. albopictus* in the New Orleans Metropolitan area by measuring oviposition intensity using oviposition traps. Since 2009, a total of 74 study sites have been monitored weekly. We have found that both species are common in New Orleans and exhibit species-specific spatial and temporal variation in their distributions. Using multiple regression analysis, we have determined that the egg laying intensity of *Ae. aegypti* and *Ae. albopictus* can be partially explained by variables such as human population density, household income, and housing age. Furthermore, employing a regression model with time lags, we investigated the temporal variation of egg counts and hatched *Aedes spp.* counts in relation to weather data. The relationship between mosquitoes and weather variables will be discussed. This study provides insight into the mosquito-human-weather interactions that may aid in targeted vector control efforts and preparations to combat potential vector-borne pathogen transmission in southern Louisiana.

Funding provided by NIH grant, R43 AI115782-01B1

ABSTRACT

Regulatory effects of Interleukin (IL)-15 on allergen-induced airway obstruction

Sathisha Upparahalli Venkateshaiah*, Murli Manohar*, Alok K. Verma* and Anil Mishra*

*Department of Medicine, Tulane Eosinophilic Disorders Center (TEDC), Section of Pulmonary Diseases, Tulane University School of Medicine, New Orleans, LA 70112, USA.

Airway obstruction is a highly specific term that represents physiologic abnormalities of the airways and induced levels is observed in steroid treated asthmatic patients. We tested the hypothesis that regulation of IL-15 is critical for the preservation of allergen-induced airway hyperresponsiveness (AHR), airway resistance and compliance in response to methacholine. Airway inflammation, AHR, resistance and compliance were assessed in IL-15-deficient mice and IL-15 overexpressed mice in allergen-induced murine model of asthma. Lung histological analysis for eosinophils by anti-MBP immunostaining, Goblet cells hyperplasia by PAS staining, cytokines and chemokine levels by qPCR and ELISA analyses. Herein, we made a novel observation that IL-15 deficiency promotes baseline airway resistance in naïve mice. Moreover, rIL-15 delivery to the lung downregulates expression of inflammatory cytokines, and improves allergen-induced AHR, resistance and compliance. These observations were further validated in DOX-inducible CC-10-IL-15 transgenic mice. DOX exposed Aspergillus extract challenged CC-10-IL-15 bitransgenic mice exhibited significantly reduced levels of inflammatory cytokines (IL-4, IL-5, IL-13) and goblet cell hyperplasia. Airway obstruction, including AHR and resistance was diminished in allergen challenged DOX exposed compare to no-DOX exposed CC-10-IL-15 bitransgenic mice. Mechanistically, we observed that IL-15-induced protection of airway obstruction is associated with the induced IL-10-producing regulatory $CD4^{+}CD25^{+}Foxp3^{+}$ T cells. We report our novel finding that IL-15 has a potent inhibitory effect on the airway obstruction that occurs in response to environmental allergens/pollutants.

This work was funded by: NIH R01 DK067255 (AM), NIH R01 AI080581 (AM)

Differentiation of THP-1 cells and primary human monocytes with LT-derived adjuvants dmLT and LTA1.

Eduardo Valli[1]*, Robin L. Baudier[1], Elizabeth B. Norton[1]

[1]Department of Microbiology and Immunology, Tulane University School of Medicine, New Orleans, Louisiana, USA
*Corresponding author

Enterotoxigenic *Escherichia coli* (ETEC) produces heat-labile toxin (LT), which is also a powerful mucosal adjuvant. Detoxified versions of LT without its secretion-inducing properties have been made, including dmLT (LT(R129G/L211A)) and the enzymatic LTA1 domain. Several vaccines with dmLT have exhibited success in recent clinical trials. We have previously shown in a mouse model that dmLT or LTA1 triggers dendritic cell maturation, increases IgG levels and stimulates T-cells to shift towards a Th1/Th2/Th17 profile. The mechanism of action of these adjuvants in human antigen presenting cells (APC), however, is not well understood. Primary human monocytes or the human-derived monocyte cell line THP-1 are widely studied to examine immunologic mechanisms in APC. We evaluated THP-1 cells for their responses to dmLT and LTA1 adjuvants compared with untreated or PMA-treated cells. We confirmed key results using primary human monocytes. Our results show that dmLT- and LTA1-treated THP-1 cells diminished in size; increased secretion of IL-1 beta, IL-21, and TNF-alpha cytokines; upregulated HLA-DR, CD14 and CD11b and downregulated CD123 surface markers; and showed no change in CD11c and CD16 with respect to untreated cells. Interestingly, these changes were clearly distinguishable from PMA-treated THP-1 cells. PMA treatment, a known macrophage-like phenotype inducer, resulted in adherent, bigger cells with characteristic macrophage-like marker expression ($CD11b^{+}$, $CD11c^{+}$, $CD14^{+}$, $CD123^{lo}$, $HLA\text{-}DR^{lo}$). Primary culture results showed increased CD14, but contrary to THP-1 results, the expression of the CD123 was upregulated. In conclusion, dmLT and LTA1 alter the phenotype of THP-1 and human monocytes to a unique phenotype distinct from monocyte or monocyte-derived macrophages, likely towards a dendritic cell phenotype.

AGE-DEPENDENT ALTERATIONS IN CORTICAL DENDRITIC SPINE DYNAMICS FOLLOWING WHISKER STIMULATION

Vandemark KM*, Voglewede RL*, DeWitt AR*, Heffler MD*, Trimmer EH**, Mostany R*,**

*Neuroscience Program, Tulane Brain Institute, New Orleans, LA; **Department of Pharmacology, Tulane University School of Medicine, New Orleans, LA

Within the brain, stability and plasticity of synaptic connectivity are cooperative forces that operate in tandem during learning and memory processes. Previous research (Mostany et al., 2013) shows that aged mice display an elevated dendritic spine turnover ratio in the apical dendritic tufts of Layer V pyramidal neurons of the primary somatosensory cortex (S1) when compared to young adult mice, suggesting that synapses of aged animals are less stable over time. In addition, this research finds that aged animals have no significant difference in the proportions of dendritic spine morphology types compared to young adult mice. The present study explores the functional implications that less stable, more plastic synaptic connections within the aged cortex may have for learning and memory as animals undergo a sensory experience (whisker stimulation) designed to produce long term potentiation (Megevand et al., 2009, Gambino et al., 2014). Using chronic *in vivo* two photon imaging through a cranial window, we followed apical tuft dendrites of layer V pyramidal neurons within S1 of Thy1-eGFP-M male mice of two ages: young adult (3-5 months) and aged (18-22 months). Mice were imaged over 46 days spanning before, throughout, and following sessions of stimulation, occurring from days 8 – 11, and that consisted of continuous whisker stimulation with a piezoelectric actuator at 8 Hz for 10 minutes a day over 4 days. Imaging sessions occurred every 4 days (days 0 - 20, 38 - 46) to observe long-term changes in spine dynamics. We observe an acute increase in dendritic spine turnover ratio immediately following whisker stimulation in the young adult mice. For the aged mice, we observe an opposite effect: a decrease in turnover ratio following their initially higher baseline. The age-gap in baseline turnover ratio between the two age groups disappears following the whisker stimulation, suggesting that aged mice experience a form of synaptic stabilization following this sensory manipulation that returns them to young adult levels. We performed morphological and volumetric analysis of the dendritic spines to examine these changes from an additional angle. While we found no significant changes in volume following whisker stimulation for either age group, we found a roughly proportional decrease in mushroom spines and increase in thin spines in the aged mice. This suggests that although their synapses may be stable (in that they are still present), subtler structural changes may be occurring in terms of synaptic strength. Our ongoing analysis aims to explore how these bidirectional, age-dependent responses may serve as a compensatory mechanism that the aged brain employs during sensory processing.

Support: NIA/NIH R01AG047296, COBRE on Aging and Regenerative Medicine P20GM103629, Louisiana Board of Regents RCS LEQSF(2016-19)-RD-A-24, Newcomb College Institute Research Grant, and startup funds from the Tulane University School of Medicine to RM.

DEVELOPMENT OF AN AGENT-BASED MODEL TO PREDICT THE SALIENT FEATURES OF AGE-RELATED PATELLAR TENDON DEGENERATION

Vanosdoll MK*, Heard WMR**, Savoie FH**, Miller KS*

*Department of Biomedical Engineering, Tulane University, New Orleans, LA
**Department of Orthopaedic Surgery, Tulane University, New Orleans, LA

Age-related tendinopathy is a prevalent and debilitating disorder affecting up to one in three adults over the age of 50. It is associated with degenerative changes including altered mechanical response, microstructural composition, and cross-sectional area; however, the underlying cellular and molecular mechanisms of age-related degeneration are not well understood. Agent-based models (ABM) have emerged as powerful tools capable of predicting dynamic systems such as mechanosensitive collagen fiber remodeling in scar tissue formation, but few tendon studies to date have leveraged ABMs. Therefore, the objective of this study is to develop an ABM of the murine patellar tendon capable of predicting the salient features of age-related dynamics. ABMs represent cell behaviors through the use of literature-derived rules that govern the interactions of each cell type with adjacent cells and their environment. A first generation model of age-related degeneration of the murine patellar tendon was developed (NetLogo 5.3.1) by compiling data relevant to both tendon aging and the maintenance of homeostatic conditions at the cell and tissue levels. The model considers the effects of age on growth factors (PDGF, IGF, TGF-B), IL-1B, tissue inhibitors of matrix metalloproteinases (TIMPs), and nonenzymatic cross-linking of collagen due to the accumulation of advanced glycation endproducts (AGEs). These changes govern fluctuations in matrix metalloproteinases (MMP-1), collagen content, and the apoptotic and proliferative capacities of each cell. The model currently demonstrates that, with advancing age, AGE cross-links accumulate and growth factor and TIMP expressions decline, stimulating increased MMP-1 levels, and inducing tendon atrophy as collagen removal is favored over production. The preliminary model demonstrates capability to predict the salient features of age-related tendon degeneration including altered collagen content, increased AGE cross-linking, reduced cell number, and elongated cell shape. This preliminary ABM demonstrates the ability of ABM to provide a unique opportunity to elucidate the key cellular and molecular mechanisms of age-related tendon dynamics to allow for the rational design of informed and targeted treatment plans.

This work was supported by NIH/NIGMS P20GM103629 and the Tulane Honors Program.

RESPONSE TO HYPOXIA MAY GOVERN THE FITNESS AND VIRULENCE OF THE TUBERCLE BACILLI

Veatch AV*,**, Gautam US **, Caskey J ***, Mehra S ***, and Kaushal D **
* Department of Microbiology and Immunology, Tulane University (SOM), New Orleans, LA, USA
** Division of Bacteriology & Parasitology, Tulane National Primate Research Center, Covington, LA, USA
*** Department of Pathobiological Sciences, LSU School of Veterinary Medicine, Baton Rouge, LA, USA

Mtb, the causative agent of tuberculosis, demonstrates different virulence not only between lineages but between strains in the same lineage as well. Genomes of any two strains of *Mtb* regardless of lineage are genetically very close with an average difference of 0.03%; thus it is unlikely that genetic differences could explain differential virulence. While the immune response to strains of *Mtb* with different virulence has been studied, the underlying bacterial mechanism of differential virulence between strains has not. We hypothesized that differential response to in-vivo stress may be responsible for differential virulence. We studied two strains, one known to exhibit low virulence, CDC1551, and the other, generally considered to exhibit high virulence, Erdman, to determine mechanisms of differential responses to *in vivo*-relevant stress *in vitro*. Erdman exhibited greater fitness upon culturing in a hypoxic environment relative to CDC1551 and replicated significantly better relative to CDC1551 in an *in-vitro* model of reactivation (re-aeration). In order to determine a possible mechanism for these differences, we characterized the early hypoxia/re-aeration transcriptome. During early hypoxia, the expression of the DosR regulon was induced to significantly higher levels, both in magnitude and breadth, in Erdman relative to CDC1551. The DosR signaling pathway is critical for the persistence of Mtb in lungs. We postulate that one or more DosR-regulated proteins mediate the survival of Mtb in hypoxia and its transition to an environment of normoxia; The greater fitness of Erdman during hypoxia and reaeration may result from its ability to invoke the expression of this pathway to much higher levels. Erdman also exhibited significantly higher resistance to thiol-oxidative stress and intra-phagosomal growth relative to CDC1551.

SIGNIFICANCE OF VIP AND VIP RECEPTOR INTERACTION IN PROMOTING PATHOGENESIS OF EOSINOPHILIC ESOPHAGITIS

Verma AK*, Venkateshaiah SU*, Manohar M*, Mishra A*

*Department of Medicine, Tulane Eosinophilic Disorder Center, Pulmonary Diseases Department, Tulane University School of Medicine, New Orleans, LA 70112

Vasoactive intestinal peptide (VIP) is shown to have a role in the esophageal sphincter contraction and relaxation, and its role in pathogenesis of eosinophil associated allergic diseases like asthma and rhinitis is reported. Therefore, we tested the hypothesis that VIP may have an important role in the eosinophils accumulation in the esophagus that promote the pathogenesis of eosinophilic esophagitis (EoE). Accordingly, we performed flow cytometer analysis for VIP receptors expression in the blood eosinophils and real time PCR for VIP transcript analysis in the biopsies of human EoE. Herein, we show that human eosinophils highly express VIP associated receptor CRTH2, not VAPC1 or VAPC2. Further, VIP mRNA and protein is induced in esophageal biopsies of human EoE compare to the normal individuals. Additionally, we show that *in vitro* VIP has a similar chemoattractant activity for eosinophils as eotaxin. Further, we show that *in vivo* CRTH2 expressed eosinophils accumulated around the VIP producing nerves in the esophageal biopsies of EoE patients. Interestingly, we also observed VIP receptor VPAC2 on mast cells and their accumulation near the nerve cells in EoE biopsies. Taken together, we show the significance of VIP and its receptors interaction in the recruitment of eosinophils and mast cells that may have an important role in promoting chronic EoE pathogenesis in human.

Funding: NIH R01 AI080581 (AM)

ANTIMICROBIAL OUTER MEMBRANE VESICLES DISRUPT GRAM-POSITIVE AND GRAM-NEGATIVE BIOFILMS

Wang Y, Baker SM, Bitoun JP, Höner zu Bentrup K, Morici LA

Department of Microbiology and Immunology, Tulane University School of Medicine, New Orleans, LA, USA

Biofilms are extracellular matrices produced by many multidrug-resistant organisms (MDROs). These highly heterogeneous matrices, composed primarily of polysaccharides, proteins, and lipids, encase and protect MDROs from antibiotic penetration, obstructing the eradication of infections caused by biofilm-forming pathogens. Biofilm-forming MDROs are a common cause of many different infections, including pneumonia, otitis media, diabetic foot infections, dental caries, and infections of medical device implants. Previous studies indicate bacteria within biofilms are 10 to 1000-fold more resistant to antibiotics, making it imperative to develop new antimicrobial agents with an ability to diffuse into or disrupt biofilms and kill persisting cells. Outer membrane vesicles (OMVs) produced by Gram-negative bacteria contain outer membrane and periplasmic bacterial components, which in previous studies have demonstrated the ability to kill both Gram-negative and -positive planktonic bacteria. Additionally, the nano-particle size and membrane composition of OMVs may allow them to diffuse into biofilms. Thus, we hypothesized that OMVs could penetrate biofilm matrices and kill resident bacterial cells. We tested the antimicrobial activity of OMVs derived from *Burkholderia* species against Methicillin-resistant *Staphylococcus aureus* (MRSA), *Acinetobacter baumannii,* and the dental pathogen *Streptococcus mutans* using well-established biofilm assays. Minimal biofilm eradication concentration (MBEC) was determined and compared to the antibiotic gentamicin. *Burkholderia* OMVs significantly inhibited biofilm formation and reduced biomass of pre-formed biofilms in a dose-dependent manner against all bacterial species tested in a microtiter plate assay. Additionally, *S. mutans* biofilms harvested from a glass surface were highly susceptible to OMV treatment. These findings support the pursuit of OMVs as a novel antimicrobial agent in combating biofilm-forming MDROs.

Cockroach exposure as a driver of asthma symptom disparities in children

Derek Werthmann, MPH*, Felicia A. Rabito, PhD,MPH*

*Department of Epidemiology, Tulane University School of Public Health and Tropical Medicine

Background: Pronounced disparities in asthma outcomes exist between race and income groups. The factors influencing these disparities are not well understood. Studies show that exposure to cockroach allergen may be responsible for the disparate asthma outcomes because high risk groups are highly exposed and because cockroach antigen is more allergenic than other indoor allergens. However, these studies were limited by lack of control for important covariates. The aim of this analysis is to assess the association between exposure to cockroaches in the home and asthma symptom days, controlling for known covariates. **Methods:** Data was analyzed on 68 moderate to severe asthmatic children aged 5-17 years living in the New Orleans metro area. Neighborhood violence, caregiver stress, asthma symptoms, medication adherence, and demographic information was collected during in-home interviews. Cockroach counts were assessed via trapping in children's homes. Multiple regression analysis was performed to assess the association between maximum symptom days and cockroach counts. **Results:** In the adjusted model, cockroach counts were significantly associated with maximum symptom days (β=.011, $p<.0001$). For each 100 cockroaches trapped in homes there is an increase in 1.1 maximum symptom days. No other covariates in the model were significantly associated with the outcome. **Conclusion:** These results show that exposure to cockroaches is an important predictor of symptom days even after controlling for important covariates. This suggests that cockroach may be a driver of asthma outcome disparities especially for populations at higher risk of exposure.

Funded by: The Department of Housing and Urban Development, Healthy Homes Technical Studies, Grant No: LAHH0228-10

FACTORS ASSOCIATED WITH COMPLEMENTARY AND ALTERNATIVE MEDICINE USE AMONG ADHERENT VERSUS NONADHERENT OLDER WOMEN AND MEN

Williams, L[*,**]; Peacock E**; Bazzano L[***]; Sarpong D[*]; Krousel-Wood M[**,***,****]

[*]Xavier University of Louisiana College of Pharmacy, Division of Clinical and Administrative Sciences
[**]Tulane University School of Medicine, Department of Medicine
***Tulane University School of Public Health and Tropical Medicine, Department of Epidemiology
[****]Ochsner Health System, Research Division

Objective: Complementary and alternative medicine (CAM) use is highly prevalent among older women and men with cardiovascular disease, and has been associated with low antihypertensive medication adherence. An understanding of how the factors associated with CAM use differ among adherent versus nonadherent older women and men may help explain this relationship. We examined the factors associated with CAM use among adherent versus nonadherent older women and men using data from the Cohort Study of Medication Adherence among Older Adults (CoSMO).

Methods: We conducted a cross-sectional analysis including 2,122 older women and men with hypertension. Questions assessing CAM use were derived from a previously validated survey; CAM use was defined as the use of health food, herbal supplements, or relaxation techniques at least several times in the year prior to the baseline survey. Pharmacy fill adherence was calculated as proportion of days covered (PDC) using all antihypertensive prescriptions filled in the year prior to the survey; low adherence was classified as PDC less than 80%. Multivariable logistic regression was used to examine the factors associated with CAM use, stratified by adherence. We tested for effect modification by adherence in separate multivariable models. Interaction was tested at α=0.05 level of significance.

Results: Participants were 59.2% female, 30.7% black with a mean age of 75 years and prevalence of low adherence of 29.1%. Prevalence of CAM use among low adherers and non-low adherers was 30.9% and 24.5%, respectively. Engaging in 2 or more lifestyle modifications was associated with CAM use among both low (odds ratio (OR) 2.18; 95% confidence interval (CI) 1.22, 3.87) and non-low adherers (OR 2.29, 95% CI 1.55, 3.37). Additional factors associated with CAM use among low adherers were low satisfaction with communication (OR 1.79; 95% CI 1.04, 3.08), reduced medications because of cost (OR 1.87; 95% CI 1.00, 3.48) and reduced medications because of side effects (OR 1.87; 95% CI 1.02, 3.45). Having high hypertension knowledge (OR 1.39; 95% CI 1.04, 1.86) and high stress (OR 1.36; 95% CI 1.05, 1.77) were associated with CAM use among non-low adherers. There was no evidence of effect modification by adherence.

Conclusion: Factors associated with CAM use differ among low adherers compared to non-low adherers. Further understanding of these differences may help to explain the relationship between CAM use and low adherence, and may lead to approaches to improve medication adherence and blood pressure control among older women and men with hypertension.

Acknowledgment: This work was supported, in part, by Award Number R01 AG022536 from the National Institute on Aging (Krousel-Wood-PI) and K12HD043451 from the Eunice Kennedy Shriver National Institute of Child Health & Human Development of the National Institutes of

Health (Krousel-Wood-PI; Williams-Building Interdisciplinary Research Careers in Women's Health (BIRCWH) Scholar). The content is solely the responsibility of the authors and does not necessarily represent the official views of the NIA or the National Institutes of Health (NIH).

IMPACT OF SPATIAL SHORT-TERM MEMORY LOAD ON AUDITORY SPATIAL ATTENTION GRADIENTS

Golob, EJ[*,**,***], Winston, JL[**,***], Mock, JR[*,**]

Department of Psychology, University of Texas, San Antonio[*]

Department of Psychology[**] and Tulane Brain Institute[***], Tulane University

Background: Attentional biases on information flow happen over a wide range of timescales, from milliseconds to hours. Thus there is a need to consider how short-term memory processes that are needed to retain information over time relate to attention control. Here we used an auditory spatial attention task to test whether short-term memory load influences auditory attention gradients, and whether verbal vs. spatial information in memory have differential effects.

Methods: Young adults performed short blocks of an auditory spatial attention task while maintaining a spatial (1 sound location, n=21) short-term memory load. After encoding memory items subjects performed an attention task by attending to a standard location in space and discriminated among noise stimuli based on amplitude modulation rate (25 or 75 Hz button press, 90% AM depth). Stimuli were presented using insert headphones at 5 virtual locations in the frontal azimuth plane (-90°, -45°, 0° midline, +45°, +90°). Stimuli came from the standard location on most trials (p=.84), but occasionally the shifted (p=.04/shift location). Reaction times and accuracy were analyzed as a function of stimulus location (5) and memory load (no load, STM memory), and memory location (spatial task).

Results: No load conditions replicated prior results showing that reaction times increased on shift trials but decreased for farthest shifts, specific to the left and midline standard conditions (p's<.001). In the spatial memory task load increased reaction times at lateral locations, with no effect at the attended midline location (p<.001). The load effect was also significantly greater in the left vs. right hemispace (p<.05). There was no significant association between memorized and stimulus locations. Comparison of verbal and spatial load effects in the 0° standard showed opposite load effects among tasks. The maximal load effect was at midline for verbal memory but at lateral locations for spatial memory (p<.02).

Conclusions: Findings show that short-term memory influences the distribution of auditory attention over space; and the specific pattern depends on the type of information in short-term memory.

This work was supported by a grant from the National Institute of Health.

THE USE OF XENODIAGNOSIS TO EVALUATE TREATMENT EFFICACY IN A MOUSE MODEL OF LYME DISEASE

Worthy RS, Jacobs MB, Hasenkampf NR, Martin DS, and Embers ME*

*Division of Bacteriology and Parasitology, Tulane National Primate Research Center, Tulane University Health Sciences, Covington, Louisiana

Abstract

With an estimated incidence of 300,000+ new cases annually, Lyme disease is the most common tick-borne infection in North America. The causative agent of Lyme disease is the spirochete *Borrelia burgdorferi (Bb)*, which infects humans systemically, causing rash, arthritis, carditis, myalgia, extreme fatigue and neurological dysfunction. The efficacy and accepted regimen of antibiotic treatment has been a hotly contested issue surrounding Lyme disease for many years. Even though antibiotic treatment has been generally effective in treating Lyme disease patients, a proportion of patients continue to experience symptoms after the completion of their treatment. In animal models, the presence of *Bb* post-antibiotic treatment has been demonstrated, yet the organisms recovered are not cultivable. Our laboratory aims to test an antibiotic treatment/therapeutic vaccination strategy in mice infected with *Bb*. Following infection and treatment, persistence of *Bb* was evaluated by placing uninfected ticks on mice for feeding (xenodiagnosis), culture and PCR of tissues. Antibiotic levels in mice were measured by the Kirby-Bauer assay. Xenodiagnostic tick contents were scored either positive or negative by immunofluorescent staining of *Bb*, culture, and PCR. Our results indicate that xenodiagnosis is a sensitive method to evaluate persistence of the *Bb* pathogen when organ culture fails.

This research was supported by the Bay Area Lyme Foundation.

CHRONIC SINONASAL TRACT INFLAMMATION AS A PRECURSOR TO NASOPHARYNGEAL CARCINOMA AND SINONASAL MALIGNANCY IN THE UNITED STATES

Wu EL*, Riley CA*, Hsieh MC**, Marino MJ***, Wu XC**, McCoul ED****,*****

* Department of Otolaryngology-Head and Neck Surgery, Tulane University School of Medicine, New Orleans, LA 70112, USA
** Louisiana Tumor Registry, School of Public Health, Louisiana State University Health Sciences Center, New Orleans, LA 70112, USA
*** Otorhinolaryngology-Head and Neck Surgery, University of Texas Medical School of Houston, Houston, TX 77030, USA
**** Department of Otorhinolaryngology, Ochsner Clinic Foundation, New Orleans, LA 70120, USA
***** Ochsner Clinical School, University of Queensland School of Medicine, New Orleans, LA 70121, USA

Background: Chronic inflammatory states have been linked to the development of malignancy. Chronic rhinosinusitis (CRS) and allergic rhinitis (AR) have been associated with nasopharyngeal carcinoma (NPC) in population-based studies in Asia. A similar association with NPC and paranasal sinus malignancy (PSM) has not been defined in a North American population. Our purpose was to investigate the impact of CRS and AR on the risk of NPC and PSM.
Methods: The Surveillance, Epidemiology, and End Results (SEER)-Medicare linked database was queried as a case-control study of adults aged 65 years and greater. The study cohort included 2,009 patients diagnosed with NPC and/or PSM diagnosed in 2003-2011, and 2,009 propensity score matched controls selected from a 5% random sample of Medicare beneficiaries without cancer. CRS and AR were examined as exposures. Multivariable unconditional logistic regression was employed.
Results: Overall, NPC and PSM patients were more likely to have previous CRS diagnosis than the controls (9.2% vs. 3.0% and 11.1% vs. 2.7%, respectively). CRS was associated with greater odds of developing NPC (OR: 3.51; 95% CI, 2.12-5.79) and PSM (OR 5.30; 95% CI, 3.55-7.92). AR was associated with greater odds of developing NPC (OR: 4.23; 95% CI, 2.96-6.06) and PSM (OR: 3.35; 95% CI, 2.49-4.49). The number needed to harm in the exposed population was 311.
Conclusions: CRS and AR are associated with the development of NPC and PSM in the United States elderly population. This epidemiological association will need to be examined for causative pathophysiological mechanisms and utility in clinical diagnosis.

Conflicts of Interest: The authors declare no financial disclosures or conflicts of interest.

CIRCADAIN/MELATONIN DISRUPTION BY DIM LIGHT AT NIGHT DRIVES HUMAN EPITHELIAL BREAST CANCER TO A METASTATIC PHENOTYPE

Xiang S, Dauchy RT, Wren-Dail MA, Abdelegan M, Rowan B, Blask DE, and Hill SM

Department of [1]Structural and Cellular Biology, Tulane Cancer Center, and Tulane Center for Circadian Biology, Tulane University School of Medicine

Statement of Scientific Premise: examined if dLAN-induced circadian/MLT disruption can promote epithelial-to-mesenchymal transition (EMT) of epithelial MCF-7 breast tumor xenografts leading to the development of metastatic foci in the lungs, livers, and brains of circadian complete (MLT-producing) athymic nude female rats and mice.

Background & Data: Cancer patients with disrupted 24-hour (circadian) rhythms are reported to have poorer survival as compared to those with normal rhythms. Severe alterations in circadian rhythms predict an increased risk of death in patients with colorectal and breast cancer, suggesting that circadian disruption impact tumor progression and metastasis. We have reported that circadian/melatonin (MLT) disruption by exposure to dim light at night (dLAN) resulted in constitutive phospho-activation of ERK1/2, CREB, NF-kB, and STAT3 in breast tumor xenografts promoting resistance to Tamoxifen and Doxorubicin therapy.

Female nude rats with ERα+ MCF-7 or T47D human epithelial breast cancer xenografts were housed in LD,12:12 and LD,12:12dLAN (dLAN) photoperiods or in dLAN supplemented with nighttime MLT (0.05 μg/ml) in the drinking water, with lights on at 0600 hrs and off at 1800 hrs. Blood samples collected during the mid-dark phase (2400 hrs) showed elevated nocturnal melatonin (118.4 pg/ml) in the LD,12:12 group, but significantly suppressed melatonin (10.0 pg/ml) in the dLAN group. Tumor xenografts from rats housed in dLAN showed a ~3-fold decrease in latency-to-onset and a ~2.8-fold increase in growth rates vs. those from rats in dLAN + MLT. Tumor cAMP levels, as well as numerous signaling pathways involved in promoting EMT (Vimentin, β-catenin, and SNAIL) and metastasis (HER2/HER3, pCREB, pERK1/2, pRSK2, and pSTAT3), showed increased expression/phospho-activation at 2400 hrs in response to dLAN but repressed expression in tumors from rats in dLAN + MLT.

Follow-up studies with Foxn1^{nunu} athymic female mice implanted with non-metastatic luciferase expressing MCF-7 breast cancer cells showed that exposure to dLAN suppressed the nighttime serum levels of MLT by 93% compared to those in a LD,12:12 photoperiod. Exposure of mice to dLAN induced the rapid growth of MCF-7luc tumor xenografts and, after 5 weeks, induced the metastatic outgrowth of MCF-7 xenografts to form luciferase identifiable metastatic foci in the lungs, livers, and brains of all mice, as measured by IVIS small animal imaging system. Conversely, MCF-7luc tumor xenografts from mice exposed to dLAN and supplemented with nighttime MLT showed a reduced tumor development, 3-fold slower tumor growth, and a small metastatic lesion in one lung of a single mouse. This study is the first to show that circadian/MLT disruption by host exposure to dLAN is able to drive EMT in human epithelial breast cancer xenografts to generate metastatic foci in lung, liver, and brain of mice.

Using a MT_1-MLT receptor knock out (KO) MCF-7 breast cancer clone developed using the CRISPR approach, we found that MT1-KO cells exhibited a modest but significant 47% increase in cell proliferation in MLT sufficient media after 5 days compared to parental and vector controls. Employing the Matrigel-coated transwell in vitro invasion assay approach we found that MCF-7 MT1-KO cells exhibited a 20-fold increase in invasion as compared to parental control cells.

Conclusions: Our studies clearly demonstrate that disruption of circadian nighttime MLT by dLAN in rats and mice drives epithelial (luminal A) MCF-7 breast cancer cell xenografts to undergo EMT and to metastasize to lung, liver, and brain and that administration of exogenous MLT during dLAN can almost completely block/repress this metastatic process. The anti-metastatic actions of melatonin are mediated via its MT1 receptor as in vivo KO of the MT1 receptor drives EMT in MCF-7 cells resulting in a 20-fold increase in their invasive capacity compared to parental and vector MCF-7 controls.

Funding: *NIH/NCI R56 to SMH and DEB & Tulane U. School of Medicine Bridge Funding*

TISSUE-SELECTIVE ESTROGEN COMPLEXES ENHANCE ENDOPLASMIC RETICULUM-ASSOCIATED PROTEIN DEGRADATION AND PREVENT DIABETES IN A MOUSE MODEL OF INSULIN MISFOLDING

Xu B, Allard C, Mauvais-Jarvis F
Diabetes Discovery Research and Gender Medicine Laboratory, Section of Endocrinology, Department of Medicine, Tulane University Health Sciences Center, New Orleans, LA

Menopausal hormone therapy using conjugated estrogens (CE) reduces the incidence of T2D in women but the mechanism is unknown. The endoplasmic reticulum (EndoRetic) stress is now recognized as an important contributing factor in β-cell dysfunction in T2D. Estrogens protect pancreatic β-cell survival and function via estrogen receptor alpha (ERα) in β-cells suggesting that CE may protect β-cell from EndoRetic stress via ERα. CE pairing with the selective estrogen receptor modulator bazedoxifene (BZA) is a novel menopausal therapy. We investigated the effects of CE, BZA and the combination of CE with BZA in preventing EndoRetic stress in the Akita mouse model of β-cell insulin misfolding. CE and the combination of CE+BZA prevented β-cells apoptosis, protected β-cell mass and reduced the severity of diabetes in ovariectomized (OVX) female and male Akita mice. In cultured male and female Akita β-cells, CE decreased the intensity of thapsigargin-induced EndoRetic stress predominantly through ERα. However, while BZA alone provided a protection from β-cell destruction and EndoRetic stress in female Akita mice and cultured β-cells, in contrast, BZA showed no protective effect in male mice and β-cells. The Endoplasmic Reticulum Associated Protein Degradation (ERAD)-proteasome pathway is a major engine for the removal of misfolded proteins and is composed of the ubiquitin ligase HRD1 and its scaffold SEL1L. In male Akita cells, CE did not increase proinsulin folding. Rather, CE stabilized the expression of the ERAD proteins HRD1 and SEL1L by preventing their proteasomal degradation. Finally, CE activation of ERα repressed the expression of the ubiquitin-conjugating enzyme UBC6e, a SEL1L degrader and a natural break to the ERAD. In summary, CE activation of ERα in Akita β-cells stabilizes the ERAD pathway, thus promoting the degradation of misfolded insulin and preventing EndoRetic stress-induced β-cell death. Thus, menopausal therapy with CE may protect β-cell function and prevent T2D by mitigating EndoRetic stress in β-cells. Interestingly, while BZA acts as an ERα agonist in female β-cells, in contrast, BZA seems to behave as an ERα antagonist in males.

Funded by NIH grants DK074970 and DK107444

Detecting genetic associations by LASSO based regression under extreme phenotype sampling

Xu C*, Shen H*, Deng HW*
* Center for Bioinformatics and Genomics, Department of Global Biostatistics and Data Science, Tulane University, New Orleans, LA, USA 70112.

Genetic association study is a method to identify candidate variants, genes or genomic regions which contribute to specific diseases. Extreme phenotype sampling (EPS) is a widely used study design in genetic association studies. By enriching the causal variants in the extreme phenotypic samples within top and bottom percentiles, EPS can boost the study power compared with the random sampling with the same sample size. The existing statistical methods for EPS data can be categorized into two groups: case-control methods, which test the variants/regions individually but ignore the non-normally distributed traits under EPS, and likelihood methods, which model the non-normality data but still test the associations individually. However, many disorders are caused by multiple genetic factors. Therefore, it is critical to simultaneously model the effects of genetic markers, which may increase the power of current genetic association studies and identify novel disease associated genetic markers under EPS. The challenge of the simultaneous analysis for genetic data is that the number ($p \sim 10{,}000$) of genetic markers is typically greater than the sample size ($n \sim 1{,}000$) in a single study. The standard linear model would be inappropriate for this $p>n$ problem due to the rank deficiency of the design matrix. An alternative solution is to apply a penalized regression method – the least absolute shrinkage and selection operator (LASSO). LASSO is capable of dealing with the high dimensional ($p>n$) problem by forcing certain regression coefficients to be zero. The application of LASSO in genetic association studies under random sampling have been widely studied. We propose to employ the LASSO based approach to investigate the genetic associations under EPS, including the gene expression and rare variant analyses. By a hypothesis testing considering non-normality data in LASSO, we are able to fully use the extreme phenotypic information to simultaneously detect the disease associated genes or variants.

This work was supported by the grants from NIH (R01-AR050496-11, R01-AR057049-06, R01-AR059781-03) and Edward G. Schlieder Endowment at Tulane University.

THE ASSOCIATION BETWEEN OBESITY AND CARDIOVASCULAR RISK FACTORS IN US ADULTS WEAKENS OVER TIME: EXPERIENCE IN NHANES 1999-2014

Xu J*, Chen W*, Li S*

* Department of Epidemiology, Tulane University School of Public Health and Tropical Medicine, New Orleans, LA, USA

The prevalence of obesity, a major cardiovascular risk factor, has increased over the last four decades. During the same period, cardiovascular mortality has decreased. We hypothesized that the association between obesity and cardiovascular risk factors has changed over time. In this study, obesity status was evaluated by Waist-to-height ratio (WHtR), and cardiovascular disease risk was evaluated by triglycerides. The current study included 23,231 US adults (aged 20-85 years) from the National Health and Nutrition Examination Survey (NHANES) 1999-2014 who did not take any anti-hypertensive, lipids-lowering, and anti-diabetic medications. Association between WHtR and triglycerides levels was examined by correlation analysis and general linear models, adjusted for race, sex, age, smoking, and education levels by examination cycle. WHtR was significantly associated with triglycerides levels in all examination cycles from 1999-2014 ($P<0.0001$) after adjustment for covariates. Further, partial correlation coefficient between WHtR and triglycerides levels decreased over time, from 0.26280 in 1999-2000 to 0.19486 in 2013-2014, with a significant interaction between examination cycle and WHtR on triglycerides levels ($P<0.0001$). The results suggest that at least from 1999 to 2014, the association between obesity and cardiovascular risk factors in US adults has weakened, which may have partly contributed to the paradox between the increasing obesity prevalence and the decreasing cardiovascular mortality. The underlying reasons for this secular change remain to be explored.

ACTIVATION OF THE ANDROGEN RECEPTOR IN B-CELLS AMPLIFIES THE INCRETIN EFFECT OF GLUCAGON-LIKE PEPTIDE-1 IN THE MALE

Xu W*, Mauvais-Jarvis F*

* Department of Medicine, Tulane University School of Medicine, New Orleans, LA, USA

Although aging men with testosterone deficiency are at increased risk of type 2 diabetes (T2D), previous studies have ignored the role of testosterone and the androgen receptor (AR) in pancreatic β–cell function. We generated an inducible β–cell AR knockout (βARKO) mouse using the β-cell specific Ins1-Cre/ERT transgenic mouse. Male βARKO with AR deletion induced in adulthood using tamoxifen exhibited decreased glucose-stimulated insulin secretion (GSIS) leading to glucose intolerance compared to controls. The AR agonist dihydrotestosterone (DHT) enhanced GSIS in cultured male mouse and human islets, an effect that was abolished in βARKO islets and human islets treated with the AR antagonist flutamide. In β-cells, unlike in prostate, DHT-activated AR remains predominantly extranuclear. Accordingly, a novel androgen dendrimer conjugate (ADC), which cannot cross the nuclear membrane and is incapable of exerting AR nuclear function also enhances GSIS. AR stimulates GSIS by increasing islet cAMP and activating the protein kinase A in a manner similar to incretins. Accordingly, DHT amplified the effect of glucagon-like peptide-1 (GLP-1) in enhancing mouse and human islet GSIS. Further, the insulinotropic action of DHT was abolished in the presence of the selective GLP-1 receptor antagonist exendin (9-39) demonstrating that DHT amplifies the incretin effect of islet-derived GLP-1 and requires the GLP-1 receptor. Moreover, glucose tolerance was only altered following intraperitoneal glucose challenge in βARKO without change following and oral glucose challenge, indicating that AR mainly enhance islet-derived GLP-1 (not gut-derived) to regulate the glucose homeostasis. Our study identifies AR as a novel receptor that enhances β-cell function as an incretin sensitizer in males, a novel finding with important implications for prevention of T2D in aging men.

This work was supported by NIH (DK074970, DK007169, HD044405) and ADA (7-13-BS-101).

RENAL RESPONSE TO ACIDOSIS: RNA-SEQ

Yadav S*, Huang W*, Hamm LL*, Hering-Smith KS*

*Department of Medicine, Section of Nephrology, Tulane University School of Medicine, New Orleans, Louisiana

Purpose of Study: Metabolic acidosis is a common pathophysiologic condition that can occur either acutely or chronically in a variety of settings and diseases. Acidosis has a number of adverse effects including progression of chronic kidney disease, bone loss, and muscle wasting. The kidneys are the main organs which respond to acid loads to protect against systemic acidosis.
Methods Used: C57Bl/6 mice were fed either normal or acid diet (X3d), kidney RNA extracted & integrity validated. RNAseq was performed at Tulane Center for Aging Genomics and Biostatistics Core on Ion Proton platform with 20M reads/sample. Bioinformatics was completed at the Cancer Crusaders NGS Analysis Core. For qPCR, RNA was isolated from same kidneys & mRNA relative expression was calculated by delta delta Ct.
Summary of Results: We identified 1173 transcripts differentially expressed >1.5 fold (each statistically significant), 525 transcripts upregulated and surprisingly 648 down regulated. Among those upregulated, many have been previously reported to be involved in the response to acidosis: PCK1, GLUD1, SNAT1, SNAT3, SLC13A2, SLC26A6. But we also identified many additional genes that indicate a broader cellular metabolic response to acidosis. Of note gene transcripts exponentially upregulated were: FGF18, PCK1, SOX14, BCL6, Fam25c; and down-regulated Mir6239, Mir6236, RNU12 and SNORD13. Also 36 genes from SLC family were identified and differentially expressed under acidosis. By qPCR SLC genes 13a2,13a3, 16a9, 26a6 & 38a3 were upregulated & consistent with RNAseq. Ingenuity Pathway Analysis (Qiagen) revealed many of the genes part of canonical pathways: dTMP de novo biosynthesis, superpathway of cholesterol biosynthesis, glutathione-mediated detoxification, NRF2-mediated oxidativestress response.
Conclusions: Acidosis alters (both up and down) many genes and pathways. Many of these genes have been reported in renal fibrosis/damage, tubule injury, hypertrophy & glomerular injury. Since acidosis activates a variety of critical pathways in addition to the known pathways, this information may be useful in designing approaches to a variety of renal and systemic disorders.

This study is supported by NIH/NIDDK (KSH-S)

A NOVEL COMPUTAIONAL STRATEGY FOR DNA METHYLATION IMPUTATION

Yu F*, Deng HW*, Shen H*

*Center for Bioinformatics and Genomics, Department of Global Biostatistics & Data Science, School of Public Health and Tropical Medicine, Tulane University, New Orleans, LA, USA

Whole-genome bisulfite sequencing (WGBS) is the most comprehensive, unbiased method for characterization of genome-wide DNA methylation profiles, but is still too expensive to apply for large-scale studies. On the other hand, the Illumina HumanMethylation450 BeadChip (450K) array is a cost-effective and the most widely used method for DNA methylation analysis. Previous epigenomic studies have generated millions of 450K array data on various samples to study the methylation patterns associated with various diseases/traits. However, the 450K array only measures <2% of all the 28 million CpG sites in the human genome, which considerably limited the scope of the DNA methylation analysis in those studies. In this project, we developed a novel computational strategy to expand the existing 450K data by predicting DNA methylation levels at the unassayed CpG sites based on local DNA methylation patterns and other epigenomic functional annotations. Specifically, we first explored the co-methylation region based on the correlation pattern in a reference WGBS data. Then within each region, we trained a kernel logistic regression model to predict a DNA methylation local score based on the local upstream and downstream DNA methylation information. Finally, we incorporated the local score with other functional annotation information in a linear model to predict the DNA methylation levels at unmeasured CpG sites. This strategy will allow us to expand the existing 450K data and uncover new disease-related epigenetic signals without re-analyzing those samples by WGBS with high cost.

This work is supported by grants from the NIH (R01AR059781, P20GM109036) and Edward G. Schlieder Endowment as well as the Drs. W. C. Tsai and P. T. Kung Professorship in Biostatistics from Tulane University.

Interferon-alpha induced hepatitis C virus clearance restores p53 tumor suppressor stronger than direct-acting antivirals

Yucel Aydin [2], Animesh Chatterjee[1], Partha K Chandra[1], Srinivas Chava[1], Weina Chen[1], Anamika Tandon[1], Asha Dash[1], Milad Chedid[1], Martin W Moehlen[2], Frederic Regenstein[2], Luis A Balart[2], Ari Cohen[3], Hua Lu[4], Tong Wu[1] and Srikanta Dash[1, 2]

1-Department of Pathology and Laboratory Medicine, 2-Department of Medicine, Division of Gastroenterology and Hepatology, 3-Liver Transplant Surgery Section, Ochsner Medical Center, New Orleans, Louisiana, USA, 4-Department of Biochemistry, Tulane University Health Sciences Center, New Orleans, Louisiana, USA.

Hepatitis C virus (HCV) clearance by direct-acting antiviral drugs (DAAs) does not eliminate the risk of hepatocellular carcinoma (HCC) among patients with advanced cirrhosis. The mechanism is unclear. Many viral and bacterial infections degrade p53 in favor of cell survival to adapt endoplasmic stress (ER) response. In this study, we examined whether HCV clearance by IFN-✔ or DAAs normalizes the ER-stress and restore p53 expression in cell culture. We found that HCV infection induces chronic ER-stress and unfolded protein response (UPR) in untransformed primary human hepatocytes (PHHs). The UPR response induces chaperone-mediated autophagy (CMA) in infected PHHs and Huh-7.5 cells that results in degradation of p53 and induced expression of Mdm2. Inhibition of p53/Mdm2 interactions by small molecule (Nutlin-3) or silencing Mdm2 did not rescue the p53 degradation, indicating that HCV infection induces degradation of p53 independent of the Mdm2 pathway. Interestingly, our results show that HCV infection degrades p53 in a lysosome-dependent mechanism since LAMP2A silencing restored p53 degradation. Our results show that HCV clearance induced by interferon-based antiviral normalizes ER-stress response and restores p53 whereas HCV clearance by DAAs does neither. High ER-stress and CMA response (HSC70 and LAMP2A) also decreased expression of p53 in HCV-infected cirrhotic livers. *Conclusions:* Our results

indicate that HCV induced ER-stress and CMA promote p53 degradation in advanced liver cirrhosis. HCV clearance by DAAs does not restore p53, which provides a potential explanation why viral cure by DAAs does not eliminate HCC risk among patients with advanced liver disease. We propose that resolving the ER-stress response is an alternative approach to reduce HCC risk among cirrhotic patients after viral cure.

Discovery of Aberrant Brain Connectivity in Schizophrenia using Gaussian Graphical Models

Aiying Zhang[1], Jian Fang[1], Vince Calhoun[2], Yu-Ping Wang[1]

[1]Department of Biomedical Engineering, Tulane University, New Orleans, LA,
[2]Department of Electrical and Computer Engineering, UNM, Albuquerque, NM

Schizophrenia (SZ) has long been considered as a disorder of brain connectivity. By incorporating the graph theoretical approaches into connectivity analysis, we can gain a new understanding of the characteristics of human brain, from a microscale connectivity between single neurons to a macroscale connectivity between regions of interest (ROIs) or voxels in brain images. Region-based networks fail to illustrate the connectivity within the ROIs and can't give more precise location information. Voxel-based networks can cover the shortfalls, but it is still a challenge to construct them efficiently and accurately due to computational burden and small sample size. In this paper, we adopted a novel high-dimensional Gaussian Graphical Model (GGM)---- ψ-learning method, which can solve these issues by providing more accurate inference for underlying graphs with less CPU cost. The computational complexity is only $O(p^2)$ for $p>n$, whereas other methods have usually higher than $O(p^3)$. The main idea is to find the reduced neighborhood for each variable through a correlation screening, then calculate the ψ-score which is the partial correlation coefficient conditioned on the reduced neighborhood and finally only keep the significant edge through the so-called ψ-screening. The ψ-score is equivalent to the partial correlation coefficient in the sense that $\psi_{ij} = 0 \Leftrightarrow \rho_{ij|V\setminus ij} = 0$, where V denotes the set of indices of all variables. Since the ψ-score is an equivalent measure of the partial correlation coefficient, it keeps similar properties. Thus we can make network comparison for the case-control study by conducting a multiple hypothesis test. Multiple hypothesis tests are also required in the correlation screening and the ψ-screening which can be accomplished via Fisher's transformation. We applied the method to the fMRI data collected by The Mind Clinical Imaging Consortium (MCIC) which has 208 subjects in total: 92 SZ patients and 106 healthy controls. We followed the same preprocessing procedures as outlined by Lin. We set the significance levels for correlation screening and ψ-learning screening $\alpha 1 = \alpha 2 = 0.01$. For a run with 41236 voxels on a 2.8 GHz computer, it only took 24h 18mins. Finally, we got 33721 links in the case group and 40470 links in the control group. Reduced hub structure was observed in SZ patients as compared to the control group. Furthermore, we made a network comparison and set the significance level $\alpha = 0.01$. We got 12012 significant different edges and identified 15 affected hubs. The affected hubs are mostly located on the temporal lobe and the parietal lobe. The hub with highest number of aberrant connections is the Inferior temporal gyrus (R), followed by the Cerebellum 4 5(L). Additionally, we found some asymmetric brain connectivity in SZ patients. Several conclusions have been verified in the literature. For instance, it has been founded schizophrenic patients have left-right volume asymmetries in anterior hippocampus, parahippocampal gyrus and middle temporal gyrus on the temporal lobe and abnormal hemispheric specialization of the caudate nucleus. All these findings further demonstrate the biological significance or implications of our results.

The work is funded by NIH (R01GM109068, R01MH104680, R01MH107354), and NSF (#1539067)

GENE NETWORK ANALYSIS REVEALS A NOVEL 22-GENE SIGNATURE OF CARBON METABOLISM IN HEPATOCELLULAR CARCINOMA

Zhang J[*], baddoo M[**], Han C[*], Strong MJ[**], Cvitanovic J[***], Moroz K[*], Dash S[*], Flemington EK[*], Wu T[*]

* Department of Pathology and Laboratory Medicine, Tulane University School of Medicine, New Orleans, LA

** Bioinformatics Core, Tulane Health Sciences Center and Tulane Cancer Center, New Orleans, LA

*** Biospecimen Core, Louisiana Cancer Research Consortium, New Orleans, LA

Cancer metabolism alterations may represent convergent effects of key oncogenic signaling pathways. Although much progress has been made in understanding cancer cellular metabolism adaptation, the co-regulations between genes of metabolism and cancer pathways and their interactions remain poorly characterized. In this study, we applied weighted gene co-expression network analysis to 1509 metabolic gene microarray expression data generated from 120 Hepatocellular Carcinoma (HCC) and 180 non-tumor human samples. Our analyses reveal that genes in metabolism can be classified into different co-expression modules based on their expression patterns and associations with HCC related traits. In addition, We applied BioLayout Express3D analysis, which is a powerful way for the visualization and analysis of network graphs, to characterize the different co-regulation status of genes involved in Carbon Metabolism Pathway (KEGG hsa01200) and Pathway in Cancer (KEGG hsa05200) between HCC and non-tumor liver tissues. Results show that the majority of genes in these two pathways are well co-regulated and there exists an intertwined edges network in non-tumor liver tissues, suggesting a complex and well-organized association among genes of these two pathways. In HCC, the regulation network associations between Carbon Metabolism and Pathway in Cancer genes become weaken generally, but a number of genes' interactions with cancer related genes are enhanced. These results indicate that the co-regulation mechanism of the carbon metabolism genes in normal liver tissues was interrupted and reprogrammed to adapt the cell's specific requirements during the processes of carcinogenesis. In parallel, we performed RNAseq analysis of human HCC and matched non-neoplastic liver tissues, which revealed the spectrum of carbon metabolism pathway genes that are differently expressed between HCC and non-neoplastic liver tissues. Our transcriptomics analysis led to identification of a unique 22-gene signature of carbon metabolism, whose expression levels are elevated in HCC tissues. This gene signature was further verified in multiple microarray data sets. Analysis of The Cancer Genome Atlas (TCGA) database showed that the elevated expression of these 22 carbon metabolism genes is associated with poor survival prognosis of HCC patients. Additionally, the tumorigenic function of two representative genes citrate synthesis (CS) and acetyl-CoA synthetases short-chain family member 1 (ACSS1), were validated *in vitro*. We observed that knockdown of these two genes by siRNA significantly reduced HCC cell growth and

hepatic spheroid formation. Conclusions: The current study reveals a unique 22-carbon-metabolism-gene-expression signature in HCC, and this signature could be used to predict patient prognosis. Strategies targeting these genes may represent new therapeutic approaches for the treatment of HCC.

The work in the authors' laboratory is supported by NIH grant R01 CA102325

Reveal gene expression pattern change at transcriptional and post-transcriptional levels respectively

Zhang JG*, Xu C*, Shen H* and Deng HW*

* Center for Bioinformatics and Genomics, Department of Global Biostatistics and Data Science, Tulane University, New Orleans, LA, USA 70112.

Abstract:

Aberrant gene expression contributes to variety of complex diseases. Gene transcription is regulated with distinct sets of regulatory factors at multiple levels. Transcriptional regulation (e.g. by transcription factors) and post-transcriptional regulation (e.g. by microRNAs) constitute two major modes of regulation of gene expression to either activate or repress the initiation of transcription and thereby control the amount of proteins synthesized during translation. Disruptions of the proper regulation patterns by mutations at transcriptional and post-transcriptional regulation levels are increasingly recognized as causes of human disease. For this reason, identifying the gene differential expression at transcriptional and post-transcriptional levels respectively is vital to understand the role played by various regulatory factors on gene expression regulation. To this end, we proposed a method with a mixed model that can identify a set of differentially expressed genes at transcriptional and post-transcriptional levels. The simulation study shows that our method can provide an accurate way to identify genes subject to differential transcriptional and post-transcriptional regulation and infer an accurate regulatory network that contributes to the diseases of interest.

This work was supported by the grants from NIH (R01-AR050496-11, R01-AR057049-06, R01-AR059781-03) and Edward G. Schlieder Endowment at Tulane University.

NETWORK-BASED TRANSCRIPTOME-WIDE EXPRESSION STUDY FOR POSTMENOPAUSAL OSTEOPOROSIS

Lan Zhang[1], Wei Zhu[1, 2], Yong Zeng[1, 3], Hong-Wen Deng[1]*

1. Center for Bioinformatics and Genomics, Department of Biostatistics and Bioinformatics, Tulane University, New Orleans, LA, USA, 70112.
2. College of Life Sciences, Hunan Normal University, Changsha, Hunan, China, 410081.
3. College of Life Sciences and Bioengineering, Beijing Jiaotong University, Beijing, China, 100044.

Abstract:

Menopause is one of the crucial physiological events during the life of women. Transition of menopause status is accompanied by increased risks of various health problems like osteoporosis. Peripheral blood monocytes (PBMs) can differentiate into osteoclasts and produce cytokines important for osteoclast activities. To identify osteoporosis-related genes, we performed transcriptome-wide expression analyses for human PBM using Affymetrix 1.0 ST arrays in 40 Caucasian postmenopausal women with discordant bone mineral density (BMD) levels. 716 genes were significantly differentially expressed (P_{adjust}<0.05) in subjects with extremely low *vs.* high BMD. We performed Multiscale Embedded Gene Co-expression Network Analysis (MEGENA) to study functionally orchestrating clusters of differential expressed genes in the form of networks. MEGENA showed that the module containing *ZFP36* as hub gene was significantly correlated with BMD variation, and “T cell receptor signaling pathway” as well as “osteoclast differentiation pathway” were significantly enriched in this identified compact network. Gene Sets Net Correlations Analysis (GSNCA) was applied to see how the co-expression structure of pre-defined gene set differs in high and low BMD groups. GSNCA revealed that the co-expression structure of “Signaling by TGF-beta Receptor Complex pathway” is significantly different between two groups, and the hub genes in postmenopausal high and low BMD group are *FURIN* and *SMAD3* respectively. The present study suggested that biological signals involved in monocyte recruitment, monocyte/macrophage lineage development, osteoclast formation, osteoclast differentiation might function together in PBMs that contributes to the pathogenesis of postmenopausal osteoporosis.

TH17-IL-17 PATHWAY AS A TARGET IN PROSTATE CANCER PREVENTION

Zhang Q*,**, Liu S*, Ge D*, Cunningham DM*, Ma L*, You Z*,**,***,****

*Department of Structural & Cellular Biology, **Tulane Center for Aging, ***Tulane Cancer Center and Louisiana Cancer Research Consortium, and Tulane Center for Stem Cell Research and Regenerative Medicine, ****Department of Orthopaedic Surgery, Tulane University School of Medicine, New Orleans, LA.

Chronic inflammation predisposes an individual to cancer including prostate cancer. However, the exact role of the inflammatory Th17-IL-17 pathway in prostate cancer remains unknown. In this study, we aimed to determine the importance of IL-17 and Th17 cells in a prostate-specific *phosphatase and tensin homolog* (*Pten)* knockout (KO) mouse model. The prostate-specific *Pten* KO mice were treated by anti-mouse IL-17 monoclonal antibody or a small molecule inhibitor (SR1001) of Th17 cell differentiation from 6 weeks of age up to 12 weeks of age. For IL-17 antibody treatment, the mice were injected i.v. once every two weeks with control IgG or rat anti-mouse IL-17 monoclonal antibody, which was dissolved in PBS. The injection time points were at 6, 8, and 10 weeks of age. For SR1001 treatment, the mice were injected i.p. twice a day with vehicle or SR1001, which was dissolved in a dimethylsulfoxide (DMSO) solution. All mice were euthanized for necropsy at 12 weeks of age. We found that either anti-IL-17 antibody or SR1001 treatment decreased the formation of prostatic intraepithelial neoplasia (PIN) and invasive prostate cancer in *Pten* KO mice. The anti-IL-17 antibody or SR1001 treated mouse prostates had reduced proliferation, increased apoptosis, and reduced angiogenesis, as well as reduced inflammatory cell infiltration. By assessing the epithelial-to-mesenchymal transition (EMT) markers, we found that anti-IL-17 antibody or SR1001 treated prostate tissues had reduced EMT compared to the control treated prostates. These results demonstrated that Th17-IL-17 pathway plays a key role in the development of prostate cancer in *Pten* KO mice. Targeting Th17-IL-17 pathway could prevent prostate cancer in mice.

Grant sponsor: Z.Y. was partially supported by National Institutes of Health (R01CA174714 and P20GM103518), Department of Defense (W81XWH-14-1-0050, W81XWH-14-1-0149, W81XWH-14-1-0458(PI: Feng Chen; Co-I: Z.Y.), and W81XWH-15-1-0444)); the Developmental Fund of Tulane Cancer Center (TCC), Louisiana Cancer Research Consortium (LCRC) Fund; Q.Z. was partially supported by NIH-National Institute of General Medical Sciences (P20GM103629) (PI: S. Michal Jazwinski; Pilot Project PI: Q.Z.).

MONITORING p53 BY MDM2 AND MDMX IS REQUIRED FOR ENDOCRINE PANCREAS DEVELOPMENT AND FUNCTION IN A SPATIO-TEMPORAL MANNER

Zhang Y*, Zeng S*, Hao Q* and Lu H*

Department of Biochemistry & Molecular Biology and Tulane Cancer Center, Tulane University School of Medicine, New Orleans, LA, USA.

Although p53 is not essential for normal embryonic development, it plays a pivotal role in many biological and pathological processes, including cell fate determination-dependent and independent events and diseases. The expression and activity of p53 largely depend on its two biological inhibitors, MDM2 and MDMX, which have been shown to form a complex in order to tightly control p53 to an undetectable level during early stage of embryonic development. However, more delicate studies using conditional gene-modification mouse models show that MDM2 and MDMX may function separately or synergistically on p53 regulation during later stages of embryonic development and adulthood, in a cell and tissue-specific manner. Here, we report the role of the MDM2/MDMX-p53 pathway in pancreatic islet morphogenesis and function maintenance, using mouse lines with specific deletion of MDM2 or MDMX in pancreatic endocrine progenitor cells. Interestingly, deletion of MDM2 results in the defects of embryonic endocrine pancreas development, followed by neonatal hyperglycemia and lethality, by inducing pancreatic progenitor cell apoptosis and inhibiting cell proliferation. However, unlike MDM2-knockout animals, mice lacking MDMX in endocrine progenitor cells grow up normally. But surprisingly, compared to control mice, the survival rate of adult MDMX-knockout mice drastically declines, which is because of the blockage of neonatal development of endocrine pancreas by inhibiting cell proliferation, subsequent islet dysfunction and hyperglycemia, eventually leading to type 1 diabetes-like disease with advanced diabetic nephropathy. As expected, both MDM2 and MDMX deletion-caused pancreatic defects are completely rescued by loss of p53, verifying the crucial role of the MDM2 and/or MDMX in regulating p53 in a spatio-temporal manner during the development, function maintenance and related disease progress of endocrine pancreas. Also, our study suggests a possible mouse model of advanced diabetic nephropathy, which is complementary to other established diabetic models and perhaps useful for the development of anti-diabetes therapies.

This work was supported in part by NIH-NCI grants R01 CA095441, R01CA172468, R01CA127724, R21 CA201889-01A1, and R21 CA190775 to Hua Lu.

AMPHIPHILIC POLYPEPTOIDS SERVE AS THE CONNECTIVE GLUE TO TRANFORM LIPOSOMES INTO MULTILAMELLAR STRUCTURES WITH CLOSELY SPACED BILAYERS

Zhang Y*, Xuan S**, Owoseni O*, Omarova M*, Li X***, McPherson GL****, Raghavan SR*****, Zhang D** and John VT*

*Department of Chemical and Biomolecular Engineering, Tulane University, New Orleans, LA

**Department of Chemistry, Louisiana State University, Baton Rouge, LA

****Louisiana Consortium for Neutron Scattering, Louisiana State University, Baton Rouge, LA*

****Department of Chemistry, Tulane University, New Orleans, LA

*****Department of Chemical and Biomolecular Engineering, University of Maryland, College Park, MD

We report the ability of hydrophobically modified polypeptoids (HMPs) with decyl groups randomly along the backbones, to connect across lipid bilayers and thus form layered structures. While native polypeptoids (without hydrophobes) have no effect on liposomal structure, the HMPs remodel the unilamellar liposomes into structures with comparable diameters but with multiple concentric bilayers. The transition from single bilayer to multiple bilayer structures is revealed by small angle neutron scattering (SANS) and cryo-transmission electron microscopy (cryo-TEM). The spacing between bilayers is found to be relatively uniform at ~ 6.7 nm. We suggest that the amphiphilic nature of the HMPs explains the formation of multi-bilayered liposomes; i.e., the HMPs insert their hydrophobic tails into adjacent bilayers and thereby serve as the connective glue between bilayers. At higher HMP concentrations, the liposomes are entirely disrupted into micelle-like structures through extensive hydrophobe insertion. Interestingly, these small structures can reattach to fresh unilamellar liposomes and self-assemble to form two-bilayered liposomes. The observations have significance to designing new nanoscale carriers for drug delivery and amphiphilic surfactants for membrane protein extraction.

This work was supported by the U.S. Department of Energy under EPSCoR Grant No. DE-SC0012432.

The Role of GLP-1R in pancreatic α-cells

Yanqing Zhang, Genevieve E. Fava, Rajesh Gupta, Weiwei Xu, Lauren U Nguyen, Anadil Zakaria, Franck Mauvais-Jarvis, Vivian A. Fonseca, Kyle Sloop, and Hongju Wu
Department of Medicine, Section of Endocrinology, Tulane University.

GLP-1R is a G-protein coupled receptor responsible for glucagon-like peptide 1 (GLP-1) action in target cells, including pancreatic β-cells. It stimulates insulin expression, β-cell survival, and proliferation. However, whether GLP-1R also resides in the glucagon producing α-cells remains controversial. Moreover, GLP-1 inhibits glucagon secretion, though it remains uncertain whether its inhibitive effect is direct owing to interactions with GLP-1R on α-cells, or indirect via paracrine suppression by insulin. To investigate this matter, we first confirmed that GLP-1R was expressed by α-cells. We found that GLP-1R was expressed by α-cells and β-cells in both mouse and human pancreas as assessed by western blotting and immunostaining assays. Then, we generated α-cell specific GLP-1R knockout (αGLP-1R KO) mice by crossing hGLP-1R-loxP mice with glucagon-cre mice, and examined whether it affected glucose metabolism/diabetes development. GLP-1R deletion from α-cells of αGLP-1R KO mice was verified by triple-staining with insulin, glucagon and GLP-1R antibodies. To test their glucose metabolism, we performed glucose tolerance tests. We found that αGLP1R KO female mice had glucose intolerance by the age of four months' old. Interestingly, fasting and non-fasting glucagon concentrations in blood were significantly higher in αGLP1R KO mice than that in wildtype mice, whereas insulin levels were similar among different groups. In addition, we found glucose stimulated insulin secretion (GSIS) was maintained in the αGLP1R KO mice. Furthermore, the αGLP1R KO mice responded to the GLP1R agonist, exendin-4, during glucose tolerance test in the same manner as wildtype mice did, indicating that deletion of GLP1R from α cells had no effect on β-cell function. Taken together, these data suggested that glucose intolerance of αGLP1R KO mice was due to interference with glucagon suppression. Knockout of GLP-1R from α-cells disrupted GLP-1-mediated glucagon inhibition, which led to elevated glucagon level in circulation and impaired glucose tolerance, whereas insulin secretion was not affected. We thus concluded that GLP-1 suppresses glucagon secretion by directly acting on α-cell expressed GLP-1R.

ANTIMICROBIAL ACTIVITY AND BIOCOMPATIBILITY OF A HYALURONIC ACID-VANCOMYCIN CONJUGATE POLYMER

Authors: Zhang Z*, Sahiner N**, Blake D***, Ayyala RS*

Affiliations: * Tulane University Department of Ophthalmology, New Orleans, LA

** Canakkale Onsekiz Mart University, Department of Chemistry, Canakkale, Turkey

*** Tulane University Department of Biochemistry and Department of Ophthalmology, New Orleans, LA

Surgical outcome and patient quality of life would be greatly improved by a controlled release antibiotic that could be administered during ophthalmic surgery to decrease risk of post-operative infections while also eliminating or minimizing the need for post-operative topical medications. In this study, we evaluated the drug release rate, antimicrobial activity, and biocompatibility of a hyaluronic acid (HA) - vancomycin polymer.

HA and vancomycin were conjugated in DMSO solution with 1,1'-carbonyldiimidazole and precipitated under sterile conditions. Drug release rate of the HA-vancomycin particle was examined between 1 hour and 4 weeks by measuring the absorbance of released supernatants using UV-vis spectrophotometry at 280 nm. Antimicrobial activity of the released drug was assessed based on ability to inhibit growth of Methicillin-resistant *Staphyloccocus aureus* (MRSA) using standardized filter disks on Mueller-Hinton plates. Biocompatibility of cytotoxicity were assessed by incubating fibroblasts in the presence or absence of the polymer for 5 days. Cell viability was assessed by fixation in glutaraldehyde and nuclear staining using toluidine blue followed by quantification by cell counter.

There was an immediate fast release of 15-40 mg/g of vancomycin hourly in the first 3 hours. 185 mg/g was released in the first 24 hours. 271 mg/g was released over 3 weeks. The rate of drug release was linear after the first 24 hours. 10 ug of vancomycin was sufficient to provide a zone of inhibition of 8 mm. The released vancomycin from 30 mg of polymer was able to provide sufficient inhibition of pseudomonas growth at every time point of collection between 1 hour and 3 weeks.

The polymer was biocompatible with eukaryotic cells even at 3x the concentration required to achieve adequate antimicrobial activity. There was no change in cell density or viability after 5 days of incubation in the control group compared to the groups incubated with the conjugate polymers.

The HA-vancomycin conjugate polymer effectively releases vancomycin at a controlled rate over 4 weeks at a concentration that effectively prevents MRSA growth. The polymer is biocompatible without any toxic effects to eukaryotic cells in vitro. This delivery vehicle has great potential for post-operative infection prevention while minimizing cost and improving quality of life for patients.

Patent is pending for the HA-vancomycin polymer

This work was supported in part by the Tulane Department of Ophthalmology

Geographical difference of osteoporosis, obesity, and sarcopenia related traits in US white population

Yu Zhou[1], Kehao Wu[1], Lan-Juan Zhao[1], Tingjie Zhao[1], Jigang Zhang[1], Hong-Wen Deng[1]

[1]Center for Bioinformatics and Genomics, Department of Biostatistics and Bioinformatics, Tulane University School of Public Health and Tropical Medicine, New Orleans, LA 70112, USA

It has been reported that geographical variation influences bone mineral density (BMD), obesity, and sarcopenia related traits in other countries. However, there is lack of similar studies for US population. In the study, we compared three study cohorts: Louisiana Osteoporosis Study, Kansas City Osteoporosis Study, and Omaha Osteoporosis Study data to evaluate the geographical variation of BMD and body composition. Dual-energy X-ray absorptiometry (DXA) is the gold standard for BMD measurement in human, which can measure both fat mass and lean mass at the same time. All data in the present study were collected from same DXA machine model (Hologic QDR-4500). ANCOVA and Chi-square test were used to compare the difference of BMDs from different regional sites, obesity and sarcopenia related traits, whole body fat mass percentage, relative appendicular muscle mass, basic characteristics for continuous and binary traits, respectively. Age, height, weight, alcohol use, smoking, and regular exercise were treated as covariates in ANCOVA. Eta-squared and Cohen's D were used to measure the effect size of such difference since effect sizes are the most important outcomes of empirical studies. A total of 11,315 Caucasians from our previous 3 study cohorts were compared. There was trivial geographical difference of hip BMD for male (p-values <0.01, η^2=0.001) and female (p-values <0.01, η^2<0.001). There were significant geographical differences with medium effect size (p-value <0.001, 0.01<η^2<0.14) of whole body fat mass percentage and relative appendicular skeletal mass. For Caucasian population in United States, there is few geographical effects on hip BMD. The obesity and sarcopenia related traits are significant different from the three studies.

Gene-based Comparative analysis for consecutive studies of GEFOS

Wei Zhu[1,2], Chao Xu[2], Hao He[2], Ji-Gang Zhang[2], Ke-Hao Wu[2], Lan Zhang[2], Yong Zeng[2,3], Yu Zhou[2], Kuan-Jui Su[2], Lei Zhang[4], Hong-Wen Deng[2]

1. College of Life Sciences, Hunan Normal University, Changsha, Hunan, China 410081.
2. Center for Bioinformatics and Genomics, School of Public Health and Tropical Medicine, Tulane University, New Orleans, LA, USA 70112.
3. College of Life Sciences and Bioengineering, Beijing Jiaotong University, Beijing, China 100044.
4. Jiangsu Key Laboratory of Preventive and Translational Medicine for Geriatric Diseases, School of Public Health, Soochow University, Suzhou, Jiangsu, China, 215123.

Background

To date, conventional genome-wide association studies (GWASs) that have been largely based on individual SNP analyses, have identified about 100 loci associated with bone mineral density (BMD), but these loci only explain a small proportion of heritability to osteoporosis risk. Since gene-based analyses may be more powerful in some situations for GWAS analyses, we performed a gene-based analysis of the largest GWASs in the filed by combining the information of SNPs across individual genes to further identify BMD-associated candidate genes for some un-identified heritability

Methods

We examined BMD-associated genes by analyzing the summary statistics of two consecutive meta-analysis GWASs datasets from Genetic Factors for Osteoporosis (GEFOS) consortium, and subsequently investigated the differential expression of the identified genes in transcriptomics data with the purpose to explore the potential functionality of the identified genes. Additionally, between the two GEFOS datasets, the Pearson correlation coefficient was applied to estimate the correlation levels of the p-values of the common SNPs/genes with BMD.

Results

Additional BMD-associated genes were identified in the two datasets compared with the original SNP-based GWASs. In addition, we found an increased mutual replication between these two largely overlapped datasets with gene-based analyses than with the SNP-based analyses. Among the identified genes, 6 previously identified candidate genes for bone metabolism (*RPS6KA5*, *MEPE*, *LRP5*, *SHFM1*, *FAM3C*, and *ESR1)* and 3 novel genes (*UBTF, AAAS,* and *C11orf58*) were partially validated at the gene expression level. Between the two GEFOS projects that share the majority of their study samples, the correlation levels of p-value of common genes are higher than those of SNPs, and they both reached only a medium correlation level, indicating relatively poor replication of the genes identified from GWASs even from the same large study consortium based on largely the same cohorts.

Conclusion

We explored and identified some novel genes for BMD by gene-based analysis, which empirically showed increased statistical power for novel gene identification. Between individual GWASs, the heterogeneities of system errors and populations only accounted for a small proportion of the insufficient replication of candidate genes.

Acknowledgment

This study was partially supported by and/or benefited from grants from National Institutes of Health [P50AR055081, R21AG27110, R01AR057049, R01AR059781], and Edward G. Schlieder Endowment to Tulane University.